UNIVERSIDAD NACIONAL AUTÓNOMA DE MÉXICO

Maestría y Doctorado en Ciencias Bioquímicas
INSTITUTO DE BIOTECNOLOGIA

DEPARTAMENTO DE GENÉTICA DEL DESARROLLO Y FISIOLOGIA MOLECULAR

Estudio del papel de los productos del gen *dADD1* en la organización de la cromatina

TESIS
QUE PARA OPTAR POR EL GRADO DE:
Doctor en Ciencias

PRESENTA:
M en C. Silvia Meyer Nava

TUTOR PRINCIPAL:
Dra. Viviana del Carmen Valadez Graham
Instituto de Biotecnología

MIEMBROS DEL COMITÉ:
Dra. Leonor Pérez – Instituto de Biotecnología
Dr. David Romero – Centro de Ciencias Genómicas

Cuernavaca, Morelos. Junio, 2021

Agradecimientos

Gracias al laboratorio de Transcripción, Epigenética y Desarrollo, tanto al Dr. Mario Zurita por guiarnos como a todos sus integrantes actuales y pasado. En especial a mi tutora La Dra. Viviana Valadez, por su tiempo y dedicación después de muchos años.

A mi mamá y mi hermana por estar conmigo a pesar de la distancia, el cansancio y algunas ausencias en las Navidades.

A Adolfo por aguantarme en los malos momentos, por acompañarme el fin de semana y por siempre creer en mí.

A mi comité tutoral por toda la guía recibida en estos años. A CONACyT y Dgapa por proporcionar los fondos para la realización de este proyecto.

INDICE

ABREVIATURAS

µg microgramos
µl microlitros
ADD: Dominio conservado solo en ATRX, DNMT3 y DNMT3L
SNF2: Del inglés “Sucrose Non Fermenting 2”
HP1a: Del inglés “Heterochromatin Protein 1”
ATPasa: una clase de enzimas que catalizan la descomposición de ATP en ADP y un ion de fosfato libre, con lo que se libera energia
H3K9me3: Trimetilación de la lisina 9 de la histona 3
H3K4: lisina 4 de la histona 3
ALT: Del inglés “Alternative lengthening of telomere”
PML: Del inglés “Promyelocytic leukaemia”
ATRX : Del inglés “Alpha-Thalassemia mental Retardation syndrome X-related”
DAXX: Del inglés “Death domain associated protein”
COSMIC: Del inglés “Catalogue Of Somatic Mutations In Cancer”
THPA: Del inglés “The Human Protein Atlas”
Sp: Marcador del cromosoma 2, del inglés “Sternopleural”
CyO: Cromosoma balanceador, del inglés “Curly of Oster”
TM6B, Tb1: Cromosoma balanceador, del inglés “Tubby 1”
TPM: Transcritos por millón
UAS: Del inglés “Upstream activating sequence”
MADF: Del inglés “Myb/SANT-like domain in Adf-1”
RT-PCR: Del inglés “Reverse transcription polymerase chain reaction”
Wt: Del inglés “wild type”
MBT: Del inglés “Mid-Blastula Transition”
pan-dAdd1: Anticuerpo diseñado para reconocer todas las isoformas de dADD1

RESUMEN

Las proteínas dADD1 y dXNP son respectivamente los ortólogos en *Drosophila melanogaster* de los dominios ADD y SNF2 del remodelador de cromatina de vertebrados llamado ATRX. Estas proteínas suprimen fenotipos de variegación con efecto de posición y participan en el mantenimiento de la heterocromatina. En el presente trabajo se realizó una búsqueda en bases de datos de cáncer humano y se encontró que los niveles de proteína ATRX se encontraban elevados en más del 4,4% de las muestras analizadas. Usando el modelo de *Drosophila*, abordamos los efectos de sobreexpresión y la falta de la proteína dADD1 en las células de cromosomas politénicos. Los niveles elevados de dADD1 en los tejidos de la mosca causaron diferentes fenotipos, por ejemplo, la disrupción del cromocentro y la pérdida del patrón de bandas en los brazos de los cromosomas. Los análisis de la proteína de mantenimiento de la heterocromatina HP1a y la marca de histona H3K9me3 revelaron cambios en la localización de la marca en la cromatina acompañados de defectos transcripcionales leves, principalmente en los genes incrustados en regiones heterocromáticas cuando se sobreexpresan las proteínas dAdd1. En las glándulas salivales con pérdida de función de dadd1, la expresión de genes embebidos en la heterocromatina es menor que en la condición silvestre. Como observamos una relación entre nuestra proteína de interés y la proteína de heterocromatina 1a, analizamos en la literatura los diferentes complejos y subcomplejos asociados con HP1a. También discutimos las implicaciones de las diferentes interacciones con el mantenimiento de la heterocromatina, la dinámica de la heterocromatina y su relación directa con la regulación génica. Estos datos indican que la sobreexpresión de dADD1 induce cambios en la cromatina que probablemente afectan la estequiometría de HP1a que contiene complejos que conducen a cambios transcripcionales y arquitectónicos. Nuestros resultados colocan a las proteínas dADD1 como actores importantes en el mantenimiento de la arquitectura de la cromatina y la expresión génica heterocromática.

ABSTRACT

dADD1 and dXNP proteins are respectively orthologs in *Drosophila melanogaster* of the ADD and SNF2 domains, of the ATRX vertebrate's chromatin remodeler. They suppress position effect variegation phenotypes and participate in heterochromatin maintenance. We performed a search in human cancer databases and found that ATRX protein levels were elevated in more than 4.4% of the samples analyzed. Using the *Drosophila* model, we addressed the effects of increasing or decreasing the expression levels of dADD1 proteins in polytene cells. Elevated levels of dADD1 in fly tissues caused different phenotypes such as chromocenter disruption and loss of banding pattern at the chromosome arms. Analyses of the heterochromatin maintenance protein HP1a and the histone post-translational modification H3K9me3 revealed changes in their chromatin localization accompanied by mild transcriptional defects of genes embedded in heterochromatic regions. In null dadd1 salivary glands, the expression of heterochromatin embedded genes is lower than in wild-type conditions. Since we observed this relationship between our protein of interest and heterochromatin protein 1, we analyzed the different partners and the possible complexes and subcomplexes associated with HP1a in the literature. We will also discuss the implications of the different interactions with heterochromatin maintenance, heterochromatin dynamics, and its direct relation to gene regulation. These data indicate that dADD1 overexpression induces chromatin changes probably affecting the stoichiometry of HP1a containing complexes which lead to transcriptional and architectural changes. Our results place dADD1 proteins as important players in the maintenance of chromatin architecture and heterochromatic gene expression

1.- INTRODUCCIÓN

1.1 La organización tridimensional de la cromatina

En una célula eucariota, el material genético se encuentra almacenado en un organelo especializado llamado núcleo (Webster, Wikin, and Cohen-Fi 2009; Jorgensen et al. 2007). Con este espacio confinado, por ejemplo en *Drosophila melanogaster* el tamaño de su genoma es de 120 Megabases (Adams et al. 2000) dentro de un núcleo aproximado de 5µm, el ADN se tiene que compactar junto con nucleoproteínas para formar la cromatina (Felsenfeld and Groudine 2003). En células somáticas, la cromatina se compone del ADN y de proteínas ligeramente positivas llamadas histonas, debido a esto el ADN con su carga negativa se enrolla alrededor de las histonas cada 146 pares de bases con lo cual se neutralizan las cargas y de manera eficiente se condensa el material genético (Mariño-Ramírez et al. 2005). La subunidad primaria de la cromatina es el nucleosoma (Figura 1), el cual está formado por un octámero de histonas, es decir dos copias de cada una: H2A, H2B, H3 y H4 (Luger et al. 1997), además está asociado a una histona adicional, la histona H1 que actúa como unión al ADN "linker" (Bayona-Feliu et al. 2017). Así, el ADN enrollado en el nucleosoma forma una cadena llamada cromatina (Luger, Dechassa, and Tremethick 2012).

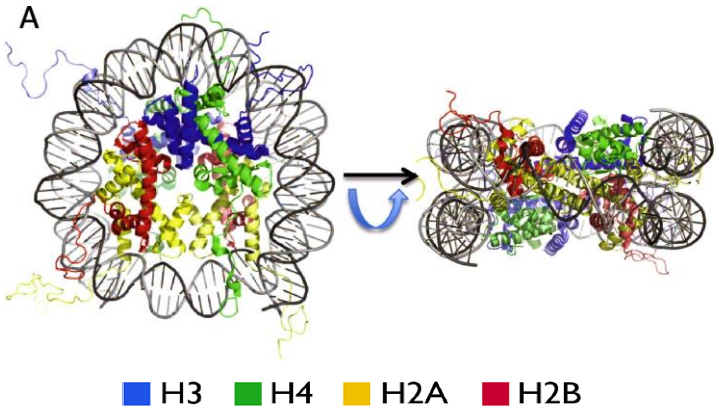

Figura 1. Estructura del nucleosoma. Modelo estructura cristalina del núcleo de nucleosoma (PDB: 1KX5 (Davey et al. 2002)). En la figura se muestra una vista hacia abajo del eje superhelical y una vista girada 90 ° alrededor de un eje horizontal. H2A amarillo, H2B rojo, H3 azul y H4 verde. (Imagen modificada de Cutter and Hayes 2015).

Mediante el uso de métodos más sofisticados que combinan la nanoscopía de superresolución, obteniendo fotografías con una resolución de ~20 nm para analizar la cromatina de distintas células se pudo demostrar que los nucleosomas se agrupan en *"clutches"* que son dominios discretos a lo largo de la fibra de cromatina intercalados y distribuidos heterogéneamente (Ricci et al, 2015). Así, la cromatina se va organizando en el interior del núcleo en distintos grados, siendo la interacción entre nucleosomas o mejor

conocida como *"clutches"* el nivel más básico (Ricci et al. 2015). Los *"clutches"* se pueden agregar de diversas formas dependiendo de las modificaciones postraduccionales que presenten los nucleosomas, lo cual coincide con la clasificación histórica de la cromatina en dos configuraciones: la eucromatina y la heterocromatina (Richards and Elgin 2002) que más a adelante se desarrollaran en detalle.

El siguiente nivel de organización está conformado por asas de cromatina, estas son estructuras que se forman cuando la fibra de la cromatina se pliega sobre si misma para promover el contacto entre elementos regulatorios distales, por ejemplo "*enhancer*", promotores, silenciadores o "*insulators*". Las asas normalmente tienen un tamaño en kilobases y necesitan de proteínas de arquitectura que promuevan este acercamiento entre las fibras de la cromatina (Fudenberg et al. 2016; Rowley et al. 2017; Rowley and Corces 2018).

A continuación, viene el siguiente nivel de organización que esta dado por los Dominios Topológicamente Asociados (TADs) que representan regiones de los cromosomas que muestran una alta frecuencia de interacción entre las secuencias dentro de este mismo domino y una menor frecuencia con dominios contiguos (Dixon et al. 2012; Sexton et al. 2012). Los TADs se identificaron por medio de ensayos tipo 5C y Hi-C (que son técnicas de captura de conformación cromosómica, a menudo abreviadas como tecnologías 3C o métodos basados en 3C donde se capturan las interacciones entre loci genomicos) (Pope et al. 2014; Rao et al. 2014; Wolff et al. 2020) y su tamaño está en la escala de megabases (Dixon et al. 2012; Nora et al. 2012) (ver Figura 2).

Consecutivamente, dentro del núcleo, se ha descrito cierta preferencia por la organización de la cromatina en compartimentos, estos son mega estructuras clasificadas como compartimento A (una cromatina más abierta) y compartimento B (cromatina más cerrada). Los compartimentos de tipo A se caracterizan por un alto contenido de genes transcripcionalmente activos y correlacionan con marcas activas de histonas que incluyen H3K9ac y H3K27ac, alto contenido de GC, así como hipersensibilidad a la ADNasa I. Por lo tanto, los compartimentos A tienen entorno transcripcional permisivo, aunque genes que se encuentran silenciados también pueden existir en menor medida dentro de estas regiones (Guelen et al. 2008; Giorgetti et al. 2016).

Por otro lado, los compartimentos tipo B se definen por las características opuestas, incluido un alto contenido de genes silenciados y se correlacionan con marcas de histonas represivas como H3K9me2, H3K9me3 y H3K27me3, pobre o nula hipersensibilidad a la ADNasa I y una sincronización tardía de la replicación. Además, como en el caso de compartimentos de tipo A, los compartimentos de tipo B también pueden contener excepciones en términos de genes que son transcripcionalmente activos (Guelen et al. 2008; van Steensel and Belmont 2017). La localización de los compartimentos de cromatina no es aleatoria en el núcleo, y esta distribución preferencial está muy correlacionada con sus características intrínsecas. Los datos de Hi-C han demostrado que los compartimentos A se encuentran preferentemente en la región central del núcleo (Stevens et al. 2017;

Buchwalter, Kaneshiro, and Hetzer 2019). Los compartimentos B se ubican preferentemente en la periferia del núcleo, interactuando con elementos de la lámina nuclear, lo que constituye un entorno predominantemente represivo. Estos resultados están respaldados por estudios de microscopía electrónica que han demostrado que la heterocromatina se localiza preferentemente y agrupada cerca de la lámina nuclear en la mayoría de los tipos de células (Capelson and Hetzer 2009; Stevens et al. 2017; Buchwalter, Kaneshiro, and Hetzer 2019) (ver Figura 2).

Finalmente, los territorios cromosomales representan el mayor nivel de organización de los cromosomas en interfase y fueron observados con hibridaciones in situ, donde se pudo detectar que los cromosomas tienen cierta tendencia a ocupar siempre el mismo espacio dentro del núcleo. Datos experimentales han revelado, que globalmente, las secuencias contenidas en cada cromosoma tienden a interactuar con secuencias ubicadas en el mismo cromosoma, y al mismo tiempo tienden a ser excluidos de secuencias en otros cromosomas. Así, de esta forma, los cromosomas se restringen a locus específicos en lugar de estar esparcidos por el núcleo (Cremer and Cremer 2010; Fritz et al. 2019).

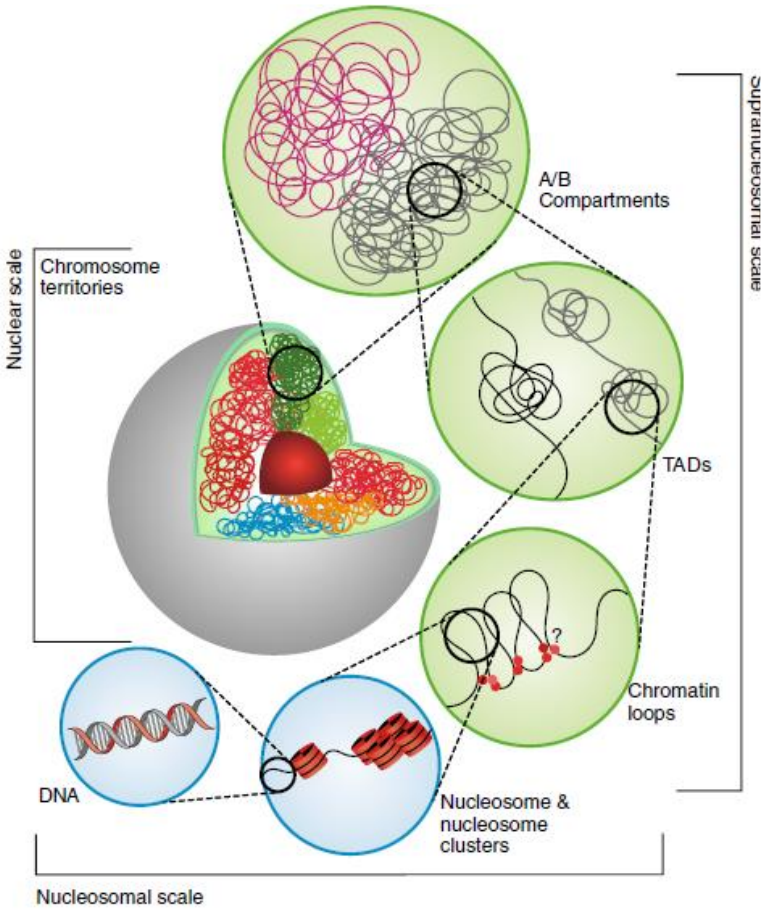

Figura 2. Representación esquemática de los distintos niveles de organización dentro del núcleo (Tomado de Doğan and Liu 2018). Los cromosomas individuales ocupan un subespacio en el núcleo y formas los llamados territorios cromosómales, estos últimos a su vez pueden estar divididos en los compartimentos A y B, que están enriquecidos para

cromatina activa y reprimida, respectivamente. A continuación, se forman regiones genómicas dentro de los TAD que muestran interacciones aumentadas, mientras que las interacciones con regiones fuera de los TAD son bastante limitadas. Un número limitado de asas de cromatina se conectan por medio de elementos reguladores a sus loci objetivo. Finalmente tenemos los "*clutches*" de nucleosomas, el nucleosoma y el ADN que se enrolla en ellos.

1.2 Tipos de cromatina

Antes de que existieran las tecnologías basadas en 3C para el estudio de la estructura 3D del núcleo, en lo que ahora conocemos como nivel de "*clutches*" de nucleosomas, históricamente la cromatina se clasifica en dos tipos: heterocromatina y eucromatina (Richards and Elgin 2002) (Figura 3). La eucromatina es el estado en que la cromatina se encuentra descondensada debido a la baja densidad de nucleosomas proporcionando una composición laxa que permite la entrada de la maquinaria de la transcripción para que esta se lleve a cabo, e incluye la mayoría de los genes transcripcionalmente activos (Piacentini et al. 2009). Por el contrario, la heterocromatina se correlaciona con secuencias compactadas, altamente condensadas, silenciadas y repetitivas que se encuentran cerca de ubicaciones centroméricas y teloméricas (Murzina et al. 1999). A través de la tinción de diferentes tipos de células, Emil Heitz concibió el término "heterocromatina" hace más de 90 años, observando la retención de esta estructura más compacta a lo largo del ciclo celular (Berger 2019). Estas estructuras heterocromáticas se han convertido en un área esencial de estudio debido a su papel en el silenciamiento de genes (Dillon 2004).

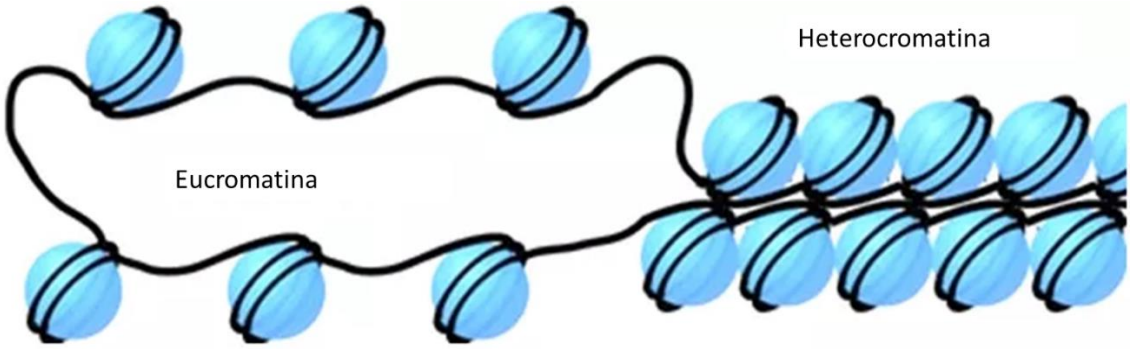

Figura 3. Representación de los tipos de cromatina. La eucromatina tiene una baja densidad de nucleosomas y más abierta para procesos transcripcionales. La heterocromatina se encuentra más compacta en cantidad de nucleosomas (círculos azules).

En los eucariotas, la heterocromatina puede clasificarse como constitutiva, que se encuentra permanentemente compacta, contiene pocos genes y está formada principalmente por secuencias repetitivas localizadas en regiones coincidentes con centrómeros y telómeros. Este tipo de cromatina se encuentra permanentemente silenciada y los genes son rara vez expresados. Con base a criterios citológicos, un tercio del genoma de *Drosophila melanogaster*, incluyendo los telómeros, las regiones pericéntricas y el cromosoma 4, se considera como la heterocromatina (Fanti and Pimpinelli 2008). El

otro tipo de heterocromatina es la facultativa, que puede pasar de un estado compacto a uno más relajado dependiendo de la actividad transcripcional que varía por su condición entre los distintos tipos celulares o en diferentes etapas del desarrollo (Britten and Kohne 1968). En algunos trabajos han encontrado alteraciones de la heterocromatina constitutiva en diversos tipos de cáncer. En particular, se ha observado una disminución de la proteína HP1, que normalmente se localiza en la regiones heterocromáticas de los cromosomas en cáncer de mama y se utiliza como biomarcador para este cáncer (Vad-Nielsen and Nielsen 2015; Zhu et al. 2011; Y.-H. Lee et al. 2015).

La heterocromatina constitutiva se establece temprano en el desarrollo y en el caso de *Drosophila*, comienza en el ciclo 13 del desarrollo embrionario (Armstrong and Duronio 2019; Seller, Cho, and Farrell 2019). El modelo propuesto implica un complejo que contiene una metiltransferasa (Eggless/SetDB1) de la marca H3K9 y la proteína HP1a "*Heterochromatin protein 1*". HP1a es uno de los factores involucrados en la compactación de la cromatina (Joel C. Eissenberg and Elgin 2014) y está compuesta por dos dominios altamente conservados, el cromodominio en la parte N-terminal (CHD) (Grewal and Jia 2007) y un dominio *cromoshadow* en la parte C-terminal (CSD), que están separados por una región *hinge* de longitud variable. La histona H3K9me (di o tri metilada) actúa como un sitio de unión para HP1a, que se une a través de su CHD a estas marcas de cromatina, posiblemente con la participación de otras interacciones estabilizadoras (Bannister et al. 2001; Jacobs and Khorasanizadeh 2002; Lechner et al. 2000). Para promover la condensación, los nucleosomas con esta marca son reconocidos por HP1 y se fortalece la asociación con la metiltransferasa, por ejemplo SUV39H1, que a su vez reconoce las colas de H3 no metiladas cercanas a la lisina 9 a través de su dominio SET, creando nuevos sitios de unión H3K9me para HP1a. Por lo tanto, este sistema de tres componentes podría explicar la propagación y el mantenimiento de silenciamiento de genes heterocromáticos (Fuks et al. 2003; Muramatsu et al. 2016). Esta interacción se conserva tanto en mamíferos como en Drosophila (H. Ito et al. 2012; Schotta et al. 2002; Yamamoto and Sonoda 2003).

Aunado a esto, estudios bioquímicos e *in vivo* de las últimas décadas han implicado que las diversas funciones de la heterocromatina dependen de la capacidad de estas estructuras para propagarse a través de grandes regiones del genoma, para compactar el ADN subyacente, y para reclutar diferentes tipos de actividades. Observaciones recientes han sugerido que la heterocromatina puede poseer propiedades similares a gotas líquidas con una participación importante de HP1 para definir la separación de fases (Larson and Narlikar 2018), donde se ha demostrado que HP1a, tanto de humano como de *Drosophila*, promueve la separación de fase de la heterocromatina de la eucromatina (Larson et al. 2017; Y. C. G. Lee et al. 2020).

Un claro ejemplo de grandes bloques de heterocromatina son los centrómeros, que se definen como loci cromosómicos donde los cinetocoros se ensamblan. La mayoría de los centrómeros eucariotas están compuestos de repeticiones de ADN, mismas que están incrustadas en heterocromatina dependiente de la marca H3K9me. Además, el ADN de estas regiones se encuentra fuertemente metilado en células somáticas de mamíferos. Sin

embargo, los parches de estas repetidas tienen nucleosomas inusuales, ya que la histona canónica H3 es reemplazada por su variante centromérica CENP-A. Estos nucleosomas específicos del centrómero forman la base física para que se una el cinetocoro (McKinley and Cheeseman 2016). Los cromocentros juegan un papel importante en el mantenimiento y estabilidad del genoma a medida que garantizan la baja transcripción de estas repetidas de ADN mientras que aseguran que centrómeros se unan correctamente al cinetocoro y se lleve a cabo la división celular (X. Liu et al. 2020; Corless, Höcker, and Erhardt 2020).

La separación de fases podría entonces representar un estado menos accesible y más reprimido de genes regulados en el desarrollo a medida que las células avanzan a través de la diferenciación. También puede estar asociado con regiones del genoma que tienen heterocromatina constitutiva como los centrómeros. Se especula que, un estado similar al gel formado por heterocromatina con HP1, puede desempeñar un papel estructural parcial, como proporcionar un ancla para el cinetocoro durante la segregación cromosómica (Larson and Narlikar 2018).

Debido a este complejo grado de organización tridimensional y la importancia de la compactación de la cromatina, se sugiere que ésta es una estructura dinámica propensa a la remodelación y reestructuración (Wang, Allis, and Chi 2007), y por lo tanto se requieren de diversas estrategias para que la maquinaria de transcripción pueda identificar sus secuencias blanco y tener acceso a las mismas (Li, Carey, and Workman 2007). Estos cambios, permiten el fácil ingreso y la interacción de los factores de transcripción con la cromatina y por ende permiten que se lleve a cabo el proceso de transcripción. Las distintas estrategias epigenéticas pueden ser modificaciones postraduccionales de histonas, reemplazo de histonas canónicas por variantes de histonas, metilación del ADN, remodelación de cromatina dependiente de ATP y unión de ARN no codificantes. Cada mecanismo ha sido ampliamente estudiado, revelando que están altamente coordinados, interactuando funcionalmente e influyendo entre ellos (Gray 2014; Torres and Fujimori 2015). A continuación, se describirán con mayor profundidad los complejos remodeladores de la cromatina.

1.3 Remodeladores de la cromatina

Los complejos remodeladores de la cromatina son maquinarias multiprotéicas especializadas que permiten el acceso al ADN alterando la estructura, la composición o el posicionamiento de los nucleosomas de manera temporal ya sea por desplazamiento o por remoción de éstos (Cairns et al. 1996). Estos factores determinan la arquitectura de la cromatina ayudando a remodelar los nucleosomas que se encuentran cubriendo regiones promotoras y reguladoras como por ejemplo las llamadas “enhancers” las cuales regulan el inicio de la transcripción de un gen e incrementan los niveles de transcripción respectivamente. Los complejos remodeladores de la cromatina, permiten que se lleve a cabo una regulación en la transcripción, activan o reprimen controlando los distintos estados de la cromatina (entre eucromatina y heterocromatina). Los promotores pueden

encontrarse bajo dos condiciones distintas: abiertos, como ocurre en el caso de los genes constitutivos (se expresan de manera constante) y cubiertos, como ocurre en los genes altamente regulados (solo se expresan bajo condiciones adecuadas, por ejemplo, en algún momento del desarrollo y en tejidos específicos) (Cairns 2009).

Los complejos remodeladores de la cromatina requieren de la hidrólisis de ATP para cumplir sus funciones de remodelación. Es por ello por lo que todos los complejos remodeladores poseen una subunidad con un dominio de ATPasa altamente conservado (Saha, Wittmeyer, and Cairns 2006). Por lo general estos han sido clasificados de acuerdo con sus funciones principales, el grado de conservación que existe entre sus dominios de ATPasa y de acuerdo con la presencia de otros dominios cerca de la región C-terminal que actúan como sitios blancos o de regulación para la interacción y el reconocimiento del ADN (Saha, Wittmeyer, and Cairns 2006).

Existen al menos 4 familias de remodeladores de la cromatina reportados en mamíferos y se encuentran conservados en la evolución: NURD/Mi-2/CHD, INO80, ISWI y SWI/SNF2, (Saha, Wittmeyer, and Cairns 2006). A continuación, se describen algunas características de ellas (Figura 4):

- Familia NURD/Mi-2/CHD ("Chromodomain-Helicase-DNA binding"), al igual que otras familias de complejos remodeladores, el complejo NuRD tiene funciones importantes en procesos como la transcripción, el ensamblaje de cromatina, la progresión del ciclo celular y la estabilidad genómica (Clapier et al. 2016); pero también en la represión de la transcripción y el silenciamiento regulado de ciertos genes (Saha, Wittmeyer, and Cairns 2006). Fue descrito por primera vez en *X. laevis* (Marfella and Imbalzano 2007).

- Familia INO80 ("Inositol requiring 80"), participa en procesos de reparación, transcripción del ADN y recombinación homóloga. Fue purificado y caracterizado por primera vez en *Saccharomyces cerevisiae*. (Saha, Wittmeyer, and Cairns 2006; Clapier and Cairns 2009; Kusch, Mei, and Nguyen 2014). INO80 se transloca a lo largo del ADN y promueve el intercambio del dímero H2A.Z-H2B de manera más eficiente que H2A-H2B (Brahma et al. 2017).

- Familia ISWI ("Imitation switch") la cual ayuda a conducir el ensamblaje y la organización de la cromatina (Längst et al. 1999; T. Ito et al. 1997), manteniendo el espaciamiento convencional de los cromosomas. Actúan sobre nucleosomas no acetilados confinando su actividad a nucleosomas en regiones transcripcionalmente inactivas (Corona et al. 2002). Fue descrito por primera vez en *D. melanogaster* (Tsukiyama et al. 1995; T. Ito et al. 1997; Varga-Weisz et al. 1997).

- Familia SWI/SNF2 ("Switch defective/sucrose nonfermenting") brinda acceso al ADN por medio del desplazamiento de nucleosomas (Whitehouse et al. 1999) o por la liberación de los mismos (Lorch and Kornberg 2017). Su función generalmente se

encuentra correlacionada a la movilización de los nucleosomas y a la activación transcripcional (Clapier et al. 2016). Fue descrita por primera vez en *S. cerevisiae* y esta familia se caracteriza por un dominio DExx / helicasa separado en dos por una inserción corta (Rein Aasland, Stewart, and Gibson 1996; Boyer et al. 2002; Tsukiyama et al. 1995)

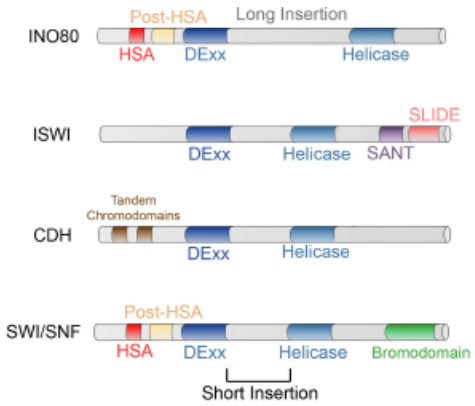

Figura 4. Representación de las cuatro familias principales de remodeladores de la cromatina (Tomado de Magaña-Acosta and Valadez-Graham 2020). Se muestran las principales características y dominios de las familias INO80, ISWI, CHD y SWI/SNF2.

En humanos, en algunas ocasiones, la desregulación o las mutaciones relacionados con los factores que se encuentran involucrados en la estructuración de la cromatina, como los complejos remodeladores de la cromatina, son causas de diversas enfermedades y síndromes como lo es el caso de la proteína ATRX que es un remodelador de la cromatina miembro de la familia SWI/SNF2 (Drané et al. 2010; Goldberg et al. 2010; Peter W. Lewis et al. 2010) que se describirá a continuación.

1.4 ATRX

El gen hATRX de humanos que fue descrito en 1995 (Gibbons et al. 1995). Mutaciones en hATRX ("Alpha-Thalassemia mental Retardation syndrome X- related") se asocian con un síndrome ligado al cromosoma X que incluye una serie de fenotipos como retraso mental de moderado a severo, fallas psicomotoras, α-talasemia, anormalidades urogenitales, microcefalia, entre otras (Garrick et al. 2004).

El gen hATRX se encuentra en la posición Xq13.1-q21.1, por lo que la mayor parte de los individuos afectados son hombres (Gibbons et al. 1995). El gen hATRX comprende aproximadamente 300 kb de ADN genómico (Gibbons et al. 1995) y consta de 36 exones (Picketts et al. 1996) que codifican al menos dos transcritos que dan lugar a dos proteínas ligeramente distintas: una de 280 kDa que se localiza preferencialmente en heterocromatina y en los cuerpos PML, los cuales están compuestos principalmente por material proteico no cromático. Esta isoforma puede unirse a las proteínas Daxx ("Death domain associated protein") y MeCP2 ("Methyl CpG binding protein 2")(ver Figura 5). Además, se produce otro transcrito por "splicing" diferencial en donde el intrón 11 es

retenido generando un codón de terminación. Este transcrito da origen a otra isoforma proteica llamada ATRXt de aproximadamente 180 kDa (Garrick et al. 2004). El resultado es un péptido que conserva el dominio ADD pero carece de la parte C-terminal donde se encuentra el dominio ATPasa/Helicasa y pierde la unión a las proteínas Daxx, MeCP2 y la localización en los cuerpos PML aunque se ha visto que se sigue asociando a heterocromatina (Garrick et al. 2004).

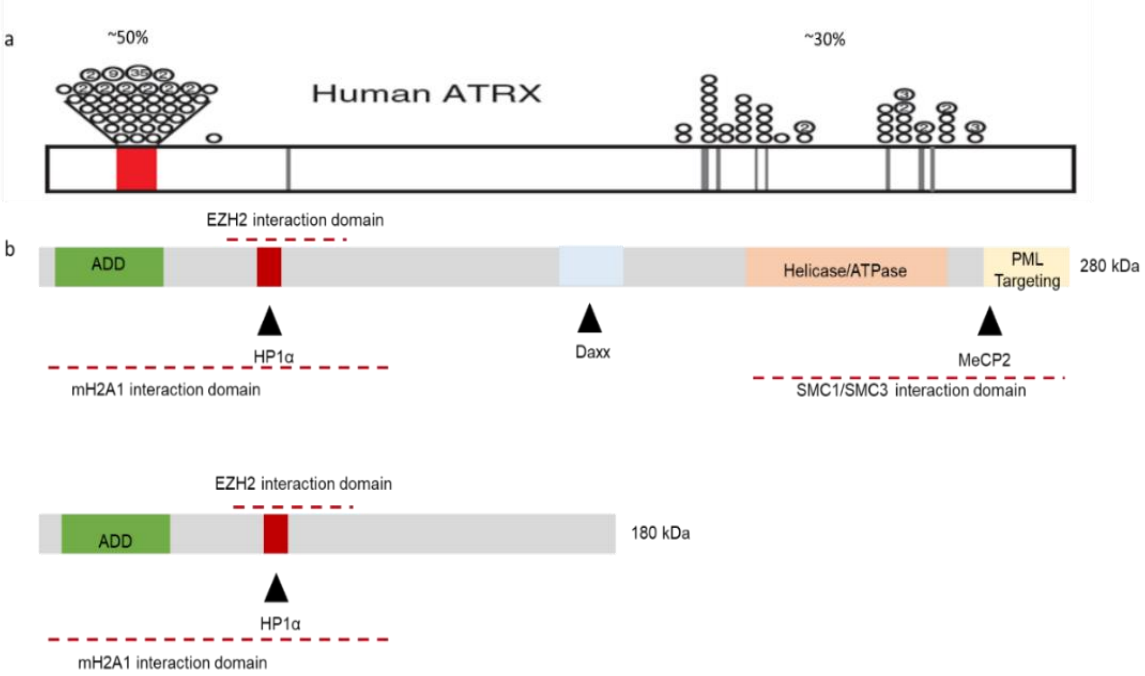

Figura 5. Las dos isoformas de ATRX y las mutaciones en el gen descritas. a) Distintas mutaciones hasta la fecha descritas en la proteína ATRX sobre los dominios ADD (~50%) y Helicasa/ATPasa (~30%) (Modificado de Eustermann et al. 2011). b) La isoforma de la proteína ATRX (280KDa) con sus dominios y sitios de interacción con distintas proteínas y la isoforma alternativa ATRXt (180 kDa) (Modificado de Dyer et al. 2017).

Los individuos con el síndrome ATRX tienen diversas mutaciones en diferentes sitios atraves del cuerpo del gen (ver Figura 5a), lo que ocasiona cambios en los aminoácidos conservando el marco de lectura, productos truncados o deleciones (Garrick et al. 2004). Estas mutaciones por lo general dan lugar a un cambio en la funcionalidad de la proteína y en su mayoría afectan los principales dominios conservados a lo largo de la evolución.

Uno de los principales dominios es del tipo ATPasa-helicasa localizado en el carboxilo terminal de la proteína, este dominio la clasifica como miembro de la familia SWI/SNF2 de remodeladores de la cromatina (Xue et al. 2003) y es capaz de deslizar y reposicionar nucleosomas (Clapier and Cairns 2009), cerca del 30% de las mutaciones descritas hasta la fecha afectan este dominio (Eustermann et al. 2011).El otro dominio se encuentra en la porción amino y está compuesto por un dedo de zinc del tipo PHD (“Plant homeo-domain”) y un dedo de zinc del tipo GATA (A. Argentaro et al. 2007). Esta organización de dedos de

zinc está presente únicamente en las ADN metil-transferasas DNMT3-DNMT3L y por lo tanto es conocido como ADD (**A**TRX-**D**NMT3-**D**NMT3L). Aproximadamente el 50% de las mutaciones que producen la enfermedad afectan este dominio (Anthony Argentaro et al. 2007).

Se ha propuesto que el dominio ADD podría estar involucrado en el reconocimiento de distintas modificaciones postraduccionales de las histonas e incluso se ha demostrado que puede unirse a ellas, en particular con la combinatoria de H3K9me3 y H3K4me0 (Dhayalan et al. 2011). Por otro lado, el dominio ADD de las proteínas DNMT reconoce solo la ausencia de metilación de H3K4, el dominio ADD de ATRX es único ya que tiene la capacidad de reconocer H3K9me3 junto con H3K4me0, uniéndose más eficientemente a histonas que contienen esta combinación de marcas (Iwase et al. 2011; Eustermann et al. 2011; Dhayalan et al. 2011).

Eustermann et al., (2011) realizaron experimentos en células de ratón donde vieron que esta combinación de marcas es necesaria para la localización de ATRX en la heterocromatina pericentromérica, donde este reclutamiento se ve aumentado por la interacción con HP1α que también reconoce la marca de H3K9me3.

También se ha propuesto que hATRX tiene un papel en la represión transcripcional o que participa en la formación de la heterocromatina debido a que mediante ensayos de inmunolocalización, la forma larga de la proteína interacciona físicamente y co-localiza con la proteína HP1α la cual se asocia a regiones heterocromáticas y es una proteína represora de la transcripción y tiene una participación importante en el mantenimiento de la heterocromatina (McDowell et al. 1999).

Durante la mitosis en *Drosophila*, la quinasa Aurora B fosforila H3 en su posición serina 10, este mecanismo se ha visto que desplaza a HP1a y quizás a otras proteínas de la heterocromatina mitótica (Hirota et al. 2005; Williams et al. 2019). Entonces, el cromodominio de HP1 no es capaz de unirse a la a marca de H3K9me3 si la serina se encuentra fosforilada, mientras que el dominio ADD si puede continuar unido a pesar de la fosforilación y entonces ATRX es una de las pocas proteínas que continua unida a la cromatina durante la mitosis, probablemente funcionando como marcador en la cromatina (Hendzel et al. 1997a; Bérubé, Smeenk, and Picketts 2000).

hATRX también interacciona con un miembro de la familia *Polycomb* EZH2, involucrado en el silenciamiento de genes durante el desarrollo (Cardoso et al. 1998). También se ha descrito que hATRX se une a elementos repetidos y es necesario para la formación de heterocromatina constitutiva (Sadic et al. 2015).

Por otra parte, en la región C-terminal ATRX presenta siete dominios colineales conservados, típicamente encontrados en la familia SNF2 (SWI/SNF2) de proteínas asociadas a complejos remodeladores de la cromatina que le confiere actividad de ATPasa (Gibbons et al. 1995). Miembros de la familia SNF2 se encuentran en grandes complejos

proteicos donde emplean la energía derivada de la hidrólisis de ATP para modular el contacto histonas-ADN (Bérubé 2011).

La caracterización bioquímica ha mostrado que ATRX en conjunto con la proteína DAXX exhibe una actividad de ATPasa que se ve estimulada por la presencia de ADN y de nucleosomas (Tang et al. 2004) y por estudios in vitro se observó una actividad de translocasa en el ADN (Xue et al. 2003); es decir, que son capaces de desplazarse cortas distancias por el ADN o de desplazar el ADN. Dicho desplazamiento crea una torsión que se traduce en superenrollamiento del ADN y por lo tanto se sugiere que ATRX puede interrumpir la interacción ADN-histona, pero no altera el posicionamiento de los nucleosomas (Xue et al. 2003) y esta actividad es esencial para el intercambio de la H3.3 junto con DAXX (Peter W. Lewis et al. 2010)

Durante mi proyecto de maestría realicé un dendograma utilizando el programa PhyML con 12 organismos modelos para observar la relación de la proteína ATRX entre ellos. Se pueden observar dos grupos principalmente, los vertebrados y los invertebrados junto con Arabidopsis (que si presenta el dominio ADD). Los vertebrados mantienen una alta conservación de los aminoácidos en ambos dominios de la proteína y los organismos invertebrados presentan el dominio Helicasa/ATPasa pero carecen del dominio ADD (López-Falcón et al. 2014). Asimismo, realicé un esquema comparativo entre los dominios de la proteína ATRX en los mismos 12 organismos, donde podemos observar el dominio ADD en verde, el SNF2 en naranja, la Helicasa/ATPasa en amarillo y la posición de los aminoácidos dentro de la proteína. Los vertebrados conservan ambos dominios mientras que en los invertebrados se ve la ausencia del dominio ADD en la región N-terminal de la proteína (Figura 6).

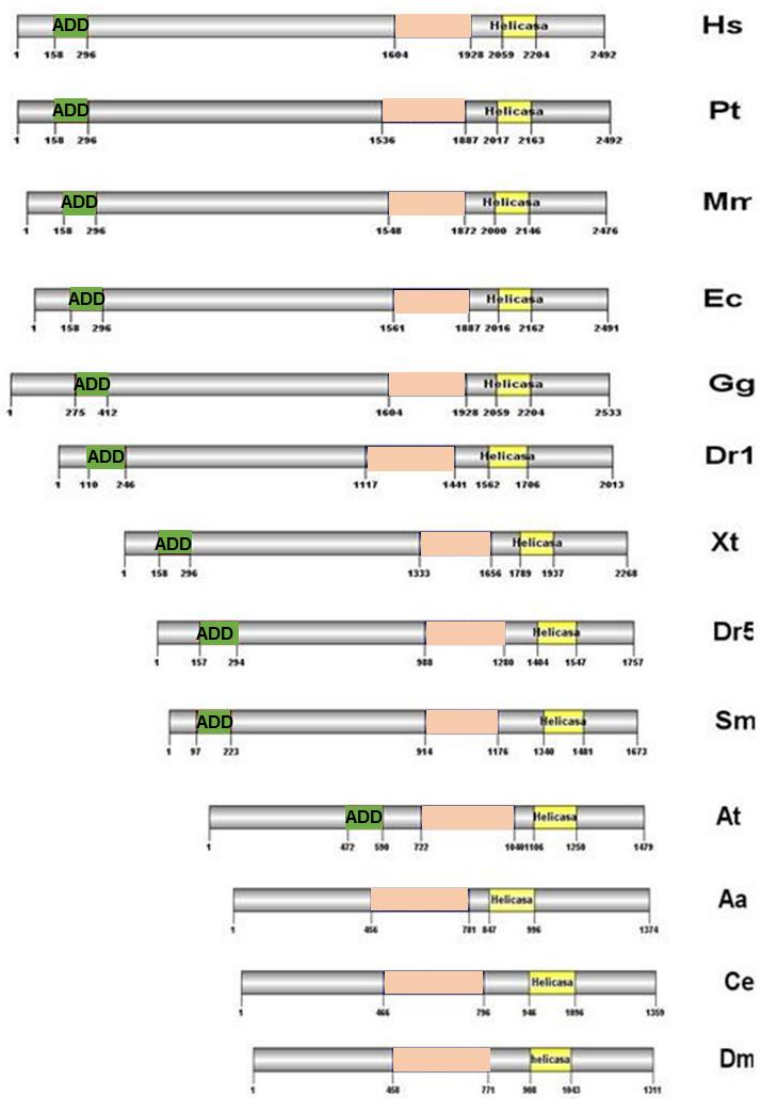

Figura 6. Conservación de los dominios ADD (verde), SNF2 (naranja) y Helicasa (amarillo) de ATRX en los distintos organismos. Dr1 y 5: *Danio rerio* , Gg: *Gallus gallus*, Pt: *Pan troglodytes*, Hs: *Homo sapiens*, Ec*: Equus ferus caballus*, Mm: *Mus musculus*, Xt: *Xenopus tropicalis*, Sm: *Schistosoma mansoni*, Dm: *Drosophila melanogaster*, Aa: *Anopheles*, Ce: C*aenorhabditis elegans*, At: *Arabidopsis thaliana*.

hATRX se encontró en regiones teloméricas co-localizando con la variante de histona H3.3 y se observó como regulador clave de la cromatina telomérica (Wong et al. 2010). Se encontró que hATRX es esencial para incorporar a H3.3 y participa en la unión de HP1α a los telómeros, por lo que se sugiere que estas proteínas pueden actuar para lograr un equilibrio en el estado de condensación de la cromatina que permite la renovación de los telómeros, pero sin perder su estructura compacta para mantener estas regiones heterocromáticas (P. W. Lewis et al. 2010).

Otro descubrimiento fue realizado por Law et. al., (2010) donde observa que hATRX se une a secuencias en tándem tanto en los telómeros como en la eucromatina. Muchas de estas secuencias repetidas pueden formar in vitro una estructura en el ADN que es llamada cuádruple hélice (G-cuádruplex) y que hATRX se une a estas estructuras donde puede jugar un papel importante. En células de pacientes con mutaciones en hATRX, los genes asociados a estas secuencias repetidas se desregulan ocasionando los variados fenotipos que se presentan en pacientes con el Síndrome, uno de estos genes es el de la alfa-globina, lo que apoya su papel en la regulación transcripcional de este gen (Law et al. 2010).

A pesar de que ATRX es una proteína muy conservada a lo largo de la evolución, en análisis previos realizados en el laboratorio observamos una clara separación de los organismos vertebrados e invertebrados (Figura 7), donde los vertebrados mantienen una alta conservación de los aminoácidos en ambos dominios de la proteína y los invertebrados por su parte presentan únicamente el dominio Helicasa/ATPasa, pero carecen del dominio ADD. Anteriormente se habían reportado posibles ortólogos de esta proteína en *Drosophila melanogaster* o *Caenorhabditis elegans* carentes del dominio ADD (Argentaro et al., 2007). Cuando realizamos análisis a mayor detalle observamos que en la clase Insecta, por medio de un evento de fisión, estos dominios quedaron separados y ahora cada uno es codificado por un gen diferente (López-Falcón et al., 2014).

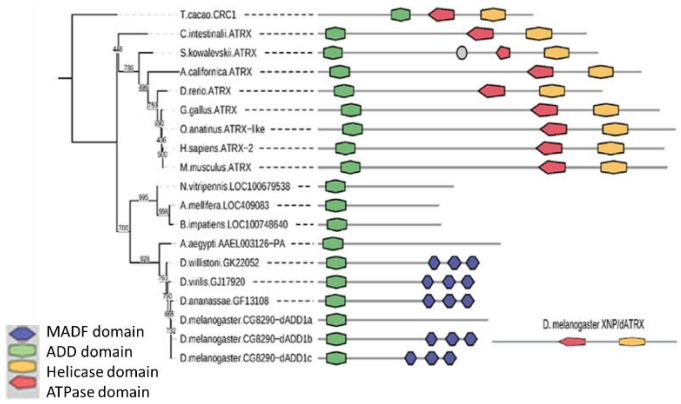

Figura 7. Análisis filogenético del dominio ADD. La proteína ATRX se encuentra completa en plantas y vertebrados, pero parece que sufrió un evento de fisión durante la evolución de los insectos. El dominio ADD (verde) y el dominio Helicasa/SNF2 (amarillo/rojo). Las proteínas homologas para el dominio ADD en el género de *Drosophila* adquirieron dominios MADF (azul), es probable que este dominio sea funcional dada su conservación dentro del género. *Theobroma cacao* (arbol de cacao), *Ciona intestinalis* (urocordado*), Saccoglossus kowalevskii* (gusano), *Artemisia californica* (arbusto), *Danio rerio* (pez cebra), *Gallus gallus* (gallo), *Ornithorhynchus anatinus* (ornitorrinco), *Homo sapiens* (humano), *Mus musculus* (ratón), *Nasonia vitripennis* (avispa), *Apis mellifera* (abeja), *Bombus impatiens* (abejorro), *Aedes aegypti* (mosquito), *Drosophila willistoni, Drosophila vinilis, Drosophila ananassae, Drosophila melanogaster* (mosca de la fruta).

2.- ANTECEDENTES

En *D. melanogaster* se ha reportado que existe un posible gen homólogo a hATRX, (dXnp) que codifica dos isoformas proteicas de distinto peso molecular. Una isoforma larga llamada dXnp-L de 148 kDa y una corta llamada dXnp-S, que se genera por un sitio alterno de la traducción, de 110 kDa (Bassett et al. 2008). La isoforma larga presenta un 48% de identidad y un 66% de similitud en aminoácidos con hATRX. Ambas isoformas comparten la región C-terminal Helicasa/ATPasa con la proteína humana, sin embargo, ninguna posee en su región N-terminal el dominio ADD (N. G. Lee et al. 2007) lo cual la hace una diferencia interesante entre la proteína de humano y la de mosca. Se sabe que dXnp-L se encuentra localizada en heterocromatina pericentromérica y que al igual que hATRX interacciona físicamente con HP1α y se han colocalizado juntas en cromosomas politénicos (Bassett et al. 2008).

Por otra parte, Schneiderman et. al., (2009) mediante inmuno-histoquímica, observaron co-localización entre dXNP y la ARN Polimerasa II en la etapa de elongación del ARN en algunos lugares, lo que implica que la proteína está presente en zonas de eucromatina. Al igual que en los humanos, existen datos que indican que en *Drosophila* ATRX también co-localiza con H3.3 en sitios de intercambio de nucleosomas y en regiones de heterocromatina en el cromosoma X (Schneiderman et al. 2009). En nuestro laboratorio mediante un ensayo de doble híbrido, se encontró que dXNP-L interacciona con el factor de transcripción DREF que tiene una secuencia de unión consenso al ADN y funciona como un regulador positivo de la transcripción, particularmente de genes involucrados en la proliferación celular. Mediante ensayos in vivo e in vitro se determinó que DREF es capaz de unirse a la secuencia promotora del gen pannier *(pnr),* un gen importante en diversos procesos del desarrollo de la mosca, y activar su transcripción, y que dXNP es reclutado por DREF para reprimir la transcripción de pnr cuando este gen ya no necesita ser expresado (Valadez-Graham et al. 2012).

Aunque dXNP se observa en ambos procesos, tanto transcripción activa como represión, se sugiere que está más involucrada en el silenciamiento de genes y su reclutamiento a heterocromatina (Bassett et al. 2008; Emelyanov et al. 2010). A pesar de todos estos avances en el conocimiento de dXNP, se desconoce el papel exacto que juega en la regulación de la transcripción. Nuestro grupo y el grupo de la Dra. Kuroda identificamos al ortólogo del dominio ADD en la mosca el cual está codificado por un gen al que se nombró *dadd1* (Brenda López-Falcón et al. 2014; Alekseyenko et al. 2014). Nuestro grupo realizó un análisis *in silico* donde se encontró el gen, "*CG8290",* el cual codifica para tres isoformas que contienen el dominio ADD. Por medio de la técnica de RT-PCR encontramos los tres transcritos provenientes del gen *dadd1*. Una de las isoformas nombrada dAdd1-a tiene un peso reportado de 130 kDa. La segunda isoforma tiene un peso reportado de 127 kDa, y fue nombrada dAdd1-b y tiene tres dominios MADF (myb/SANT-like domain in Adf-1) (Bhaskar and Courey, 2002) que son una subfamilia de los dominios SANT (nombrado por: Switching-defective protein 3 (Swi3), adaptor 2 (Ada2), nuclear receptor co-repressor (N-CoR) and transcription factor (TF)IIIB) (R Aasland and Stewart 1995). Los dominios SANT tienen un papel clave en el reconocimiento de las colas de las histonas, principalmente en aquellas

que no poseen modificaciones (Boyer et al. 2002; Yu et al. 2003) y al parecer se ha encontrado que reconocen secuencias consenso en el ADN. Por el punto isoeléctrico teórico los dominios SANT de dAdd1-b reconocerían al ADN. La tercera isoforma llamada dAdd1-c tiene dividido el exón tres produciendo un nuevo intrón. Este transcrito se encuentra representado a lo largo de todo el desarrollo y genera una proteína de 112 kDa de peso como se muestra en la figura 8 (López-Falcón *et al,* 2014).

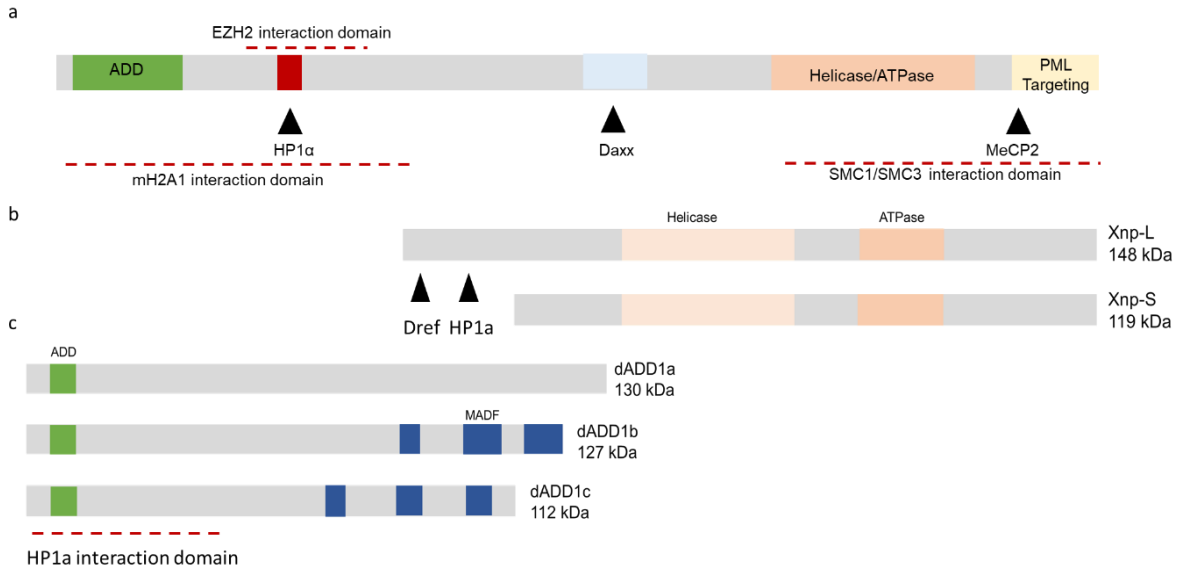

Figura 8. La proteína ATRX en humanos y en *Drosophila*. a) La isoforma de la proteína ATRX de mamíferos (280KDa) con sus dominios (ADD en verde y Helicasa/ATPasa en naranja) y sitios de interacción con distintas proteínas (Modificado de Dyer et al. 2017). b) En *Drosophila*, dXNP codifica para dos isoformas proteicas que contienen el dominio Helicasa/ATPasa (naranja) de distinto peso molecular: Xnp-L la isoforma larga de 148 kDa que interacciona físicamente y colocaliza con la proteína HP1-a, y Xnp-S la isoforma corta de 110 kDa (Modificado de Bassett et al. 2008; Valadez-Graham et al. 2012). c) El gen dADD1 codifica para 3 isoformas proteícas de distinto peso molecular que contienen el dominio ADD (verde) y 2 isoformas además presentan dominios tipos MADF (azul marino) (Modificado de Alekseyenko et al. 2014; López-Falcón et al. 2014).

Durante mi trabajo de investigación en la maestría determinamos que dAdd1 es el ortólogo del dominio ADD de ATRX de humanos, tiene una alta homología en secuencia y en estructura 3D, demostramos por medio de pull-down y CoIP que interaccionan físicamente con dXnp y HP1a, además de co-localizar en el cromocentro, y se confirmó por análisis de ChIP que las proteínas dAdd1 están presentes en regiones de heterocromatina. Además, demostramos una interacción genética, las moscas que llevan combinaciones transheterocigóticas de alelos mutantes de *dadd1* y *dxnp* son semi-viables y presentan la aparición de masas melanóticas (Basset et al 2008). Finalmente se encontró que estas proteínas tienen un papel en el mantenimiento de la heterocromatina.

Posteriormente en el laboratorio, se descubrió que las mutaciones en los genes que codifican las proteínas dXNP y dAdd1 afectan la estabilidad cromosómica, causando aberraciones cromosómicas, incluidos defectos teloméricos, similares a los observados en mutantes de *Su(var)205* (el gen que codifica para HP1a). En células somáticas, se observó que dXNP y dAdd1 participan en el silenciamiento de retrotransposones HTT teloméricos. Además, la falta de dAdd1 da como resultado la pérdida de HP1a de las regiones teloméricas y las mutaciones de pérdida de función de dXNP también afectan la localización de HP1a, pero no en todos los telómeros, lo que sugiere un papel especializado para las proteínas dAdd1 y dXNP en la localización de HP1a en los extremos de los cromosomas. Estos resultados colocan a dAdd1 como un regulador esencial de la localización y función de HP1a en el dominio heterocromático de los telómeros (Chavez et al. 2017).

Conservar los niveles correctos de estas proteínas resulta importante para mantener la estabilidad del genoma, perder a las proteínas dAdd1 y a dXNP tiene efectos en la localización de HP1a y estos efectos se observaron en los telómeros, sin embargo, condiciones en donde se sobreexpresaran estas proteínas hasta el momento no habían sido evaluadas. Adicionalmente, previamente las investigaciones del laboratorio se enfocaron en los telómeros, pero un área severamente afectada también son los centrómeros. Por lo tanto, en este trabajo se propuso examinar con mayor profundidad la organización de esta zona heterocromática tan abundante llamada cromocentro, y los efectos transcripcionales que se producen en respuesta a cambios en la cantidad de las proteínas dAdd1 y dXNP.

3.- HIPÓTESIS

Fallas en el mantenimiento de la heterocromatina pericéntrica afectarán la correcta expresión de ciertos genes embebidos en dicha región. Por lo que variaciones en la concentración de expresión de Add1 afectarán la estructura de la heterocromatina.

4.- OBJETIVOS

4.1.- Objetivo general

- Determinar el papel de las proteínas dAdd1 en el mantenimiento de la estructura de la cromatina.

4.2.- Objetivos particulares

1. Determinar si la modificación de los niveles basales de las proteínas dAdd1 afectan la estructura de la cromatina.

2. Examinar la localización subcelular de la proteína HP1a en condiciones donde se sobreexpresan todas y las diferentes isoformas de dADD1 de manera individual.

3. Evaluar la presencia de marcas heterocromáticas en las histonas y su posible modificación en respuesta a los cambios niveles de las proteínas dADD1.

4. Analizar si los cambios en la expresión de las proteínas dADD1 inducen cambios en la abundancia de genes localizados en regiones heterocromáticas.

5. MATERIALES Y MÉTODOS

- Cepas de moscas

La línea "white" se usó como cepa silvestre (w^{1118}). Todas las cepas se mantuvieron en comida estándar a 25 °C (para 1 litro de medio: 100 gramos de levadura, 100 gramos de azúcar de caña sin refinar, 16 gramos de agar, 10 ml de ácido propiónico y 14 gramos de gelatina. Se disolvieron todos los ingredientes excepto la levadura en 800 ml de agua del grifo y luego disuelva la levadura. Autoclave inmediatamente durante 30 minutos. Posteriormente, dejar enfriar el medio a 60° C y agregar ácido propiónico, concentración final 0.01%, dejar reposar la botella hasta que se forme una gelatina). Las cepas transgenicas se cruzaron con la línea w^{1118}*; Sp/CyO; TM6B,* Tb^{1}*/MKRS* para balancear y tener todas en el mismo fondo genético. Para realizar las cruzas se empleó una temperatura de 28°C (ver tabla 1).

Tabla 1. Cepas de moscas empleadas

Stock	**Lugar del que proviene**	**Finalidad**
UAS-dADD1	Kyoto ID 200280	sobreexpresión de todas las isoformas de dADD1
Tub-GAL4	BL ID 5138	"Driver" para inducir la expresión en todo el organismo
Act5C-GAL4	BL ID 4414	"Driver" para inducir la expresión en todo el organismo
Sgs3-GAL4	BL ID 6870	"Driver" para inducir la expresión en glándulas salivares de larva de tercer instar
dadd1²	Donado del laboratorio Dr. Mitzi Kuroda	Es una línea a la cual se le removió el gen por lo cual carece de la función de dADD1

UAS-XNP	BL ID 26645	Promueve la sobreexpresión de todas las isoformas de XNP usando el sistema Gal4
Xnp^2	BL ID 26643	Alelo hipomorfo que se realizó con un transposón con el cual se eliminó la parte del promotor del gen XNP y disminuye la cantidad de ARNm producido
Xnp^3	BL ID 26644	Alelo hipomorfo que se realizó con un transposón con el cual se elimina el codón de inicio XNP y los primeros 105 aminoácidos de la región codificante
His2Av-RFP	BL ID 23651	Mosca transgénica fluorescente que se usó para revisar el contenido de cromatina en los distintos fondos genéticos

- Generación de moscas transgénicas para sobreexpresar ADN de dos isoformas de dADD1

Para generar las moscas transgénicas que sobreexpresan las isoformas *dadd1-a* y *dadd1-b*, se tomó el cDNA que codifica para dichas isofromas y fue subclonado en el vector pUAST que contiene cinco secuencias UAS. Se llevaron a cabo una serie de digestiones para la construcción de los vectores; el vector de donde se obtuvo el fragmento de "dadd1-a" fue el pAc5.1/V5-HisdAdda-Flag en el cual previamente se había insertado el fragmento dAdd1 de 3612 pb digerido con EcoRI y NotI. Entonces el fragmento se extrajo digiriendo con las mismas enzimas de restricción (Roche) para obtener un fragmento de 3612 pb. Simultáneamente, el vector pUAST se digirió con NotI y EcoRI (Figura 9).

El vector que contiene el fragmento de "dadd1-b" fue el pAc5.1/V5-HisdAddb-Flag donde se insertó el fragmento de dAdd1-b por medio de PCR insertando un sitio EcoRV con el oligo forward. La inserción de este nuevo sitio de corte fue muy importante ya que el fragmento que codifica para dAdd1-b contiene un sitio EcoRI que lo fragmentaría a la mitad. Entonces se decidió realizar la clonación del fragmento con las enzimas de restricción Not1 y EcoRV (Roche) para obtener un fragmento de 3378 pb. El vector pUAST se digirió con EcoRI y posteriormente fue recortado con la enzima "*Mung Bean nuclease*" (Roche) para generar

extremos romos para poder insertar el fragmento que proviene de la digestión con EcoRV. Después se digirió con NotI para generar el otro extremo y poder tener una clonación direccional (Figura 9).

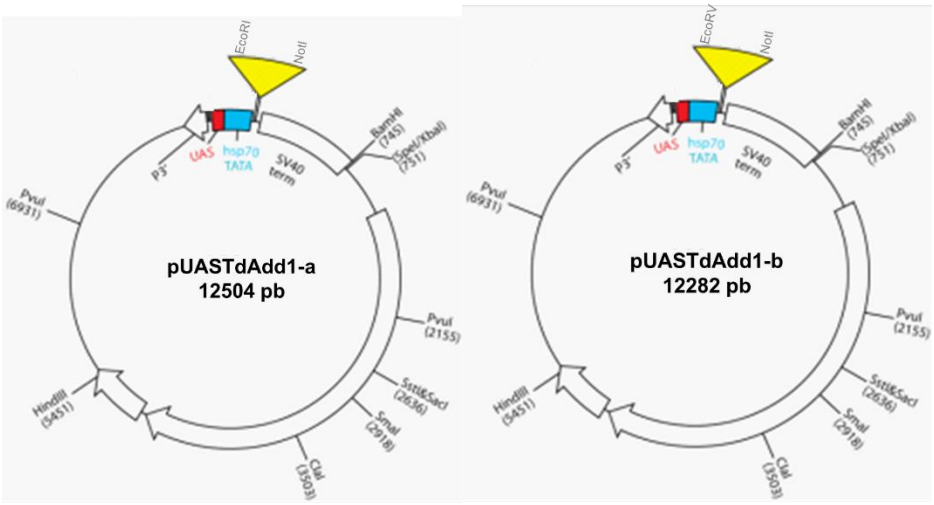

Figura 9. Esquema del vector pUAST con los respectivos insertos que contienen aAdd1-a o dAdd1-b. En este vector se ligaron los fragmentos obtenidos de los vectores pAc5.1/V5-his y estas construcciones fueron las que se mandaron microinyectar para generar las moscas transgénicas.

Se decidió empezar con estas dos isoformas debido a que ya se cuenta con el cDNA completo de estas dos isoformas clonado en vectores de expresión pAc5.1/V5-his con resistencia a ampicilina (ver Figura 9) proporcionados por Dra. Brenda López Falcón además que las isoformas b y c son muy parecidas y solo difieren en un exón en la parte media (B. López-Falcón et al. 2014), con lo cual podemos discernir de sus posibles funciones empezando con las isoformas a y b. Una vez obtenidas las construcciones deseadas se realizaron midipreps empleando kit de QUIAGEN (QIAprep cat no 27106) para obtener la cantidad necesaria de ADN para mandar microinyectar embriones de *Drosophila*.

La microinyección de los plásmidos con los respectivos fragmentos de cada isoforma se llevó a cabo por la compañía Best Gene (https://www.thebestgene.com/). Consistió en microinyección de embriones de la línea w^{118}/w^{118} antes de la formación de las células polares ya que estas células darán origen a la línea germinal y es necesario inyectar antes de este momento para poder heredar la construcción. La microinyección se llevó a cabo con los plásmidos pUAST que contiene cinco secuencias de levadura UAS ("Upstream Activator Sequences") inducibles por Gal4 también de levadura. Es un sistema ventajoso que permite el control temporal y espacial de la expresión de genes ectópicos que fue propuesto en 1993 por Brand y Perrimon (Brand and Perrimon 1993). Es un sistema de dos componentes, uno de ellos es la proteína GAL4, que es un factor transcripcional endógeno de levaduras y no presenta homólogos en Drosophila. El segundo componente son las secuencias UAS a las cuales se une GAL4 para activar la transcripción de genes en *Drosophila* que se encuentran río abajo de la misma (Fischer, J.A., Giniger, E., Maniatis, T.&Ptashne 1988) (Figura 10).

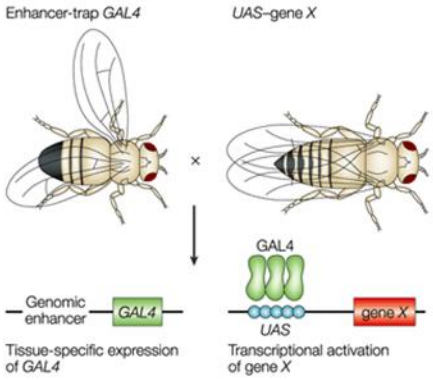

Figura 10. El sistema UAS-GAL4 se puede usar como regulador de la expresión de genes en *Drosophila*. Esquema el cual ejemplifica como se lleva a cabo la activación específica de un gen haciendo uso del sistema UAS-Gal4. Uno de los individuos posee únicamente la secuencia activadora Gal4 y el otro posee solamente la secuencia UAS. Esto permite asegurarnos que en toda la progenie de la F1 se active o inactive nuestro gen de interés (gene X) (Tomado de St Johnston 2002).

En la tabla 2 se muestra la lista con la descripción de las transgénicas que se obtuvieron para la construcción que contiene *dadd1-a.*

Tabla 2. Líneas transformadas con la construcción pUASTdadd1-a.

Número de vial	**Etiqueta**	**Localización (cromosoma)**
1	16710-1-1M	3
2	16710-1-2M	3
3	16710-1-3M	2
4	16710-1-4M	3
5	16710-1-5M	3
6	16710-1-6M	3
7	16710-1-7M	3
8	16710-1-8M	3
9	16710-1-9M	2

En la tabla 3 se muestra una lista con la descripción de las moscas transgénicas que se obtuvieron para la construcción que contiene *dadd1-b.*

Tabla 3. Líneas transformadas con la construcción pUASTdadd1-b.

Número de vial	Etiqueta	Localización (cromosoma)
1	16710-2-1M	2
2	16710-2-2M	3
3	16710-2-3M	3
4	16710-2-4M	3
5	16710-2-5M	3
6	16710-2-6M	2

Con el objetivo de poder inducir la expresión de las isoformas de dADD1, las líneas transgénicas se establecieron cruzándolas con la mosca "balancer" *w*^{1118}*; Sp/CyO; TM6B, Tb1/MKRS* y así tener todas con el mismo fondo genético para no perder la inserción de las isoformas. Posteriormente, se realizaron cruzas con el "driver" Sgs-Gal4 (glándula salival) y se extrajo en ARN total de las glándulas salivales (siguiendo las instrucciones del proveedor Trizol Invitrogen) para analizar con oligos específicos si se estaban sobreexpresando las isoformas de manera individual sin afectar la expresión de las otras (Figura 11).

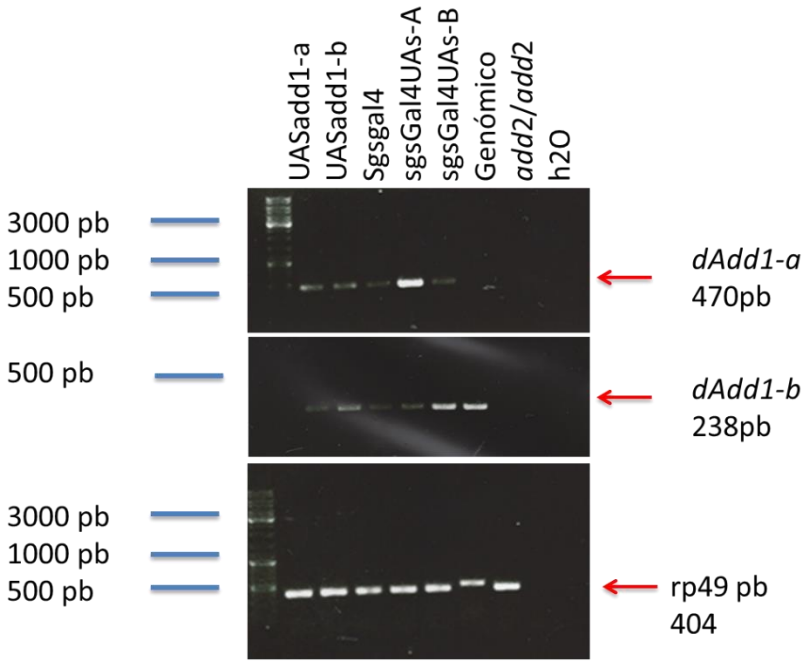

Figura 11. Las líneas transgénicas sobreexpresan específicamente cada isoforma cuando se cruzan con un Gal4. En los primeros dos carriles se encuentran las líneas sin inducción

(progenitores de la cruza). El carril Sgs-Gal4 es la línea progenitor materna en ambos casos. Los carriles 4 y 5 son los organismos resultantes de la cruza con la sobrexpresiones de cada una de las isoformas. Finalmente se muestran los controles, ADN genómico "*wild type*", cDNA de la condición nula dadd2^{1}/ dadd2^{1} y H_2O. Como control de carga se usó Rp49.

Para la amplificación por PCR se mezclaron los siguientes componentes en un tubo estéril de 0.5 ml: 2.5 µl de búfer 10x (Thermo®), 2 µl MgCl2 (Thermo®), 1 µl de dNTPS (Invitrogen®) a 10mM cada uno, 1.5 µl del oligo A (10uM), 1.5 µl del oligo B (10uM), 0.5 µl de la enzima "Taq DNA Polymerase" (Thermo®), 1 µl de cDNA (para obtener cDNA se convirtió 1 µg de ARN total en 20µl finales) y 15 µl de agua estéril. Bajo las siguientes condiciones de amplificación: 94°C por 5 minutos (1 ciclo); 94°C por 30 segundos, 55°C por 30 segundos para Rp49 y 60°C por 30 segundos para los oligos de ADD, 72°C por 30 segundos (30 ciclos); 72°C por 7 minutos (1 ciclo). El control de carga que se empleó es Rp49 y finalmente se visualizó por electroforesis en geles de agarosa al 1%.

- Inmunofluorescencia de cromosomas politénicos

Se seleccionaron larvas de tercer instar, que son aquellas que salieron del alimento adhiriéndose a las paredes del tubo y presentan movilidad antes de prepararse para la pupación. Estas larvas fueron enjuagadas con agua destilada para quitar los excesos de comida. Posteriormente las larvas se colocaron sobre un vidrio de reloj en una solución de NaCl 0.7%. Con la ayuda de un microscopio estereoscópico y unas pinzas de disección se tomó la larva por ambos extremos, la cola y la probóscide, extendiéndola cuidadosamente hacia lados opuestos para extirpar las glándulas. Las glándulas fueron recolectadas y se removieron los excesos de grasa y otros órganos. Los cromosomas politénicos fueron fijados y extendidos siguiendo el protocolo reportado por Engels (1986). Primeramente, fueron tratados los portaobjetos y cubreobjetos; los portaobjetos se lavaron en una solución de 25 mL de Poli-L-lisina y puestos a secar durante una hora. Los cubreobjetos se lavaron en solución de 10 mL de sigmacote y puestos a secar durante una hora, posteriormente se sumergieron en 10 mL de etanol al 100% y después se ponen a secar.

Se realizó la preparación de las soluciones de lisis y fijación para el proceso de "squash". La solución de lisis contiene: 69.38 µl de paraformaldehído 16% + 80.62 µl de H_2O + 150 µL de ácido acético. La solución fijadora está compuesta por: 69.38 µl de paraformaldehído 16% + 227.62 µl de PBS 1X + 3µl de tritón. Estas soluciones fueron separadas en el momento de uso y se desecharon al pasar 2 horas.

Se tomaron 2 cubreobjetos tratados con Sigmacote® y se colocaron en uno 25 µL de la solución fijadora en uno y en el otro 25 µL de la solución de lisis. Haciendo uso de las pinzas de disección, fueron colocadas dos pares de glándulas durante un periodo de 10 segundos en la solución de fijación e inmediatamente después en la solución de lisis durante 1 minuto y medio. Una vez transcurrido el tiempo se dejó caer suavemente sobre el cubreobjetos un portaobjetos tratado con Sigmacote®. Se tomó el portaobjetos y con ayuda de una pinza se deslizó de un lado a otro el cubreobjetos con el objetivo de romper el tejido, hasta el punto

en que las glándulas quedaron esparcidas. Se cortó un fragmento de papel cromatográfico de 3MM “Whatman” aproximadamente del tamaño de un cubreobjetos, se colocó a lo ancho de la muestra asegurándonos de abarcar todo el cubreobjetos y se deslizó el pulgar apoyado de abajo hacia arriba varias veces con la finalidad de extender los cromosomas politénicos "squash".

Las muestras fueron congeladas en nitrógeno líquido y finalmente fueron almacenadas a 4° C en solución de metanol para su posterior uso en la inmunotinción. Para hidratar las preparaciones se enjuagan dos veces con PBS 1X durante 30 min. Después se incuban con un anticuerpo de interés:

- anti-HP1a (C1A9 de DSHB 1:1000)

-anti-paddADD1 (New england peptide 1:50)

-anti-Histona H3K9me3 (Abcam 8898 1:50)

-anti-dXNP (New england peptide 1:10)

El respectivo anticuerpo se puso en leche Carnation en polvo al 1% (diluida en PBS 1X con Igepal al 0.1%), y se deja incubando toda la noche a 4° C. Posteriormente las preparaciones se lavaron 6 veces con Igepal al 0.1% diluido en PBS 1X por 15 minutos para después aplicar el anticuerpo secundario (Alexa de Invitrogen) a una concentración 1:100 Alexa Flour verde 488 antirabbit para α-H3K9me3, α-ADD y α-dXNP y 1:500 antimouse Alexa Flour rojo 564 para α-HP1 en leche Carnation en polvo al 1% (diluida en PBS 1X con Igepal al 0.1%) y se deja incubar 3 horas a temperatura ambiente. Por último, cada preparación se lava 6 veces con Igepal al 0.1% diluido en PBS 1X por 15 minutos en agitación, se agregan 20 µl de citifluor y se sellan. Las imágenes se tomaron en el microscopio confocal (Olympus FV1000) con un aumento de 60x y posteriormente se analizaron en ImageJ.

- Inmunotinción de glándulas salivales

Se extrajeron 15 pares de glándulas salivales o la mayor cantidad de glándulas que se pudiera en media hora en PBS frío con inhibidores de proteasa (Aprotinina 10 µg/mL, Leupeptina 10 µg/mL, 1x Complete Roche y PMSF 250 mM) bajo el microscopio estereoscópico. Posteriormente se fijaron con búfer 1X Ruvkun, más metanol (añadir 0,5 ml de metanol al 100%) más 2% de formaldehído y se incubaron durante 2 horas a 4 grados Celsius con rotación suave (Ruvkun 2x solución: 160mM KCl, 40mM NaCl, 20mM EGTA, 30mM PIPES pH 7.4). Se realizó un lavado de rotación de 5 minutos con Tris/Triton (100 mM tris pH 7.4, 1% Triton X-100 y 1 mM EDTA) añadiendo 1 ml. Se incubaron las glándulas salivales en 1 ml de Tris/Tritón X-100 (igual que el anterior) + 1% de β-mercaptoetanol durante 2 horas a 37 °C con agitación leve (300 rpm). Luego se realizó la permeabilización con un lavado con 1 ml de búfer BO_3 (0.01 M H3BO3 pH 9.2 + 0.01 M NaOH) y luego se incubaron en BO_3 / 10 mM TDT a 37 ° C con agitación leve (300 rpm) durante 15 minutos. Al final del período de incubación, se realizó un lavado con 1 ml de Búfer BO_3 solo. Para bloquear, se incubaron las glándulas salivales en 1 ml de búfer B (PBS + 0,1% BSA + 0,5%

Tritón X-100 + 1 mM EDTA) durante 2 horas a temperatura ambiente con rotación. Para la inmunotinción, eliminar todo el búfer B y se añadió el búfer A (búfer B con 1% BSA) más anticuerpos de interés (en este caso usamos HP1a C1A9 de Hybridoma Bank 1:3000) durante la noche a 4ºC con rotación. Al siguiente día se dieron 3 lavados de 15 minutos cada uno con búfer B y después, las glándulas se transfirieron al búfer B junto con el anticuerpo secundario acoplado a un fluoróforo durante 2 horas bajo rotación a 4ºC (anticuerpo secundario Alexa fluor 568 Invitrogen se utilizaron 1:3000). Posteriormente, se lavaron 2 veces durante 15 minutos a temperatura ambiente mientras se hace la rotación con 1ml de búfer C (búfer B sin EDTA). Incubar con un marcador de ADN como Hoechst (tomar 1µl de caldo 10 mg/mL y disolver en 1 ml de búfer B) durante 10 minutos a temperatura ambiente con rotación. Se realizó un lavado con búfer B y una vez con PBS, cada lavado de 10 minutos. Finalmente, se montaron las glándulas salivales en un portaobjetos, haciendo una alberca con un cubreobjetos. Se pusieron las glándulas salivales en el centro de la alberca y se cubrieron con citifluor para posteriormente sellar todos los lados con esmalte de uñas claro. Se observaron bajo un microscopio de fluorescencia o confocal.

- Ensayo tipo “Western blot”

Se colectaron 10 pares de larvas de tercer instar en PBS más inhibidores de proteasas (Aprotinina 10 µg/mL, Leupeptina 10 µg/mL, 1x Complete Roche y PMSF 250 mM) de cada genotipo analizado. Las muestras se hirvieron en búfer de Laemmli y se cargaron en un gel SDS-PAGE al 8% donde corrieron 10 minutos a 80 Volts y durante 2 horas a 110 Volts (Maniatis, et al 1987).

Para realizar la inmunodetección, la membrana se bloqueó con leche Carnation en polvo al 10% en PBS 1X + 0.1% Tween20, en agitación durante 1 h. Se agregó la solución con el anticuerpo primario: Leche Carnation en polvo al 5% en PBS 1X + 0.1% Tween20 en una dilución de 1:3000 del anticuerpo α-βTubulina (E7 de DSHB) y 1:1000 del anticuerpo α-ADD (New england peptide). Posteriormente se realizaron lavados con PBS+ 0.1% Tween20 y se agregaron los anticuerpos secundarios acoplados a HRP (Zymed) 1:3000 “goat-antimouse” y 1:5000 “goat-antirabbit” respectivamente. La detección se realizó con el “Kit” de Amersham para la detección por Quimioluminiscencia.

- Análisis de expresión relativa qRT-PCR

Se extrajeron 10 pares de glándulas salivales y se guardaron en Trizol (Invitrogen). El ARN se extrajo siguiendo el protocolo del proveedor, se cuantificó y almacenó a -70°C en etanol 75% para su posterior utilización. La integridad del ARN se comprobó corriendo 1µl en un gel desnaturalizante de agarosa al 1%. Para obtener cDNA se convirtió 1 µg de ARN total disuelto en 20µl finales, más 1µl de oligo dT (Invitrogen), 1µl de dNTPs y agua inyectable. Esta mezcla se calentó por 5 minutos a 65°C, se pasó por hielo y se le añadió 4µl de búfer 5x, 2µl DTT 0.1M y 0.5µl de inhibidor de RNAsa, se mezcló con pipeta y se puso 2 minutos a 37°C, finalmente se añadió 1µl de transcriptasa reversa (ThermoFisher) y se dejó en el termociclador por 1 hora a 37°C. Para inactivar la enzima se le dio un ciclo de 15 minutos a 65°C.

Para analizar las distintas isoformas de dADD1 se cuentan con varios oligos, a continuación, se muestra un esquema (Figura 12) con las distintas isoformas y los oligos que se requieren para ver cada isoforma de manera específica.

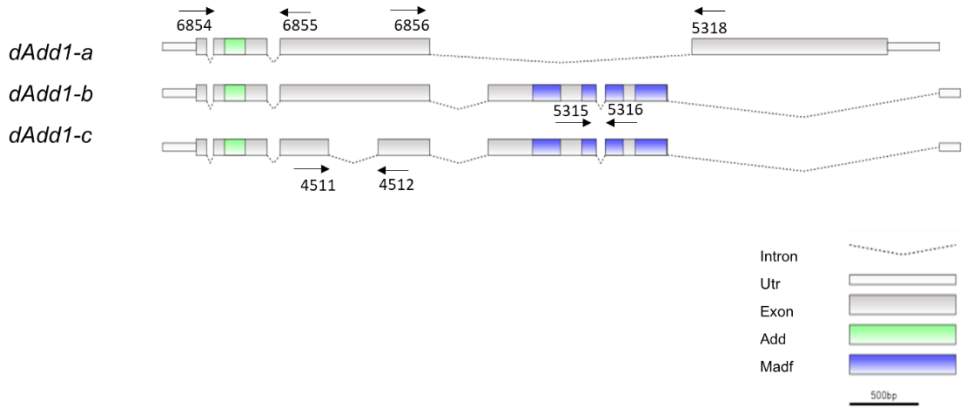

Figura 12. Esquema de los ARNm de *dadd1* generados por "splicing" alternativo. Los dominios ADD (verde) y MADF (azul) se representan como recuadros. Los oligos utilizados para amplificar los ADNc se indican mediante flechas horizontales y el numero proporcionado por la unidad de secuenciación.

Las secuencias de los oligonucleótidos que se emplearon para la amplificación de transcritos señalados en la Figura 15 se muestran en la siguiente tabla:

Tabla 4. Oligonucleótidos empleados para amplificar el transcritos

Nombre	**Forward**	**Reverse**
Su(var)3-9	GTGCGCTTCAAGAACGAACT	GCGGCCTTTTGGCAATTACT
Su(var)205	GGGCAAGAAAATCGACAACCC	GGCCATTATTGTCGGAGGCA
Act5C	GGTTGCAGCTTTAGTGGTCG	GGCACAGTATGGGAGACACC
Sgs8	TGCTCGTTGTCGCCGTC	GCCGCTCAAGACCCTCCATA
Psi	TCCAGGGAAAGAACGACGAA	CGCTCCAGATTGCTGGTTGA
Kraken	CGGAACTTTCGCCAGAGACAA	CTATCCGGCGAATCAGGCAT
Toy	CGTTGCGGAACGAACATCAT	CATCGTTGCAATCGGTTGTG
Lgs	GTACCACAACAGCAAACCCC	TGGGCTTGGTCGCCTACTTT
Cin	ACACGGTACAAAAGACCGCC	TCCACTTGCACTACGCAATCT
Msps	GTATCGCAGTCCTATGCGCT	CTACGGATTGAGCCGATGGT
Vtd	CATAATGTCCCTTCGCCTGC	TCGACACCTCCAGTTTCTTTCC

CG7742	ATGGCCAAGTGGAACGAACT	AATCCTCTGGCACTGAACCG
NipB	TTTGGCGAGCAAAACCACTC	CCGTACGGAGACACCAGTAT
Ank	TTTCGTTCTTACGTGCTGCTC	TGTGCAAAGGGGTGAATCCT
Cta	ACGCGGCTTTGAGGAGTAC	GACTAGCTACCACAATATCC
Rl	TCGTATTGCAGATCCCGAGC	TGCAAGAGCTTCCTCGACAG
Lt	TTTGAGGAGGCAATGGAACTT	CAGCCAGGCCGTCATAAAGA

La RT-qPCR se llevó a cabo por duplicado y se utilizó el instrumento LightCycler Fast Start DNA Master SYBR Green 1 (Roche). Para realizar la mezcla para el tiempo real se empleó 2.5 µl de cDNA diluido (para hacer el cDNA se convirtió 1 µg de ARN total en 100 µl) más 7.5 µl de mix (1µl de cada oligo 2.5 picomolar, 2 µl de mix con syber green y 3.5 µl agua inyectable de la farmacia). Las condiciones de PCR fueron de 95 °C durante 10 minutos, seguidas de 40 ciclos a 95 °C por 10 s, la temperatura de alineación para 10 s, y 72 °C por 18 s. La temperatura de alineación fue de 65-60 °C. El ciclo de umbral (Ct) se utilizó para evaluar los niveles relativos de respeto al gen de control interno Rp49. Se compararon los niveles relativos de genotipos mutantes con los niveles correspondientes de la cepa silvestre para obtener la diferencia utilizando la fórmula 2-ΔΔCT = [(CT gen de interés − CT control interno) muestra A − (CT gen de interés − CT control interno) muestra B]. Se midió la abundancia de transcritos con duplicados técnicos y se analizaron tres réplicas biológicas independientes.

- Inmunoprecipitación de la cromatina en glándulas salivales

En cada uno de los ensayos se emplearon 120 pares de glándulas salivales previamente disectadas en PBS más inhibidores de proteasas (Aprotinina 10 µg/mL, Leupeptina 10 µg/mL, 1x Complete Roche y PMSF 250 mM). Las glándulas se guardaron conforme se fueron extrayendo en pequeños lotes de 20 a 30 pares de glándulas a -70ºC. El entrecruzamiento de las glándulas se realizó añadiendo formaldehido al 1% final en 100 µl de PBS y se incubaron por 15 minutos a 37ºC. Las glándulas se lavaron 2 veces con 1ml de PBS. Finalmente se guardaron en 100 µl de PBS a -70ºC.

Al momento de realizar el experimento, las glándulas se descongelaron en hielo, se lavaron 2 veces con PBS y se juntaron los lotes hasta obtener 120 pares. Posteriormente se le añadió 150 µl de búfer de lisis nuclear de sarcosinato (Tabla 5) más inhibidores de proteasas.

Tabla 5. Búfer de lisis nuclear de sarcosinato

Concentración de reactivos stock	**Concentración final**
Tris.HCl, pH 8, 1M	10 mM

NaCl	100 mM
Deoxicolato de sodio	0.1%
Lauroil sarcosinato de sodio	0.5%
EDTA	1 mM
EGTA	0.5 mM
+ inhibidores de proteasa (complete 1 tableta 100x, PMSF 100	**Añadir fresco cada vez

Se realizó la incubación en el búfer mencionado en la tabla anterior colocándose en hielo por 20 minutos y posteriormente se realizó el proceso de sonicación en un aparato Biotuptor (Configuración 30on/30off) durante 11 ciclos (para obtener fragmentos de cromatina de 200-800 pares de bases). Una vez finalizados los ciclos de sonicado se le añadió triton-100 a una concentración final de 1%. Los tubos se centrifugaron a 13,000 rpm por 10 minutos a 4ºC y el sobrenadante se transfirió a tubos que contienen perlas con "prelimpiado" (estas perlas magnéticas estuvieron previamente incubadas una hora con un anticuerpo irrelevante) y se dejaron en rotación por 1 hora a 4ºC. Las perlas se colectaron con la gradilla magnética y el extracto se transfirió a un nuevo tubo que contenía las perlas previamente acopladas al anticuerpo de interés, en este caso HP1a (C1A9 de DSHB) y un anticuerpo irrelevante, que fue el "Mock" (IgG de ratón empleado como control negativo). Las muestras se dejaron durante toda la noche en rotación a 4ºC. A las 12 horas se colectaron las perlas con la gradilla magnética, el sobrenadante se desechó y se lavaron las perlas 2 veces con búfer de baja sal, seguido de un lavado con búfer de alta sal, posteriormente un lavado con cloruro de litio y finalmente un lavado con búfer TE. Los fragmentos de cromatina se recuperan eluyendo 2 veces con 100 µl de búfer de elución IP preparado en el momento (0.1 M NaHCO3, 1% SDS) (cada elución se incuba a 65ºC por 15 minutos, posteriormente se recupera el sobrenadante removiendo las perlas). Al finalizar, se mezclaron los 2 eluyentes y se añade NaCl (10ul de 5M), EDTA (4ul de 0.5M), Tris (8ul de 1M) para revertir el entrecruzamiento por 2 horas a 65ºC (este paso puede prolongarse hasta 6 horas).

Se añadió 2µl de Proteinasa K grado ARN 20mg/ml por 2 horas a 65ºC y finalmente se realizó la extracción del ADN con fenol:cloroformo:isoamílico (25:24:1). Se añadió 1 µl de glicógeno 20 mg/ml para dejar precipitando toda la noche junto con 1/10 de volumen de 3M de acetato de sodio, pH=5.2 junto con 2 volúmenes de etanol toda la noche a 4ºC. Al siguiente día se centrifugó durante 20 minutos a 13000 rpm a 4ºC, se lavó una vez con etanol al 70% para remover la sal y se dejó secar el tubo. El pellet resultante se disolvió en 20µl de H_2O inyectable. El ADN recuperado se analizó mediante PCR tiempo real que se llevó a cabo por duplicado (2 réplicas técnicas) y se empleó el reactivo LightCycler Fast Start DNA Master SYBR Green 1 (Roche). Para realizar la mezcla para el tiempo real se empleó 2.5µl de ADN diluido 1:100 para el input o directo del ChIP, más 7.5µl de mix (1µl de cada oligo 2.5 pico molar, 2µl del mix con syber green y 3.5µl agua inyectable de la farmacia). Las condiciones de PCR fueron de 95 °C durante 10min, seguidas de 40 ciclos a 95 °C para 10s, la

temperatura de alineación para 10s, y 72 °C para 18s. La temperatura de alineación fue de 65-60 °C. Se emplearon los siguientes olinucleotidos diseñados para la región promotora de estos genes:

Tabla 6. Secuencias de los oligonucleótidos empleados para amplificar ensayos de inmunoprecipitación de la cromatina

Nombre	**Forward**	**Reverse**
Het-A	ACAGATGCCAAGGCTTCAG	GCCAGCGCATTTCATGC
Sgs8	TTTGGCACTTACCAATGACGGCGA	TTCCATTGATCCTATAACACATTT
Psi	TCCAGGGAAAGAACGACGAA	CGCTCCAGATTGCTGGTTGA
Ank	TTTCGTTCTTACGTGCTGCTC	TGTGCAAAGGGGTGAATCCT
Cta	ACGCGGCTTTGAGGAGTAC	GACTAGCTACCACAATATCC
Lt	TTTGAGGAGGCAATGGAACTT	CAGCCAGGCCGTCATAAAGA
Hsp70Aa	GGTCGTTGGCGATAATCTCC	CTGCAACTACTGAAATCAAC

El enriquecimiento relativo al anticuerpo irrelevante o “mock “ (IgG de ratón) se calculó empleando la siguiente formula % Input = 100*log2(dCt normalizado ChIP), donde dCt normalizado ChIP = Ct muestra − [Ct input*Input factor de dilución)]

6. RESULTADOS

6.1.- La sobreexpresión de dADD1 causa letalidad en el organismo y ruptura de la cromatina

Con base en los resultados obtenidos en los trabajos previos del laboratorio donde se muestra que dADD1 está involucrado en la unión de HP1a a los telómeros, además del hecho de que mutaciones en ATRX se han asociado con varios tipos de cáncer, incluyendo glioblastoma y cáncer de páncreas (Mukherjee et al. 2018; Singhi et al. 2017) decidimos hacer una búsqueda bioinformática de los niveles de transcritos de ATRX en una variedad de cánceres somáticos humanos utilizando la base de datos COSMIC (Catalogue Of Somatic Mutations In Cancer) (Harsha et al. 2018) y THPA (The Human Protein Atlas) (Uhlén et al. 2015), esto con la finalidad de evaluar tanto la presencia de niveles más altos de la proteína como los niveles más bajos.

Esta búsqueda fue realizada por la Dra. Amada Torres que se encontraba realizando una estancia postdoctoral con la Dra. Viviana Valadez en ese momento. Ella encontró que ATRX se presenta con valores altos de TPM (“Transcripts Per Million”) en todos los tipos de células revisadas en la base de datos de THPA, principalmente en tejidos como la paratiroides y las glándulas tiroideas, corteza cerebral y endometrio. Los umbrales utilizados para categorizar

como “sobreexpresion” y la “subexpresión” de los niveles normales se explica en la base de datos. La proteína está presente en casi todos los tipos de tejidos humanos (https://www.proteinatlas.org/) y (https://cancer.sanger.ac.uk/cosmic).

Las alteraciones en su expresión se encuentran en el 7,79% de los casos notificados (795/10,202 casos). La Dra. Torres realizó una consulta filtrada en la base COSMIC donde reportó 174 (4.45%) casos de sobreexpresión y 39 (0.99%) subexpresión que tuvieron niveles modificados de ATRX, donde en paréntesis se muestra el porcentaje respecto al total de casos registrados (n = 3910), respectivamente. La Dra. Torres curó los datos de forma manual para seleccionar los pacientes sin antecedentes de tratamiento para descartar posibles efectos secundarios de cualquier tratamiento, lo que nos dio un total de 144 casos de sobreexpresión y 33 de subexpresión.

En la figura 13a se muestra la distribución de la sobreexpresión de ATRX en diferentes tipos de tumores como tumores de pulmón (19%, franja color mostaza) y de mama (26%, franja color rosa fuerte) que son los tipos más abundantes de cáncer con alteraciones en la expresión; no encontramos ningún registro de tumores del sistema nervioso central representados en este grupo. La figura 13b muestra los tipos de tumores asociados con una menor cantidad de expresión de ATRX, como pulmón (38%, franja color mostaza) y tracto aerodigestivo superior (18%, azul claro). La subexpresión no está correlacionada con cambios en el número de copias del gen, lo que indica que, como en los casos de sobreexpresión, estos cambios podrían ser el resultado de otros eventos moleculares como la represión génica o quizás mutaciones en secuencias reguladoras y de codificación.

En la parte inferior de la Figura 13, se seleccionaron tejidos que representan los distintos casos que encontramos y que en la base de datos THPA tuvieran varias imágenes con inmunotinciones empleando el anticuerpo de Santa Cruz sc-15408 que reconoce a ATRX de humanos. En la Figura 13c podemos ver la localización nuclear en las células glandulares de una paciente sana. En la figura 13d se muestra un tejido con cáncer de seno que presenta bajos niveles de ATRX, y en la 13e y 13f podemos ver niveles altos de la proteína ATRX en muestras de cáncer de seno. La inmunotinción del tejido pulmonar sano con el mismo anticuerpo se muestra en g y en h se observa una inmunotincion baja.

Las Figura 13i y 13j son ejemplos de carcinoma de pulmón en los que ATRX se sobreexpresa con tinción fuerte y localización nuclear. Estos datos asocian la sobreexpresión de ATRX con varios tipos de tumores somáticos, por lo tanto, un análisis más profundo de los efectos moleculares de la sobreexpresión ATRX es esencial para estudiar su papel como uno de los factores que pueden conducir a la aparición o mantenimiento de un fenotipo tumoral transformado.

.

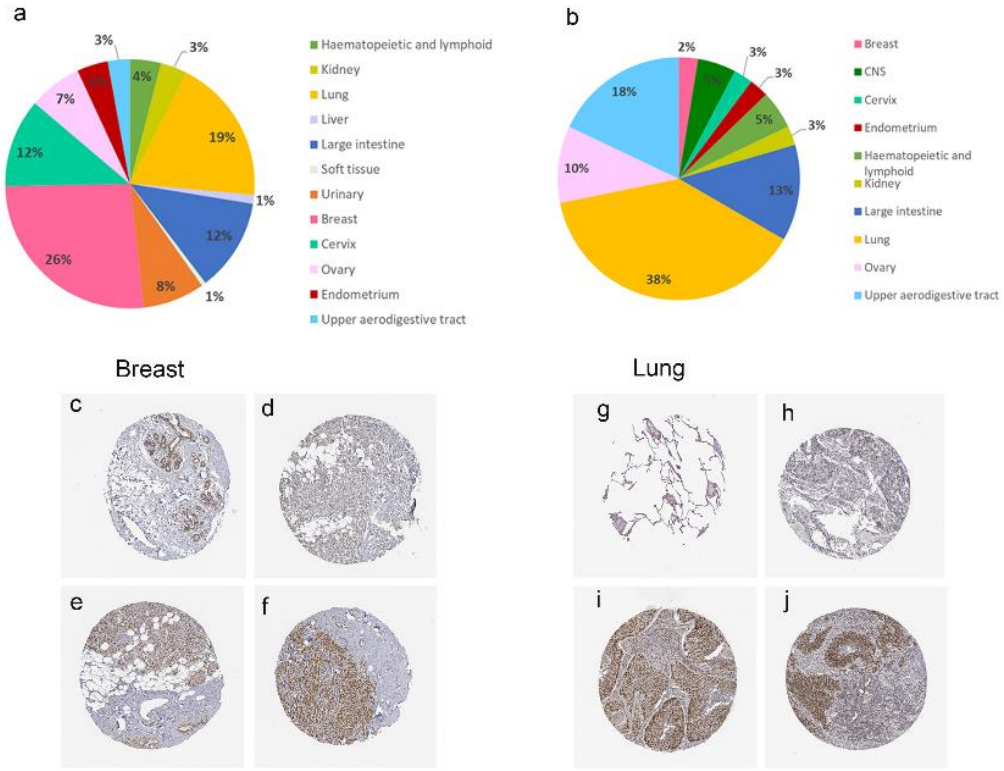

Figura 13. Distribución de los casos por tipo de cáncer, presentada en porcentaje con a) sobreexpresión de ATRX y b) subexpresión de ATRX. c) Muestra de tejido mamario sano (id del paciente: 3544) de una paciente de 45 años que presenta inmunohistoquímica contra la proteína ATRX, d) Muestra de carcinoma de conducto mamario (id del paciente: 1874) de una paciente de 80 años. e) Muestra de carcinoma de conductos mamarios (id del paciente: 4193) de una paciente de 43 años con alta señal de ATRX. f) Muestra de carcinoma lobular (id del paciente: 4789) de un paciente de 49 años con una alta señal de ATRX. g) Tejido sano pulmonar (id del paciente:1678) de una paciente de 57 años que presenta inmunohistoquímica contra la proteína ATRX, h) Adenocarcinoma de mujer de 51 años (id del paciente: 2041) que muestra baja señal de ATRX, i) Carcinoma de células escamosas de hombre de 64 años (id del paciente:4090), j) Carcinoma de células escamosas de hombre, de 72 años (id:4896). Imágenes tomadas de la base de datos THPA.

Con las observaciones encontradas que muestran que ATRX se sobreexpresa en una amplia variedad de cánceres humanos (Figura 13), se decidió estudiar cuáles serían los efectos moleculares de la sobreexpresión de las proteínas dADD1 en el modelo de *Drosophila*.

Como una primera aproximación para estudiar el papel de las proteínas dAdd1 en el desarrollo del organismo, se sobreexpresaron todas las isoformas de dAdd1 de manera ubicua con el sistema UAS-GAL4 y se observó una letalidad del 100% (Tabla 7). Se lograron resultados similares cuando se sobreexpresaron las isoformas de manera individual, ya sea dADD1a o dADD1b, y en todos los casos los organismos no alcanzaron el estadio de larva, muy probablemente murieron en las primeras etapas de desarrollo (datos no mostrados).

Tabla 7. Efecto de la sobreexpresión de dADD1 en la viabilidad de los organismos

Genotipo	Viabilidad [a] (%)
+/+;Tub-GAL4/+	352/372 (94)
+/ UAS-dADD1;+/+	361/361 (100)
+/+; UAS-dADD1a/+	558/558 (100)
+/+; UAS-dADD1b/+	273/273(100)
+/UAS-dADD1;Tub-GAL4/+	0/361 (0)
+/+;Tub-GAL4/UAS-dADD1a	0/558 (0)
+/+;Tub-GAL4/UAS-dADD1b	0/273 (0)

[a]El número de moscas adultas esperadas de acuerdo con la clase más saludable en cada cruza

Como la sobreexpresión resultó letal en el organismo, decidimos analizar las glándulas salivales de las larvas del 3° instar. El ADN de estas células se encuentra amplificado cerca de 1000 veces por un proceso llamado endoreplicación, además los cromosomas politénicos tienen una arquitectura bien definida y pueden diferenciarse zonas eucromáticas y heterocromáticas (Jamrich, Greenleaf, and Bautz 1977).

Se realizó la sobreexpresión de todas las isoformas de dAdd1 en las glándulas salivales haciendo uso del sistema GAL4 (*Sgs3-Gal4* que es el "*driver*" de glándulas salivares) y se obtuvieron cromosomas politénicos. En el cromosoma tipo "*wild type*", se muestra el patrón característico de bandas (representan cromatina más compacta) e interbandas (cromatina más abierta y transcripcionalmente activa) (I. F. Zhimulev et al. 2004), también podemos ver el cromocentro (cuadro discontinuo en 14a y 14a'), los telómeros (cuadros de línea continua en 14a y 14a'') y la integridad general de los cromosomas. Las características estructurales fáciles de visualizar son la alineación muy cercana de la cromátida a lo largo del cromosoma, a menudo con poca o ninguna separación visible entre las cromátidas. Esta estrecha alineación se debe en parte, al emparejamiento de los cromosomas somáticos, en el que los cromosomas homólogos se alinean uno al lado del otro de una manera dependiente de la secuencia (Stormo and Fox 2017)(Figura 14a). La sobreexpresión de dADD1 resulta en una pérdida general de la estructura de la cromatina (Figura 14b), el cromocentro se vuelve frágil (comparar los cuadros discontinuos de las Figuras 14a y 14b), hay una pérdida del patrón de bandas en algunas regiones en los brazos cromosómicos, en los telómeros (flechas y cuadros de líneas continuas en la Figura 14b y una imagen amplificada en 14b'') y copias de cromosomas disociados.

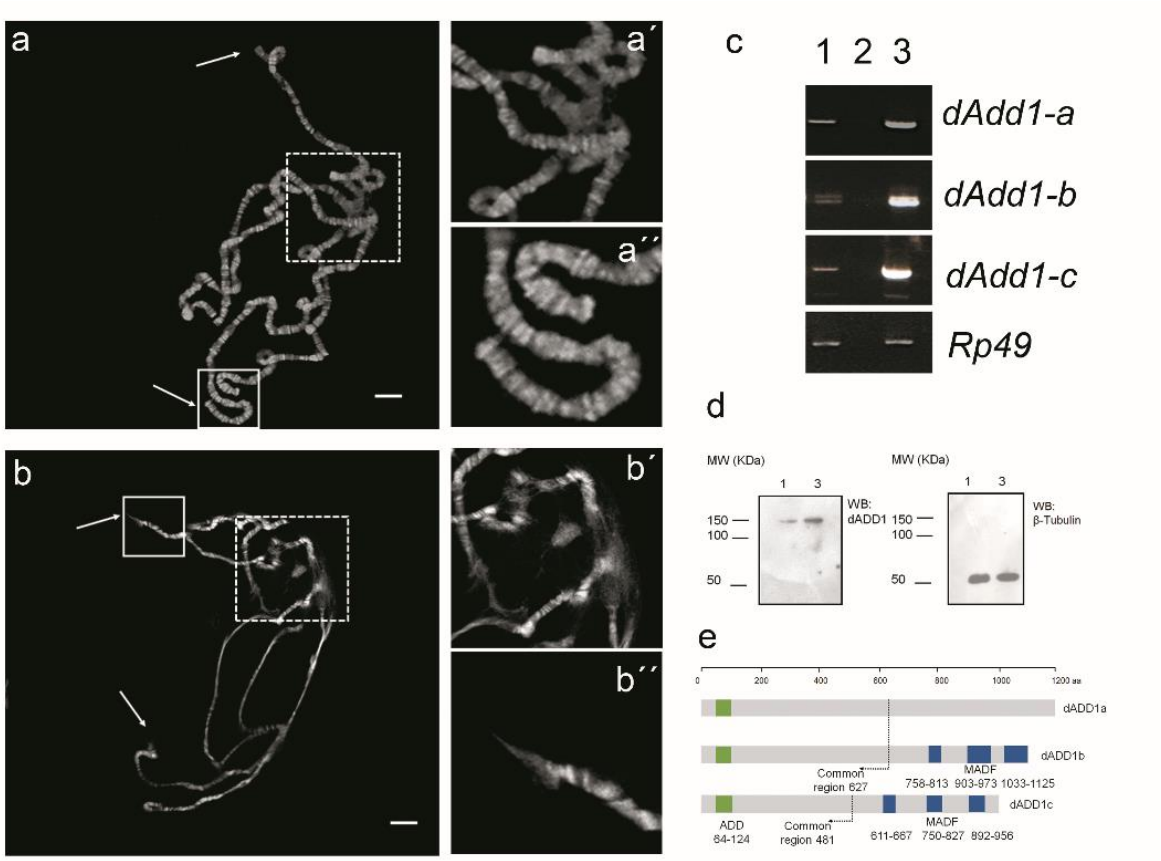

Figura 14. Modificar los niveles de expresión de dADD1 da como resultado una desorganización cromosómica. a) Cromosoma politénico "*wild type*". El ADN se tiñó con DAPI (se muestra en gris), las flechas apuntan a regiones teloméricas, el cromocentro se muestra dentro del cuadro punteado y un aumento del cromocentro se muestra en a´, un aumento de los telómeros se observa en a´´. b) Cromosoma politénico de glándulas salivales en las que se sobreexpresaron todas las isoformas de dADD1 utilizando el sistema UAS-GAL4, las flechas apuntan a regiones teloméricas y el cromocentro está en el cuadro discontinuo, en b' se muestra un aumento del cromocentro y en b´´ un aumento de una región telomérica. La barra de escala es de 20 µm. c) Análisis semicuantitativo de los niveles de transcritos de las isoformas de dADD1 en las glándulas salivales. Los carriles en el gel corresponden a 1) "*wild type*", 2) H_2O, 3) *UAS-dadd1;Sgs3-GAL4*. El transcrito de *Rp49* se utilizó como control. Todas las isoformas de dADD1 están sobreexpresadas (ver carril 1 vs 3). d) Western blot de extractos de proteínas totales de glándulas salivales donde se usaron anticuerpos pan-dADD1 y anti-β tubulina. Los carriles corresponden a 1) "*wild type*" y 3) *UAS-dadd1; Sgs3-GAL4*, los marcadores de peso molecular se muestran al lado izquierdo de los paneles. En el lado derecho los anticuerpos utilizados para cada membrana se especifican. e) Representación esquemática de las isoformas de la proteína dADD1. Se muestra el dominio ADD compartido por todas las isoformas en verde; una línea discontinua delimita la región común. Los dominios MADF de las isoformas dADD1b y c se muestran en azul. dADD1a es de 1199 aa (130 kDa), dADD1b es 1125 aa (127 kDa) y dADD1c es 979 aa (112 kDa).

Para confirmar la sobreexpresión de ARNm de dAdd1, analizamos los niveles de los transcritos de dADD (a, b y c en las glándulas salivales), empleando los oligos específicos para cada isoforma de la figura 12, obtenidas del genotipo *UAS-dADD1;Sgs3-Gal4* y comparamos con las glándulas salivales "*wild type*". Los oligos de *Rp49* se utilizaron como control. Se descubrió que todos los niveles de ARNm de las isoformas eran de dos a tres veces más altos que los "*wild type*", (comparar los carriles 1 y 3 en la Figura 14c). Además, utilizamos el anticuerpo pan-dADD1 descrito anteriormente para realizar un ensayo tipo Western blot con extractos de proteínas totales de las glándulas salivales (Brenda López-Falcón et al. 2014) y encontramos una sobreexpresión de las proteínas dADD1 al menos tres veces en comparación con los niveles de proteína "*wild type*" (comparar los carriles 1 y 3 en la Figura 14d).

Como los brazos de los cromosomas se veían notablemente más delgados, se quiso descartar que hubiera cambios en la cantidad de ADN ni en los ciclos de replicación. Para esto se usaron métodos indirectos, como emplear la fluorescencia, para ver la cantidad de ADN teñido con un colorante (DAPI) y se analizaron las imágenes obtenidas en el microscopio confocal respecto a la intensidad de la señal (Figura 15a). Para ver la cantidad de cromatina en las glándulas salivales, se evaluaron los cambios en el contenido de ADN e histonas tanto en condiciones "*wild type*" como sobreexpresadas, se utilizó una línea transgénica que expresa la histona H2Av fusionada a un fluoróforo rojo y no se observó un cambio cualitativo significativo entre las condiciones de sobreexpresión de dADD1 versus "*wild type*" (Figura 15b). Al no observar cambios, se puede concluir que el fenotipo observado no se debe a diferencias en la cantidad de ADN, sin embargo, no puede descartarse que se deba a problemas en la cohesión de las cromátidas hermanas. La sobreexpresión de las proteínas dADD1 podría estar alterando los procesos de condensación y segregación de los cromosomas debido a que hay un reporte de interacción directa entre estas proteínas y mod(mdg4), y esta proteína participa en esos procesos.

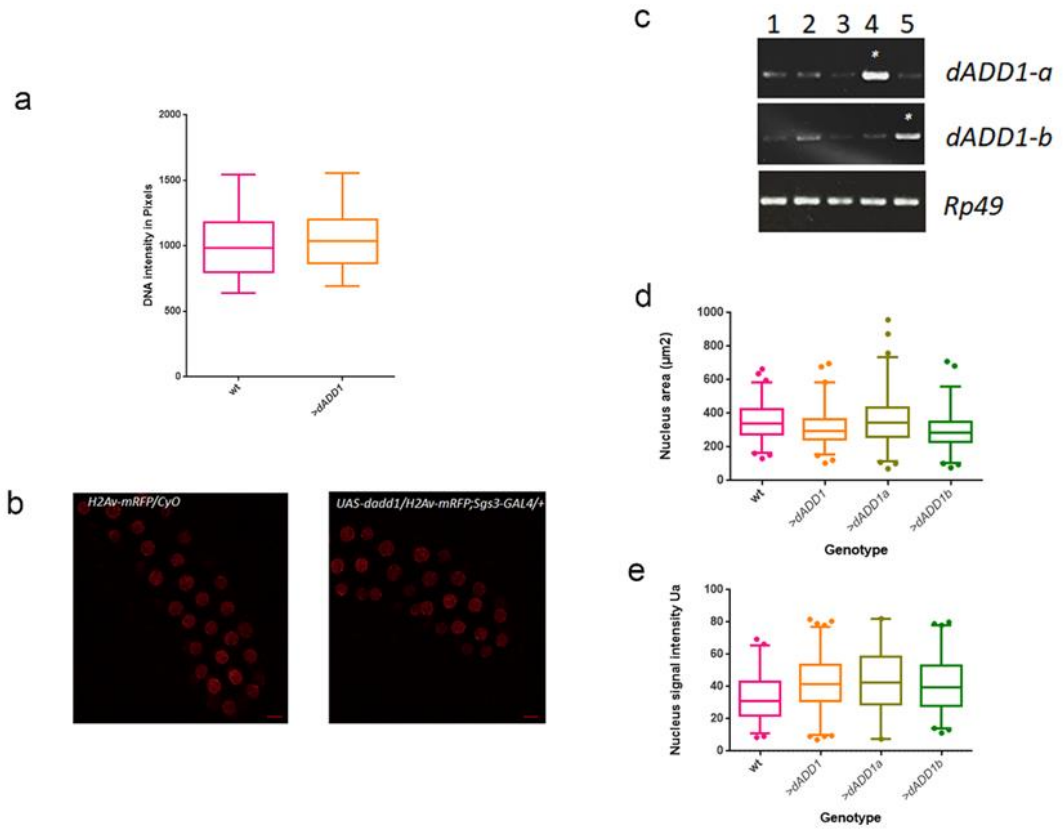

Figura 15. La cantidad de ADN y cromatina no se modifica durante la sobreexpresión de dADD1. a) Cuantificación del ADN en las glándulas salivales sobreexpresando todas las isoformas. Se realizó una prueba t no emparejada para determinar la significación. No se encontraron diferencias significativas. b) Visualización H2Av-RFP de glándulas salivales con una línea transgénica H2Av-RFP (señal roja) usada como "*wild type*" y la sobreexpresión de dADD1. c) Análisis de los transcritos de dADDa y dADDb por medio de RT-PCR 1) *Sgs3-GAL4*, carril 2) *UAS-dADD1a*, carril 3) *UAS-dAD1b*, carril 4) *Sgs3-GAL4/UAS-dADD1a* y carril 5) *Sgs3-GAL4/UAS-dAD1b*. Se utilizó Rp49 como control. Se cuantificaron los parámetros de área (d) e intensidad (e) de las condiciones de tipo salvaje y sobreexpresión. Se realizó ANOVA unidireccional ordinaria para determinar la significación. No se encontraron diferencias significativas. Para cada genotipo contamos el número de núcleos wt n = 303, *UAS-dADD1; Sgs3-GAL4* n = 307, *Sgs3-GAL4/UASdADD1a*, n = 296, *Sgs3-GAL4/UAS-dADD1b* n = 219. Las cuantificaciones se realizaron utilizando el programa ImageJ.

El fenotipo observado de la pérdida general de patrones de bandeo y compactación cromosómica cuando sobreexpresamos dADD1 fue algo inesperado ya que recientemente datos publicados del laboratorio indican que dADD1 participa en el silenciamiento y compactación de los retrotransposones teloméricos y previene las fusiones teloméricas (Chavez et al. 2017). Por lo tanto, esperábamos que la sobreexpresión pudiera conducir a un efecto opuesto, es decir, mayor compactación en ciertas regiones de los cromosomas. Por el contrario, se observó una descompactación de regiones heterocromáticas, como el

cromocentro y los telómeros, indicando una sensibilidad de estas regiones a los cambios en los niveles de dAdd1. Con anterioridad habíamos descrito una interacción física y genética con la proteína HP1a, que es un factor importante para la formación de la heterocromatina en estas regiones (López-Falcón et al. 2014) lo que nos llevó a la siguiente pregunta de este trabajo que se aborda en el punto 6.2.

6.2 La proteína HP1a se deslocaliza en respuesta a la sobreexpresión de las proteínas dADD1

HP1a es uno de los factores involucrados en la compactación de la cromatina (Joel C. Eissenberg and Elgin 2014) y está compuesta por dos dominios altamente conservados, el cromodominio en la parte N-terminal (CHD) (Grewal and Jia 2007) y un dominio cromoshadow en la parte C-terminal (CSD), que están separados por una región "Hinge" de longitud variable. Las proteínas HP1 se unen específicamente a H3K9 dimetilada y trimetilada (H3K9me2 y H3K9me3) a través de su CHD (Hendzel et al. 1997b; Hirota et al. 2005). Los dos dominios presentan una función crítica para la formación de heterocromatina (Azzaz et al. 2014) , ya que el CHD reconoce la marca de H3K9 para dirigirlo a heterocromatina, y el dominio CSD facilita la dimerización de las proteínas HP1 y a su vez puede tener interacción con otras proteínas que portan el motivo pentapéptido conservado, PxVxL, como lo es el caso de las metiltransferasas para depositar una nueva marca de heterocromatina (Hinde, Cardarelli, and Gratton 2015).

Como se mencionó en los antecedentes, HP1a interacciona con dADD1 (Brenda López-Falcón et al. 2014; Alekseyenko et al. 2014) y por lo tanto surgió el interés de conocer si el efecto de la sobreexpresión de dADD1 afectaba a este factor y era crucial para heterocromatinizar. Entonces se realizaron inmunolocalizaciones de HP1a en cromosomas donde sobreexpresamos todas las isoformas de dADD1 y se observaron por medio de imágenes tomadas en el microscopio confocal. En general se percibieron muchos cromosomas con una menor cantidad de señal de HP1a en el cromocentro, además de que con anterioridad ya habíamos observado un patrón de pérdida de bandas (Figura 14). Para evaluar si había una correlación entre la pérdida del patrón de bandeo y la localización de HP1a, cuantificamos el número de cromosomas que presentaban un patrón de pérdida de bandas y dividimos los cromosomas en tres grupos de acuerdo con la severidad de la pérdida del patrón de bandas:

- organizados (bandas bien definidas, cromocentro con señal HP1a)
- moderadamente afectados (aún con señal HP1a en el cromocentro, pero con irregularidades en el patrón de bandas)
- severamente afectados (muy poca o ninguna señal de HP1a en el cromocentro, muchos defectos en el patrón de bandeo y grosor del brazo cromosómico)

En la Figura 16a se muestran ejemplos de cada fenotipo y el resultado de esta clasificación. Los cromosomas "*wild type*" conservaron el patrón de bandas a lo largo de los brazos y también la señal pericentromérica de HP1a (98,3%). En los cromosomas que sobreexpresan

dADD1 (> dADD1), la gran mayoría no mantienen una estructura de cromatina organizada y presentan menor señal de HP1a (90.3%). Al observar estos datos decidimos cuantificar el área de la señal de HP1a en los cromocentros y se puede observar una disminución de esta área en los cromosomas que sobreexpresan dADD1 (Figura 16b). Para evaluar si existe una correlación entre la pérdida del patrón de bandas en el cromosoma con la pérdida de HP1a en el cromocentro, se midieron los resultados obtenidos de cada genotipo y la intensidad de la señal de HP1a, y observamos que, de hecho, los cromosomas que tienen una pérdida severa del patrón de bandas tenían menos HP1a unido al cromocentro (Figura 16c). Estos experimentos indican que la sobreexpresión de dADD1 resulta en una pérdida de la estructura de regiones heterocromáticas que se localizan a lo largo de los brazos de los cromosomas y también una disminución de la señal de HP1a en el cromocentro.

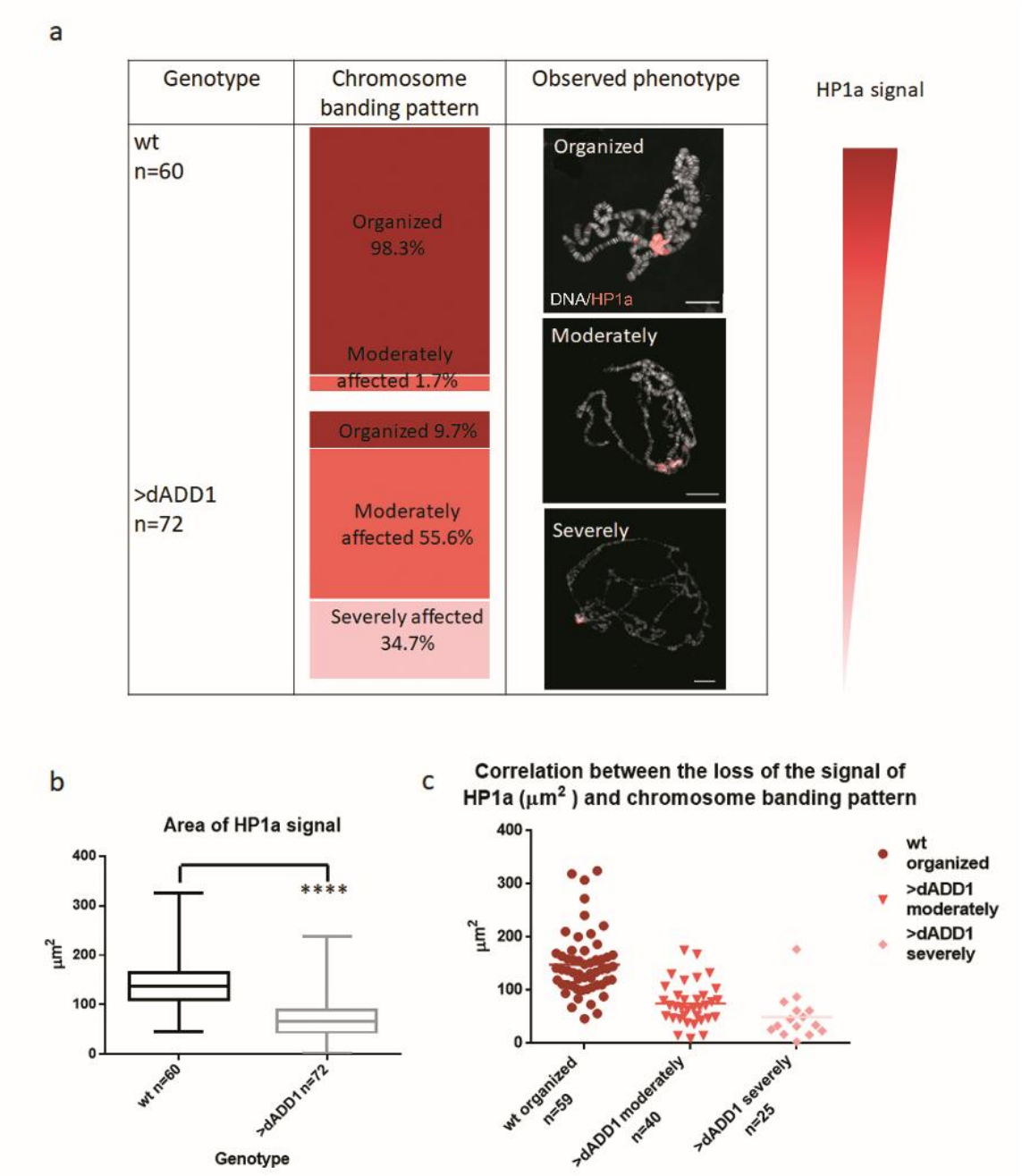

Figura 16. La sobreexpresión de dADD1 induce la deslocalización de HP1a, que se correlaciona con la pérdida de la señal de HP1a. a) Clasificación del grado de los fenotipos y la cantidad de señal de HP1a observada en los cromosomas de politénicos. La primera columna indica los genotipos analizados; la segunda columna muestra la clasificación de los cromosomas de acuerdo con su patrón de bandas en organizado, moderado y gravemente afectado (ver el texto para una explicación detallada sobre la clasificación). Diferentes tonos de rojo indican la intensidad de la señal HP1a. La tercera columna muestra un ejemplo de cada uno de estos cromosomas donde el ADN se observa por la tinción DAPI (se muestra en gris), la tinción contra HP1a (rojo) y la barra de escala de 20 µm. b) El área de la señal HP1a

disminuye en los cromosomas donde se sobreexpresa dADD1, el área se cuantificó con el programa ImageJ. El número de cromosomas analizados para cada la condición se muestra con "n" y se realizó una prueba t no emparejada. c) Correlación entre HP1a y la pérdida del patrón de bandas cromosómicas. **** equivale a un valor de p <0.0001, se realizó una ANOVA unidireccional, wt oraganizado n=59, > dAdd1 moderado= 40, > dAdd1 severo=25.

Una posibilidad de la pérdida de HP1a era que esta proteína cambiara su localización subnuclear, ya que dejo de estar unida al cromocentro. Para determinar si este era el caso, realizamos inmunofluorescencias de HP1a en las glándulas salivales con los núcleos intactos para evaluar si la pérdida de HP1a de la cromatina fue el resultado de un cambio en su localización subnuclear. Dirigimos la expresión de dADD1a, b y todas las isoformas usando el "driver" *Sgs3-GAL4* y analizamos la localización de HP1a mediante inmunofluorescencia. En las glándulas salivales "*wild type*", HP1a aparece como un punto focalizado único que marca el cromocentro (J C Eissenberg and Elgin 2000) (ver Figura 17a), donde el 92% de los núcleos contados presentaron este único punto y su localización es nuclear ya que no se observa en citoplasma. La sobreexpresión de todas las isoformas genera un cambio en la distribución de HP1a, donde el 70% de los núcleos presentan una distribución amplia. Cuando se realiza la sobreexpresión de manera individual podemos ver que la sobreexpresión de dADD1a produce una distribución amplia de HP1a en 48% de los núcleos. Por el contrario, las células que sobreexpresan dADD1b exhibían una distribución amplia en el 18% de las células analizadas y 19% de ellos mostraban una distribución de HP1a en dos puntos focales, pero la mayoría tenía una distribución de HP1a tipo "wild *type*". Si examinamos los porcentajes con mayor detalle, la sobreexpresión combinada de dADD1a y dADD1b es responsable de casi el 70% (48% más 18% = 66%) de la distribución amplia de HP1a Figura 17b. Sin embargo, dADD1a tiene el efecto más marcado en la distribución de HP1a, esto podría ser el resultado de la interacción entre estas dos proteínas (Alekseyenko et al. 2014; Swenson et al. 2016; Brenda López-Falcón et al. 2014).

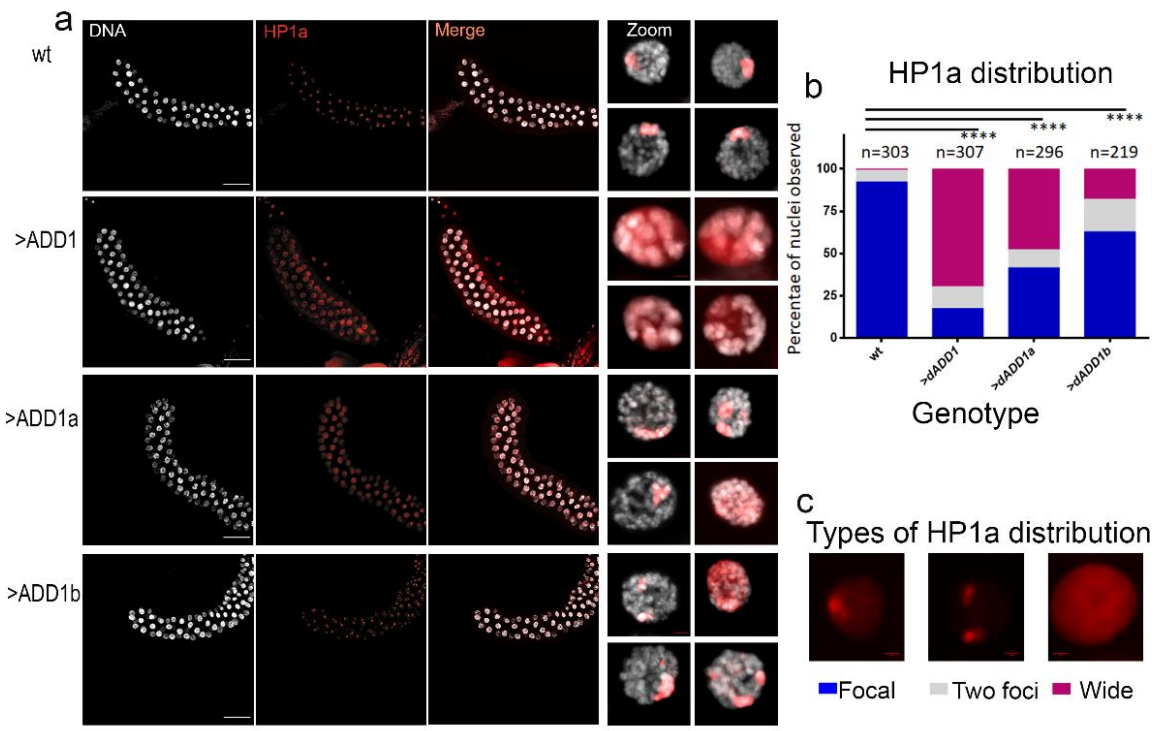

Figura 17. La sobreexpresión de las proteínas dADD1 cambia la distribución de HP1a en las glándulas salivales completas. a) Inmunohistoquímica de una glándula salival "*wild type*" con el anticuerpo contra HP1a (wt), *UAS-dADD1;Sgs3-GAL4* (> dAdd1), *Sgs3-GAL4/UAS-dADD1a* (> dAdd1a) y *Sgs3-GAL4/UAS-dADD1b* (> dADD1b), HP1a (señal roja), ADN (señal gris) y barra de escala de 100 µm. La columna de la derecha muestra una imagen ampliada de varios núcleos con una barra de escala de 5 µm. b) Distribucion de HP1a en los núcleos, se le asignó una escala de"1" para focal, "2" para dos puntos y "4" para amplio, "n" representa el número de núcleos analizados en cada genotipo. . **** equivale a un valor de p <0.0001, se realizó una la prueba de Kruskal-Wallis. c) Clasificación de las distribuciones de HP1a (señal roja) encontradas en los núcleos, focal, dos puntos y amplio, la barra de escala es de 5 µm.

Para determinar si existían diferencias en diámetro del núcleo cuantificamos el área de los núcleos para ver si cambiaba con la sobreexpresión de dADD1, pero no pudimos encontrar diferencias significativas cuando lo comparamos con los núcleos control, esto también nos dio una idea que no estaba incrementando la cantidad de ADN dentro del núcleo y por eso medimos la intensidad del DAPI y no observamos diferencias. Estos datos sugieren que la sobreexpresión de dADD1 no afecta el tamaño de los núcleos aun cuando parece haber una descompactación de la cromatina ni la cantidad de ADN en estas las células (Figura 15).

Como se mencionó anteriormente, las isoformas de la proteína dADD1 conservan una región común que incluye el dominio ADD, la diferencia entre ellas es la presencia en la parte del carboxi-terminal de dominios MADF adicionales en la isoforma dADD1b que no están presentes en la isoforma dADD1a (Figura 14e). Por lo tanto, es posible que la región

común tenga un papel esencial en la alteración de la localización focal de HP1a. El dominio ADD reconoce y se une a H3K9me3 en combinación con H3K4 sin ninguna modificación; por lo tanto, consideramos como una posibilidad que la sobreexpresión de dADD1 pudiera "competir" con HP1a para unirse al H3K9me3.

6.3 La marca de H3k9me3 disminuye en respuesta a la sobreexpresión de las proteínas dADD1

Se anticiparon al menos dos escenarios posibles, en el primero las proteínas dADD1 podrían "agotar o eliminar" a HP1a del cromocentro de las glándulas salivales directamente a través de interacciones proteína-proteína. En el segundo escenario podría existir una competencia entre HP1a y dADD1 por el sitio de unión H3K9me3.

Se ha demostrado ampliamente que la modificación postraduccional de H3K9me3 es necesaria para mantener la heterocromatina pericéntrica y que esta marca de histona se enriquece en el cromocentro de los cromosomas politénicos (Schotta et al. 2002). Cualquier perturbación de esta marca conduce a la pérdida de HP1a del cromocentro (Rudolph et al. 2007; Wood et al. 2010). La heterocromatina constitutiva se establece temprano en el desarrollo. En *Drosophila*, comienza durante MBT ("*Mid-Blastula Transition*") (en el ciclo 13 del desarrollo embrionario de Drosophila) (Seller, Cho, and Farrell 2019). El modelo propuesto involucra un complejo que contiene una metiltransferasa (Eggless / SetDB1) de histona H3 lisina 9 y HP1a. La marca de histona H3K9me (di o tri metilada) actúa como un sitio de unión para HP1a, que se une a través de su CHD a estas marcas de cromatina (Jacobs et al. 2001). Posteriormente también participa la metiltransferasa *Su(var)3-9* que se encarga de depositar la marca de trimetilación y forma un complejo con HP1a (Yamamoto and Sonoda 2003). Por lo tanto, se decidió evaluar si esta marca se conservaba en las células que sobreexpresan dADD1.

Se realizó una doble inmunotinción de H3K9me3 y HP1a en cromosomas politénicos de células "*wild type*" o que sobreexpresan dADD1. Las imágenes confocales representativas se muestran en la Figura 18a. En los cromosomas "*wild type*", las señales H3K9me3 (verde) y HP1a (rojo) se enriquecen en el cromocentro como se ha descrito anteriormente (Schotta et al. 2002), todos los cromosomas "*wild type*" analizados presentaron ambas señales (100%) (Figura 18a, primera columna).

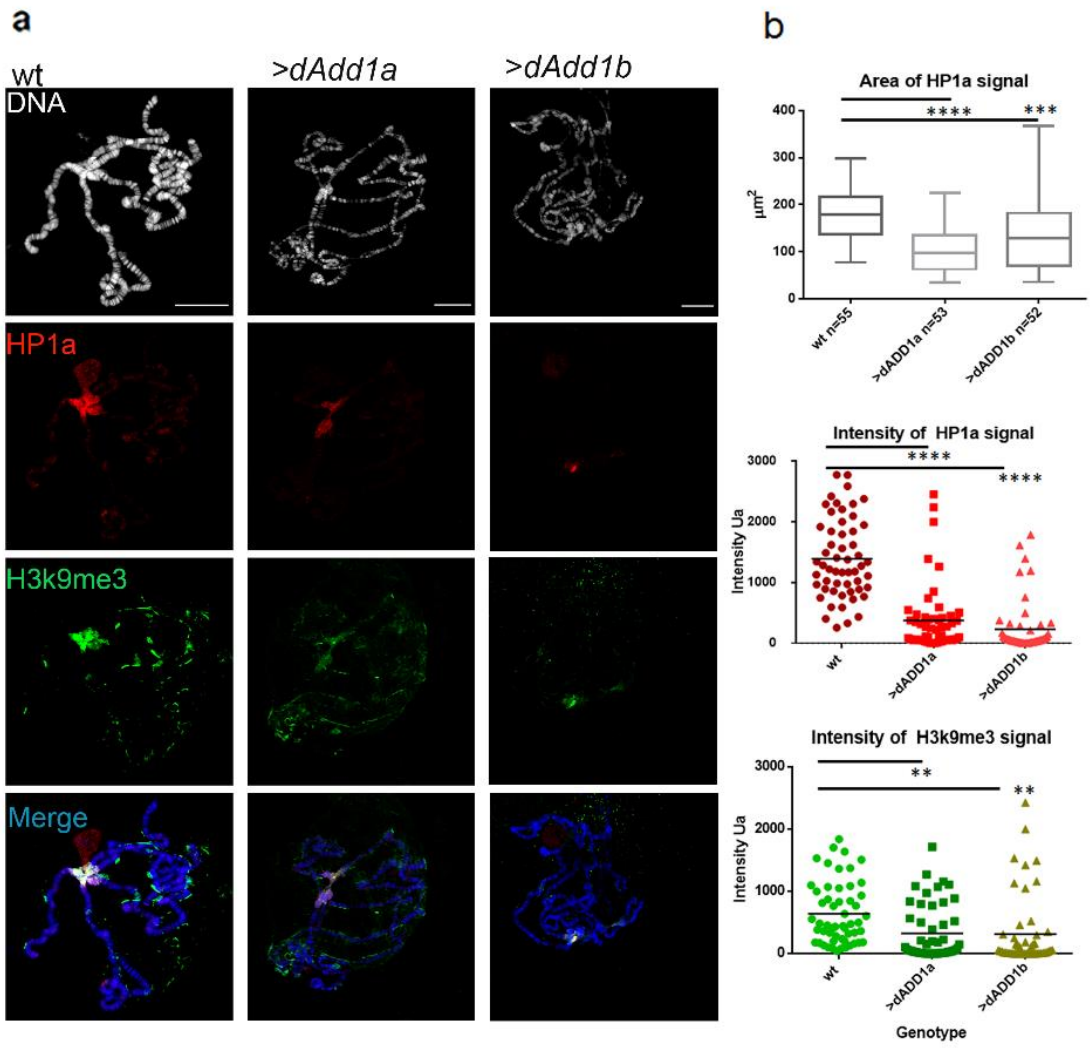

Figura 18. La sobreexpresión de las proteínas dADD1 perturba la señal de H3K9me3. a) Inmunotinción de cromosomas politénicos "*wild type*", *Sgs3-GAL4/UASdADD1a* (> dAdd1a) y *Sgs3-GAL4/UAS-dADD1b* (> dADD1b), ADN (la tinción DAPI se muestra en gris), HP1a (señal roja), H3K9me3 (señal verde) y la fusión de colores, la barra de escala es de 20 µm. b) El área de señal de HP1a se cuantificó mediante ImageJ, así como la intensidad de la señal de HP1a y H3K9me3, "n" representa el número de cromosomas analizados en cada genotipo; Se realizó una prueba ANOVA unidireccional ordinaria para determinar si fue significativo p <0.05 *, <0.01 **, <0.001 ***, <0.0001 ****

Al sobreexpresar las isoformas dADD1a o b, el patrón de bandas del cromosoma se mantiene, pero hay menos señal de HP1a (Figura 18a columna media y derecha), y el área cuantificada de HP1a se ve ligeramente menos afectada con la sobreexpresión de dADD1b. Sin embargo, este efecto podría deberse a que la mayoría de los cromosomas tenían una señal de HP1a "dividida" (se muestra un cromosoma representativo en la Figura 19a, columna derecha y gráfico de área de la Figura 18b) como si el cromocentro fuera más frágil y propenso a "romperse" con el procedimiento mecánico para obtener los cromosomas.

Estos resultados coinciden con los observados en la figura anterior (Figura 17a), donde la sobreexpresión de dADD1b produce mayor presencia del fenotipo de dos foci en la señal de HP1a.

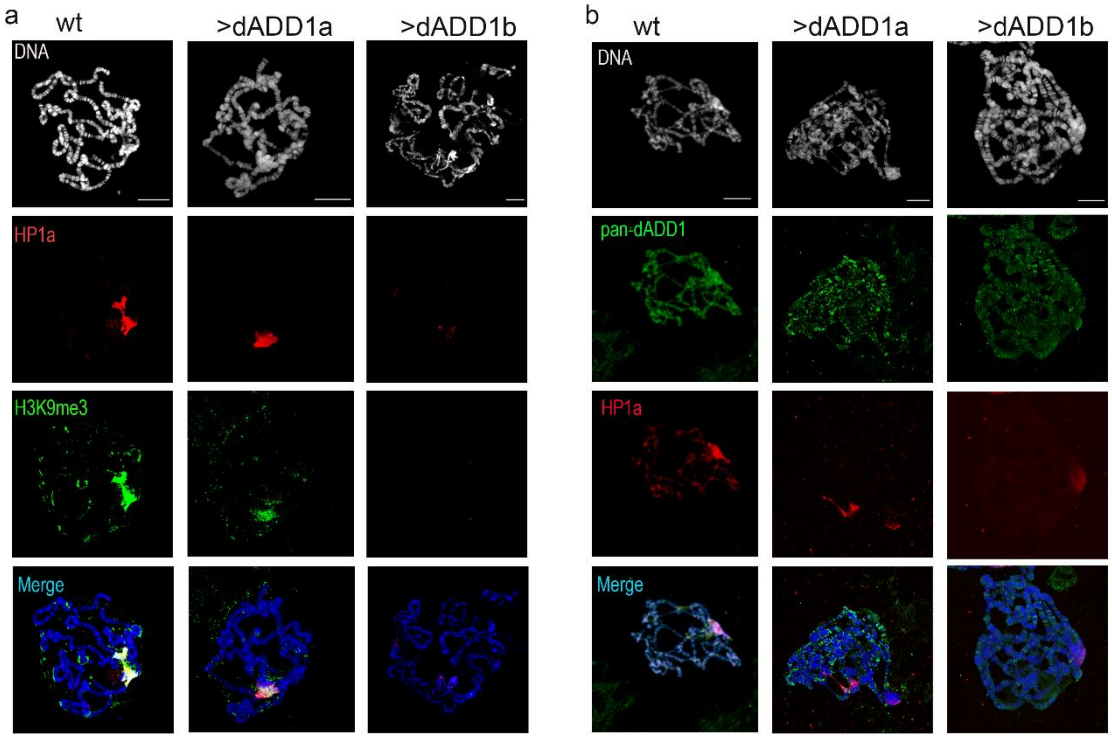

Figura 19. La sobreexpresión de las isoformas dADD1 a y b, perturba la señal H3K9me3 y dADD1. a) Inmunotinción de cromosomas politenicos *wild type*, y sobreexpresión de las proteínas dADD1 a y b, ADN (señal gris), HP1a (señal roja), H3K9me3 (verde) y "*merge*", barra de escala 20 µm. b) Inmunotinción de los cromosomas politenicos a partir de proteínas dADD1 de tipo silvestre y sobreexpresión. Genotipo: *Sgs3-GAL4/ UAS-dADD1a* y *Sgs3-GAL4/UAS-dADD1b*, ADN (señal gris), pan-dAdd1 (verde), HP1a (señal roja) y "*merge*", barra de escala 20 µm.

Estos resultados indican que la sobreexpresión de dADD1 no compite con HP1a para unirse a su sitio de reconocimiento en la cromatina, pero podría afectar de alguna manera al cromocentro titulando los complejos que contienen HP1a. Uno de los complejos que se forma en el cromocentro y que afectaría estas dos señales es el que se forma de la unión de HP1a junto con la metiltransferasa Su(var)3-9, que es una enzima con actividad de histona metiltransferasa, gracias a su dominio SET, es específica para la lisina 9 de la histona 3 (Tschiersch et al. 1994; Greil et al. 2003a; Figueiredo et al. 2012). HP1a y la metiltransferasa interaccionan por medio del dominio CSD (Schotta et al. 2002; H. Ito et al. 2012; Swenson et al. 2016), por medio de este dominio también interaccionan HP1a y XNP (que es el dominio helicasa/ATPasa para completar el homólogo de mamíferos) (Bassett et al. 2008). Por medio de una búsqueda bioinformática, encontramos que dADD1 tiene un pentapéptido putativo de unión a HP1a, PxVxL, conocido por unirse a la interfaz del dominio CSD (Meyer-Nava et al. 2020). Hipotetizamos que un exceso de proteínas dADD1 podrían

estar saturando el dominio CSD y evitando que se unan otras proteínas a HP1a y eso afectaría los complejos que se unen al cromocentro. Las proteínas que podrían verse afectadas cuando dADD1 está saturando el sistema son: Hip/HP4 (Schwendemann et al. 2008; Hines et al. 2009), Su(var)3-7 (Cléard and Spierer 2001; Delattre et al. 2000), Kdm4A (Alekseyenko et al. 2014; Lin et al. 2008; Swenson et al. 2016), Ssrp (Kwon et al. 2010), Su(var)2-HP2 (Shaffer et al. 2002; Mendez, Mandt, and Elgin 2013), HP6 (Joppich et al. 2009), egg (D. H. Lee et al. 2019) y G9a (D. H. Lee et al. 2019) entre otras que aun desconocemos.

6.4 Los niveles de dADD1 determinan cambios en la abundancia de transcritos heterocromáticos

Algunos genes se encuentran integrados en la heterocromatina y necesitan este contexto circundante para su correcta expresión y también requieren la presencia de HP1a (Cryderman, Vitalini, and Wallrath 2011). Dado que HP1a se deslocalizó de muchas regiones tras la sobreexpresión de dADD1, se decidió analizar si los transcritos de genes ubicados en heterocromatina, tenían una expresión anormal.

Para realizar el siguiente experimento se seleccionaron algunos genes que previamente habían sido descritos por medio de la técnica de perfilado de cromatina DamID, que es un protocolo para mapear los sitios de unión de proteínas de unión a ADN y cromatina. DamID identifica los sitios de unión expresando la proteína de unión al ADN de interés con una proteína de fusión con la metiltransferasa del ADN. La unión de la proteína de interés al ADN localiza la metiltransferasa en la región del sitio de unión. La metilación de adenina no ocurre naturalmente en eucariotas y, por lo tanto, se puede concluir que la metilación de adenina en cualquier región ha sido causada por la proteína de fusión, lo que implica que la región está ubicada cerca de un sitio de unión. DamID es un método alternativo a ChIP-on-chip o ChIP-seq (Greil et al. 2003b). Estos genes se encuentran ubicados en regiones pericéntricas y necesitan de HP1a para su expresión adecuada en glándulas salivales. Entre ellos se encuentran: “cinnamon” (*cin*), “mini spindles” (*msps*), CG7742 (Fanti et al. 2003), light (*lt*), “rolled” (*rl*)(Lu et al. 2000) y concertina (*cta*)(T. J. R. Penke et al. 2016). Estos genes se ubican en diferentes cromosomas y regiones heterocromáticas (Greil et al. 2003b; T. J. R. Penke et al. 2016). Además decidimos evaluar otros genes porque están silenciados en las glándulas salivales, como “Kraken” (*kra*) y ”*P-element somatic inhibitor*” (*psi*) o porque son parte de los complejos necesarios para la cohesión cromosómica adecuada, como “verthandi” (*vtd*) y “Nipped-b” (Hallson et al. 2008). También evaluamos genes eucromáticos como controles negativos ya que no están regulados directamente por HP1a o Su (var)3–9.

Usando PCR tiempo real (qRT-PCR), se analizó la abundancia de transcritos de estos genes en glándulas salivales “*wild type*” (barra gris), glándulas salivales que sobreexpresen dADD1a (barra roja) o b (barra azul oscuro) y también glándulas salivales de organismos nulos dADD1 (barra aqua) (ver Figura 20). Con anterioridad habíamos encontrado una colocalización de las proteínas HP1a y dADD1 particularmente en el cromocentro de

cromosomas politénicos y también en algunas bandas a lo largo de los brazos (Brenda López-Falcón et al. 2014) por lo que decidimos evaluar todas las condiciones posibles de expresión de dADD1.

Para normalizar los datos se utilizó *Rp49* (un gen que codifica una proteína ribosomal) ya que los niveles de este transcrito se mantuvieron muy similares entre todos los genotipos. Para tener la certeza de que el experimento se estaba llevando a cabo de forma adecuada primero se realizó el análisis de los transcritos de las isoformas sobreexpresadas de manera individual dADD1a o b (Fig. 20a panel superior etiquetado como "controles"). Como era de esperarse cada isoforma se sobreexpresó más de 3 veces (Fig. 20a comparar barras rojas vs barras grises, barra azul vs barra gris).

Posteriormente se analizaron los transcritos de las proteínas encargadas de mantener silenciados estos genes, como lo son S*u(var)3-9* (la metiltransferasa que pone la marca de trimetilación) y *Su(var)205* (el gen que codifica HP1a) y sus niveles de expresión no se vieron afectados en todos los genotipos analizados (Fig. 20a). Esto sugiere que los efectos previamente observados sobre la pérdida de la localización de HP1a y H3K9me3 (Figs. 17 y 18) no se deben a un defecto en la transcripción de estos genes.

De igual manera los genes eucromáticos como *A*ct5C y Sgs8, así como los genes regulados por Su (var) 3-9 no fueron afectados (Fig. 20b y c). Los únicos genes afectados fueron los genes regulados por HP1a tales como *t*oy y *l*gs (Fig. 20d) y los genes regulados por las dos proteínas Su(var)3-9/HP1a como *Ank* (Fig 20e) y genes pericéntricos como *cta* y *light* (Fig. 20f).

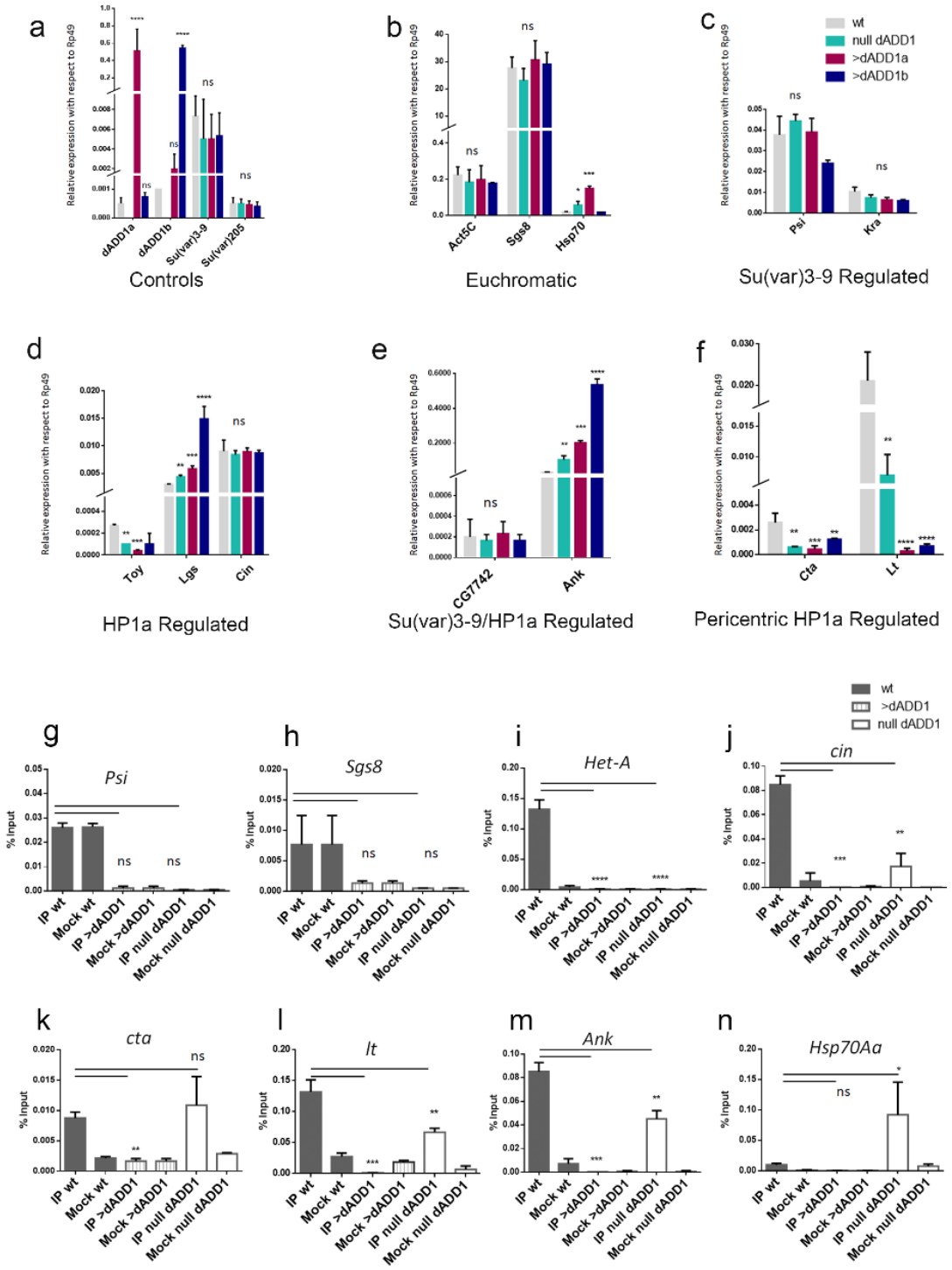

Figura 20. La sobreexpresión de dADD1 da como resultado el silenciamiento transcripcional y la ausencia de la proteína HP1a en algunos genes. Análisis qRT-PCR(a-f), "*wild type*" (barras grises), nulo dADD1 (barras de aqua), *Sgs3-GAL4/UAS-dADD1a* (barras rojas) y *Sgs3-GAL4/UAS-dADD1b* (barras de color azul oscuro). Tres réplicas biológicas independientes junto con dos replicas técnicas fueron realizadas. Los datos se muestran como expresión

relativa a la transcripción de *Rp49*. Se realizó una prueba de ANOVA unidireccional ordinaria para determinar si era significativo con valores de p: (p <0.05 *, <0.01 **, <0.001 ***, <0.0001 ****, ns, no significativo). a) controles, b) genes de eucromatina, c) genes regulados por Su(var)3–9, d) genes regulados por HP1a, e) genes regulados por Su(var)3-9 y HP1a, f) genes pericéntricos. Se realizaron ensayos de inmunoprecipitación de la cromatina usando el anticuerpo C1A9 (anti-HP1a) y la IgG de ratón como control en glándulas "*wild type*" (barra gris oscuro), glándulas sobreexpresando todas las isoformas (> dADD1 barra con líneas), glándulas nulas (barra blanca) (g-n). Psi, Sgs8 y Hsp70 son genes eucromáticos sin la presencia de HP1a (g, h y n) por lo que no hay enriquecimiento vs la condición "*wild type*". El promotor del retrotransposón Het-A (i) y Cin (j) se evaluaron como regiones teloméricas y subteloméricas en las que se localiza HP1a. Cta (k) y Lt (l) son pericentroméricos, y HP1a también los regula. Ank está regulado por Su(var)3-9 y HP1a (m). Las barras de error representan la desviación estándar. Valores p (p <0.05 *, <0.01 **, <0.001 ***, <0.0001 ****, ns, no significativo).

Debido a que aún no contamos con datos de ChIP-seq en estas células, decidimos analizar los datos de ChIP-seq del Laboratorio de la Dra Kuroda previamente publicados. En estos experimentos se utilizó una etiqueta para identificar los sitios a los que se une dADD1a en experimentos ChIP-seq en células S2 (Alekseyenko et al. 2014) y así evaluar la presencia de dADD1a en los mismos genes de la Fig. 20 (a-f). Aunque las células S2 son embrionarias, la posición de los genes en el cromosoma no cambia, y tampoco lo hace la heterocromatina constitutiva; por lo tanto, los datos de ChIP-seq ayudan a obtener más información sobre la posición de dADD1a en regiones heterocromáticas. Se encontró que dADD1a no está presente en genes eucromáticos como *sgs8* y *actina*, ni en *su(var)205* y *su (var)3–9*, ni en genes controlados por Su(var)3–9 como *psi* y *kraken* (Figura 21), esto coincide con que la transcripción de estos genes que no fue alterada. Cuando se examinaron los genes controlados exclusivamente por HP1a (J C Eissenberg et al. 1990), solo se encontró a dADD1a en *toy* y *lgs*, que están ubicados en el cromosoma cuatro, que es principalmente heterocromático, mientras que en *cin* no hay presencia de dADD1a. Cabe resaltar que el efecto en la transcripción es diferente en estos genes cuando no hay dADD1 o cuando se sobreexpresa, y pareciera que es mayor la afectación cuando hay un exceso, como si se satura el sistema. En los genes controlados por HP1a/Su(var)3–9, dADD1a se localiza en *Ank* pero no en *CG7742* (ver Figura 21) y esto correlaciona con el cambio en la expresión analizado en la figura 20e, ya que a mayor expresión de dADD1 se ve que hay más expresión en el transcrito de A*nk*. También existe la presencia de dADD1a en los genes pericentroméricos, *lt* y *cta*, donde dADD1a se encuentra en el promotor, pero también sobre el del cuerpo del gen. Esto nos sugiere que la presencia de dADD1 tiene un efecto en la regulación de la transcripción de estos genes, principalmente los que se encuentran en la heterocromatina.

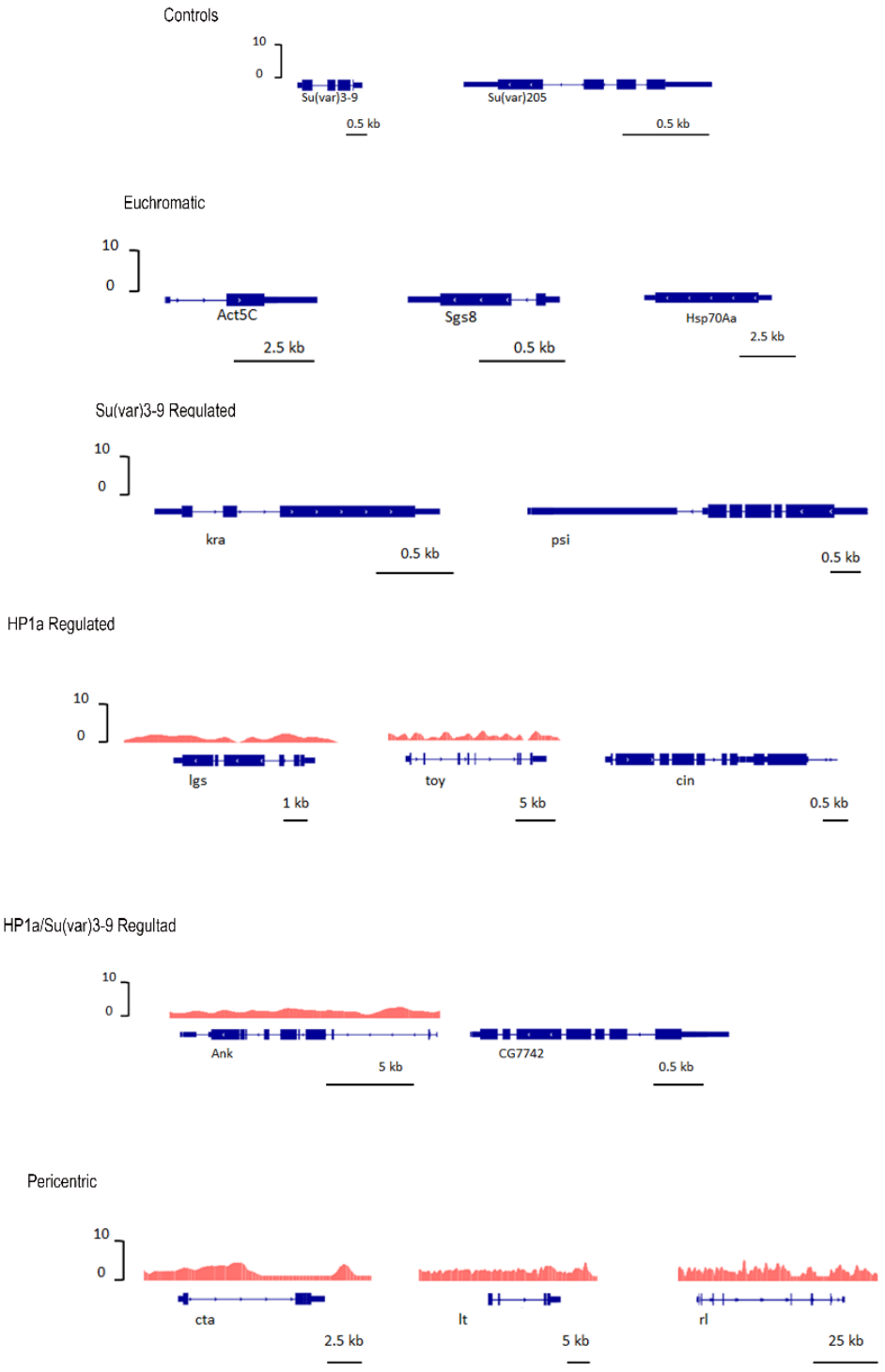

Figura 21. Localización de la proteína dADD1a en los genes analizados. La proteína dADD1a (picos rosados) se encuentra principalmente en el promotor, y a través de los cuerpos del gen en los genes pericéntricos (cta y lt). También en Ank que se encuentra controlado por HP1a/Su (var)3-9. dADD1a no está presente en genes eucromáticos como Sgs8, Actina y

Hsp70Aa. Tampoco se encuentra presente en genes controlados por Su (var)3-9 como Psi y kraken, de igual forma que genes exclusivamente controlados por HP1a como toy o lgs.

La mayoría de los genes de la Figura 20a-f se encuentran regulados a la baja en los organismos nulos dADD1 o en la sobreexpresión de las isoformas dADD1a o b. Es importante mencionar que todos estos genes tienen la presencia de dADD1 en células S2 (Figura 21). Los únicos dos genes que mostraron una sobreexpresión en condiciones nulas de dADD1 o de ganancia de función fueron *lgs* y *Ank* (Fig 20d y e). Un gen interesante fue el gen de respuesta a choque térmico *Hsp70*, el cual parece aumentar su transcripción tanto en la falta de dADD1 como en la sobreexpresión de la isoforma a, mas no la b (Figura 20b).

La disminución de la transcripción de varios genes en las distintas condiciones de sobreexpresión de dADD1 o nulas en dADD1 también puede deberse a su localización en el cromosoma o en el tipo de cromatina a la que se encuentran asociados. Por ejemplo, *cta* y *light* están en regiones pericéntricas (Figura 22) y tuvieron el mismo comportamiento, es decir se disminuyó su transcripción en cualquiera de las condiciones de dADD1 respecto al "*wild type*". Los genes *lgs* y *Ank* se encuentran ubicados en el cromosoma 4 (Figura 22) que es altamente heterocromático, pero no son pericéntricos ni teloméricos. Por lo tanto, la falta o aumento de dADD1 podría dar diferentes resultados dependiendo del gen analizado y su localización en el cromosoma. En la literatura se ha descrito que la regulación a la baja de los genes pericéntricos se debe a la pérdida de HP1a (J C Eissenberg et al. 1990; Joel C. Eissenberg and Elgin 2014).

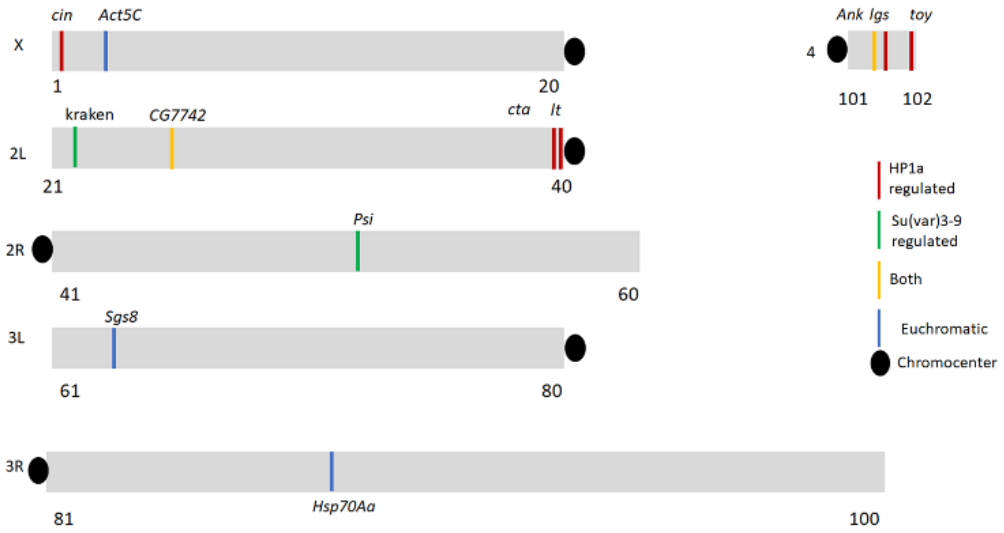

Figura 22. Representación de los cromosomas politénicos de *Drosophila* y la ubicación de los transcritos analizados en la Fig. 20. Los números debajo de cada cromosoma corresponden a ubicaciones del mapa citogenético. Los genes regulados por HP1a se muestran en rojo, los genes regulados por Su (var)3-9 se muestran en verde y en amarillo,

los genes que están regulados por ambas proteínas. Los genes eucromáticos se representan con líneas azules. Un círculo negro representa el cromocentro.

Para investigar los cambios en la unión de HP1a en estos genes que fueron afectados respecto a su transcripción, se realizó una inmunoprecipitación de la cromatina seguida de PCR cuantitativa (ChIPqPCR). Primero, se analizaron dos genes que no están regulados por HP1a, los cuales son *Psi* y *Sgs8*, que no muestran ningún enriquecimiento de HP1a versus el control (anticuerpo IgG, ver Figs. 20g y h). Posteriormente se analizó una región que sabemos que es blanco de HP1a, el promotor de Het-A, como podemos ver en la Fig. 20i, donde hay un enriquecimiento de HP1a en esta región en los organismos "*wild type*". En organismos que carecen de proteínas dADD1, HP1a ya no está presente en este sitio, coincidiendo con la publicación anterior (Chavez et al. 2017); de igual forma la sobreexpresión de todas las proteínas dADD1conduce a la pérdida de HP1a en esta región telomérica. El mismo efecto se puede ver en *light*, *Ank* y *cin* (Fig 20l, m y j). En el caso de *light* y *ank*, se puede observar que la pérdida de HP1a conduce a efectos opuestos en la transcripción, *light* se regula negativamente y *Ank* está regulado positivamente, esto indica que hay un papel diferencial para HP1a y posiblemente para dADD1 en estos sitios.

Sorprendentemente, aunque en el gen *cin* se pierde HP1a, tanto en la sobreexpresión como en la condición nula, la transcripción no se ve afectada (Fig. 20 d y j). *Cta*, que también es un gen con localización pericéntrica, obtuvo menores niveles de transcritos en todas las condiciones analizadas, conserva HP1a en las glándulas nula (Fig. 20k). Otro resultado inesperado fue cuando se analizó la expresión de *Hsp70Aa*; en organismos nulos de dADD1 y en la sobreexpresión de dADD1a, el gen se está sobreexpresando, esta respuesta podría ser indirecta, ya que la proteína dADD1 no se encuentra presente en el gen de Hsp70Aa y este transcrito se sobreexpresa en condiciones de estrés, sin embargo, en condiciones nulas HP1a se enriquece en el promotor de este gen (Fig. 20n). Este dato podría ser interesante ya que pudiera existir un mecanismo de regulación transcripcional, por ejemplo, este gen podría estar regulado por la presencia de HP1a.

En general, los datos encontrados en el presente trabajo indican que la expresión incorrecta de dADD1, ya sea aumentada o nula, tiene un impacto importante en la estructura de la cromatina y algunas veces en la localización de HP1a, lo que conduce a diferencias en la expresión de genes principalmente heterocromáticos. Esto sugiere que dADD1 coopera con HP1a para mantener la expresión de estos genes. La transcripción de genes de eucromatina no se vio afectada pero un gen interesante de analizar posteriormente sería el gen de respuesta a calor Hsp70Aa que parece estar regulado positivamente en las condiciones que analizamos dADD1. Nuestros resultados indican que dADD1 podría ser un regulador de este gen (Elmallah, Cordonnier, and Vautrot 2019).

6.5 La localización de dXNP en cromosomas politénicos se altera con cambios en la expresión de dADD1

En el trabajo previo de nuestro laboratorio se identificó a dXNP como un interactor de dADD1 (Brenda López-Falcón et al. 2014), ya que dXNP carece de un sitio de unión al ADN, se propuso que otras proteínas la llevaban a sus sitios blanco en la cromatina. Debido a lo anterior, se decidió analizar si la sobreexpresión de dXNP fenocopia la pérdida de heterocromatina observada en la sobreexpresión de dADD1. La sobreexpresión de la parte helicasa/ATPasa se realizó de la misma forma usando el sistema UAS-GAL4 y el mismo "driver" de glándulas salivales Sgs3. De primera instancia se observó la distribución de HP1a en las glándulas salivales completas donde se encontró que la distribución focal de HP1a se mantiene. Sin embargo, cuando se realizó la comparación de la sobreexpresión de dXNP en las glándulas salivales respecto a las "*wild type*", la cromatina parece más compacta, y la señal HP1a, aunque presente se puede observar disminuida (ver Fig. 23a).

Observando esto, se midió el área de los núcleos y se encuentran significativamente más pequeños cuando se sobreexpresa dXNP (Fig. 23b). No se cuantificó la cantidad de ADN, ni se hicieron experimentos respecto a la replicación, es decir si presentaban menor cantidad de ciclos de endoreplicación en este genotipo. Otra posible explicación de este fenotipo es que se estén reclutando otras proteínas que promuevan la formación de heterocromatina de forma independiente de HP1a. Finalmente se observaron los cromosomas politénicos y se apreció que en condiciones "*wild type*", estas proteínas colocalizan y también se observó la localización telomérica de dXNP, como se esperaba (Fig. 23d primera fila e imágenes ampliadas). Tras la sobreexpresión de dXNP, el número de bandas aumentaba, así como la señal en ciertas regiones heterocromáticas, como los telómeros (Fig. 23d). Entonces se puede concluir que se está sobreexpresando correctamente dXNP y que esta sobreexpresión afecta el tamaño del núcleo, a pesar de que se sigue observando la señal de HP1a.

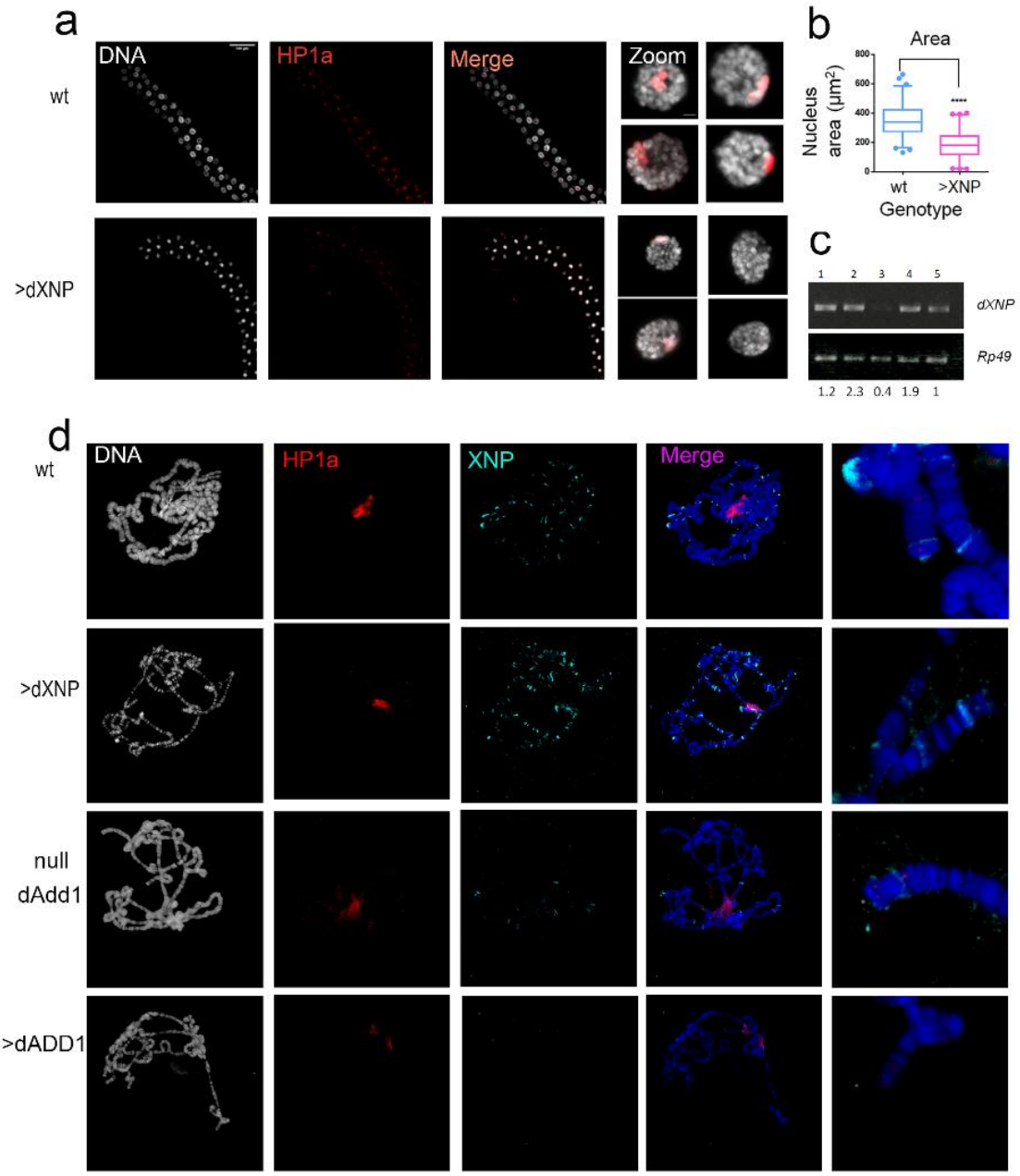

Figura 23. La sobreexpresión de dADD1 provoca cambios en la unión de dXNP. a) inmunotinción de una glándula salival "*wild type*" con el anticuerpo HP1a (wt) y sobreexpresión de dXNP (> dXNP) *Sgs3-GAL4/UAS-dXNP*. HP1a (señal roja), ADN (señal gris) y fusión de colores (barra de escala 100 µm). En la columna de la derecha se muestra la ampliación de varios núcleos (barra de escala de 5 µm). b) Cuantificación del área del núcleo que muestra una reducción en el área nuclear, wt n = 341 y >dXNP n = 344. c) Análisis de RT-PCR de los niveles de transcritos de dXNP en glándulas salivales. Los carriles en el gel corresponden a los siguientes genotipos 1)"*wild type*" (wt) 2) *Sgs3-Gal4/UASXNP* (>dXNP),

3) *xnp^2/xnp^3* (condición heteroalélica en la que disminuyen los transcritos de dxnp), 4) *dadd1^2 / dadd1^2* (nulo dADD1) y 5) *UAS-dadd1;Sgs3-GAL4* (>dADD1). El transcrito de *Rp49* se utilizó como control; los números en la parte inferior son las cuantificaciones de la intensidad de las bandas con respecto a *Rp49* . d) Inmunotinción de cromosomas politénicos "*wild type*" (wt), *Sgs3-GAL4/UAS-XNP* (> XNP), *dadd1^2 / dadd1^2* (nulo dAdd1) y *UAS-dADD1;Sgs3-GAL4* (> dADD1), ADN (tinción DAPI en gris), HP1a (señal roja), dXNP (señal cian) y fusión de colores. La columna derecha presenta un aumento de las regiones teloméricas.

En organismos nulos para dADD1 o bien en la sobreexpresión de dADD1, la señal dXNP disminuye, y solo se conservan pocas bandas con la señal de la proteína dXNP en los cromosomas politénicos (ver Fig. 23d color cian últimas dos filas). Posteriormente, se examinaron los transcritos producidos por el gen dXNP y se expresan normalmente en todos los genotipos analizados (comparar líneas 1 vs 4 y 5 en la figura 23c). Por lo tanto, la falta o la sobreexpresión de dADD1 no afecta la transcripción de dXNP, solo la ubicación de la proteína en la cromatina. Estos resultados demuestran que ante la pérdida de dADD1, dXNP pierde su localización en la cromatina y esto podría conducir a la pérdida de la compactación de la cromatina. Curiosamente, tras la sobreexpresión de dXNP, parece que la cromatina se compacta de manera general y esto a su vez coincide con la presencia de más bandas dXNP en cromosomas politénicos. El que los fenotipos sean completamente opuestos podría dar indicios de lo que hace cada dominio en la proteína completa de mamíferos. Usando *Drosophila* podemos observar que al incrementar la presencia del dominio ADD la cromatina se ve más laxa, lo cual podría inhibir la correcta formación de la heterocromatina como se ha propuesto en conjunto con HP1a y una metiltransferasa. Por otro lado, el dominio Helicasa (dXNP) podría estar actuando como Helicasa/ATPasa y favoreciendo la compactación de la cromatina, inclusive podría estar interactuando con otros factores de transcripción que promuevan el cerrado de la cromatina.

7. DISCUSIÓN

Cada vez son más las evidencias que indican que los mecanismos epigéneticos son importantes para la regulación de la expresión genética y la estabilidad del genoma. La cromatina es una macromolécula que presenta un alto nivel de dinamismo y dada su importancia y participación en diversos procesos, como la transcripción y duplicación, ha sido blanco de estudios durante los últimos años. Entre los procesos más estudiados se encuentra la regulación de la transcripción génica. La complejidad de los mecanismos se refleja en la gran cantidad de proteínas que intervienen en el proceso. A nivel mundial son varios los laboratorios que estudian el papel de la pérdida de función de muchos factores transcripcionales y remodeladores de la cromatina en células cancerosas, y muchas bases de datos han podido concentrar estos datos para entender mejor esta importante enfermedad. Justamente una de las líneas de investigación del laboratorio es la proteína ATRX que toma mayor relevancia como un factor involucrado en la regulación transcripcional y la estabilidad del genoma en células de mamíferos.

Se han asociado mutaciones de pérdida de función de ATRX con varios tipos de cáncer, desde glioblastoma hasta cáncer de páncreas (Singhi et al. 2017). El número de estas mutaciones ha aumentado en los últimos años, y muchas de ellas afectan los dominios que son esenciales para la función de la proteína (Schwartzentruber et al. 2012). Si bien la mayoría de los estudios se han concentrado en la pérdida de función, también hay informes que muestran la sobreexpresión de ATRX en diferentes tipos de cáncer. Muchos genes se desregulan y sobreexpresan durante el proceso de transformación de las células. Durante la investigación que se llevó a cabo en este trabajo encontramos varios casos de cáncer en células o en tejido somático que tienen sobreexpresión de ATRX en las principales bases de datos a las que tuvimos acceso (Figura 13). En la bibliografía hay una única publicación donde se ha evaluado la sobreexpresión de ATRX en ratón observando los mismos fenotipos que con la pérdida de función (Berubé et al. 2002), que son retraso del crecimiento, defectos del tubo neural y una alta incidencia de muerte embrionaria. Además, si los ratones sobrevivían el nacimiento tenían un alto índice de muerte perinatal, así como convulsiones, anomalías craneofaciales leves y comportamiento anormal (Berubé et al. 2002).

La sobreexpresión de las proteínas dADD1 dio como resultado la pérdida de la estructura de la cromatina, y causó una descompactación general y la disociación de las fibras de cromatina alrededor del cromocentro (Figs. 14 y 16). Estos fenotipos fueron más fuertes cuando la sobreexpresión se realizó con todas las isoformas de dADD1. En las glándulas salivales "*wild type*", los niveles de transcripción de dADD1 son bajos en comparación a otros transcritos analizados (ver Fig. 20). Estos resultados indican que los niveles de dADD1 en los cromosomas politénicos deben mantenerse constantemente regulados en cantidades óptimas para lograr una correcta estructura de cromatina. El complejo de cohesinas es un factor importante para mantener unidos los brazos de los cromosomas. En *Drosophila* se ha caracterizado la distribución del complejo formado por Vtd (Rad21), Smc1, Nip-B, SA y Smc3 (Pherson et al. 2019) y podría existir un complejo entre estas proteínas o una interacción indirecta aun no reportada (Meyer-Nava et al. 2020).

El dominio ADD está compuesto por un dominio PHD y un dedo de zinc del tipo GATA (Argentaro et al. 2007). Es notorio que mutaciones en los genes que codifican para proteínas que contienen el dominio PHD, están involucrados en distintas enfermedades en humanos como leucemia, cáncer de mama y melanoma así como en distintos síndromes como el "Weaver, Rubinstein–Taybi" y "Borjeson Forssman Lehmann" que afectan a las líneas germinales como lo hace el síndrome de ATRX (Baker, Allis, and Wang 2008). En todas estas enfermedades se han reportado mutaciones en los PHD y se propone que la mala interpretación o la falta del reconocimiento de modificaciones de las histonas es la causa de los padecimientos por lo tanto es importante entender su funcionamiento.

Eustermann et. al (2011) e Iwase et. al (2011) observaron que el dominio ADD de la proteína ATRX de humano reconocía la trimetilación de la lisina 9 de la histona H3 y la lisina 4 cuando se encuentra libre de modificaciones y describieron los aminoácidos importantes para que se lleve a cabo el reconocimiento de esta marca. Además, Dhayalan et. al. 2011 realizaron un modelo 3D del dominio ADD donde muestran los aminoácidos importantes para el

reconocimiento de esta marca. En *Drosophila* el dominio ADD también tiene la capacidad de reconocer esta marca (López-Falcón et al. 2014; Alekseyenko et al. 2014).

Recientemente, en el laboratorio de la Dra Kuroda se identificó a dADD1 como un fuerte interactor de HP1a, y también de otros factores, como las metiltransferasas Eggless/dSETDB1 y Su(var)3–9. Estas metiltransferasas participan en la formación y mantenimiento de la heterocromatina pericéntrica (Schwartzentruber et al. 2012; Brower-Toland et al. 2009). La pérdida de cualquiera de estas metiltransferasas o un cambio en sus niveles afectan la heterocromatina pericéntrica, la metilación de H3K9 y la localización de HP1a. Dado que dADD1 interactúa con estas histonas metiltransferasas, una posibilidad es que la sobreexpresión de dADD1 produce el rompimiento de la estequiometría de los complejos que contienen estas proteínas, y esto a su vez afecta la actividad de las metiltransferasas, que conduce a la pérdida de la marca de metilación, y a la perdida de HP1a (ver Figuras 17 y 18). Es fundamental considerar que para el mantenimiento y la propagación de H3K9me3, es necesaria HP1a, ya que recluta Su(var) 3–9; por lo tanto, la interrupción de la unión de HP1a desde el cromocentro podría conducir a los cambios observados en H3K9me3.

Si tomamos los datos anteriores de la bibliografía junto con nuestros datos, podemos presentar la posibilidad de un "loop" donde dADD1 se recluta a la heterocromatina a través de la unión del dominio ADD a H3K9me3 y recluta a la enzima "Eggless" (Alekseyenko *et al*., 201; Seller et al., 2019). A su vez, Eggless contribuiría a la trimetilación de las zonas aledañas, facilitando una mayor unión de dADD1. Este puede ser un mecanismo que mantiene dominios ricos en dADD1 en heterocromatina y promueven la formación de gotas ricas en heterocromatina (Fig. 17) (Larson and Narlikar 2018; Meyer-Nava et al. 2020). Muramatsu et al., (2013) realizaron la mutación de la metiltransferasa que pone la marca de H3K9me3 en células ESCs de ratón, y observaron que no se recluta correctamente HP1a ni ATRX a la heterocromatina. En células de ratón se ha observado que ATRX está involucrado en la deposición de la variante H3.3 junto con la chaperona DAXX (Goldberg et al., 2010).

En *Drosophila*, se ha demostrado que DAXX "*Death-associated protein 6*" coopera con ASF1 " *Anti-silencing factor 1*" para la deposición de H3.3 y también con dXNP en ciertas regiones heterocromáticas (Fromental-Ramain C., Philippe Ramain 2017). También se sabe que la falta de dXNP no modifica la incorporación de la variante H3.3, aunque se observa una localización de la proteína dXNP en sitios donde se realiza el intercambio de esta variante, como es el locus de "*heat shock"* (Schneiderman et al. 2012). En la literatura, hay informes de mutantes que fenocopia la pérdida de organización del cromocentro que observamos cuando sobreexpresamos dADD1. Mutantes que afectan niveles de H3.3 o un mutante que sustituye a la lisina 9 de la cola de la histona 3 por una arginina conduce a una desorganización del cromocentro (Pencik et al. 2016; T. Penke et al. 2018). Sería bastante interesante en un futuro evaluar cual es el papel de las isoformas de dADD1 en la incorporación de la variante H3.3 y si la afectación en la incorporación de la H3K9me3 (Anexo 1).

Siguiendo con la regulación del locus de "*heat shock*", además de la explicación mediante la deposición de la variante H3.3 también cabe la posibilidad que el locus esté regulado por HP1a, por ejemplo, un grupo demostró que Jra, el homólogo de Drosophila de c-Jun, interactúa y recluta a HP1a en la región de su propio cuerpo del gen (Jra). A su vez, HP1a recluta a la histona desmetilasa KDM4A para reducir los niveles de metilación de H3K36, lo que da como resultado altos niveles de acetilación de histonas en la región del cuerpo del gen y, por lo tanto, promueve transcripción de este gen. Estos datos hablan de un bucle de autorregulación para promover su propia transcripción vía HP1a (Y. Liu and Zhang 2015).

La reducción de la señal de H3K9me3 y HP1a en el cromocentro cuando se sobreexpresa dADD1, explica parcialmente la pérdida de la estructura global de la cromatina observada en los cromosomas politénicos. Nuestro grupo ha demostrado que dADD1 también interactúa física y genéticamente con la ATPasa dXNP; y esta proteína no tiene un dominio de unión a ADN o cromatina, por lo que probablemente se está uniendo por medio de dADD1 y de otros interactores que conservan un dominio de reconocimiento al ADN o a la cromatina (López-Falcón et al. 2014). La sobreexpresion del dominio helicasa/ATPasa (dXNP) podría estar ocasionando cambios en el posicionamiento de los nucleosomas, como se ha visto cuando se desregulan otros remodeladores de la cromatina y conducen a cambios importantes en la estructura general de la cromatina (Corona et al. 2007), aunque esta idea habría que analizarla con mayor profundidad con diversos experimentos. dXNP es importante para el mantenimiento de beta heterocromatina y se ha demostrado que interactúa también con HP1a (Bassett et al. 2008; Emelyanov et al. 2010). Los niveles de las proteínas dADD1 pueden cambiar la localización de HP1a, y también afectar la unión de dXNP a la cromatina que conduce a una desregulación de la actividad ATPasa y la pérdida de la estructura de la cromatina (ver Fig. 23) (Emelyanov et al. 2010).

La sobreexpresión de dXNP en el ojo y el ala durante el desarrollo temprano causa apoptosis a través de la vía JNK (N. G. Lee et al. 2007; Hong et al. 2009). En otros estudios, la sobreactivación de JAK-STAT y STAT92E produce la interrupción de HP1a y pérdida de la estabilidad de la cromatina (Xu et al. 2014). En contraste, reducir los niveles de STAT92E fosforilada, causa inestabilidad en la heterocromatina (Shi et al. 2008). JNK y JAK-STAT son dos de las señales que juegan un papel principal durante la determinación del destino de una célula (Ahmed-de-Prado, Diaz-Garcia, and Baonza 2018). Estos datos pueden ser notables para nuestro trabajo ya que la sobreexpresión de las proteínas dADD1 podría conducir a la apoptosis a través de la vía de JNK, y es bien sabido que la activación anormal de JAK-STAT por fosforilación está relacionada a cánceres humanos (Pencik et al. 2016) (ver Anexo 2, 3 , 4 y 5).

Continuando con la sobreexpresión de dXNP, en los cromosomas politénicos (ver figura 23) sería importante en un futuro demostrar si existe más o menos endoduplicación en estos cromosomas donde se observa un área nuclear menor, o simplemente se encuentran más condensados, y esto se podría observar mediante marcadores del ciclo celular y cuantificando la cantidad de ADN, ya que es bien sabido que estos cromosomas tienen 10 rondas de endoreplicación que producen 2^{10}=1024 copias de ADN (Lilly and Duronio 2005; Igor F Zhimulev and Koryakov 2009).

Otro dato importante es que cuando se sobreexpresan por separado las isoformas de dADD en fondo "*wild type*" también causan 100% de letalidad (Tabla 7), y al parecer la condición nula de estas proteínas parece tener un 40% de supervivencia (Chavez et al. 2017). Al sobreexpresar cada una de las isoformas en el fondo nulo se logra apenas un 20% de supervivencia, lo cual sugiere que para el organismo es un fenotipo más penetrante en la letalidad tener las proteínas en exceso que no tenerlas (datos no mostrados). Esto podría explicarse con la desregulación que se da a nivel transcripcional, además de evaluar en qué momento clave del desarrollo embrionario se están muriendo para determinar la posible interacción o participación en una vía de regulación, o la unión con un factor transcripcional importante en el desarrollo del embrión.

En una publicación previa del laboratorio, en un fondo nulo de dadd1 demostraron que HP1a se restauró a la región telomérica cuando el rescate se realizó con dADD1a pero no con dADD1b (Chavez et al. 2017). dADD1 también interactúa significativamente con las proteínas asociadas a telómeros como HP2, lo que sugiere que dADD1 puede ser importante para la regulación de telómeros. HP2 a su vez interacciona con HP1a en los telómeros, lo cual podría contribuir al estado de compactación general de la cromatina en esta región (Alekseyenko et al. 2014).

En eucromatina, tanto dADD1 como dXNP probablemente interactúan con HP1b, que es un parálogo de HP1a que tanto en humanos como en *Drosophila* se localiza tanto en heterocromatina como eucromatina (Nielsen et al. 2001), y esto puede ser uno de los mecanismos por el cual estas proteínas se reclutan para la eucromatina (Alekseyenko et al. 2014). Recientemente se comprobó que el cromodominio de HP1b se une a H3K9me3 de manera similar al cromodominio de HP1a, pero con menor afinidad (D. H. Lee et al. 2019). Dado que H3K9me3 se localiza muy específicamente en heterocromatina y HP1b se localiza en la eucromatina, puede existir un gradiente donde se pueden seguir formando pequeñas islas heterocromáticas y tal vez no se encuentran bien aisladas para que HP1a se una. dADD1 también interactúa con Bonus, donde Bonus, dADD1 y HP1b se pudieran estar asociando a la marca de trimetilación probablemente en conjunto con otras marcas. El mecanismo y el orden exacto aún se desconoce, pero se deben realizar más trabajos para comprender la naturaleza de esta interacción y la función de este complejo en la eucromatina.

En *Drosophila* este es el primer estudio donde se evalúa el efecto de la sobreexpresión del dominio ADD, utilizando el homólogo de humano ATRX. En investigaciones futuras sería bastante interesante evaluar cual es el fenotipo sin llevar a la letalidad del organismo y observar la conversión al cáncer. Además, con este estudio pudimos entender mejor la sobreexpresión de ATRX en células tumorales y que parece bastante tóxico para la estabilidad cromosomal tener un exceso de esta proteína, lo que muy posiblemente contribuya al fenotipo canceroso.

8. CONCLUSIONES

- ✓ La sobreexpresión de dADD1 de forma ubicua causa letalidad del organismo.
- ✓ La sobreexpresión de dADD1 altera la estructura de la cromatina, principalmente afecta las estructuras heterocromáticas como el cromocentro y los telómeros.
- ✓ La sobreexpresión de dADD1 induce la deslocalización de la proteína HP1a del cromocentro y esto a su vez correlaciona con la pérdida del patrón de bandeo.
- ✓ El área de la señal de HP1a en cromosomas politénicos se ve reducida cuando se sobreexpresan todas las dADD1, a o b.
- ✓ La proteína HP1a cambia su distribución en las glándulas salivales cuando se están sobreexpresando todas las isoformas, a o b de dADD1.
- ✓ La señal de la marca de H3k9me3 se ve disminuida cuando aumentamos la expresión de dADD1a o b.
- ✓ Las proteínas dADD1 se requieren para la correcta transcripción de genes heterocromáticos
- ✓ La sobreexpresión de dADD1 afecta la unión a la cromatina de la proteína HP1a en algunos genes heterocromáticos.
- ✓ La unión de dXNP se ve afectada cuando incrementamos o disminuimos la expresión de dADD1 en cromosomas politénicos.

9. PERSPECTIVAS

- Determinar si la letalidad que observamos con la sobreexpresión de todas las isoformas es por medio de apoptosis, por la vía de la Jun quinasa como en la sobreexpresión de XNP (Ver Anexo 2-5).
- Determinar si la sobreexpresión de dXNP casusa un fenotipo de menor área nuclear debido a menos rondas de duplicación o a mayor compactación de la cromatina.
- Realizar un RNA-seq en las glándulas salivales de condición nula para evaluar que transcritos se están afectando con la falta de dADD1.
- Analizar si existe una asociación entre la falta de las proteínas dADD1 y la falta de la deposición de H3.3 como posible analogía de lo que sucede en mamíferos (ver Anexo 1).
- Llevar a cabo un ensayo de ChIP-seq de la isoforma b de ADD1 para poder discernir entre los blancos de las distintas isoformas.
- Construir moscas que sobreexpresen la isoforma c para ver si presentan el mismo fenotipo o inclusive hacer combinaciones entre las isoformas para observar distintos fenotipos.
- Evaluar la presencia de dADD1 en el locus de Hsp70 y su posible papel en respuesta a estrés por choque térmico.

10. BIBLIOGRAFÍA

Aasland, R, and A F Stewart. 1995. "The Chromo Shadow Domain, a Second Chromodomain in Heterochromatin-Binding Protein1, HP1." *Nucleic Acids Res.* 23 (16): 3168–73.

Aasland, Rein, A. Francis Stewart, and Toby Gibson. 1996. "The SANT Domain: A Putative DNA-Binding Domain in the SWI-SNF and ADA Complexes, the Transcriptional Co-Repressor N-CoR and TFIIIB." *Trends in Biochemical Sciences* 21 (3): 87–88. https://doi.org/10.1016/S0968-0004(96)30009-1.

Adams, M. D., S. E. Celniker, R. A. Holt, C. A. Evans, J. D. Gocayne, P. G. Amanatides, S. E. Scherer, et al. 2000. "The Genome Sequence of Drosophila Melanogaster." *Science* 287 (5461): 2185–95. https://doi.org/10.1126/science.287.5461.2185.

Ahmed-de-Prado, Sara, Sandra Diaz-Garcia, and Antonio Baonza. 2018. "JNK and JAK/STAT Signalling Are Required for Inducing Loss of Cell Fate Specification during Imaginal Wing Discs Regeneration in Drosophila Melanogaster." *Developmental Biology* 441 (1): 31–41. https://doi.org/10.1016/j.ydbio.2018.05.021.

Alekseyenko, Artyom A., Andrey A. Gorchakov, Barry M. Zee, Stephen M. Fuchs, Peter V. Kharchenko, and Mitzi I. Kuroda. 2014. "Heterochromatin-Associated Interactions of Drosophila HP1a with DADD1, HIPP1, and Repetitive RNAs." *Genes and Development* 28 (13): 1445–60. https://doi.org/10.1101/gad.241950.114.

Argentaro, A., J.-C. Yang, L. Chapman, M. S. Kowalczyk, R. J. Gibbons, D. R. Higgs, D. Neuhaus, and D. Rhodes. 2007. "Structural Consequences of Disease-Causing Mutations in the ATRX-DNMT3-DNMT3L (ADD) Domain of the Chromatin-Associated Protein ATRX." *Proceedings of the National Academy of Sciences* 104 (29): 11939–44. https://doi.org/10.1073/pnas.0704057104.

Argentaro, Anthony, Ji Chun Yang, Lynda Chapman, Monika S. Kowalczyk, Richard J. Gibbons, Douglas R. Higgs, David Neuhaus, and Daniela Rhodes. 2007. "Structural Consequences of Disease-Causing Mutations in the ATRX-DNMT3-DNMT3L (ADD) Domain of the Chromatin-Associated Protein ATRX." *Proceedings of the National Academy of Sciences of the United States of America* 104 (29): 11939–44. https://doi.org/10.1073/pnas.0704057104.

Armstrong, Robin L., and Robert J. Duronio. 2019. "Phasing in Heterochromatin during Development." *Genes and Development* 33 (7–8): 379–81. https://doi.org/10.1101/gad.324731.119.

Azzaz, Abdelhamid M., Michael W. Vitalini, Andrew S. Thomas, Jason P. Price, Melissa J. Blacketer, Diane E. Cryderman, Luka N. Zirbel, et al. 2014. "Human Heterochromatin Protein 1α Promotes Nucleosome Associations That Drive Chromatin Condensation." *Journal of Biological Chemistry* 289 (10): 6850–61. https://doi.org/10.1074/jbc.M113.512137.

Baker, Lindsey A., C. David Allis, and Gang G. Wang. 2008. "PHD Fingers in Human Diseases: Disorders Arising from Misinterpreting Epigenetic Marks." *Mutation Research - Fundamental and Molecular Mechanisms of Mutagenesis* 647 (1–2): 3–12. https://doi.org/10.1016/j.mrfmmm.2008.07.004.

Bannister, Andrew J., Philip Zegerman, Janet F. Partridge, Eric A. Miska, Jean O. Thomas, Robin C. Allshire, and Tony Kouzarides. 2001. "Selective Recognition of Methylated

Lysine 9 on Histone H3 by the HP1 Chromo Domain." *Nature* 410 (6824): 120–24. https://doi.org/10.1038/35065138.

Bassett, Andrew R, Sarah E Cooper, Anan Ragab, and Andrew A Travers. 2008. "The Chromatin Remodelling Factor DATRX Is Involved in Heterochromatin Formation." *PLoS ONE* 3 (5). https://doi.org/10.1371/journal.pone.0002099.

Bayona-Feliu, Aleix, Anna Casas-Lamesa, Oscar Reina, Jordi Bernués, and Fernando Azorín. 2017. "Linker Histone H1 Prevents R-Loop Accumulation and Genome Instability in Heterochromatin." *Nature Communications* 8 (1). https://doi.org/10.1038/s41467-017-00338-5.

Berger, F. 2019. "Emil Heitz, a True Epigenetics Pioneer." *Nature Reviews Molecular Cell Biology* 20 (10): 572. https://doi.org/10.1038/s41580-019-0170-y.

Berubé, N. G., Magdalena Jagla, Cecelia Smeenk, Yves De Repentigny, Rashmi Kothary, and David J. Picketts. 2002. "Neurodevelopmental Defects Resulting from ATRX Overexpression in Transgenic Mice." *Human Molecular Genetics* 11 (3): 253–61. https://doi.org/Doi 10.1093/Hmg/11.3.253.

Bérubé, Nathalie G. 2011. "ATRX in Chromatin Assembly and Genome Architecture during Development and Disease." *Biochemistry and Cell Biology* 89 (5): 435–44. https://doi.org/10.1139/o11-038.

Bérubé, Nathalie G., Cecilia A. Smeenk, and David J. Picketts. 2000. "Cell Cycle-Dependent Phosphorylation of the ATRX Protein Correlates with Changes in Nuclear Matrix and Chromatin Association." *Human Molecular Genetics* 9 (4): 539–47. https://doi.org/10.1093/hmg/9.4.539.

Boyer, Laurie A., Michael R. Langer, Kimberly A. Crowley, Song Tan, John M. Denu, and Craig L. Peterson. 2002. "Essential Role for the SANT Domain in the Functioning of Multiple Chromatin Remodeling Enzymes." *Molecular Cell* 10 (4): 935–42. https://doi.org/10.1016/S1097-2765(02)00634-2.

Brahma, Sandipan, Maheshi I. Udugama, Jongseong Kim, Arjan Hada, Saurabh K. Bhardwaj, Solomon G. Hailu, Tae Hee Lee, and Blaine Bartholomew. 2017. "INO80 Exchanges H2A.Z for H2A by Translocating on DNA Proximal to Histone Dimers." *Nature Communications* 8. https://doi.org/10.1038/ncomms15616.

Brand, A. H., and N. Perrimon. 1993. "Targeted Gene Expression as a Means of Altering Cell Fates and Generating Dominant Phenotypes." *Development* 118 (2): 401–15.

Britten, R. J., and D. E. Kohne. 1968. "Repeated Sequences in DNA." *Science* 161 (3841): 529–40. https://doi.org/10.1126/science.161.3841.529.

Brower-Toland, Brent, Nicole C. Riddle, Hongmei Jiang, Kathryn L. Huisinga, and Sarah C.R. Elgin. 2009. "Multiple SET Methyltransferases Are Required to Maintain Normal Heterochromatin Domains in the Genome of Drosophila Melanogaster." *Genetics* 181 (4): 1303–19. https://doi.org/10.1534/genetics.108.100271.

Buchwalter, Abigail, Jeanae M. Kaneshiro, and Martin W. Hetzer. 2019. "Coaching from the Sidelines: The Nuclear Periphery in Genome Regulation." *Nature Reviews Genetics* 20 (1): 39–50. https://doi.org/10.1038/s41576-018-0063-5.

Cairns, Bradley R. 2009. "The Logic of Chromatin Architecture and Remodelling at Promoters." *Nature* 461 (7261): 193–98. https://doi.org/10.1038/nature08450.

Cairns, Bradley R., Yahli Lorch, Yang Li, Mincheng Zhang, Lynne Lacomis, Hediye

Erdjument-Bromage, Paul Tempst, Jian Du, Brehon Laurent, and Roger D. Kornberg. 1996. “RSC, an Essential, Abundant Chromatin-Remodeling Complex.” *Cell* 87 (7): 1249–60. https://doi.org/10.1016/S0092-8674(00)81820-6.

Capelson, Maya, and Martin W. Hetzer. 2009. “The Role of Nuclear Pores in Gene Regulation, Development and Disease.” *EMBO Reports* 10 (7): 697–705. https://doi.org/10.1038/embor.2009.147.

Cardoso, Carlos, Serge Timsit, Laurent Villard, Michel Khrestchatisky, Michel Fontès, and Laurence Colleaux. 1998. “Specific Interaction between the XNP/ATR-X Gene Product and the SET Domain of the Human EZH2 Protein.” *Human Molecular Genetics* 7 (4): 679–84. https://doi.org/10.1093/hmg/7.4.679.

Chavez, Joselyn, Juan Manuel Murillo-Maldonado, Vanessa Bahena, Ana Karina Cruz, América Castañeda-Sortibrán, Rosario Rodriguez-Arnaiz, Mario Zurita, and Viviana Valadez-Graham. 2017. “DAdd1 and DXNP Prevent Genome Instability by Maintaining HP1a Localization at Drosophila Telomeres.” *Chromosoma* 126 (6): 697–712. https://doi.org/10.1007/s00412-017-0634-9.

Clapier, Cedric R., and Bradley R. Cairns. 2009. “The Biology of Chromatin Remodeling Complexes.” *Annual Review of Biochemistry* 78: 273–304. https://doi.org/10.1146/annurev.biochem.77.062706.153223.

Clapier, Cedric R., Margaret M. Kasten, Timothy J. Parnell, Ramya Viswanathan, Heather Szerlong, George Sirinakis, Yongli Zhang, and Bradley R. Cairns. 2016. “Regulation of DNA Translocation Efficiency within the Chromatin Remodeler RSC/Sth1 Potentiates Nucleosome Sliding and Ejection.” *Molecular Cell* 62 (3): 453–61. https://doi.org/10.1016/j.molcel.2016.03.032.

Cléard, Fabienne, and Pierre Spierer. 2001. “TPosition-Effect Variegation in Drosophila: The Modifier Su(Var)3-7 Is a Modular DNA-Binding Protein.” *EMBO Reports* 2 (12): 1095–1100.

Corless, Samuel, Saskia Höcker, and Sylvia Erhardt. 2020. “Centromeric RNA and Its Function at and Beyond Centromeric Chromatin.” *Journal of Molecular Biology* 432 (15): 4257–69. https://doi.org/10.1016/j.jmb.2020.03.027.

Corona, Davide F.V., Cedric R. Clapier, Peter B. Becker, and John W. Tamkun. 2002. “Modulation of ISWI Function by Site-Specific Histone Acetylation.” *EMBO Reports* 3 (3): 242–47. https://doi.org/10.1093/embo-reports/kvf056.

Corona, Davide F.V., Giorgia Siriaco, Jennifer A. Armstrong, Natalia Snarskaya, Stephanie A. McClymont, Matthew P. Scott, and John W. Tamkun. 2007. “ISWI Regulates Higher-Order Chromatin Structure and Histone H1 Assembly in Vivo.” *PLoS Biology* 5 (9): 2011–21. https://doi.org/10.1371/journal.pbio.0050232.

Cremer, Thomas, and Marion Cremer. 2010. “Chromosome Territories.” *Cold Spring Harbor Perspectives in Biology* 2 (3): 1–23. https://doi.org/10.1101/cshperspect.a003889.

Cryderman, Diane E., Michael W. Vitalini, and Lori L. Wallrath. 2011. “Heterochromatin Protein 1a Is Required for an Open Chromatin Structure.” *Transcription* 2 (2): 95–99. https://doi.org/10.4161/trns.2.2.14687.

Cutter, Amber R., and Jeffrey J. Hayes. 2015. “A Brief Review of Nucleosome Structure.” *FEBS Letters* 589 (20): 2914–22. https://doi.org/10.1016/j.febslet.2015.05.016.

Davey, Curt A, David F Sargent, Karolin Luger, Armin W Maeder, and Timothy J Richmond. 2002. “Solvent Mediated Interactions in the Structure of the ˚ Resolution † Nucleosome Core Particle at 1 . 9 A” 2836 (02): 1097–1113. https://doi.org/10.1016/S0022-2836(02)00386-8.

Delattre, M, A Spierer, C H Tonka, and P Spierer. 2000. “The Genomic Silencing of Position-Effect Variegation in Drosophila Melanogaster: Interaction between the Heterochromatin-Associated Proteins Su(Var)3-7 and HP1.” *Journal of Cell Science* 113: 4253–61. http://jcs.biologists.org/content/joces/113/23/4253.full.pdf.

Dhayalan, Arunkumar, Raluca Tamas, Ina Bock, Anna Tattermusch, Emilia Dimitrova, Srikanth Kudithipudi, Sergey Ragozin, and Albert Jeltsch. 2011. “The ATRX-ADD Domain Binds to H3 Tail Peptides and Reads the Combined Methylation State of K4 and K9.” *Human Molecular Genetics* 20 (11): 2195–2203. https://doi.org/10.1093/hmg/ddr107.

Dillon, Niall. 2004. “Heterochromatin Structure and Function.” *Biology of the Cell* 96 (8): 631–37. https://doi.org/10.1016/j.biolcel.2004.06.003.

Dixon, Jesse R., Siddarth Selvaraj, Feng Yue, Audrey Kim, Yan Li, Yin Shen, Ming Hu, Jun S. Liu, and Bing Ren. 2012. “Topological Domains in Mammalian Genomes Identified by Analysis of Chromatin Interactions.” *Nature* 485 (7398): 376–80. https://doi.org/10.1038/nature11082.

Doğan, Ezgi Süheyla, and Chang Liu. 2018. “Three-Dimensional Chromatin Packing and Positioning of Plant Genomes.” *Nature Plants* 4 (8): 521–29. https://doi.org/10.1038/s41477-018-0199-5.

Drané, Pascal, Khalid Ouararhni, Arnaud Depaux, Muhammad Shuaib, and Ali Hamiche. 2010. “The Death-Associated Protein DAXX Is a Novel Histone Chaperone Involved in the Replication-Independent Deposition of H3.3.” *Genes and Development* 24 (12): 1253–65. https://doi.org/10.1101/gad.566910.

Dyer, Michael A., Zulekha A. Qadeer, David Valle-Garcia, and Emily Bernstein. 2017. “ATRX and DAXX: Mechanisms and Mutations.” *Cold Spring Harbor Perspectives in Medicine* 7 (3). https://doi.org/10.1101/cshperspect.a026567.

Eissenberg, J C, T C James, D M Foster-Hartnett, T Hartnett, V Ngan, and S C Elgin. 1990. “Mutation in a Heterochromatin-Specific Chromosomal Protein Is Associated with Suppression of Position-Effect Variegation in Drosophila Melanogaster.” *Proceedings of the National Academy of Sciences of the United States of America* 87 (24): 9923–27. https://doi.org/10.1073/pnas.87.24.9923.

Eissenberg, Joel C., and Sarah C.R. Elgin. 2014. “HP1a: A Structural Chromosomal Protein Regulating Transcription.” *Trends in Genetics* 30 (3): 103–10. https://doi.org/10.1016/j.tig.2014.01.002.

Elmallah, Mohammed I Y, Marine Cordonnier, and Valentin Vautrot. 2019. “Membrane-Anchored Heat-Shock Protein 70 (Hsp70) in Cancer.” *Cancer Letters*, no. August: 0–1. https://doi.org/10.1016/j.canlet.2019.10.037.

Emelyanov, Alexander V., Alexander Y. Konev, Elena Vershilova, and Dmitry V. Fyodorov. 2010. “Protein Complex of Drosophila ATRX/XNP and HP1a Is Required for the Formation of Pericentric Beta-Heterochromatin in Vivo.” *Journal of Biological Chemistry* 285 (20): 15027–37. https://doi.org/10.1074/jbc.M109.064790.

Eustermann, Sebastian, Ji Chun Yang, Martin J. Law, Rachel Amos, Lynda M. Chapman, Clare Jelinska, David Garrick, et al. 2011. “Combinatorial Readout of Histone H3 Modifications Specifies Localization of ATRX to Heterochromatin.” *Nature Structural and Molecular Biology* 18 (7): 777–82. https://doi.org/10.1038/nsmb.2070.

Fanti, Laura, Maria Berloco, Lucia Piacentini, and Sergio Pimpinelli. 2003. “Chromosomal Distribution of Heterochromatin Protein 1 (HP1) in Drosophila: A Cytological Map of Euchromatic HP1 Binding Sites.” *Genetica* 117 (2–3): 135–47. https://doi.org/10.1023/A:1022971407290.

Felsenfeld, Gary, and Mark Groudine. 2003. “Controlling the Double Helix.” *Nature* 42 (January): 448–53. https://doi.org/10.1038/nature01410.

Figueiredo, Margarida L.A., Philge Philip, Per Stenberg, and Jan Larsson. 2012. “HP1a Recruitment to Promoters Is Independent of H3K9 Methylation in Drosophila Melanogaster.” *PLoS Genetics* 8 (11): 1–12. https://doi.org/10.1371/journal.pgen.1003061.

Fischer, J.A., Giniger, E., Maniatis, T.&Ptashne, M. 1988. “GAL4 Ativates Tanscription in Drosophila.” *Nature*.

Fritz, Andrew J., Nitasha Sehgal, Artem Pliss, Jinhui Xu, and Ronald Berezney. 2019. “Chromosome Territories and the Global Regulation of the Genome.” *Genes Chromosomes and Cancer* 58 (7): 407–26. https://doi.org/10.1002/gcc.22732.

Fromental-Ramain C., Philippe Ramain, Ali Hamiche. 2017. “The Drosophila DAXX-Like Protein (DLP) Cooperates with ASF1 for H3.3 Deposition and Heterochromatin Formation.” *Molecular and Cellular Biology* 37 (12): 1–18.

Fudenberg, Geoffrey, Maxim Imakaev, Carolyn Lu, Anton Goloborodko, Nezar Abdennur, and Leonid A. Mirny. 2016. “Formation of Chromosomal Domains by Loop Extrusion.” *Cell Reports* 15 (9): 2038–49. https://doi.org/10.1016/j.celrep.2016.04.085.

Fuks, François, Paul J. Hurd, Rachel Deplus, and Tony Kouzarides. 2003. “The DNA Methyltransferases Associate with HP1 and the SUV39H1 Histone Methyltransferase.” *Nucleic Acids Research* 31 (9): 2305–12. https://doi.org/10.1093/nar/gkg332.

Garrick, David, Vassiliki Samara, Tarra L. McDowell, Andrew J.H. Smith, Lorraine Dobbie, Douglas R. Higgs, and Richard J. Gibbons. 2004. “A Conserved Truncated Isoform of the ATR-X Syndrome Protein Lacking the SWI/SNF-Homology Domain.” *Gene* 326 (1–2): 23–34. https://doi.org/10.1016/j.gene.2003.10.026.

Gibbons, Richard J., David J. Picketts, Laurent Villard, and Douglas R. Higgs. 1995. “Mutations in a Putative Global Transcriptional Regulator Cause X-Linked Mental Retardation with α-Thalassemia (ATR-X Syndrome).” *Cell* 80 (6): 837–45. https://doi.org/10.1016/0092-8674(95)90287-2.

Giorgetti, Luca, Bryan R. Lajoie, Ava C. Carter, Mikael Attia, Ye Zhan, Jin Xu, Chong Jian Chen, et al. 2016. “Structural Organization of the Inactive X Chromosome in the Mouse.” *Nature* 535 (7613): 575–79. https://doi.org/10.1038/nature18589.

Goldberg, Aaron D., Laura A. Banaszynski, Kyung Min Noh, Peter W. Lewis, Simon J. Elsaesser, Sonja Stadler, Scott Dewell, et al. 2010. “Distinct Factors Control Histone Variant H3.3 Localization at Specific Genomic Regions.” *Cell* 140 (5): 678–91. https://doi.org/10.1016/j.cell.2010.01.003.

Gray, Steven G. 2014. “Book Review: Â€œEpigeneticsâ€•.” *Frontiers in Genetics* 5 (April): 1–2. https://doi.org/10.3389/fgene.2014.00104.

Greil, F, I Van Der Kraan, J Delrow, J. F. Smothers, E De Wit, Harmen J. Bussemaker, R Van Driel, S Henikoff, and B Van Steensel. 2003a. “Distinct HP1 and Su(Var)3-9 Complexes Bind to Sets of Developmentally Coexpressed Genes Depending on Chromosomal Location.” *Genes and Development* 17 (22): 2825–38. https://doi.org/10.1101/gad.281503.

Greil, F, Ineke Van Der Kraan, Jeffrey Delrow, James F. Smothers, Elzo De Wit, Harmen J. Bussemaker, Roel Van Driel, Steven Henikoff, and Bas Van Steensel. 2003b. “Distinct HP1 and Su(Var)3-9 Complexes Bind to Sets of Developmentally Coexpressed Genes Depending on Chromosomal Location.” *Genes and Development* 17 (22): 2825–38. https://doi.org/10.1101/gad.281503.

Grewal, Shiv I.S., and Songtao Jia. 2007. “Heterochromatin Revisited.” *Nature Reviews Genetics* 8 (1): 35–46. https://doi.org/10.1038/nrg2008.

Guelen, Lars, Ludo Pagie, Emilie Brasset, Wouter Meuleman, Marius B. Faza, Wendy Talhout, Bert H. Eussen, et al. 2008. “Domain Organization of Human Chromosomes Revealed by Mapping of Nuclear Lamina Interactions.” *Nature* 453 (7197): 948–51. https://doi.org/10.1038/nature06947.

Hallson, G., M. Syrzycka, S. A. Beck, J. A. Kennison, D. Dorsett, S. L. Page, S. M. Hunter, et al. 2008. “The Drosophila Cohesin Subunit Rad21 Is a Trithorax Group (TrxG) Protein.” *Proceedings of the National Academy of Sciences* 105 (34): 12405–10. https://doi.org/10.1073/pnas.0801698105.

Harsha, Bhavana, Celestino Creatore, Chai Yin Kok, Charlie Hathaway, Charlotte G Cole, Christopher C Ramshaw, Claire E Rye, et al. 2018. “COSMIC: The Catalogue Of Somatic Mutations In Cancer.” *Nucleic Acids Research* 47 (D1): D941–47. https://doi.org/10.1093/nar/gky1015.

Hendzel, Michael J., Yi Wei, Michael A. Mancini, Aaron Van Hooser, Tamara Ranalli, B. R. Brinkley, David P. Bazett-Jones, and C. David Allis. 1997a. “Mitosis-Specific Phosphorylation of Histone H3 Initiates Primarily within Pericentromeric Heterochromatin during G2 and Spreads in an Ordered Fashion Coincident with Mitotic Chromosome Condensation.” *Chromosoma* 106 (6): 348–60. https://doi.org/10.1007/s004120050256.

———. 1997b. “Mitosis-Specific Phosphorylation of Histone H3 Initiates Primarily within Pericentromeric Heterochromatin during G2 and Spreads in an Ordered Fashion Coincident with Mitotic Chromosome Condensation.” *Chromosoma* 106 (6): 348–60. https://doi.org/10.1007/s004120050256.

Hinde, Elizabeth, Francesco Cardarelli, and Enrico Gratton. 2015. “Spatiotemporal Regulation of Heterochromatin Protein 1- Alpha Oligomerization and Dynamics in Live Cells.” *Scientific Reports* 5 (August): 1–11. https://doi.org/10.1038/srep12001.

Hines, Karrie A., Diane E. Cryderman, Kaitlin M. Flannery, Yang Hongbo, Michael W. Vitalini, Tulle Hazelrigg, Craig A. Mizzen, and Lori L. Wallrath. 2009. “Domains of Heterochromatin Protein 1 Required for Drosophila Melanogaster Heterochromatin Spreading.” *Genetics* 182 (4): 967–77. https://doi.org/10.1534/genetics.109.105338.

Hirota, Toru, Jesse J. Lipp, Ban Hock Toh, and Jan Michael Peters. 2005. “Histone H3 Serine

10 Phosphorylation by Aurora B Causes HP1 Dissociation from Heterochromatin." *Nature* 438 (7071): 1176–80. https://doi.org/10.1038/nature04254.

Hong, Yoon Ki, Nam Gon Lee, Min Jung Lee, Min Soo Park, Gahee Choi, Yoon Seak Suh, Seung Yeop Han, Soojin Hwang, Gilsang Jeong, and Kyoung Sang Cho. 2009. "DXNP/DATRX Increases Apoptosis via the JNK and DFOXO Pathway in Drosophila Neurons." *Biochemical and Biophysical Research Communications* 384 (2): 160–66. https://doi.org/10.1016/j.bbrc.2009.04.112.

Ito, Hiroki, Kosei Sato, Masayuki Koganezawa, Manabu Ote, Ken Matsumoto, Chihiro Hama, and Daisuke Yamamoto. 2012. "Fruitless Recruits Two Antagonistic Chromatin Factors to Establish Single-Neuron Sexual Dimorphism." *Cell* 149 (6): 1327–38. https://doi.org/10.1016/j.cell.2012.04.025.

Ito, Takashi, Michael Bulger, Michael J. Pazin, Ryuji Kobayashi, and James T. Kadonaga. 1997. "ACF, an ISWI-Containing and ATP-Utilizing Chromatin Assembly and Remodeling Factor." *Cell* 90 (1): 145–55. https://doi.org/10.1016/S0092-8674(00)80321-9.

Iwase, Shigeki, Bin Xiang, Sharmistha Ghosh, Ting Ren, Peter W. Lewis, Jesse C. Cochrane, C. David Allis, et al. 2011. "ATRX ADD Domain Links an Atypical Histone Methylation Recognition Mechanism to Human Mental-Retardation Syndrome." *Nature Structural and Molecular Biology* 18 (7): 769–76. https://doi.org/10.1038/nsmb.2062.

Jacobs, Steven A., and Sepideh Khorasanizadeh. 2002. "Structure of HP1 Chromodomain Bound to a Lysine 9-Methylated Histone H3 Tail." *Science* 295 (5562): 2080–83. https://doi.org/10.1126/science.1069473.

Jacobs, Steven A., Sean D. Taverna, Yinong Zhang, Scott D. Briggs, Jinmei Li, Joel C. Eissenberg, C. David Allis, and Sepideh Khorasanizadeh. 2001. "Specificity of the HP1 Chromo Domain for the Methylated N-Terminus of Histone H3." *EMBO Journal* 20 (18): 5232–41. https://doi.org/10.1093/emboj/20.18.5232.

Jamrich, M, A L Greenleaf, and E K Bautz. 1977. "Localization of RNA Polymerase in Polytene Chromosomes of Drosophila Melanogaster." *Proceedings of the National Academy of Sciences* 74 (5): 2079 LP – 2083. https://doi.org/10.1073/pnas.74.5.2079.

Joppich, Christian, Sabrina Scholz, Günter Korge, and Alexander Schwendemann. 2009. "Umbrea, a Chromo Shadow Domain Protein in Drosophila Melanogaster Heterochromatin, Interacts with Hip, HP1 and HOAP." *Chromosome Research* 17 (1): 19–36. https://doi.org/10.1007/s10577-008-9002-1.

Jorgensen, Paul, Nocholas Edgington, Brandt Schneider, Ivan Rupes, Mike Tyers, and Bruce Futcher. 2007. "The Size of the Nucleus Increases as Yeast Cells Grow." *Molecular Biology of the Cell* 18 (March): 976–85. https://doi.org/10.1091/mbc.E06.

Kusch, Thomas, Amanda Mei, and Camtu Nguyen. 2014. "Histone H3 Lysine 4 Trimethylation Regulates Cotranscriptional H2A Variant Exchange by Tip60 Complexes to Maximize Gene Expression." *Proceedings of the National Academy of Sciences of the United States of America* 111 (13): 4850–55. https://doi.org/10.1073/pnas.1320337111.

Kwon, So Hee, Laurence Florens, Selene K. Swanson, Michael P. Washburn, Susan M. Abmayr, and Jerry L. Workman. 2010. "Heterochromatin Protein 1 (HP1) Connects the FACT Histone Chaperone Complex to the Phosphorylated CTD of RNA Polymerase

II." *Genes and Development* 24 (19): 2133–45. https://doi.org/10.1101/gad.1959110.
Längst, Gernot, Edgar J. Bonte, Davide F.V. Corona, and Peter B. Becker. 1999. "Nucleosome Movement by CHRAC and ISWI without Disruption or Trans-Displacement of the Histone Octamer." *Cell* 97 (7): 843–52. https://doi.org/10.1016/S0092-8674(00)80797-7.
Larson, Adam G., Daniel Elnatan, Madeline M. Keenen, Michael J. Trnka, Jonathan B. Johnston, Alma L. Burlingame, David A. Agard, Sy Redding, and Geeta J. Narlikar. 2017. "Liquid Droplet Formation by HP1α Suggests a Role for Phase Separation in Heterochromatin." *Nature* 547 (7662): 236–40. https://doi.org/10.1038/nature22822.
Larson, Adam G., and Geeta J. Narlikar. 2018. "The Role of Phase Separation in Heterochromatin Formation, Function, and Regulation." *Biochemistry* 57 (17): 2540–48. https://doi.org/10.1021/acs.biochem.8b00401.
Law, Martin J., Karen M. Lower, Hsiao P.J. Voon, Jim R. Hughes, David Garrick, Vip Viprakasit, Matthew Mitson, et al. 2010. "ATR-X Syndrome Protein Targets Tandem Repeats and Influences Allele-Specific Expression in a Size-Dependent Manner." *Cell* 143 (3): 367–78. https://doi.org/10.1016/j.cell.2010.09.023.
Lechner, M S, G E Begg, D W Speicher, and F J Rauscher. 2000. "Molecular Determinants for Targeting Heterochromatin Protein 1-Mediated Gene Silencing: Direct Chromoshadow Domain-KAP-1 Corepressor Interaction Is Essential." *Molecular and Cellular Biology* 20 (17): 6449–65. https://doi.org/10.1128/MCB.20.17.6449-6465.2000.
Lee, Dong Hoon, Hyun Wook Ryu, Go Woon Kim, and So Hee Kwon. 2019. "Comparison of Three Heterochromatin Protein 1 Homologs in Drosophila." *Journal of Cell Science*. https://doi.org/10.1242/jcs.222729.
Lee, Nam Gon, Yoon Ki Hong, Si Young Yu, Seung Yeop Han, Dongho Geum, and Kyoung Sang Cho. 2007. "DXNP, a Drosophila Homolog of XNP/ATRX, Induces Apoptosis via Jun-N-Terminal Kinase Activation." *FEBS Letters* 581 (14): 2625–32. https://doi.org/10.1016/j.febslet.2007.05.005.
Lee, Young-Ho, Xiyong Liu, Fuming Qiu, Timothy R. O'Connor, Yun Yen, and David K. Ann. 2015. "HP1β Is a Biomarker for Breast Cancer Prognosis and PARP Inhibitor Therapy." *Plos One* 10 (3): e0121207. https://doi.org/10.1371/journal.pone.0121207.
Lee, Yuh Chwen G., Yuki Ogiyama, Nuno M.C. Martins, Brian J. Beliveau, David Acevedo, C. ting Wu, Giacomo Cavalli, and Gary H. Karpen. 2020. "Pericentromeric Heterochromatin Is Hierarchically Organized and Spatially Contacts H3K9me2 Islands in Euchromatin." *PLoS Genetics* 16 (3): 1–27. https://doi.org/10.1371/journal.pgen.1008673.
Lewis, P. W., S. J. Elsaesser, K.-M. Noh, S. C. Stadler, and C. D. Allis. 2010. "Daxx Is an H3.3-Specific Histone Chaperone and Cooperates with ATRX in Replication-Independent Chromatin Assembly at Telomeres." *Proceedings of the National Academy of Sciences* 107 (32): 14075–80. https://doi.org/10.1073/pnas.1008850107.
Lewis, Peter W., Simon J. Elsaesser, Kyung Min Noh, Sonja C. Stadler, and C. David Allis. 2010. "Daxx Is an H3.3-Specific Histone Chaperone and Cooperates with ATRX in Replication-Independent Chromatin Assembly at Telomeres." *Proceedings of the*

National Academy of Sciences of the United States of America 107 (32): 14075–80. https://doi.org/10.1073/pnas.1008850107.

Li, Bing, Michael Carey, and Jerry L. Workman. 2007. "The Role of Chromatin during Transcription." *Cell* 128 (4): 707–19. https://doi.org/10.1016/j.cell.2007.01.015.

Lilly, Mary A., and Robert J. Duronio. 2005. "New Insights into Cell Cycle Control from the Drosophila Endocycle." *Oncogene* 24 (17): 2765–75. https://doi.org/10.1038/sj.onc.1208610.

Lin, Chia Hui, Bing Li, Selene Swanson, Ying Zhang, Laurence Florens, Michael P. Washburn, Susan M. Abmayr, and Jerry L. Workman. 2008. "Heterochromatin Protein 1a Stimulates Histone H3 Lysine 36 Demethylation by the Drosophila KDM4A Demethylase." *Molecular Cell* 32 (5): 696–706. https://doi.org/10.1016/j.molcel.2008.11.008.

Liu, Xing, Xu Liu, Haowei Wang, Zhen Dou, Ke Ruan, Donald L. Hill, Lin Li, Yunyu Shi, and Xuebiao Yao. 2020. "Phase Separation Drives Decision Making in Cell Division." *Journal of Biological Chemistry* 295 (39): 13419–31. https://doi.org/10.1074/jbc.REV120.011746.

Liu, Yan, and Daoyong Zhang. 2015. "HP1a/KDM4A Is Involved in the Autoregulatory Loop of the Oncogene Gene c-Jun." *Epigenetics* 10 (6): 453–59. https://doi.org/10.1080/15592294.2015.1048059.

López-Falcón, B., S. Meyer-Nava, B. Hernández-Rodríguez, A. Campos, D. Montero, E. Rudiño, M. Vázquez, M. Zurita, and V. Valadez-Graham. 2014. "Characterization of the Drosophila Group Ortholog to the Amino-Terminus of the Alpha-Thalassemia and Mental Retardation X-Linked (ATRX) Vertebrate Protein." *PLoS ONE* 9 (12). https://doi.org/10.1371/journal.pone.0113182.

López-Falcón, Brenda, Silvia Meyer-Nava, Benjamín Hernández-Rodríguez, Adam Campos, Daniel Montero, Enrique Rudiño, Martha Vázquez, Mario Zurita, and Viviana Valadez-Graham. 2014. "Characterization of the Drosophila Group Ortholog to the Amino-Terminus of the Alpha-Thalassemia and Mental Retardation X-Linked (ATRX) Vertebrate Protein." *PLoS ONE* 9 (12): 1–25. https://doi.org/10.1371/journal.pone.0113182.

Lorch, Yahli, and Roger D. Kornberg. 2017. "Chromatin-Remodeling for Transcription." *Quarterly Reviews of Biophysics* 50: 1–15. https://doi.org/10.1017/S003358351700004X.

Lu, B Y, P C Emtage, B J Duyf, a J Hilliker, and Joel C. Eissenberg. 2000. "Heterochromatin Protein 1 Is Required for the Normal Expression of Two Heterochromatin Genes in Drosophila." *Genetics* 155 (2): 699–708.

Luger, Karolin, Mekonnen L. Dechassa, and David J. Tremethick. 2012. "New Insights into Nucleosome and Chromatin Structure: An Ordered State or a Disordered Affair?" *Nature Reviews Molecular Cell Biology* 13 (7): 436–47. https://doi.org/10.1038/nrm3382.

Luger, Karolin, Armin W Mader, Robin K Richmond, David F Sargent, and Timothy J Richmond. 1997. "Crystal Structure of the Nucleosome Resolution Core Particle at 2 . 8 A." *Nature* 389: 251–60. https://doi.org/10.1038/38444.

Magaña-Acosta, Mauro, and Viviana Valadez-Graham. 2020. "Chromatin Remodelers in

the 3D Nuclear Compartment." *Frontiers in Genetics* 11 (November): 1–22. https://doi.org/10.3389/fgene.2020.600615.

Marfella, Concetta G.A., and Anthony N. Imbalzano. 2007. "The Chd Family of Chromatin Remodelers." *Mutation Research - Fundamental and Molecular Mechanisms of Mutagenesis* 618 (1–2): 30–40. https://doi.org/10.1016/j.mrfmmm.2006.07.012.

Mariño-Ramírez, Leonardo, Maricel G. Kann, Benjamin A. Shoemaker, and David Landsman. 2005. "Histone Structure and Nucleosome Stability." *Expert Review of Proteomics* 2 (5): 719–29. https://doi.org/10.1586/14789450.2.5.719.

McDowell, T. L., R. J. Gibbons, H. Sutherland, D. M. O'Rourke, W. A. Bickmore, A. Pombo, H. Turley, et al. 1999. "Localization of a Putative Transcriptional Regulator (ATRX) at Pericentromeric Heterochromatin and the Short Arms of Acrocentric Chromosomes." *Proceedings of the National Academy of Sciences* 96 (24): 13983–88. https://doi.org/10.1073/pnas.96.24.13983.

McKinley, Kara L., and Iain M. Cheeseman. 2016. "The Molecular Basis for Centromere Identity and Function." *Nature Reviews Molecular Cell Biology* 17 (1): 16–29. https://doi.org/10.1038/nrm.2015.5.

Mendez, Deanna L., Rebecca E. Mandt, and Sarah C R Elgin. 2013. "Heterochromatin Protein 1a (HP1a) Partner Specificity Is Determined by Critical Amino Acids in the Chromo Shadow Domain and C-Terminal Extension." *Journal of Biological Chemistry* 288 (31): 22315–23. https://doi.org/10.1074/jbc.M113.468413.

Meyer-Nava, Silvia, Victor E Nieto-caballero, Mario Zurita, and Viviana Valadez-graham. 2020. "Insights into HP1a-Chromatin Interactions."

Mukherjee, Joydeep, Tor Christian Johannessen, Shigeo Ohba, Tracy T. Chow, Lindsey Jones, Ajay Pandita, and Russell O. Pieper. 2018. "Mutant IDH1 Cooperates with ATRX Loss to Drive the Alternative Lengthening of Telomere Phenotype in Glioma." *Cancer Research* 78 (11): 2966–77. https://doi.org/10.1158/0008-5472.CAN-17-2269.

Muramatsu, Daisuke, Hiroshi Kimura, Kaoru Kotoshiba, Makoto Tachibana, and Yoichi Shinkai. 2016. "Pericentric H3K9me3 Formation by HP1 Interaction-Defective Histone Methyltransferase Suv39h1." *Cell Structure and Function* 41 (2): 145–52. https://doi.org/10.1247/csf.16013.

Murzina, Natalia, Alain Verreault, Ernest Laue, and Bruce Stillman. 1999. "Heterochromatin Dynamics in Mouse Cells: Interaction between Chromatin Assembly Factor 1 and HP1 Proteins." *Molecular Cell* 4 (4): 529–40. https://doi.org/10.1016/S1097-2765(00)80204-X.

Nielsen, Anders Lade, Mustapha Oulad-Abdelghani, José A. Ortiz, Eumorphia Remboutsika, Pierre Chambon, and Régine Losson. 2001. "Heterochromatin Formation in Mammalian Cells: Interaction between Histones and HP1 Proteins." *Molecular Cell* 7 (4): 729–39. https://doi.org/10.1016/S1097-2765(01)00218-0.

Nora, Elphège P., Bryan R. Lajoie, Edda G. Schulz, Luca Giorgetti, Ikuhiro Okamoto, Nicolas Servant, Tristan Piolot, et al. 2012. "Spatial Partitioning of the Regulatory Landscape of the X-Inactivation Centre." *Nature* 485 (7398): 381–85. https://doi.org/10.1038/nature11049.

Pencik, Jan, Ha Thi Thanh Pham, Johannes Schmoellerl, Tahereh Javaheri, Michaela Schlederer, Zoran Culig, Olaf Merkel, Richard Moriggl, Florian Grebien, and Lukas

Kenner. 2016. “JAK-STAT Signaling in Cancer: From Cytokines to Non-Coding Genome.” *Cytokine* 87: 26–36. https://doi.org/10.1016/j.cyto.2016.06.017.
Penke, Taylor J.R., Daniel J. McKay, Brian D. Strahl, A. Gregory Matera, and Robert J. Duronio. 2016. “Direct Interrogation of the Role of H3K9 in Metazoan Heterochromatin Function.” *Genes and Development* 30 (16): 1866–80. https://doi.org/10.1101/gad.286278.116.
Penke, Taylor, Daniel J. McKay, Brian D. Strahl, A. Gregory Matera, and Robert J. Duronio. 2018. “Functional Redundancy of Variant and Canonical Histone H3 Lysine 9 Modification in Drosophila.” *Genetics* 208 (1): 229–44. https://doi.org/10.1534/genetics.117.300480.
Pherson, Michelle, Ziva Misulovin, Maria Gause, and Dale Dorsett. 2019. “Cohesin Occupancy and Composition at Enhancers and Promoters Are Linked to DNA Replication Origin Proximity in Drosophila.” *Genome Research* 29 (4): 602–12. https://doi.org/10.1101/gr.243832.118.
Piacentini, Lucia, Laura Fanti, Rodolfo Negri, Valerio Del Vescovo, Alessandro Fatica, Fabio Altieri, and Sergio Pimpinelli. 2009. “Heterochromatin Protein 1 (HP1a) Positively Regulates Euchromatic Gene Expression through RNA Transcript Association and Interaction with HnRNPs in Drosophila.” *PLoS Genetics* 5 (10). https://doi.org/10.1371/journal.pgen.1000670.
Picketts, D J, D R Higgs, S Bachoo, D J Blake, O W Quarrell, and R J Gibbons. 1996. “ATRX Encodes a Novel Member of the SNF2 Family of Proteins: Mutations Point to a Common Mechanism Underlying the ATR-X Syndrome.” *Human Molecular Genetics* 5 (12): 1899–1907. https://doi.org/6d0165 [pii].
Pope, Benjamin D., Tyrone Ryba, Vishnu Dileep, Feng Yue, Weisheng Wu, Olgert Denas, Daniel L. Vera, et al. 2014. “Topologically Associating Domains Are Stable Units of Replication-Timing Regulation.” *Nature* 515 (7527): 402–5. https://doi.org/10.1038/nature13986.
Rao, Suhas S.P., Miriam H. Huntley, Neva C. Durand, Elena K. Stamenova, Ivan D. Bochkov, James T. Robinson, Adrian L. Sanborn, et al. 2014. “A 3D Map of the Human Genome at Kilobase Resolution Reveals Principles of Chromatin Looping.” *Cell* 159 (7): 1665–80. https://doi.org/10.1016/j.cell.2014.11.021.
Ricci, Maria Aurelia, Carlo Manzo, María Filomena García-Parajo, Melike Lakadamyali, and Maria Pia Cosma. 2015. “Chromatin Fibers Are Formed by Heterogeneous Groups of Nucleosomes in Vivo.” *Cell* 160 (6): 1145–58. https://doi.org/10.1016/j.cell.2015.01.054.
Richards, Eric J., and Sarah C.R. Elgin. 2002. “Epigenetic Codes for Heterochromatin Formation and Silencing: Rounding up the Usual Suspects.” *Cell* 108 (4): 489–500. https://doi.org/10.1016/S0092-8674(02)00644-X.
Rowley, M. Jordan, and Victor G. Corces. 2018. “Organizational Principles of 3D Genome Architecture.” *Nature Reviews Genetics* 19 (12): 789–800. https://doi.org/10.1038/s41576-018-0060-8.
Rowley, M. Jordan, Michael H. Nichols, Xiaowen Lyu, Masami Ando-Kuri, I. Sarahi M. Rivera, Karen Hermetz, Ping Wang, Yijun Ruan, and Victor G. Corces. 2017. “Evolutionarily Conserved Principles Predict 3D Chromatin Organization.” *Molecular*

Cell 67 (5): 837-852.e7. https://doi.org/10.1016/j.molcel.2017.07.022.
Rudolph, Thomas, Masato Yonezawa, Sandro Lein, Kathleen Heidrich, Stefan Kubicek, Christiane Scha, Sameer Phalke, et al. 2007. "Heterochromatin Formation in Drosophila Is Initiated through Active Removal of H3K4." *Mol. Cell* 2: 103–15. https://doi.org/10.1016/j.molcel.2007.02.025.
Sadic, Dennis, Katharina Schmidt, Sophia Groh, Ivan Kondofersky, Joachim Ellwart, Christiane Fuchs, Fabian J Theis, and Gunnar Schotta. 2015. "Atrx Promotes Heterochromatin Formation at Retrotransposons." *EMBO Reports* 16 (7): 836–50. https://doi.org/10.15252/embr.201439937.
Saha, Anjanabha, Jacqueline Wittmeyer, and Bradley R. Cairns. 2006. "Chromatin Remodelling: The Industrial Revolution of DNA around Histones." *Nature Reviews Molecular Cell Biology* 7 (6): 437–47. https://doi.org/10.1038/nrm1945.
Schneiderman, Jonathan I., Guillermo A. Orsi, Kelly T. Hughes, Benjamin Loppin, and Kami Ahmad. 2012. "Nucleosome-Depleted Chromatin Gaps Recruit Assembly Factors for the H3.3 Histone Variant." *Proceedings of the National Academy of Sciences of the United States of America* 109 (48): 19721–26. https://doi.org/10.1073/pnas.1206629109.
Schneiderman, Jonathan I., Akiko Sakai, Sara Goldstein, and Kami Ahmad. 2009. "The XNP Remodeler Targets Dynamic Chromatin in Drosophila." *Proceedings of the National Academy of Sciences of the United States of America* 106 (34): 14472–77. https://doi.org/10.1073/pnas.0905816106.
Schotta, Gunnar, Anja Ebert, Veiko Krauss, Andreas Fischer, Jan Hoffmann, Stephen Rea, Thomas Jenuwein, Rainer Dorn, and Gunter Reuter. 2002. "Central Role of Drosophila SU(VAR)3-9 in Histone H3-K9 Methylation and Heterochromatic Gene Silencing." *EMBO Journal* 21 (5): 1121–31. https://doi.org/10.1093/emboj/21.5.1121.
Schwartzentruber, Jeremy, Andrey Korshunov, Xiao Yang Liu, David T.W. Jones, Elke Pfaff, Karine Jacob, Dominik Sturm, et al. 2012. "Driver Mutations in Histone H3.3 and Chromatin Remodelling Genes in Paediatric Glioblastoma." *Nature* 482 (7384): 226–31. https://doi.org/10.1038/nature10833.
Schwendemann, A., T. Matkovic, C. Linke, A. Klebes, A. Hofmann, and G. Korge. 2008. "Hip, an HP1-Interacting Protein, Is a Haplo- and Triplo-Suppressor of Position Effect Variegation." *Proceedings of the National Academy of Sciences* 105 (1): 204–9. https://doi.org/10.1073/pnas.0705595105.
Seller, Charles A, Chun-yi Cho, and Patrick H O Farrell. 2019. "Rapid Embryonic Cell Cycles Defer the Establishment of Heterochromatin by Eggless / SetDB1 in Drosophila." *Genes & Development*, 1–15. https://doi.org/10.1101/gad.321646.118.GENES.
Sexton, Tom, Eitan Yaffe, Ephraim Kenigsberg, Frédéric Bantignies, Benjamin Leblanc, Michael Hoichman, Hugues Parrinello, Amos Tanay, and Giacomo Cavalli. 2012. "Three-Dimensional Folding and Functional Organization Principles of the Drosophila Genome." *Cell* 148 (3): 458–72. https://doi.org/10.1016/j.cell.2012.01.010.
Shaffer, C. D., G. E. Stephens, B. A. Thompson, L. Funches, J. A. Bernat, C. A. Craig, and S. C. R. Elgin. 2002. "Heterochromatin Protein 2 (HP2), a Partner of HP1 in Drosophila Heterochromatin." *Proceedings of the National Academy of Sciences* 99 (22): 14332–37. https://doi.org/10.1073/pnas.212458899.

Shi, Song, Kimberly Larson, Dongdong Guo, Su Jun Lim, Pranabananda Dutta, Shian Jang Yan, and Willis X. Li. 2008. “Drosophila STAT Is Required for Directly Maintaining HP1 Localization and Heterochromatin Stability.” *Nature Cell Biology* 10 (4): 489–96. https://doi.org/10.1038/ncb1713.

Singhi, Aatur D., Ta Chiang Liu, Justin L. Roncaioli, Dengfeng Cao, Herbert J. Zeh, Amer H. Zureikat, Allan Tsung, et al. 2017. “Alternative Lengthening of Telomeres and Loss of DAXX/ATRX Expression Predicts Metastatic Disease and Poor Survival in Patients with Pancreatic Neuroendocrine Tumors.” *Clinical Cancer Research* 23 (2): 600–609. https://doi.org/10.1158/1078-0432.CCR-16-1113.

St Johnston, Daniel. 2002. “The Art and Design of Genetic Screens: Drosophila Melanogaster.” *Nature Reviews Genetics* 3 (3): 176–88. https://doi.org/10.1038/nrg751.

Steensel, Bas van, and Andrew S. Belmont. 2017. “Lamina-Associated Domains: Links with Chromosome Architecture, Heterochromatin, and Gene Repression.” *Cell* 169 (5): 780–91. https://doi.org/10.1016/j.cell.2017.04.022.

Stevens, Tim J., David Lando, Srinjan Basu, Liam P. Atkinson, Yang Cao, Steven F. Lee, Martin Leeb, et al. 2017. “3D Structures of Individual Mammalian Genomes Studied by Single-Cell Hi-C.” *Nature* 544 (7648): 59–64. https://doi.org/10.1038/nature21429.

Stormo, Benjamin M., and Donald T. Fox. 2017. “Polyteny: Still a Giant Player in Chromosome Research.” *Chromosome Research* 25 (3–4): 201–14. https://doi.org/10.1007/s10577-017-9562-z.

Swenson, Joel M., Serafin U. Colmenares, Amy R. Strom, Sylvain V. Costes, and Gary H. Karpen. 2016. “The Composition and Organization of Drosophila Heterochromatin Are Heterogeneous and Dynamic.” *ELife* 5: 1–37. https://doi.org/10.7554/eLife.16096.001.

Tang, Jun, Shaobo Wu, Hongtu Liu, Rachael Stratt, Orr G. Barak, Ramin Shiekhattar, David J. Picketts, and Xiaolu Yang. 2004. “A Novel Transcription Regulatory Complex Containing Death Domain-Associated Protein and the ATR-X Syndrome Protein.” *Journal of Biological Chemistry* 279 (19): 20369–77. https://doi.org/10.1074/jbc.M401321200.

Torres, Idelisse Ortiz, and Danica Galonić Fujimori. 2015. “Functional Coupling between Writers, Erasers and Readers of Histone and DNA Methylation.” *Current Opinion in Structural Biology* 35: 68–75. https://doi.org/10.1016/j.sbi.2015.09.007.

Tschiersch, B., A. Hofmann, V. Krauss, R. Dorn, G. Korge, and G. Reuter. 1994. “The Protein Encoded by the Drosophila Position-Effect Variegation Suppressor Gene Su(Var)3-9 Combines Domains of Antagonistic Regulators of Homeotic Gene Complexes.” *The EMBO Journal* 13 (16): 3822–31. https://doi.org/10.1002/j.1460-2075.1994.tb06693.x.

Tsukiyama, Toshio, Carla Daniel, John Tamkun, and Carl Wu. 1995. “ISWI, a Member of the SWI2/SNF2 ATPase Family, Encodes the 140 KDa Subunit of the Nucleosome Remodeling Factor.” *Cell* 83 (6): 1021–26. https://doi.org/10.1016/0092-8674(95)90217-1.

Uhlén, Mathias, Linn Fagerberg, Björn M Hallström, Cecilia Lindskog, Per Oksvold, Adil Mardinoglu, Åsa Sivertsson, et al. 2015. “Tissue-Based Map of the Human Proteome.”

Science 347 (6220): 1260419. https://doi.org/10.1126/science.1260419.
Vad-Nielsen, Johan, and Anders Lade Nielsen. 2015. "Beyond the Histone Tale: HP1α Deregulation in Breast Cancer Epigenetics." *Cancer Biology and Therapy* 16 (2): 189–200. https://doi.org/10.1080/15384047.2014.1001277.
Valadez-Graham, Viviana, Yasuhide Yoshioka, Oscar Velazquez, Akihito Kawamori, Martha Vázquez, Adina Neumann, Masamitsu Yamaguchi, and Mario Zurita. 2012. "XNP/DATRX Interacts with DREF in the Chromatin to Regulate Gene Expression." *Nucleic Acids Research* 40 (4): 1460–74. https://doi.org/10.1093/nar/gkr865.
Varga-Weisz, Patrick D., Matthias Wilm, Edgar Bonte, Katia Dumas, Matthias Mann, and Peter B. Becker. 1997. "Chromatin-Remodelling Factor CHRAC Contains the ATPases ISWI and Topoisomerase II." *Nature* 388 (6642): 598–602. https://doi.org/10.1038/41587.
Villican, Claudia, Grisel Cruz, and Mario Zurita. 2013. "The Genetic Depletion or the Triptolide Inhibition of TFIIH in P53-Deficient Cells Induces a JNK-Dependent Cell Death in Drosophila," 2502–15. https://doi.org/10.1242/jcs.122721.
Wang, Gang G., C. David Allis, and Ping Chi. 2007. "Chromatin Remodeling and Cancer, Part II: ATP-Dependent Chromatin Remodeling." *Trends in Molecular Medicine* 13 (9): 373–80. https://doi.org/10.1016/j.molmed.2007.07.004.
Webster, Micah, Keren L. Wikin, and Orna Cohen-Fix. 2009. "Sizing up the Nucleus: Nuclear Shape, Size and Nuclear-Envelope Assembly." *Journal of Cell Science* 122 (10): 1477–86. https://doi.org/10.1242/jcs.037333.
Whitehouse, Iestyn, Andrew Flaus, Bradley R. Cairns, Malcolm F. White, Jerry L. Workman, and Tom Owen-Hughes. 1999. "Nucleosome Mobilization Catalysed by the Yeast SWI/SNF Complex." *Nature* 400 (6746): 784–87. https://doi.org/10.1038/23506.
Williams, Monique M., Angela J. Mathison, Trent Christensen, Patricia T. Greipp, Darlene L. Knutson, Eric W. Klee, Michael T. Zimmermann, Juan Iovanna, Gwen A. Lomberk, and Raul A. Urrutia. 2019. "Aurora Kinase B-Phosphorylated HP1α Functions in Chromosomal Instability." *Cell Cycle* 18 (12): 1407–21. https://doi.org/10.1080/15384101.2019.1618126.
Wolff, Joachim, Leily Rabbani, Ralf Gilsbach, Gautier Richard, Thomas Manke, Rolf Backofen, and Björn A Grüning. 2020. "Galaxy HiCExplorer 3: A Web Server for Reproducible Hi-C, Capture Hi-C and Single-Cell Hi-C Data Analysis, Quality Control and Visualization." *Nucleic Acids Research*, April. https://doi.org/10.1093/nar/gkaa220.
Wong, Lee H., James D. McGhie, Marcus Sim, Melissa A. Anderson, Soyeon Ahn, Ross D. Hannan, Amee J. George, Kylie A. Morgan, Jeffrey R. Mann, and K. H.Andy Choo. 2010. "ATRX Interacts with H3.3 in Maintaining Telomere Structural Integrity in Pluripotent Embryonic Stem Cells." *Genome Research* 20 (3): 351–60. https://doi.org/10.1101/gr.101477.109.
Wood, Jason G., Sara Hillenmeyer, Charles Lawrence, Chengyi Chang, Suzanne Hosier, Will Lightfoot, Eric Mukherjee, et al. 2010. "Chromatin Remodeling in the Aging Genome of Drosophila." *Aging Cell* 9 (6): 971–78. https://doi.org/10.1111/j.1474-9726.2010.00624.x.
Xu, Na, Alexander V Emelyanov, Dmitry V Fyodorov, and Arthur I Skoultchi. 2014.

"Drosophila Linker Histone H1 Coordinates STAT-Dependent Organization of Heterochromatin and Suppresses Tumorigenesis Caused by Hyperactive JAK-STAT Signaling." *Epigenetics and Chromatin*, 1–13.

Xue, Yutong, Richard Gibbons, Zhijiang Yan, Dafeng Yang, Tarra L. McDowell, Salvatore Sechi, Jun Qin, Sharleen Zhou, Doug Higgs, and Weidong Wang. 2003. "The ATRX Syndrome Protein Forms a Chromatin-Remodeling Complex with Daxx and Localizes in Promyelocytic Leukemia Nuclear Bodies." *Proceedings of the National Academy of Sciences of the United States of America* 100 (19): 10635–40. https://doi.org/10.1073/pnas.1937626100.

Yamamoto, Ken, and Miki Sonoda. 2003. "Self-Interaction of Heterochromatin Protein 1 Is Required for Direct Binding to Histone Methyltransferase, SUV39H1." *Biochemical and Biophysical Research Communications* 301 (2): 287–92. https://doi.org/10.1016/S0006-291X(02)03021-8.

Yu, Jiujiu, Yun Li, Takahiro Ishizuka, Matthew G. Guenther, and Mitchell A. Lazar. 2003. "A SANT Motif in the SMRT Corepressor Interprets the Histone Code and Promotes Histone Deacetylation." *EMBO Journal* 22 (13): 3403–10. https://doi.org/10.1093/emboj/cdg326.

Zhimulev, I. F., E. S. Belyaeva, V. F. Semeshin, D. E. Koryakov, S. A. Demakov, O. V. Demakova, G. V. Pokholkova, and E. N. Andreyeva. 2004. "Polytene Chromosomes: 70 Years of Genetic Research." *International Review of Cytology* 241 (SPEC.ISS.): 203–75. https://doi.org/10.1016/S0074-7696(04)41004-3.

Zhimulev, Igor F, and Dmitry E Koryakov. 2009. "Polytene Chromosomes." *Encyclopedia of Life Sciences*, no. 1881: 1–10. https://doi.org/10.1002/9780470015902.a0001183.pub2.

Zhu, Quan, Gerald M. Pao, Alexis M. Huynh, Hoonkyo Suh, Nina Tonnu, Petra M. Nederlof, Fred H. Gage, and Inder M. Verma. 2011. "BRCA1 Tumour Suppression Occurs via Heterochromatin-Mediated Silencing." *Nature* 477 (7363): 179–84. https://doi.org/10.1038/nature10371.

11. ANEXOS

Para evaluar si las proteínas dADD1 o XNP de *Drosophila* estaban involucradas en la deposición de la variante H3.3 como en mamíferos, realice inmunotinciones de cromosomas politénicos. Las mutantes y el protocolo se encuentran descritos en materiales y métodos, con la dilución de anticuerpo H3.3 millipore a una concentración de 1:10 y la polimersa serina 5 fosforilada 1:500.

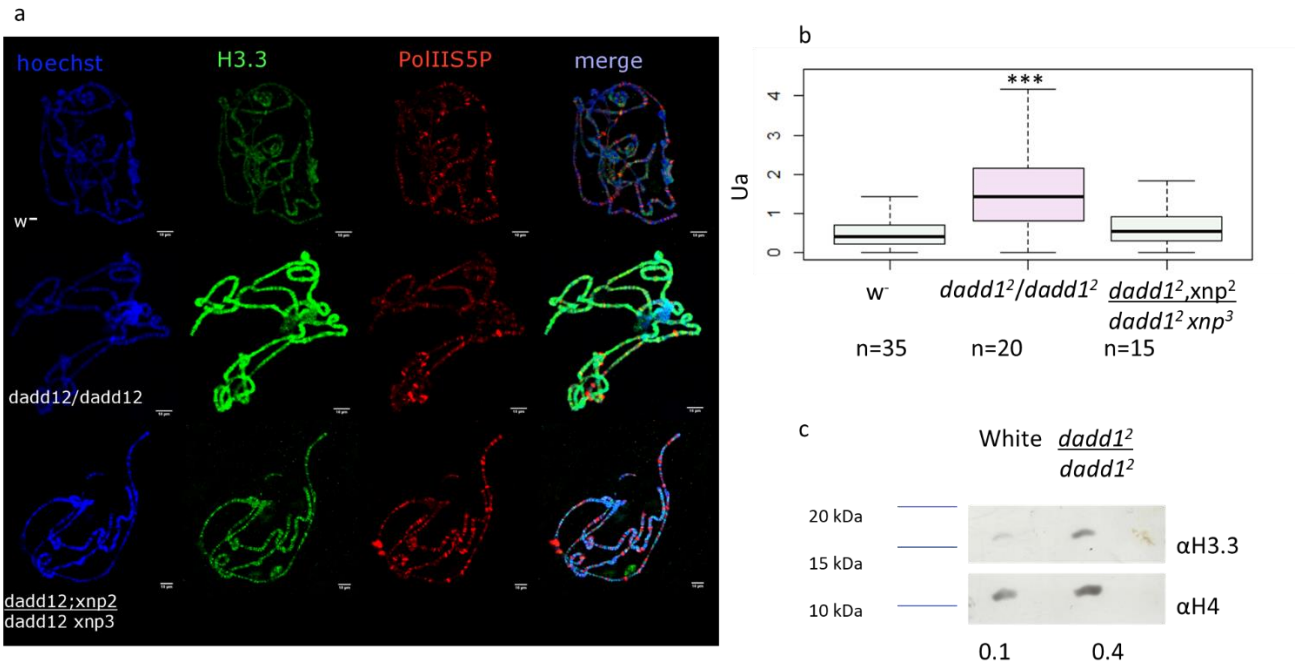

Anexo 1. Las ausencia de las proteínas dAdd1 incrementa la deposición de la variante H3.3 a) Inmunotincion de cromosomas politénicos "*wild type*", *dadd1²/ dadd1²* (nula) y *dadd1²/ dadd1²;* xnp²/xnp³ (condición heteroalélica en la que disminuyen los transcritos de dxnp más la condición nula), ADN (la tinción DAPI se muestra en azul), H3.3 (señal verde), Polimersa serina 5 fosforilada (señal roja), y la fusión de colores, la barra de escala es de 20 µm. b) La intensidad de la señal de H3.3 en unidades arbitrarias se cuantificó mediante ImageJ, "n" representa el número de cromosomas analizados en cada genotipo; Se realizó una prueba ANOVA unidireccional ordinaria para determinar si fue significativo p <0.001 ***. c) Western blot de extractos de proteínas unidas a la cromatina (modificado de Berstein & Wysocka) de glándulas salivales donde se usaron anticuerpos H3.3 y H4. Los carriles corresponden al genotipo indicado en la parte superior, los marcadores de peso molecular se muestran al lado izquierdo de los paneles. En la parte inferior se muestra un número que fue la cuantificación de la intensidad de la banda de H3.3 respecto H4 y se observa una mayor proporción de H3.3 en la mutante.

Tabla 8. Efecto de la sobreexpresión de dADD1 en el ala

Genotipo	Viabilidad	Fenotipo ala quemada
MS1096GAL4/+; UAS-dadd1/+	93/107	72/93 (77)
MS1096GAL4/Y; UAS-dadd1/+	14/107	0/14 (0)

- Ensayo de túnel

El ensayo de túnel (Terminal deoxynucleotidyl-transferase-mediated dUTP Nick end Labeling) se realizó en discos de ala de larvas de tercer estadio hembra siguiendo las instrucciones del proveedor del kit "In Situ Cell Death Detection kit TMR red", Roche (no de catálogo 11684795910). Los discos se montaron en glicerol al 80%, galato de n-propilo al 4% en 1X PBS y se almacenaron en la oscuridad hasta la observación en microscopía confocal.

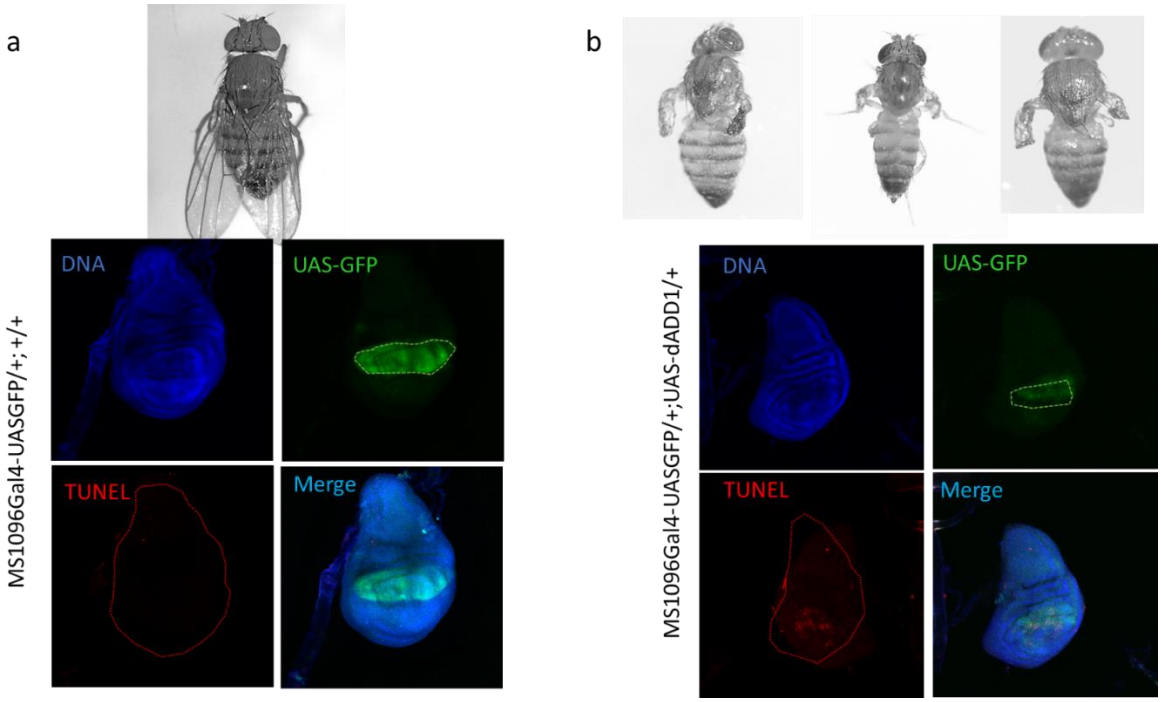

Anexo 2. La sobreexpresión de dADD1 causa una muerte celular masiva en el disco del ala por apoptosis. a) En la parte superior se muestra el control de la mosca adulta hembra y el disco del ala que muestra un fenotipo de tipo salvaje MS1096GAL4-UASGFP / +.b) En la segunda columna se muestra que la sobreexpresión de dADD1 (MS1096GAL4-UASGFP / +; UAS-dADD1/ +) que causa alas quemadas en moscas adultas hembras y cuerpos apoptóticos en la bolsa del disco del ala. ADN (azul), TUNEL (rojo), dominio de expresión MS1096GAL4-UASGFP (verde) y "merge".

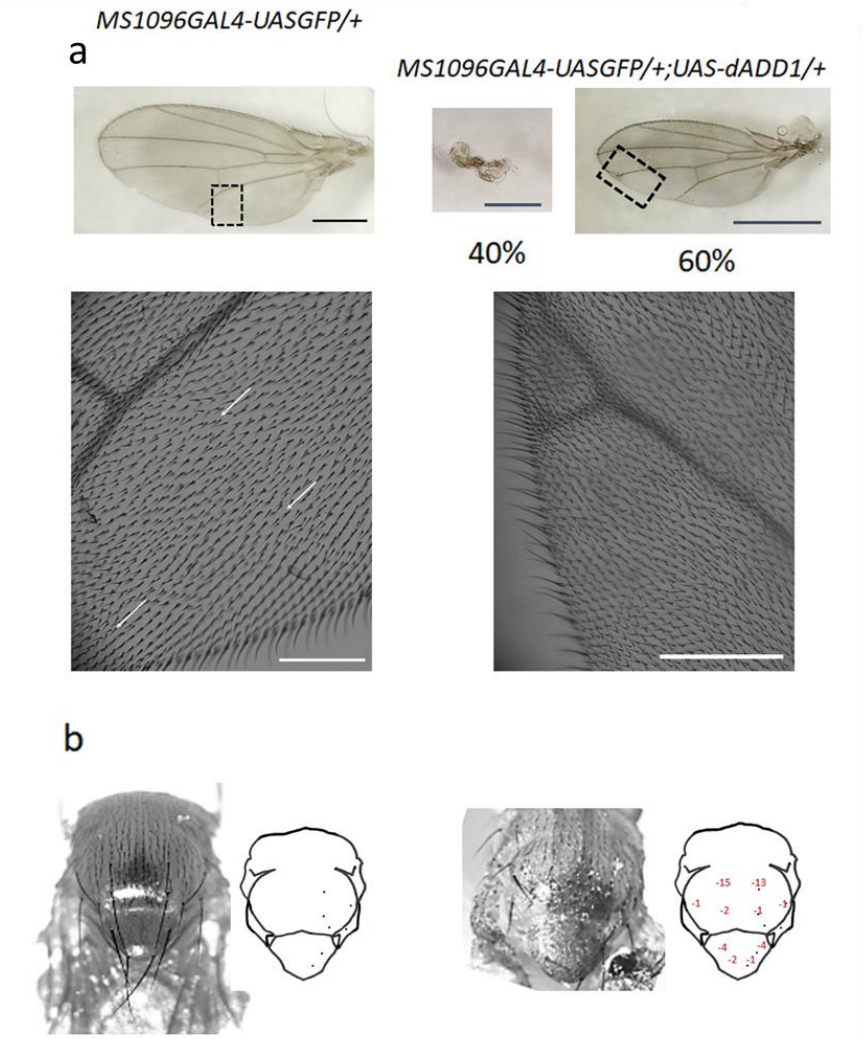

Anexo 3. La sobreexpresión de dADD1 origina defectos en las macroquetas. a)L a primera columna muestra una mosca control donde podemos ver un ala "wild-type" y un acercamiento. EN la columna derecha podemos ver la sobreexpresión de dADD1 (MS1096GAL4-UASGFP / +; UAS-dADD1 / +) que provoca el fenotipo de ala quemada cerca de un 40% (ver tabla 8). Las moscas que no tiene el ala quemada presentan venaciones extras como se muestra en la fotografía de abajo. Se añadieron flechas blancas para observar que todas las vellosidades tienen el mismo sentido en la condición wt, no siendo el caso en la mutante. b) En la parte inferior observamos el tórax de una hembra adulta como fenotipo de "*wild type*" MS1096GAL4-UASGFP / + y la caricatura representativa a su lado donde deben de estar las macroquetas. A la derecha se muestra la sobreexpresión de dADD1 (MS1096GAL4-UASGFP / +; UAS-dADD1 / +) que provoca la pérdida de macroquetas. La segunda fila es una caricatura con un resumen de las pérdidas de las macroquetas observadas con un número rojo.

- Inmunotinciones de discos imagales de alas de larvas del tercer instar

Los discos de alas se obtuvieron de larvas hembras de tercer estadio ys e siguió el protocolo exacto descrito por la Dra. Claudia Villicaña (Villican, Cruz, and Zurita 2013) . Brevemente, se disecaron discos imagales en 1X PBS frío y se fijaron con paraformaldehído al 4% durante 30 min a temperatura ambiente. Los discos se lavaron con PBT (1X PBS más Triton X-100 al 0,2%), se bloquearon durante 1 h con albúmina de suero bovino al 0,1% en PBST 1X con NaCl 250 mM a 4C. Los anticuerpos primarios se añadieron a diluciones apropiadas durante la noche a 4 C°:

HP1a C1A9 de Hybridoma Bank 1:3000

anti-Histona H3K9me3 Abcam 8898 1:100

anti-Histona H3S10P 1:1000

P-JNK (Abcam) 1:100

Al día siguiente se lavaron los discos con PBT. Los anticuerpos secundarios se agregaron junto con Hoechst (0.1 ug / ml) durante 2 h a temperatura ambiente, se lavaron nuevamente con PBST y después de eliminar PBST, los discos se montaron en glicerol al 80%, galato de n-propilo al 4% en 1X PBS y se almacenaron en la oscuridad hasta la observación en microscopía confocal.

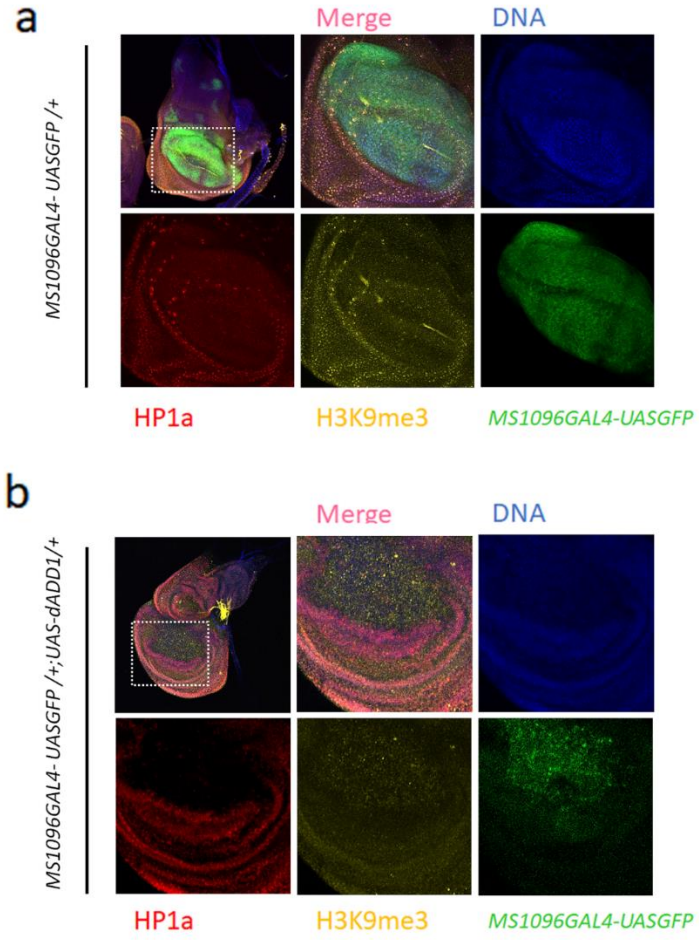

Anexo 4 La sobreexpresión de proteínas dADD1 perturba la señal de HP1a y H3K9me3 en el disco del ala. a) Inmunotinción del control del disco del ala que muestra un fenotipo de tipo salvaje MS1096GAL4-UASGFP / +. Inmunotinción del disco del ala que sobreexpresa dADD1 donde ADN (azul), HP1a (rojo), dominio de expresión MS1096GAL4-UASGFP (verde), H3K9me3 (amarillo) y “merge”.

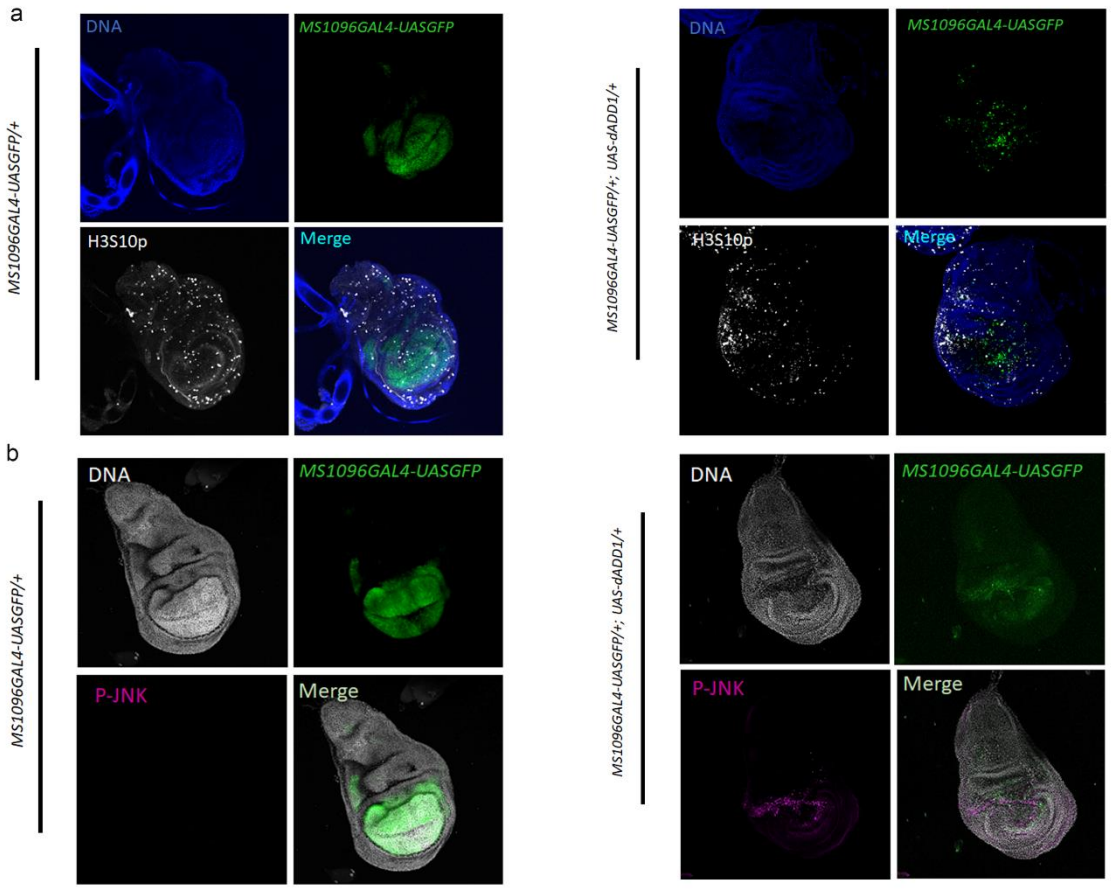

Anexo 5. dADD1 no afecta el ciclo celular, pero induce la apoptosis a través de JNK. a) Inmunotinción del control del disco del ala que muestra un fenotipo de tipo salvaje MS1096GAL4-UASGFP / + versus sobreexpresión de dADD1 con ADN (azul), H3S10P (gris), dominio de expresión MS1096GAL4-UASGFP (verde) y Merge. b) Inmunotinción del control del disco del ala que muestra un fenotipo de tipo salvaje MS1096GAL4-UASGFP / + frente a la sobreexpresión de dADD1 con ADN (gris), P-JNK (magenta), dominio de expresión MS1096GAL4-UASGFP (verde) y Merge.

12. PUBLICACIONES

- Characterization of the Drosophila group ortholog to the amino-terminus of the alpha-thalassemia and mental retardation X-Linked (ATRX) vertebrate protein. López-Falcón B, **Meyer-Nava S**, Hernández-Rodríguez B, Campos A, Montero D, Rudiño E, Vázquez M, Zurita M, Valadez-Graham V. PLoS One. 2014 Dec 1;9(12):e113182. doi: 10.1371/journal.pone.0113182. eCollection 2014.

- Molecular effects of dADD1 misexpression in chromatin organization and transcription. **Meyer-Nava S**, Torres A, Zurita M, Valadez-Graham V. BMC Mol Cell Biol. 2020 Mar 23;21(1):17. doi: 10.1186/s12860-020-00257-2.

- A cross-sectional report on melasma among Hispanic patients: Evaluating the role of oral tranexamic acid versus oral tranexamic acid plus hydroquinone. Arreola Jauregui IE, Huerta Rivera G, Soria Orozco **M, Meyer-Nava S**, Paniagua Santos JE, López Zaldo JB, Meyer-Nava I, Madrid Carrillo C, Zaldo Rolón IE, Baeza Echeverría AE, Vázquez Huerta M. J Am Acad Dermatol. 2020 Nov;83(5):1457-1458. doi: 10.1016/j.jaad.2020.02.072. Epub 2020 Mar 6.

- Insights into HP1a-Chromatin Interactions. **Meyer-Nava S**, Nieto-Caballero VE, Zurita M, Valadez-Graham V. Cells. 2020 Aug 9;9(8):1866. doi: 10.3390/cells9081866.

- Immunofluorescent Staining for Visualization of Heterochromatin Associated Proteins in Drosophila Salivary Glands. **Meyer-Nava S**, Zurita M, Valadez-Graham V. JoVE. 2021. Accepted manuscript.

PLOS ONE

RESEARCH ARTICLE

Characterization of the *Drosophila* Group Ortholog to the Amino-Terminus of the Alpha-Thalassemia and Mental Retardation X-Linked (ATRX) Vertebrate Protein

Brenda López-Falcón[1☯], Silvia Meyer-Nava[1☯], Benjamín Hernández-Rodríguez[1], Adam Campos[2], Daniel Montero[1], Enrique Rudiño[2], Martha Vázquez[1], Mario Zurita[1]*, Viviana Valadez-Graham[1]*

1. Departamento de Genética del Desarrollo y Fisiología Molecular, Instituto de Biotecnología, Universidad Nacional Autónoma de México, Cuernavaca, Morelos, México, **2.** Departamento de Medicina Molecular y Bioprocesos, Instituto de Biotecnología, Universidad Nacional Autónoma de México, Cuernavaca, Morelos, México

*vvaladez@ibt.unam.mx (VVG); marioz@ibt.unam.mx (MZ)

☯ These authors contributed equally to this work.

Citation: López-Falcón B, Meyer-Nava S, Hernández-Rodríguez B, Campos A, Montero D, et al. (2014) Characterization of the *Drosophila* Group Ortholog to the Amino-Terminus of the Alpha-Thalassemia and Mental Retardation X-Linked (ATRX) Vertebrate Protein. PLoS ONE 9(12): e113182. doi:10.1371/journal.pone.0113182

Editor: Barbara Jennings, Oxford Brookes University, United Kingdom

Received: July 17, 2014

Accepted: October 21, 2014

Published: December 1, 2014

Data Availability: The authors confirm that all data underlying the findings are fully available without restriction. All relevant data are within the paper and its Supporting Information files.

Funding: This work was supported by grant 127440 from Consejo Nacional de Ciencia y Tecnología to MZ and grants 177393, Joven Investigador, from Consejo Nacional de Ciencia y Tecnologia and IA200613 from Programa de Apoyo a Proyectos de Investigación e Innovación Tecnológica, Universidad Nacional Autónoma de México to VVG. The funders had no role in study design, data collection and analysis, decision to publish, or preparation of the manuscript.

Competing Interests: The authors have declared that no competing interests exist.

Abstract

The human *ATRX* gene encodes hATRX, a chromatin-remodeling protein harboring an helicase/ATPase and ADD domains. The ADD domain has two zinc fingers that bind to histone tails and mediate hATRX binding to chromatin. dAtrx, the putative ATRX homolog in *Drosophila melanogaster*, has a conserved helicase/ATPase domain but lacks the ADD domain. A bioinformatic search of the *Drosophila* genome using the human ADD sequence allowed us to identify the *CG8290* annotated gene, which encodes three ADD harboring- isoforms generated by alternative splicing. This *Drosophila* ADD domain is highly similar in structure and in the amino acids which mediate the histone tail contacts to the ADD domain of hATRX as shown by 3D modeling. Very recently the *CG8290* annotated gene has been named *dadd1*. We show through pull-down and CoIP assays that the products of the *dadd1* gene interact physically with $dAtrx_L$ and HP1a and all of them mainly co-localize in the chromocenter, although euchromatic localization can also be observed through the chromosome arms. We confirm through ChIP analyses that these proteins are present *in vivo* in the same heterochromatic regions. The three isoforms are expressed throughout development. Flies carrying transheterozygous combinations of the *dadd1* and *atrx* alleles are semi-viable and have different phenotypes including the appearance of melanotic masses.

Interestingly, the dAdd1-b and c isoforms have extra domains, such as MADF, which suggest newly acquired functions of these proteins. These results strongly support that, in *Drosophila*, the *atrx* gene diverged and that the *dadd1*-encoded proteins participate with dAtrx in some cellular functions such as heterochromatin maintenance.

Introduction

The human *ATRX* gene (*hATRX*) was described approximately 20 years ago as the main gene mutated in ATRX syndrome (Alpha-Thalassemia with mental Retardation X-related). *ATRX* is localized on the X chromosome in position Xq13.1–q21.1. Individuals with mutations in this gene present several phenotypic charateristics that may include mental retardation, craniofacial and urogenital deformities, psychomotor failure and alpha-thalassemia [1]. Since its description, there have been important advances in the characterization of the molecular functions of the protein encoded by this gene. In humans, there are mainly two isoforms named hATRX (289 kDa) and hATRXt (t, from truncated, 200 kDa) that are encoded by this gene [2]. Both proteins contain an amino-terminal domain which is composed of PHD and GATA-like zinc fingers, named ADD after the three proteins that contain this domain (ATRX, DNMT3b and DNMT3L). It was recently demonstrated through different *in vitro* and *in vivo* approaches that this domain recognizes the combination of K9me3 and unmethylated K4 residues of the histone H3 tail [3]. This domain directs the protein mainly to pericentric heterochromatin [4]. Mutations described in patients afflicted with the syndrome mainly affect the important amino acids that form the "pocket" of the ADD domain for the histone H3 tail recognition. The hATRX protein additionally has a helicase/ATPase domain, which classifies it as a member of the SNF2 subfamily of chromatin remodelers [5]. The hATRX SNF2 domain has *in vitro* ATPase activity, which can be stimulated both by DNA and nucleosomes [6]. About 50% of the mutations described in patients fall in the ADD domain, whereas the other 50% affect the SNF2 helicase/ATPAse and other protein domains [7]. hATRX, as many chromatin remodelers, has been identified as a component of a complex that includes the histone variant H3.3 chaperone DAXX (Death domain Associated protein). This particular histone variant is incorporated at different chromatin regions, such as promoters, enhancers and heterochromatic regions, and it has been proposed to have dual functions in promoting both an active chromatin state and the maintenance of heterochromatin [8]. hATRX ATPase activity is important for incorporation of the histone variant H3.3 by the chaperone DAXX into specific regions of the chromosomes, such as telomeres and pericentric heterochromatin [9].

Genome-wide studies have identified hATRX as a protein that is able to bind to DNA regions that can acquire a G4 structure conformation, such as telomeres and

repetitive G-rich regions [9]; however, the important domain that mediates this interaction it is not yet known.

It is clear though that both the ADD and helicase/ATPase domains play crucial roles during development [1]. The *ATRX* gene is highly conserved through eukaryotic evolution, but in invertebrates and particularly in *Drosophila*, it encodes proteins that lack the ADD N-terminal domain, i.e., the $dAtrx_L$ and $dAtrx_s$ isoforms are encoded by the same gene but lack an ADD domain. The $dAtrx_L$ isoform interacts with HP1a and is localized to heterochromatin, whereas the $dAtrx_s$ isoform is localized to euchromatin [10].

We decided to determine if there was a gene in *Drosophila* that could encode proteins with the conserved the amino-terminus of the vertebrate ATRX. Performing *in silico* analyses, we demonstrate that the annotated gene *CG8290*, recently named *dadd1* [11], encodes three proteins with a conserved ADD domain that physically interact with $dAtrx_L$. Using a genetic approach, we found that these proteins have important functions during *Drosophila* development and that they cooperate with $dAtrx_L$ in certain functions. The evidence leads us to propose that the dAdd1 proteins are orthologs of the amino-terminus of the ATRX protein in vertebrates.

Materials and Methods

Ethics statement

All animal handling was approved by the Instituto de Biotecnología Bioethics Comittee, Permit Number 344 (2011/02/10), which follows NOM-062 animal welfare mexican law. All efforts were made to minimize animal suffering. Animals were sacrificed by CO_2 euthanasia.

Protein domain structure illustration

The domain organization of dAdd1 isoforms (Fig. 1C) and the representation of the fragments assayed by pull-down were performed using the DOG 1.0 Illustrator of Protein Domain Structures [12]. For gene representation we used FancyGene [13].

Alignments and phylogenetic inference analyses

Multiple alignments were performed with CLUSTALX2 2.1 [14] and the parameters for the Phylogenetic Inferences were used as estimated by ProtTest 2.4 program [15] for selection of models of protein evolution. The Maximum Likelihood Phylogenetic Analysis was computed by PhyML 3.0 [16] with the parameters: Substitution model: WAG (ADD) & LG (Helicase/ATPase) [17]; Bootstrap: 1000; Proportion of invariable sites: 0.12 (Both); Gamma shape parameter: 2.15 (ADD) & 0.81 (Helicase/ATPase). The tree was edited using Interactive Tree Of Life (iTOL) v2 [18] with Protein Domain Architecture information of the containing proteins as predicted by ScanProsite [19].

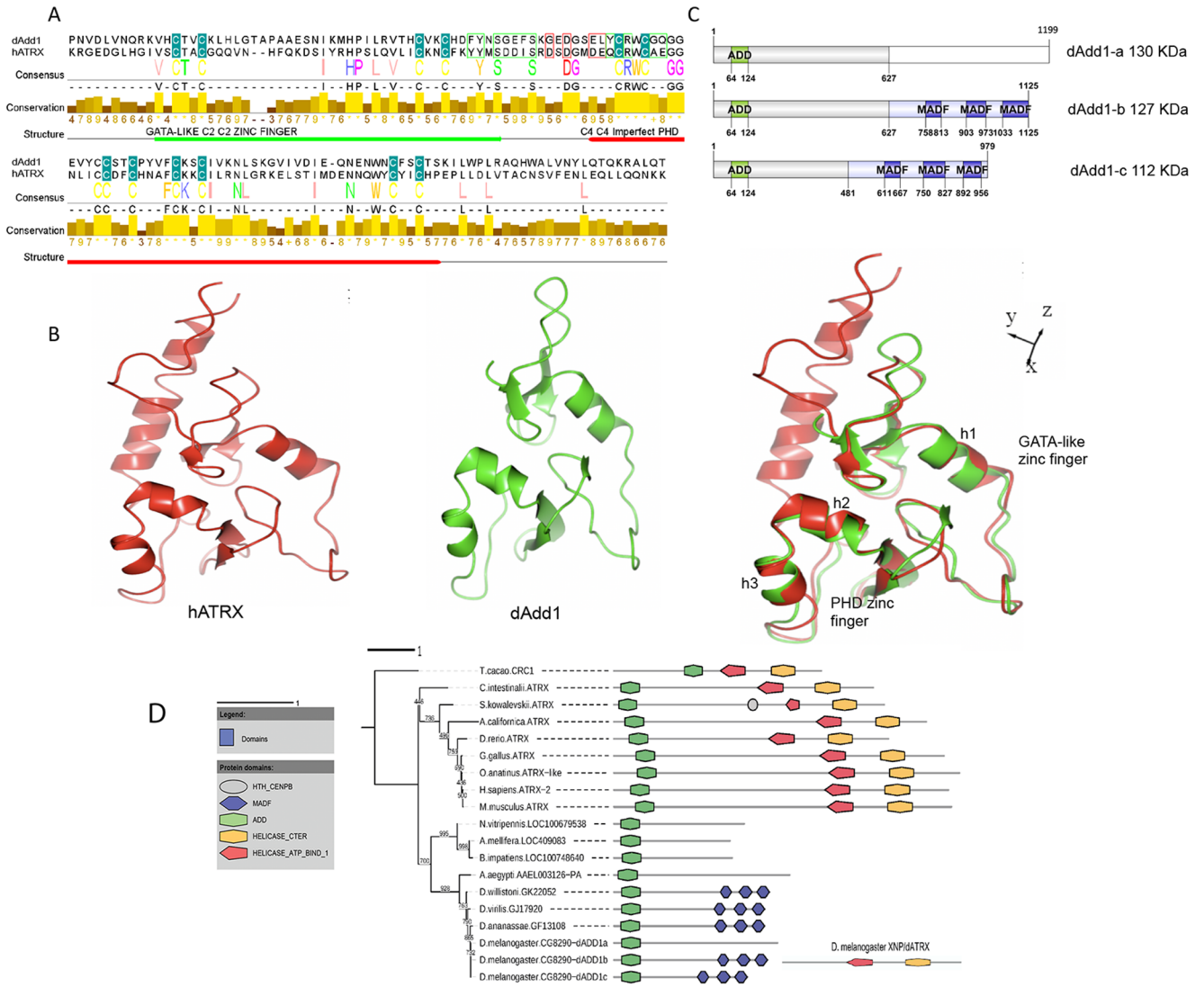

Figure 1. The ADD domain of the hATRX protein is conserved in the dAdd1 proteins of *Drosophila*. A. ADD domain prediction in the protein sequence alignment of hATRX and dAdd1 proteins. Conserved cysteines are shown as yellow letters within a cyan box. The amino acids involved in H3K9me3 and H3K4me0 recognition are marked by green and red boxes respectively. The GATA-like C2-C2 zinc finger and the C4-C4 imperfect PHD are marked by green and red boxes respectively. B. Ribbon representation of ADD domain of hATRX on red (left) and dAdd on green (center) CPH models-3.0 server was used to create the model of the ADD domain of dAdd1. Structural superposition of ADD domains of hATRX and dAdd1 (right). C. Domain organization of dAdd1 (a-c) isoforms. All of them have an N-terminal ADD domain. A C-terminal MADF domain is present in two (dAdd1-b, and dAdd1-c isoforms) copies. D. Maximum Likelihood Phylogenetic Analysis of the ADD domain and the corresponding Protein Domain Architecture information of the containing proteins as computed by PhyML [16] and ScanProsite [19], respectively. The numbers shown represent bootstrap values. Note that the ADD harboring protein underwent a gene fission event during the evolution of insects. Also note that the homologous proteins within the *Drosophila* genus have acquired a tandem MADF domain during its divergence from other insects. This domain is likely to be functional given its conservation within the genus. For the parameters used, refer to Material and Methods.

doi:10.1371/journal.pone.0113182.g001

Protein structure homology model

In an attempt to determine a protein-modeling of ADD domain (101 amino acid residues), we generated by SWISS-MODEL [20], a three-dimensional structural model of a protein target, based on identity sequence related with structures deposited in the Protein Data Bank. Basically the steps used in homology

modeling are the following: template identification, amino acid sequence alignment, model building and model verification (model quality) [21]. The crystal structure of the transcriptional regulator ATRX from *Homo sapiens* [22] PDB entry 3qla chain A, was used as a template for homology modeling. The identity between these two proteins was 37% and the structural similarity was 0.42. It is important to mention that the procedures implemented in SWISS-MODEL allow the modeling of sequences which share at least 35% identity with a known three dimensional structure. Although the resulting models do not represent the real 3D structure, it is accurate enough to learn about the general topology and a possible residue arrangement of the ADD protein sequence.

Fly stocks

The wild-type flies used in this study were Oregon R (*OreR*) or w^{1118}, and fly stocks were maintained at 25℃ with standard food. The stocks that carried the *atrx* alleles were obtained from the Bloomington Stock Center. The stocks that carried *dadd1* and *Su(var)2-5* alleles were obtained from the *Drosophila* Genetic Resource Center (DGRC), Kyoto Institute of Technology. The *xnp/atrx* alleles (called *atrx* for simplicity) were described by Bassett AR, *et al.*, (2008) [10]. The *dadd1* alleles: $dadd1^{NP0793}$ ($w^{*};P\{GawB\}^{NP0793}/CyO$) and $dadd1^{NP1240}$ ($y^{*}w^{*};P\{GawB\}^{NP1240}/CyO$, *P{UAS lacZ.UW14} UW14*), carry a *P*-element insertion at -225 and -223 bp from the translation initiation codon of the *dadd1* gene, respectively. The $Su(var)2\text{-}5^{2}$ allele is a missense mutation that has been characterized molecularly by Eissenberg *et al.*, (1992) [23]. This is a single mutation in the open reading frame: a G-A transition in the first nucleotide of codon 26, resulting in the substitution of methionine for valine that affects the chromodomain. The $Su(var)2\text{-}5^{5}$ allele is an X-ray induced mutation, in which only the first 10 amino acids of HP1a are translated [23]. The position effect variegation (PEV) reporter line BL1 is an inversion allele of the *hsp70-lacZ* transgenic reporter, with the reporter gene positioned adjacent to a 3L pericentric heterochromatin mass [24].

Genetic crosses

All stocks were outcrossed with w^{1118}; *Sp/CyO; TM6B, Tb/MKRS* flies for five generations. Chromosomes with the alleles of interest were followed by segregation with specific balancer chromosomes. To reassure the presence of the atrx alleles in these lines, females carrying alleles $atrx^{1}$, $atrx^{2}$ *and* $atrx^{3}$ chromosomes were outcrossed with males from parental $atrx^{1}$ allele and viability was assayed and compared to the previously reported viability [10]. The stocks that carried the *atrx* alleles were established and balanced with *TM6B, Tb* for chromosome 3. The stocks that carried the *dadd1* alleles were established and balanced with the *CyO* balancer for chromosome 2 and followed by *white* complementation. Fly crosses were performed according to standard procedures, three biological replicates were performed. At least 100 flies were examined for each genotype.

Antibodies

The $dAtrx_L$ antibody was previously described [25]. All antibodies were generated by New England Peptide (NEP). The pan-dAdd1 antibody was generated using the peptide: QGGEVYCCSTCPYVFCKSC wich recognizes dAdd1-a, b and c isoforms. For the dAdd1-a isoform, the CDLIKALGSPSVLP peptide was used and for the dAdd1-b isoform the CDKQFCQQLVLAM peptide was used. Specificity of these antibodies was assayed by their capability to recognize dAdd1-a or dAdd1-b fused to GST (see pull-down section and antibody specificity assays section for details) by western blot (Fig. S1). The HP1a antibody was obtained from the Developmental Studies Hybridoma Bank DSHB at the University of Iowa (C1A9). The HA antibody was obtained from Roche (Ref.11867423001). Antibodies used for mock immunoprecipitations were purified IgG from mouse GenScript (Cat. A01007); and purified IgG from rabbit Invitrogen (Cat.02-6102).

Antibody specificity assays

To test the specificity of the pan-dAdd1 antibody, a Western blot was performed with 100 μg of S2R+ protein extracts either using as primary antibody the non-depleted pan-dAdd1 antibody fraction or a supernatant from where the pan-dAdd1 antibodies were depleted (Fig. S1A). Depletion was performed by incubating the pan-dAdd1 antibody in PBS, Tween 0.01%, 5% nonfat milk for 2 hours in the presence of the dAdd1-GST fusion protein blotted onto a nitrocellulose membrane, after the incubation period, supernatant fraction was saved (depleted fraction). The GST-dAdd1 fusion protein harbors the dAdd1 QGGEVYCCSTCPYVFCKSC peptide (aa 122-137) that was used to raise the pan-dAdd1 antibody.

To test the specificity of the dAdd1-a and dAdd1-b antibodies, GST-dAdd1-a or b fusion proteins were expressed in bacteria, blotted onto a nitrocelulose membrane and incubated with either anti-dAdd1-a (Fig. S1B) or anti-dAdd1-b (Fig. S1C) showing that the different antibodies recognize their specific substrate. Detection was performed with the PIERCE quimioluminiscence substrate.

Immunostaining of polytene chromosomes

Polytene chromosomes for immunostaining were obtained from wild type *OreR* or w^{1118} lines or from $Xnp^{Scer\backslash UAS.T:Ivir\backslash HA1}/Sgs3\text{-}GAL4$ (w^{1118}; $P\{w^{+mC=Sgs3\text{-}GAL4.PD}\}TP1$) larvae. The $Xnp^{Scer\backslash UAS.T:Ivir\backslash HA1}$ allele is described in [10], and the *Sgs3-GAL4* (w^{1118}; $P\{w^{+mC=Sgs3\text{-}GAL4.PD}\}TP1$ driver line was used to direct Xnp/dAtrx (called dAtrx for simplicity throughout this manuscript) expression to salivary glands from third instar larvae. Both latter lines were obtained from the Bloomington *Drosophila* Stock Center.

Immunostaining of polytene chromosomes was performed with slight modifications of the protocol described in [25]. Salivary glands from third instar larvae were fixed in solution I (PBS, 3.7% paraformaldehyde and 1% Triton X-100) and then in solution II (3.7% paraformaldehyde, 50% acetic acid). The chromosomes were spread on poly-L-Lysine coated microscope slides. Anti-HP1a

(DSHB) antibody was used at 1:300, anti-dAtrx$_L$ antibody at 1:100, pan-dAdd1 at 1:50 and anti-HA (Roche) at 1:50. Secondary antibodies were Alexa fluor 488 used at 1:500 and Alexa fluor 568 or 594 used at 1:100 (Invitrogen). Images were taken on a confocal laser-scanning microscope (Olympus FV1000) at the Laboratoratorio Nacional de Microscopía Avanzada (LNMA, UNAM).

For the double dAdd1/dAtrx immunostaining we followed an epitope tagged version of dAtrx$_L$ (dAtrx$_L$-HA) because the dAdd1 and dAtrx$_L$ antibodies were raised in the same species and could not be used together for this experiment.

Pull-down assays

We generated fusion proteins of several fragments of dAtrx$_L$ and the dAdd1 proteins. All the clones used in this work were nucleotide-sequenced. The *Drosophila* LD28477, LD24316 and LD37351 cDNA (BDGP Gold collection of *Drosophila* Genomics Resource Center) were amplified by PCR and cloned in the *Eco*RI, *Not*I, *Sma*I, *Xho*I or *Sal*I sites of the pGEX-4T1 or pGBKT7 vector (details are available upon request). The dAtrx$_L$ and dAdd1 fragments were expressed as GST fusion proteins in a bacterial system. For interaction assays, over-expression of dAtrx$_L$ fragments fused to GST in bacteria was induced with 0.4 mM IPTG during 3 h. GST-dAtrx$_L$ fragments were purified using glutathione-sepharose (Amersham) according to manufacturer's instructions. The dAdd1 fragments were expressed and labelled with S^{35} using an *in vitro* transcription/translation system (TNT-Quick-Coupled Transcription/Translation System from Promega). Pull-down assays were performed according to the manufacturer's instructions.

Cell culture transfection and co-immunoprecipitation

The dAdd1-a cDNA was cloned into *Eco*RI/*Not*I sites of pAc5.1/V5-HisA vector (Invitrogen). *Drosophila* S2R+ cells were maintained in Schneider medium with 10% fetal bovine serum and 100 μg streptomycin/0.25 μg amphotericin. Cells were cotransfected with 10 μg of each construction by the calcium method (Invitrogen). Fourty-eight hours after transfection, the cells were collected and lysed. Lysates were clarified by centrifugation at 15.7 g at 4℃. CoIPs were performed as indicated in [26]. For embryo-stage immunoprecipitations: embryo nuclear extracts were prepared as described [27]. The Co-IP was performed as described in [28]. Antibodies used for mock immunoprecipitations were purified IgG from mouse GenScript (Cat. A01007); and purified IgG from rabbit Invitrogen (Cat.02-6102).

RT–PCR assays

RNA was obtained using the Trizol reagent (Invitrogen®) from embryos (0–3 and 3–21 hour post-fertilization), 1st, 2nd and 3rd instar larvae (L1, L2 and L3), pupae (P), pharate (Ph) and female and male adults Oregon R flies (F and M). 10 μg of total RNA was converted to cDNA using reverse transcriptase enzyme (Invitrogen) and oligo-dT and random primers (Stratagene®). To assess the

presence of the transcripts the following oligonucleotides were used for the PCR reaction: dAdd1-a forward (5′CATCTTACGGGCAAAGTGGT-3′); dAdd1-a reverse (5′CAGGCTGGCCAATATCGTGG-3′); dAdd1-b forward (5′GCTTGT-CATCGGGCATATCT-3′); dAdd1-b reverse (5′GCTCATAAGCAGCCAGCAG-T-3′); dAdd1-c forward (5′ACAGCGGCAGCAACGGAAGC-3′); dAdd1-c reverse (5′GCGGAAGTCCTTGCAGCGGT-3′); rp49 forward (5′TCAAGATGACCATC-CGCCCA-3′); rp49 reverse (5′GTTCTCTTGAGAACGCAGGC-3′). rp49 was used as an RT- PCR control.

Chromatin Immunoprecipitation

S2R+ cells or third instar larvae salivary glands from wild type organisms were fixed in 1% formaldehyde. The fixation reaction was stopped by adding glycine (125 mM). Cells or salivary glands were washed and resuspended in lysis buffer, and sonication was performed until the size of chromatin reached between 200 and 800 bp. Pre-clearing, antibody incubations, immunoprecipitation and phenol:chlorophorm extractions were performed as described in [25]. For the 'mock' condition, a pre-immune sera against dAtrx or an anti-GFP antibody was used. The following oligonucleotides were used: rover forward (5′-CAACCAAG-ACCAACCTACCC-3′); rover reverse (5′-GCTCATTTTAGTCTGTCCGC-3′) [29]; for TAS-L, TAS3L_ChIP1 (5′-TGACTGCCTCTCATTCTGTC-3′) and TAS3L_ChIP2 (5′-TATCATCTCGTTCATCCGCC-3′) [30]. qPCRs were performed using the light cycler DNA master SYBR green 1 run in a Lyght cycler 1.5 (ROCHE), and the quantification of %INPUT was performed as in [31].

β-galactosidase quantitative assay

Detection of β-galactosidase in adult flies was performed as in Gu and Elgin (2013) [32]. For quantitative β-galactosidase assays, flies were homogenized in 300 µl of assay buffer (50 mM potassium phosphate, 1 mM MgCl2, pH 7.5), followed by spinning to pellet the debris. An aliquot of 50 µg of protein extract was transferred to CPRG solution (1 mM chlorophenol red b-D-galactopyrano-side in assay buffer) and the O.D. at 574 nm was measured at intervals over a 2-hour period. The β-galactosidase activity was calculated as a function of the change in O.D.

Results

The ADD domain of Atrx is highly conserved in *Drosophila* and other invertebrates

We searched for genes encoding proteins with the ADD domain in the *Drosophila* genome using the ADD region (aa 169-268) of the hATRX protein with the BLAST (Basic Local Alignment Search Tool) of the NCBI (National Center of Biotechnology Information). Using this approach, we identified the *CG8290* annotated gene, which putatively encodes three annotated proteins that have a

conserved amino-terminal ADD domain that is 52% homologous and 36% identical to the hATRX ADD domain (Fig. 1A, B). Protein alignment (Fig. 1A) showed that there is a high conservation at the position of the cysteins that coordinate de zinc atoms in the GATA-like and PHD zinc fingers. This conservation is not as high when we align DNMT3L, a methyltransferase that also has an ADD domain (data not shown). The ADD domain in the *Drosophila CG8290* encoded proteins is more similar to the one in hATRX than in DNMT3L (data not shown). While this work was in preparation for publication Alekseyenko *et al.*, (2014) named the *CG8290* gene *dadd1* [11].

In the hATRX protein, there are some amino acids in a "hydrophobic pocket" that mediate the interaction between the H3K9me3 and unmethylated H3K4 (H3K4me0) histone tail combination. In general, it is noteworthy that the whole "hydrophobic pocket" binding site is conserved between the ADD in *Drosophila* and in hATRX (aa 110-126 in dAdd1) [33]. There are also many conserved amino acids that are not part of the "hydrophobic pocket", such as the histidine 189 and proline 190 of hATRX (which correspond to aa 96 and 97 in dAdd1) that are mutated in ATRX syndrome [22]. We constructed a three-dimensional model of the ADD domain found in the dAdd1 proteins (aa 64 to 164) and compared it to the hATRX ADD domain (Fig. 1B). The human and *Drosophila* domains mainly overlap in the GATA-like and PHD zinc fingers helices 1, 2 and 3 (h1, h2 and h3, respectively), and the pocket that is important for recognition of H3K9me3 and H3K4me0 is also conserved (Fig. 1C). In the recently published work by Alekseyenko *et al.*, (2014), the capability of this domain to bind to the H3K9me3 tail was assayed, confirming it preferentially binds to this histone modification [11].

We also compared the native structure of the ADD domain of dAdd1 to the ADD domain of DNMT3L (data not shown) and found less overlaping when we superimpose the structures. This led us to propose that during ATRX evolution, the protein may have undergone a fission event. To obtain insight into the evolutionary history of ATRX, we decided to perform a rooted phylogenetic inference analysis using homologous sequences of the ADD and the helicase/ATPase domains from ATRX of higher eukaryotes. We found that the shared common ancestor of higher eukaryotes possessed a protein with both the ADD and helicase/ATPase domains, but in insects, it underwent a fission event by which the two domains were separated, generating two different genes (Fig. 1D, Fig. S2) (perhaps involving gene duplication with subsequent partial degeneration, as has been proposed for cmi and TRR proteins or the *monkey king* (*mkg*) gene family in *Drosophila*) [34, 35].

Another interesting feature is that, in *Drosophila,* ADD harboring-proteins acquired other domains such as MADF (myb/Sant-like domain in Adf1, shown in blue hexagons), suggesting novel functions for these proteins (Fig. 1D). MADF domains can recognize repetitive sequences on DNA, for instance in Adf1 and Dip3 the MADF domain directs the binding of these transcription factors to specific promoter sequences [36]. All these data led us to propose that the proteins

encoded by *dadd1* could represent the orthologs of the amino terminal half of the hATRX protein.

The dAdd1 proteins are expressed throughout development and are preferentially nuclear proteins that can bind to different chromatin regions

Through RT-PCR analyses of cDNAs obtained from different developmental stages (see Material and Methods and Fig. 2A), we found three transcripts *dAdd1-a*, *dAdd1-b* and *dAdd1-c* (Fig. 2A, and B top panel). The transcripts (*dAdd1-a*, *dAdd1-b*, *dAdd1-c*) corresponded to the ones derived from alternatively spliced transcripts of *CG8290* described in FlyBase [37]. All of these transcripts are deposited maternally into the embryo and are later expressed through all stages of development (Fig. 2B, 0-3 lanes).

Interestingly when we amplify the *dAdd1-b* transcript, another higher molecular weight band appears (Fig. 2B top panel). We sequenced this fragment and it

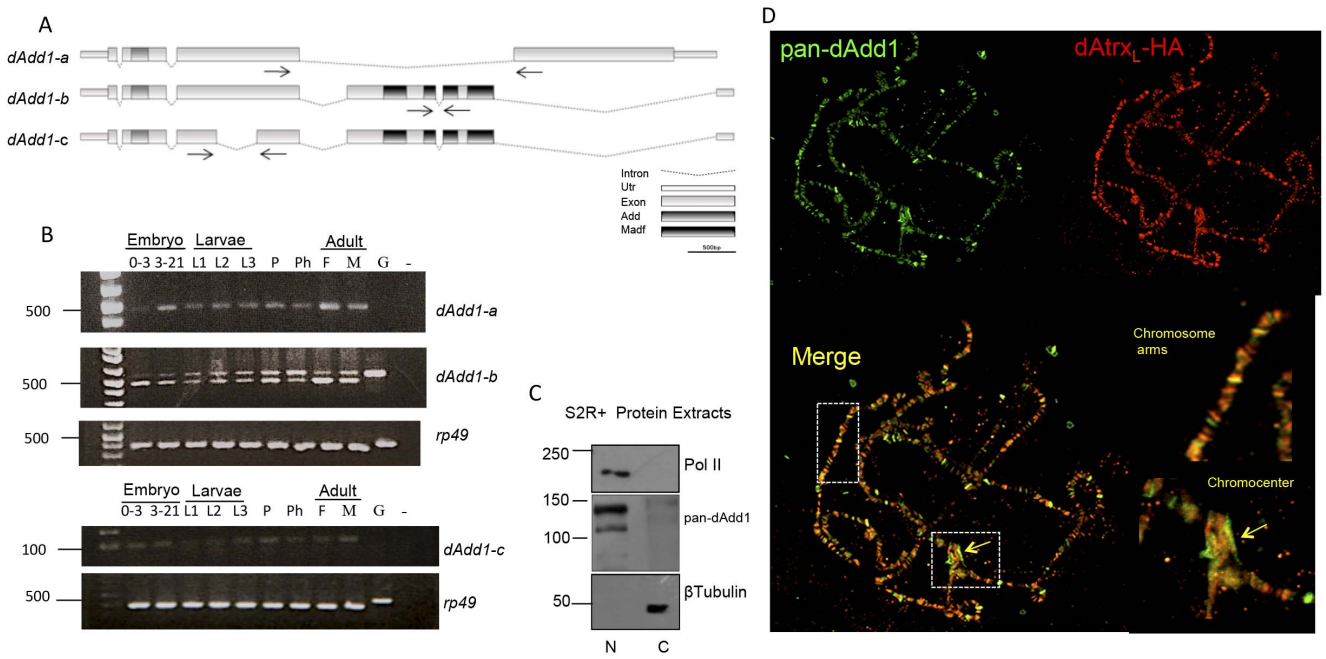

Figure 2. The dAdd1 proteins are expressed throughout development. A. Scheme of the *dadd1* mRNAs generated by alternative splicing. The nucleotide sequence of the ADD and MADF domains are represented as gray boxes. Primers used to amplify cDNAs representing mRNAs encoding Add isoforms are indicated by horizontal arrows. B. The *dadd1* transcripts were detected throughout all *Drosophila* stages of development by RT-PCR. Detection of exons from different *dadd1* mRNAs in cDNA generated from total RNA isolated from embryos (0–3 and 3–21 hour), 1st, 2nd and 3rd instar larvae (L1, L2 and L3), pupae (P), pharate (Ph) and female and male adults (F and M). *rp49* was used as a RT- PCR control. Sequence of the specific primers used to detect and sequence exons from each different *dadd1* mRNA are described in Material and Methods section. Molecular weight markers on the left of the panels represent base pairs. C. The dAdd1 (a-c) protein isoforms are mainly nuclear. Detection of dAdd1 (a-c) proteins by Western blotting using the pan-dAdd1 antibody in nuclear (N) and cytoplasmic (C) soluble fractions isolated from S2R$^+$ cells. The largest RNA polymerase II subunit and β-tubulin were used as controls of nuclear and cytoplasmic fractions, respectively. Molecular weight markers on the left of the panels represent kDa. D. dAdd1 proteins co-localize with dAtrx protein in polytene chromosomes of third instar larvae. dAtrx$_L$-HA and dAdd1 were followed with an anti-HA (red, right upper panel) and the pan-Add1 (green, left upper panel) antibodies respectively. The dAdd1 and dAtrx$_L$-HA proteins colocalize in some bands and interbands (left lower panel). They also co-localize in heterochromatic regions such as the chromocenter (see Insets, lower panel right). Note that not all the bands co-localize.

doi:10.1371/journal.pone.0113182.g002

corresponds to a transcript that retains the fifth intron. The presence of this putative transcript varies throughout development being more abundant in larval stages. Bioinformatic analyses indicate that retention of the fifth intron in this transcript would generate a stop codon which will in turn translate into a protein that conserves only one MADF domain. Further analyses are being carried out to assess the presence of this putative protein.

We found that there are three proteins derived from these transcripts that have similar predicted molecular weights ranging from 112 kDa to 130 kDa (Fig. 1C). Interestingly, the dAdd1-b and dAdd1-c proteins have several MADF domains in their carboxy-termini. We designed an antibody that recognizes the three dAdd1 isoforms (called pan-dAdd1, see Materials and Methods), and we tested the antibody's specificity through Western blot and depletion with a GST-dAdd1 fusion protein (Fig. S1A and Materials and Methods section). In the immunoblots we observe two main bands (112 and 130 kDa). Based on the predicted molecular weight of the proteins, the signals of these high-molecular weight bands probably represent the three proteins but cannot be resolved by standard SDS-PAGE electrophoresis.

We found that the dAdd1 proteins are enriched in the nuclear fraction of $S2R^+$ cells (Fig. 2C). Because the proteins are nuclear and have putative chromatin and DNA binding domains, we analyzed their location on chromatin. We made polytene chromosomes preparations from third instar larvae, and using immunostaining with the pan-dAdd1 antibody, we found that the dAdd1 proteins are located in several bands and interbands in the polytene arms (Fig. S3). The signal is also present in heterochromatic regions such as the chromocenter and on the fourth chromosome, and it co-localizes with the dAtrx signal in this region and in other heterochromatic regions (Fig. 2D and Fig. S3).

To determine whether dAdd1 colocalizes with dAtrx, we expressed an epitope tagged-$dAtrx_L$ ($dAtrx_L$-HA) [10] in larval salivary glands. This tagged $dAtrx_L$-HA version localizes to the same sites as wild type $dAtrx_L$ [25] and does not alter dAdd1 distribution (compare Fig. 2D and Fig. S3). We found that dAdd1 colocalizes with $dAtrx_L$-HA in the chromocenter and in other heterochromatic regions (Fig. 2D insets).

These results opened the possibility that dAdd1 proteins with an ADD domain could interact with the ADD-less *Drosophila* dAtrx and cooperate in some cellular functions in the organism.

The dAdd1 proteins interact directly with the $dAtrx_L$ protein

To test the proposed interaction hypothesis, we performed co-immunoprecipitation experiments using different antibodies generated against the dAdd1 proteins and $dAtrx_L$ (see Materials and Methods). As a first approach we coimmunoprecipitated dAdd1 with the pan-dAdd1 antibody and tested whether we could detect $dAtrx_L$. In addition to detecting dAdd1 (Fig. 3A, top panel, pan-dAdd1 blot) we found $dAtrx_L$ in the immunoprecipitate (Fig. 3A top panel, $dAtrx_L$ blot, IP lane), the specific bands obtained in the IP are marked with a

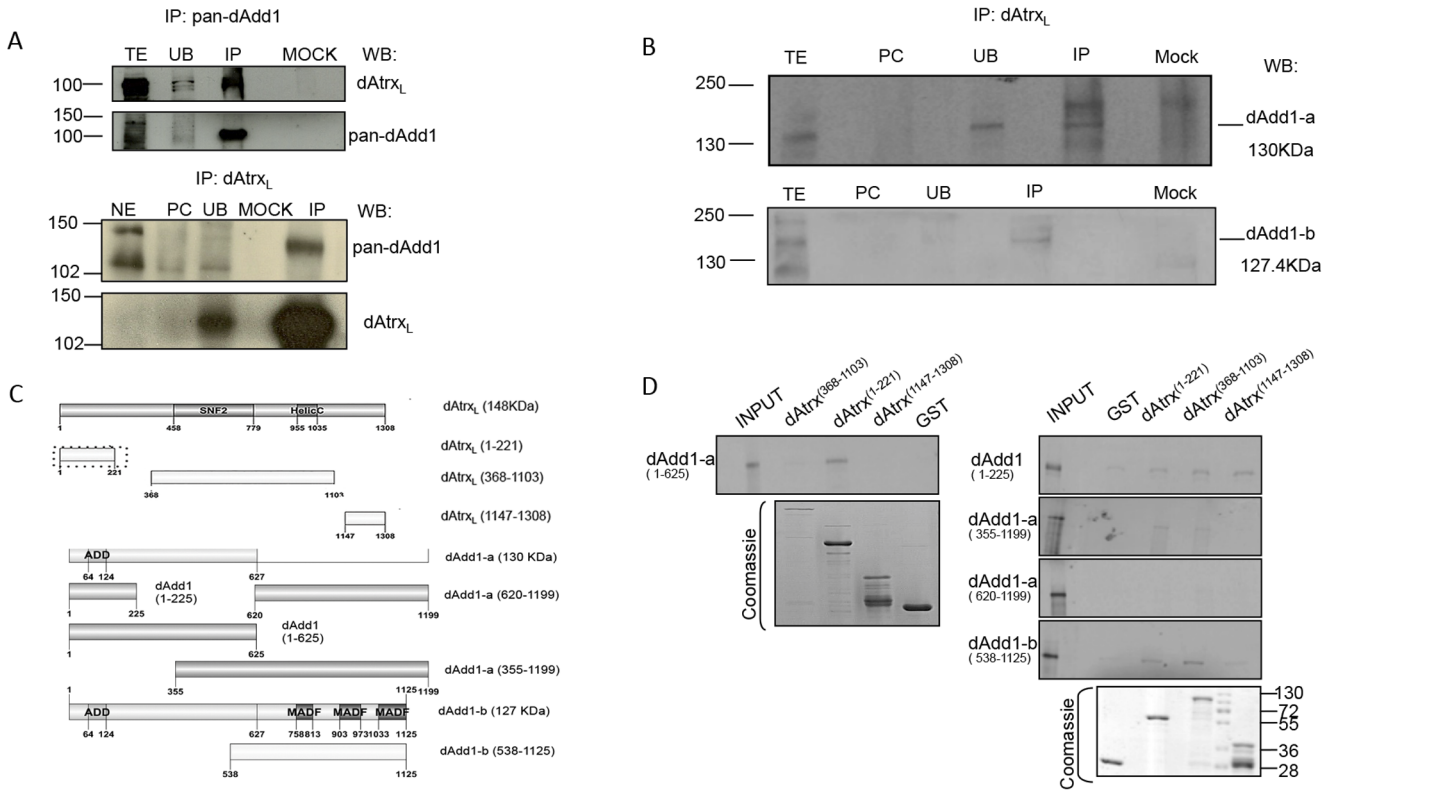

Figure 3. The dAtrx and dAdd1 proteins physically interact. A. Co-immunoprecipitation (CoIP) assays of dAdd1 and dAtrx$_L$. IP performed with pan-dAdd1 antibody (top panels) and the reciprocal CoIP assay with anti-dAtrx$_L$ antibody (bottom panels). Embryo nuclear extract (NE); S2R$^+$ cells total extract (TE); pre-clearing (PC); unbound protein fraction (UB); Mock is the IP performed with an unrelated antibody. The presence of dAdd1 and dAtrx$_L$ in the precipitated proteins was determined by Western blotting using the specific antibody. 10% of the nuclear extract (corresponding to approximately 50 μg of protein) used for the IP was loaded as the INPUT fraction. 20% of the total extract (corresponding to 150 μg of protein) was loaded as the INPUT fraction. Molecular weight markers on the left of the panels represent kDa. B. CoIP assay of dAdd1-a and dAdd1-b with dAtrx$_L$. S2R+ cells total extract (TE); pre-clearing (PC); unbound protein fraction (UB); IP was performed with anti-dAtrx$_L$. Mock is the IP performed with an unrelated antibody. The presence of dAdd1-a and dAdd1-b in the precipitated proteins was determined using the specific antibody. 20% of the total extract (corresponding to 150 μg of protein) was loaded as the INPUT fraction. The 250 kDa band observed in the INPUT lane is an unspecific band. Molecular weight markers on the left of the panels represent kDa. C. Representation of the fragments assayed by Pull-down. The important fragments for the interaction between dAtrx and dAdd are shown in dashed boxes. D. Pull-down assay. The first lane of all panels (except the coomassie panels) shows the 10% of the total amount of transcription/translation labeled protein (dAdd1 fragments) used for each experiment (input). The rest of the lanes are the experimental interaction (GST-dAtrx fragments and dAdd1 fragments) and the control interaction (GST and dAdd fragments) for each analyzed polypeptide. Coomasie staining of the loaded GST-fused proteins is shown in the bottom panels.

doi:10.1371/journal.pone.0113182.g003

white arrow. We also performed the reciprocal immunoprecipitation with the dAtrx$_L$ antibody, and we show that at least one of the dAdd1 proteins, approximately 130 kDa, co-immunoprecipitates with dAtrx$_L$ (Fig. 3A bottom panel, IP lane) the specific band is marked with a black arrow. The signal in both cases is specific because it cannot be detected when we used an irrelevant antibody to perform the immunoprecipitation assay (mock lane in all the blots).

To further characterize which of the dAdd1 proteins are in the observed immunoprecipitated band, we performed a coimmunoprecipitation assay using S2R$^+$ total extracts with antibodies generated against dAdd1-a or dAdd1-b. We found that both, dAdd1-a and dAdd1-b coimmunoprecipitate with dAtrx$_L$ (Fig. 3B, top and bottom panels), the white arrows indicate the specific bands corresponding

to the co-immunoprecipitated proteins. In the dAdd1-a blot (Fig. 3B, top panel) there is a high molecular weight band, near the 250 kDa weight marker, this band is unspecific because it also appears in the immunoprecipitation performed with a purified rabbit IgG antibody (Fig. 3B, mock lane). The fact that both proteins, dAdd1-a and dAdd1-b, can immunoprecipitate with $dAtrx_L$ indicates that the interaction domain is most likely conserved in both proteins or that a third protein is mediating the interaction.

To map the dAdd1 protein domain(s) important for the interaction with $dAtrx_L$, we performed a series of pull-down assays. We generated several fragments of $dAtrx_L$ and dAdd1 proteins and expressed them as GST-fusion proteins in a bacterial system or expressed and labeled them with S^{35} using an *in vitro* transcription/translation system (see Materials and Methods, Fig. 3C). We tested four different fragments of the dAdd1-a protein. Two of these fragments are present in the three isoforms (dAdd1 1-225, dAdd1 1-625). When we assayed the dAdd1 1-225 fragment with three different $dAtrx_L$ fragments, we observed that it binds to all of the tested fragments of $dAtrx_L$, but this fragment also binds to the negative control GST, although with less affinity (Fig. 3D top panel on the right). In contrast, the larger fragment that contains aminoacids 226-625 (fragment dAdd1 1-625) binds specifically to the amino-terminal fragment of $dAtrx_L$ (dAtrx 1-221) (Fig. 3D top left panel).

We also tested the dAdd1-a (355-1199) and dAdd1-a (620-1199) fragments. The first fragment, which contains amino acids 355-625 binds to two $dAtrx_L$ fragments (1-221 and 368-1103), corresponding to the amino-terminal and SNF2 fragments, whereas the second dAdd1-a fragment (620-1199), which lacks amino acids 355-625, fails to interact with any of the tested $dAtrx_L$ fragments (compare second and third panels from top to bottom on the right of Fig. 3D).

In these analyses, we also found that a fragment that includes the MADF domains (dAdd1-b 538-1125) interacts with the amino terminal and SNF2-containing fragments of the $dAtrx_L$ protein (Fig. 3D from top to bottom: fourth panel on the right) but this fragment also binds to the negative control GST.

From these data, we conclude that the dAdd1 domain that interacts with $dAtrx_L$ is conserved in all dAdd1 isoforms. Thus, all dAdd1 isoforms can directly interact with the amino-terminal domain of $dAtrx_L$ (a.a. 1-221) through their amino-terminal domain (a.a. 1-625). Interestingly, this $dAtrx_L$ fragment is only conserved in the long isoform, and it does not overlap with the HP1a interaction domain [22]. In contrast, it does overlap with the DREF interaction domain, which was reported by our group [25]. Based on these results, we conclude all dAdd1 isoforms can interact directly with the $dAtrx_L$ protein.

atrx and *dadd1* interact genetically

At this point we have demonstrated that dAdd1 and dAtrx physically interact; and therefore, we wanted to know whether they genetically interact in the fly. For this purpose, we made transheterozygous *atrx* and *dadd1* flies. For these analyses, we used three *atrx* alleles [20]. $atrx^1$ is a deficiency that uncovers dAtrx as well as

three more adjacent genes; $atrx^2$ is an hypomorphic allele that affects both the long and short dAtrx isoforms and $atrx^3$ is an hypomorphic allele that affects only the long isoform. The survival of heteroallelic *atrx* flies is affected, as previously reported, and they do not present any other obvious phenotype (Table 1, [10]).

We also used two *P*-element insertion lines, $dadd1^{NP1240}$ and $dadd1^{NP0793}$. These insertions lie at 83 or 81 bp, respectively, from the *dadd1* transcriptional start site (Fig. 4A). To determine whether the insertions affected the levels of the dAdd1 proteins, we extracted total proteins from adult flies of the different genotypes and analyzed the presence of the dAdd1 proteins through Western blotting using the pan-dAdd1 antibody (Fig. 4B). We found that the levels of the dAdd1 proteins are diminished in homozygous $dadd1^{NP1240}/dadd1^{NP1240}$ individuals, with respect to the heterozygous $dadd1^{NP1240}$/+ or +/+ flies (Fig. 4B). We also analyzed the *dadd1* mRNA levels of $dadd1^{NP1240}$/+ or $dadd1^{NP0793}$/+ individuals through semi-quantitative RT-PCR and found that the *dadd1* mRNA levels are diminished in the mutant individuals compared to the *dadd1* wild type flies (Fig. S4). These results indicate that these alleles are hypomorphic. Similar results were obtained with the $dadd1^{NP1240}/dadd1^{NP0793}$ heteroallelic flies (data not shown) and thus we used for the rest of our tests the $dadd1^{NP1240}$ allele. 44% and 90% of the $dadd1^{NP1240}/dadd1^{NP1240}$ and $dadd1^{NP1240}/dadd1^{NP0793}$ flies reach adulthood respectively, showing that the higher lethality present in $dadd1^{NP1240}$/

Table 1. Interaction between *dadd1*, and *atrx*.

Genotype	Viability[a] (%)	Melanotic Masses[b] (%)
$atrx^1$/+	789/789 (100)	0/789 (0)
$atrx^2$/+	202/202 (100)	0/202 (0)
$atrx^3$/+	775/789 (98)	0/775 (0)
$atrx^1/atrx^2$	80/202 (40)	0/80 (0)
$atrx^1/atrx^3$	387/789 (49)	0/387 (0)
$atrx^2/atrx^3$	130/228 (57)	0/130 (0)
$dadd1^{NP1240}$/+	180/180 (100)	0/180 (0)
$dadd1^{NP0793}$/+	255/255 (100)	0/255 (0)
$dadd1^{NP1240}/dadd1^{NP1240}$	91/206 (44)	0/91 (0)
$dadd1^{NP1240}/dadd1^{NP0793b}$	163/180 (90)	0/163 (0)
$dadd1^{NP1240}$/+;$atrx^1$/+	454/454 (100)	32/454 (7)
$dadd1^{NP1240}$/+;$atrx^2$/+	568/568 (100)	11/568 (2)
$dadd1^{NP1240}$/+;$atrx^3$/+	632/632 (100)	14/632 (2)
$dadd1^{NP0793}$/+;$atrx^1$/+	152/152 (100)	5/152 (3)
$dadd1^{NP0793}$/+;$atrx^2$/+	322/322 (100)	11/322 (3)
$dadd1^{NP0793}$/+;$atrx^3$/+	243/243 (100)	7/243 (3)
$dadd1^{NP1240}$/+;$atrx^1/atrx^3$	76/105 (72)	9/76 (12)
$dadd1^{NP1240}$/+;$atrx^2/atrx^3$	106/141 (75)	8/106 (8)
$dadd1^{NP0793}$/+;$atrx^2/atrx^3$	161/219 (73)	15/161 (9)

[a]The number of flies obtained over the number of flies expected according to the healthiest class in each cross. Percentage is in parentheses.
[b]Number of adult individuals with melanotic masses (Fig. 4B) observed over the total number of that particular class. Percentage is in parentheses.

doi:10.1371/journal.pone.0113182.t001

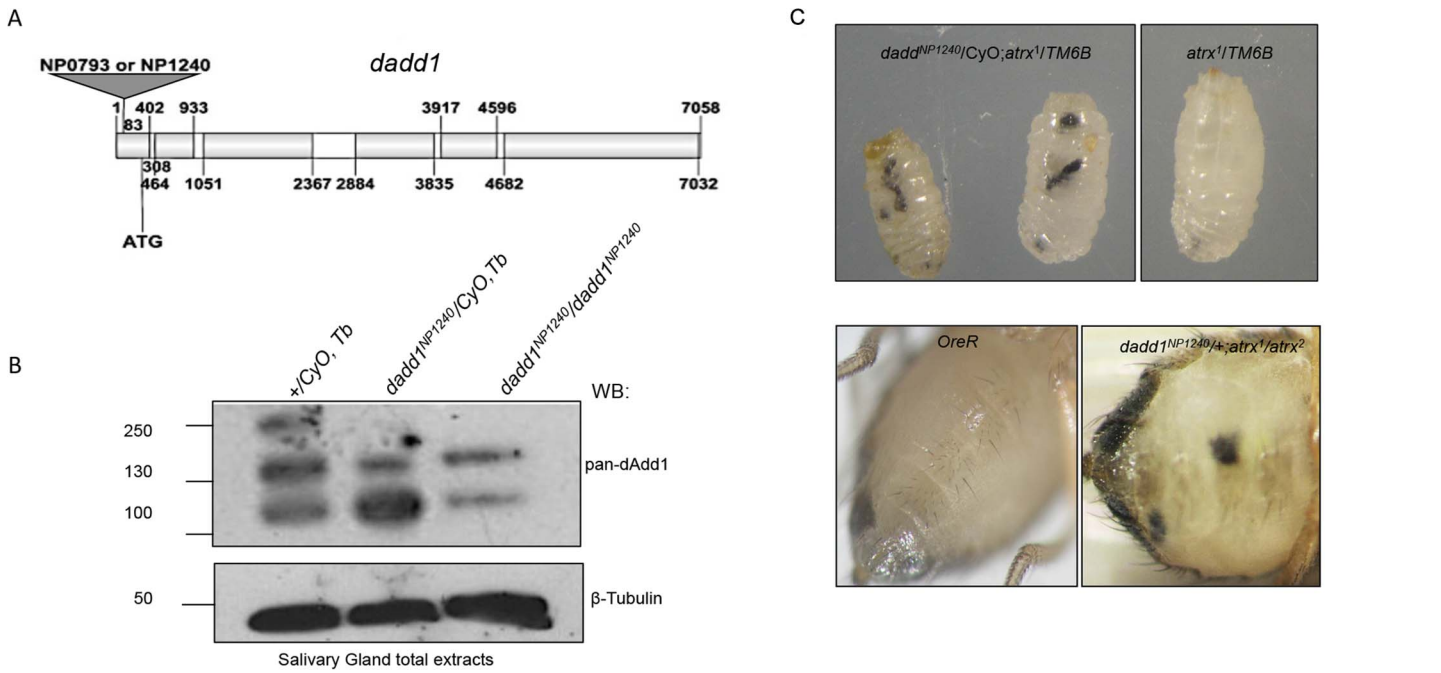

Figure 4. Genetic interaction between *dadd1* and *atrx*. A. Scheme of *dadd1* showing the position of the *EP* elements insertions (gray triangle) in $dadd1^{NP1240}$ and $dadd1^{NP0793}$ alleles, introns are represented by white boxes while exons are represented by gray boxes. The start codon at position 308 pb is also shown. *B.* $dadd1^{NP1240}$ is an hypomophic *dadd1* allele. Western blotting assay probed with the pan-dAdd1 antibody. Each lane contains 150 μg of proteins from adult flies of the indicated genotype. β-tubulin was used as a loading control. Note the low levels of the dAdd1 proteins in homozygous individuals with respect to +/+ individuals. This demonstrates the allele is hypomorphic. The 250 kDa band observed in the wild type lane is an unspecific band. Molecular weight markers on the left of the panels represent kDa. C. Some *dadd1*/*atrx* individuals present melanotic masses. Melanotic masses that appear during larval (upper panel) and adult stages (lower panel) of mutant *dadd1/atrx* individuals are shown. Wild type individuals (w^{1118} for larvae and *OreR* for adult) are shown to the left for comparison.

doi:10.1371/journal.pone.0113182.g004

$dadd1^{NP1240}$ individuals (56%) compared to the one presented by the $dadd1^{NP1240}$/$dadd1^{NP0793}$ flies (only 10%) may be caused by other lethals present in the $dadd1^{NP1240}$ chromosome (Table 1). The heteroallelic $dadd1^{NP1240}$/$dadd1^{NP0793}$ individuals are fertile and do not present any other obvious phenotype.

Survival of the transheterozygous *dadd1/atrx* flies is mildly affected, and a small percentage of these flies present melanotic masses, both in third instar larvae and adult individuals. The percentage of melanotic masses is higher in flies carrying two different alleles of *atrx* in combination with one allele of *dadd1* (Fig. 4, Table 1). We obtained similar results for all the combinations of *atrx* and *dadd1* alleles (Fig. 4, Table 1,). The masses also appear during larval stages, and these individuals fail to advance further in development (Fig. 4C). Similarly, adult flies presenting melanotic tumors die within the first 10 days post-eclosion (data not shown). These data provide evidence that, besides the physical interaction we showed in the previous sections, there is a genetic interaction between dAdd1 and Atrx functions that is essential for fly development.

The dAdd1 proteins co-localize with HP1a in heterochromatic regions and cooperate with dAtrx in the maintenance of pericentric heterochromatin

As dAdd1 proteins interact with $dAtrx_L$, we thought that they could be involved in heterochromatin maintenance; therefore, we analyzed their interaction with HP1a.

As mentioned before, the HP1α interaction domain in the $dAtrx_L$ protein (245aa-CxVxL-249aa, [10]) does not overlap with the interaction domains of the dAdd1 proteins. It is possible that dAdd1-a, b or c, $dAtrx_L$ and HP1a can co-exist in the same protein complex. If this is true, then we should be able to coimmunoprecipitate HP1α with the dAdd1 proteins. We expressed a V5 epitope-tagged dAdd1 version in $S2R^+$ cells and detected the presence of HP1a in an immunoprecipitation (IP) assay of the V5-dAdd1 protein with the V5 antibody (Fig. 5A, lower panel, white asterisk). Although the signal is faint it is specific because it cannot be detected in the mock control IP (Fig. 5A). This finding indicates that dAdd1-a is able to co-immunoprecipitate with HP1a.

We also show that dAdd1 and HP1a co-localize in heterochromatin regions and in the chromocenter of wild type polytene chromosomes (Fig. 5B yellow arrow). The dAdd1 signal is also observed in regions where no HP1a signal is detected (Fig. 5B green arrow).

The coimmunoprecipitation and immunolocalization analyses suggest that the dAdd1 proteins could be located in different regions of the chromatin. To analyze the binding of these factors at several heterochromatic and euchromatic regions in more detail, we performed chromatin immunoprecipitation (ChIP) assays using different antibodies against HP1a, $dAtrx_L$ and the dAdd1 proteins with chromatin from third instar larvae salivary glands and $S2R^+$ cells (see Material and Methods).

HP1α is not enriched in the TAS (Telomeric Associated Sequences) regions [38]. On the other hand, Antão *et al.*, (2012) [30] found through a proteomic analysis of chromatin segments (PICh) that dAtrx and of the product of *CG8290* are enriched in the telomeric associated sequences (TAS-L) but they did not find HP1a. Thus, we looked for the presence of HP1α, $dAtrx_L$ and the dAdd1 proteins in the telomeric region (TAS-L). Our ChIP experiments show, similar to Antão *et al.*, (2012) [30], that $dAtrx_L$ and the proteins, but not HP1α, are enriched in the TAS-L region (Fig. S5). We also found that $dAtrx_L$ and the dAdd1 proteins colocalize in a region that can potentially form a G quadruplex structure (G4) (Fig. S5).

In search for heterochromatic regions where the proteins did not co-localize we tested the rover retrotransposon, which we know is a constitutive heterochromatic region enriched in H3K9me3 mark [29]. Here we found $dAtrx_L$ is present but the dAdd1 proteins are not enriched in this region. This result indicates that dAdd1 and $dAtrx_L$ do not colocalize at all the heterochromatic regions in the genome (Fig. S5). Next, we looked for an euchromatic region, we decided to use the *sgs8* promoter which is actively transcribing in third instar salivary glands [29]. We observed that in this euchromatic region there is some enrichment of dAdd1

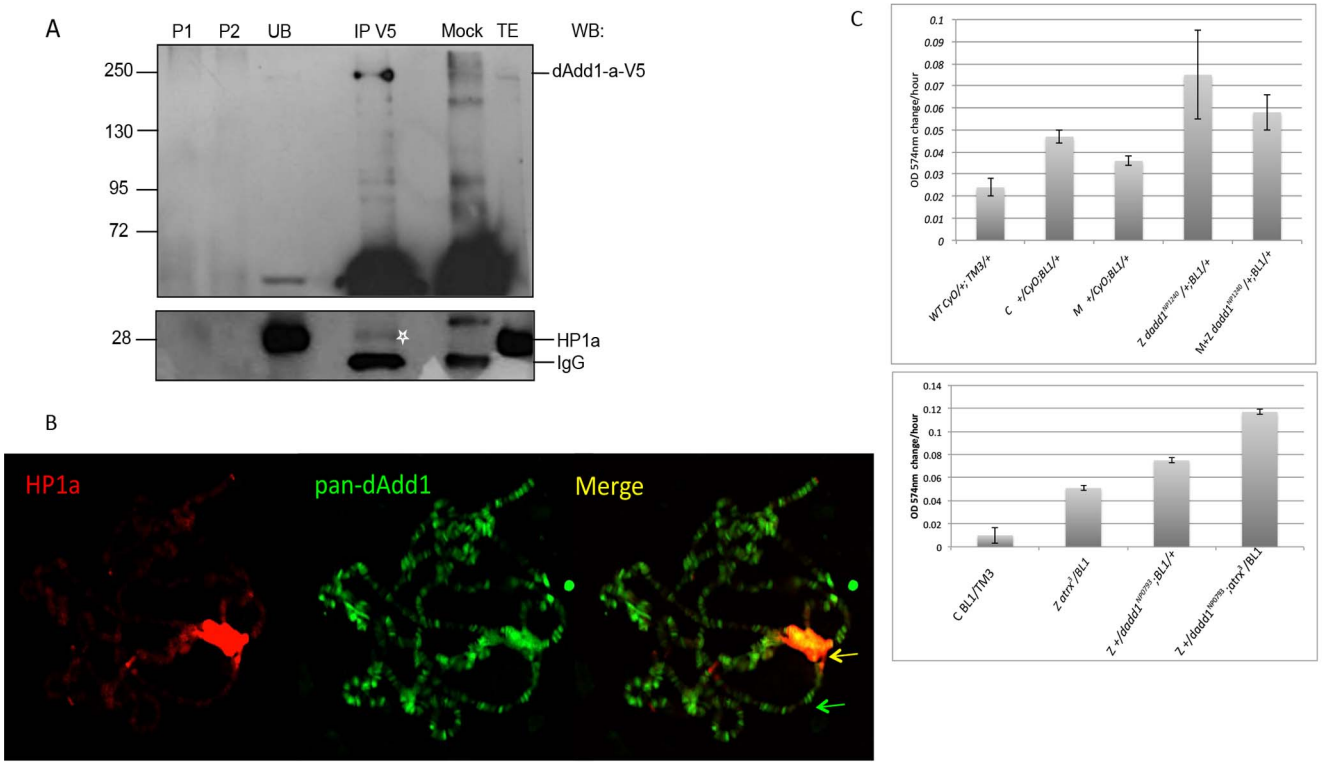

Figure 5. The dAdd1 proteins co-localize in heterochromatic regions with HP1a and cooperate with dAtrx in the maintenance of pericentric heterochromatin. A. CoIP assay of dAdd1-a and HP1a. Total extract (TE) from transiently transfected S2R^{+} cells with dAdd1-a-V5, P1 and P2 are pre-clearing 1 and 2 (see Material and Methods); unbound protein fraction (UB); IP performed with anti-V5 (upper panel); Mock is the IP performed with purified mouse IgG. The presence of dAdd1-a-V5 was determined using the anti-V5 antibody. The presence of HP1a was determined using the anti-HP1a (CIA9) antibody (lower panel). Molecular weight markers on the left of the panels represent kDa. B. Polytene chromosomes preparations from wild-type *OreR* third instar larvae were simultaneously stained with anti-HP1a (red signal) and pan-dAdd1 (a-c) antibody (green signal). Merge bands containing both factors can be visualized mainly in the chromocenter (yellow signal). *C. dadd1* is a suppressor of position effect variegation. Quantitative β-galactosidase assay. The graphs show that *dadd1* alleles can suppress position effect variegation measured by the enzymatic activity of Lac-Z. WT= wild type flies with *CyO* and *TM3* chromosome balancers; C= control flies derived from F1 progeny of paternally delivered *dadd1* alleles; M= Maternal depletion, F1 progeny flies of maternally delivered *dadd1* alleles; Z=zygotic depletion, flies derived from crossing males carrying the *dadd1* alleles to females carrying the *BL1* allele; M+Z= maternal and zygotic depletion, flies derived from crossing females carrying the *dadd1* alleles to males carrying the *BL1* reporter allele. The bottom graph shows that transheterozygous *dadd1, atrx* flies have an additive effect in the suppression of position effect variegation.

doi:10.1371/journal.pone.0113182.g005

proteins whereas dAtrx$_L$ is not enriched as expected (Fig. S5). This finding is supported by the fact that in the immunolocalization experiments shown above, we also observe dAdd1 in euchromatic regions in the chromosome arms (Fig. 2D and Fig. S3).

The results obtained in the ChIP analyses could represent the capability of the different dAdd1 proteins to bind different regions of the chromatin. The fact that dAtrx$_L$ and the dAdd1 proteins are not always together, as shown in the ChIP and the immunolocalization analyses, provide evidence that the dAdd1 proteins have functions independent of that with dAtrx$_L$. This result also shows that dAtrx$_L$ can bind to chromatin regions independent of the dAdd1 proteins, most likely through interactions with other factors such as DREF [23].

The colocalization of HP1a, dAtrx$_L$ and dAdd1 in the chromocenter raises the possibility that the dAdd1 proteins are involved in the maintenance of

heterochromatin. In a model for the maintenance of pericentric heterochromatin proposed by Eustermann S, *et al.*, (2011) [4], the ADD domain of the hATRX protein, reinforced by the interaction with HP1a, recognizes pericentric heterochromatin. Once hATRX is recruited its helicase/ATPAse domain directs deposition of the histone variant H3.3 [4].

It has not been determined conclusively whether Drosophila dAtrx is involved in the deposition of the histone variant H3.3, but both HP1a and $dAtrx_L$ localize at the chromocenter of polytene chromosomes and act as suppressors of position effect variegation for the w^{m4} allele, an inversion that lies near pericentric heterochromatin [10].

Following this hypothesis we tested the *dadd1* capability to suppress position effect variegation. We used the BL1 line, which carries a LacZ reporter construct that lies near the centromere [24, 32]. In this assay, we can determine whether *dadd1* is involved in the establishment, crossing virgin females carrying the *dadd1* alleles to males carrying the reporter BL1 (maternal effect), or maintenance, crossing males carrying the *dadd1* alleles to females carrying the reporter BL1 (zygotic effect), of heterochromatin [32] (see Material and Methods).

The results show that *dadd1* does not have a relevant role in the establishment of pericentric heterochromatin (compare M (maternal) bar and C (control) bar in Fig. 5C top graph). When we analyzed the zygotic effect, virgin BL1 females crossed to *dadd1* male carrying alleles, the activity of LacZ was consistently higher in *dadd1* mutants (compare Z (zygotic) bar to C (control) bar in Fig. 5C top graph), indicating that the *dadd1* alleles can suppress position effect variegation and that *dadd1* has a role in the maintenance of heterochromatin rather than in the establishment of heterochromatin.

Next, we tested whether a combination of *dadd1* and *atrx* alleles enhances the suppression of position effect variegation in a cooperative manner. In fact, this is what we observed. Our results show that transheterozygous *dadd1*/*atrx* flies suppress position effect variegation more efficiently than heteroallelic flies carrying either the *dadd1* or *atrx* alleles (compare third and fourth bars in Fig. 5C bottom graph).

Overall, these results indicate that dAdd1 proteins are capable of interacting with proteins, such as HP1a, that are involved in the establishment of heterochromatin and that they cooperate with $dAtrx_L$ in the maintenance of heterochromatin.

Su(var)205 interacts genetically with *dadd1*, and *atrx*

We showed that *dadd1*/*atrx* individuals present melanotic masses. The $Su(var)205^2$ is a loss-of-function HP1a allele because it carries a mutation in aminoacid 26 within the chromodomain. We tested whether the loss of function of HP1a in the presence of *dadd1* and/or *atrx* mutations affects the presence of the melanotic masses found in *dadd1/atrx* individuals.

Transheterozygous $Su(var)205^2$ flies carrying the *dadd1*, or $atrx^1$ or $atrx^2$ alleles do not present melanotic masses, whereas $Su(var)205^2$ flies carrying $atrx^3$ (which

Table 2. *Su(var)205* interaction with *dadd1*, and *atrx*.

Genotype	Melanotic Masses [a](%)
$Su(var)205^{2}$/+	0/487 (0)
$Su(var)205^{2}$/+;$atrx^{3}$/+	6/366 (2)
$Su(var)205^{2}$/$dadd1^{NP1240}$	0/201 (0)
$dadd1^{NP1240}$/+;$atrx^{3}$/+	3/69 (4)
$Su(var)205^{2}$/$dadd1^{NP1240}$; $atrx^{3}$/+	16/111(14)

[a]Number of adult individuals with melanotic masses (Fig. 4B) observed over the total number of that particular class. Percentage is in parentheses.

doi:10.1371/journal.pone.0113182.t002

affects only the long isoform of dAtrx) present melanotic masses in a small percentage (Table 2). The penetrance of melanotic masses in $dadd^{NP1240}$/+; $atrx^{3}$/+ (4%) or $Su(var)205^{2}$/+; $atrx^{3}$/+ (2%) individuals increases to 14% in $Su(var)205^{2}$/$dadd^{NP1240}$;$atrx^{3}$/+ individuals where mutations in the three genes are together (Table 2). These data show that the presence of melanotic masses in transheterozygous *dadd1*, *atrx* and *Su(var)205* flies most likely involves misregulation in the maintenance of heterochromatin.

Discussion

In vertebrates, hATRX is a protein with an ADD domain and an SNF2-helicase/ATPase motif. Through evolution, the SNF2 domain of hATRX has been highly conserved, but in invertebrates, the ADD domain is lost (Fig. 1D, [39]). In this article, we describe the characterization of the *Drosophila* dAdd1 proteins as orthologs to the amino-terminal region of Atrx. The *dadd1* gene expresses the dAdd1 proteins, which have an ADD domain (Fig. 1C), throughout development (Fig. 2B). The 3D structure of the dAdd proteins ADD domain (Fig. 1B) is more similar to the one found in hATRX than to the ADD domains found in other proteins. *Drosophila* dAdd1 and the ADD-less dAtrx interact physically (Fig. 3A, 3D) and genetically (Tables 1 and 2), and they interact with HP1a in heterochromatic regions (Fig. 5B).

The human *hATRX* gene encodes an SNF2 helicase/ATPase protein that has many different functions. It is part of a complex that includes the histone variant H3.3 chaperone DAXX, and it is involved in the deposition of this histone variant in pericentric and telomeric heterochromatin [7, 40, 41]. The hATRX protein can also bind to regions in the genome that can potentially form G-quadruplex structures and it has been proposed that this binding alleviates the quadruplex conformation and allows the deposition of H3.3 [9, 42]. Its participation in the deposition of histone variant H3.3 requires the helicase/ATPase activity, although it has not been determined whether this activity is also required for the binding and recognition of the G-quadruplex structures of the DNA. In addition to the SNF2 helicase/ATPase domain, hATRX also has an amino-terminal domain composed of two zinc fingers, a GATA-like finger and a PHD finger called the

ADD domain. This domain is able to recognize the H3K9me3 histone mark in combination with unmodified H3K4 through a "hydrophobic pocket", which is an unusual feature for a PHD zinc finger [33]. The interaction between hATRX and histone H3 chromatin marks has been shown to maintain hATRX binding to pericentric heterochromatin. A model has been proposed in which hATRX is directed to pericentric heterochromatin through the ADD domain, and this interaction is reinforced by the interaction between hATRX and HP1a. In this model, the SNF2 helicase/ATPase domain then directs histone H3.3 deposition or performs other required ATP-dependent functions [4].

dadd1 encodes three polypeptides that contain an ADD domain that is highly similar to the hATRX ADD domain (36% identity and 52% of similarity, [11] and this work). The comparison of the 3D-structure analyses of the ADD of *Drosophila* dAdd1 and hATRX reveal that these domains overlap and that the histone recognition pocket is conserved.

Our phylogenetic inference analysis using the ADD domain of hATRX indicates that the ATRX gene underwent a fission event. This fission has been described in at least another chromatin-binding-protein encoding gene, *cara mitad* (*cmi*), which is the homolog of the amino-terminal portions of mammalian *MLL2* and *MLL3* [32].

It is intriguing that there are three spliced isoforms encoded by the *dadd1* gene. The dAdd1-a isoform contains the ADD domain and no other putative domains, while the other two spliced isoforms have additional domains called MADF (myb/SANT-like domain in Adf1). The MADF domains are a subfamily of the SANT domains. They are DNA-binding domains found in all *Drosophila* species. In the case of Adf1, the first *Drosophila* factor identified to have an homology to the Myb oncoprotein [43], the MADF domain recognizes and binds certain sequences in repetitive regions [44], although there are some examples in which the MADF domains can also bind proteins, and apparently the specificity lies in the domain's isoelectric point [45].

The predicted isoelectrical point of the three MADF domains in the dAdd1 proteins is basic, which could indicate that they can bind to DNA.

The acquisition of new domains indicates that these proteins most likely have diverged functions. One indication of this could be the pattern of the immunolocalization of dAdd1 in polytene chromosomes, where not all the signals derived from the pan-dAdd1 antibody co-localize with $dAtrx_L$. This indicates that the dAdd1 isoforms could also have roles independent of their interaction with $dAtrx_L$.

The survival of transheterozygous individuals carrying the *dadd1/atrx* alleles is compromised, and some of the larvae and adult individuals show melanotic masses. We found that these proteins also colocalize with HP1a and that dAdd1-a immunoprecipitates with HP1a. Diminished HP1a levels in *dadd1/atrx* flies enhance the incidence of melanotic masses. Our results are supported by the recent report of Alekseyenko *et al.*, (2014), in which it is demonstrated that dAdd1 physically interacts with HP1a and that dAdd1 is a suppressor of variegation [11].

The generation of melanotic masses involves problems in the differentiation of hematopoietic cells in the flies. The differentiation of hematopoietic cells takes place in the early embryonic head mesoderm and in the lymph gland of late larvae, and three different types of cells are derived from the prohemocytes; the plasmatocytes, crystal cells and lamellocytes. Several different pathways regulate the differentiation of these cells [46]. One of the pathways involves a balance in the expression of the Pnr-α and Pnr-β proteins, which is controlled by the JAK/STAT pathway [48]. Jak hyperactivation results in the proliferation of hemocytes, lamellocyte differentiation and the generation of melanized pseudotumors. Pseudotumors or melanotic masses are formed by crystal cells and lamellocytes [47]. On the other hand, Stat is a positive regulator of plasmatocyte differentiation, and one of the downstream factors regulated by Stat is the GATA factor Pannier [48]. Importantly, our group had already identified *pannier (pnr)* as a gene regulated by $dAtrx_L$ and another transcriptional factor DREF [25]. In that report, we concluded that $dAtrx_L$ is recruited to the *pnr* gene promoter through DREF, and that it acts as a co-repressor of *pnr* gene expression.

Furthermore, the data obtained from the genetic interactions between the *dadd1, atrx* and *Su(var)205*^{2} alleles indicates that melanotic masses are derived from problems in the proteins involved in heterochromatin maintenance, such as $dAtrx_L$ and HP1a. The position effect variegation assay indicated that the dAdd1 proteins are involved in the maintenance of heterochromatin. Thus, an attractive hypothesis is that dAdd1, $dAtrx_L$ and HP1a cooperate and promote heterochromatinization at the promoters of the genes involved in the JAK/STAT pathway, including *pnr*. Lack of these proteins could lead to misregulation of the effectors of the pathway, giving rise to the melanotic masses. Experiments are being carried out to test this hypothesis.

In the human ATRX syndrome, the majority of the mutations identified so far affect the ADD or the SNF2 helicase/ATPAse domains. The fact that the domains are separated in flies provides a new important tool to study the individual roles these domains have in the development of the organism.

Supporting Information

Figure S1. dAdd1 antibodies recognize specifically the dAdd1 proteins. a) Western blot using the pan-dAdd1 antibody. The dAdd1 isoform signals (lane 1) observed with the pan-dAdd1 antibody are no longer observed in lane 2. This demonstrates that the GST-dAdd1 fusion protein which harbors the peptide used to raise the pan-dAdd1 antibody is able to deplete them from this fraction. The dAdd1 signals are no longer observed (lane 2) showing that the pand-dAdd1 specifically recognizes the dAdd1 isoforms (see also Materials and Methods). b) Anti-dAdd1-a antibody recognizes the dAdd1-a protein. Indicated GST fusion proteins were loaded and blotted onto a nitrocelulose membrane. The Western blot was performed with an anti-dAdd1-a antibody (top panel) or an anti-GST antibody (bottom panel). The dAdd1 specific signal is observed only where the

GST-dAdda-1 fusion protein harboring the peptide used to raise the antibody was loaded (GST-dAdd1 aminoacids 620-1199) (left lane, top panel). The antibody does not recognize a fusion protein that lacks this peptide (right lane, top panel). The GST antibody recognizes the aforementioned two GST-dAdd1 fusion proteins (bottom panel). Extra bands (asterisks, right lane, bottom panel) may be fusion protein degradation. c) Specificity test for the dAdd1-b antibody. Indicated GST-fusion proteins were induced in *E. coli*. Induced extracts were loaded and blotted onto nitrocellulose membranes. The Western blot (upper panel) was performed using the anti-dAdd1-b antibody. A specific signal is observed (lane 3, black arrow in the blot and in the Ponceau staining) which corresponds to the induced GST-dAdd1-b fragment (aa 530-1125) and not GST or GST-dAdd1-a (aa 620-1199) (lanes 1 and 2 respectively). Faint bands in the first two lanes are unspecific signals.

doi:10.1371/journal.pone.0113182.s001 (TIF)

Figure S2. The *atrx* gene suffered a fission event in the Insecta class. Maximum Likelihood Phylogenetic Analysis of Helicase/ATPase domain and the corresponding Protein Domain Architecture information of its containing proteins. The numbers shown represent bootstrap values. It can be seen that the common ancestor to plants and animals had a protein with both, the ADD and the helicase/ATPase domains, but insects show the homologous domains in different proteins. Since it is more likely that only one fusion event, instead of two independent acquisitions of the same domain, occurred during the evolution, the most parsimonious explanation is to consider a model in which a gene fission event occurred within the Insecta class. For the parameters used, see Material and Methods section.

doi:10.1371/journal.pone.0113182.s002 (DOCX)

Figure S3. The dAdd1 proteins localize at many chromatin regions in polytene chromosomes. Wild type polytene chromosome staining was performed with the pan-dAdd1 antibody (red). The dAdd1 proteins localize in heterochromatic regions such as the chromocenter and the fourth chromosome (inset, white arrow). Staining along the chromosomes arms and in euchromatic regions is also observed.

doi:10.1371/journal.pone.0113182.s003 (TIF)

Figure S4. Alleles *dadd1*^{NP1240} and *dadd1*^{NP0793} are hypomorphs. Semiquantitative RT-PCR from wild type and mutant *dadd1* flies. dadd1 mRNA level is lower in the *dadd1*^{NP1240} (upper panel) and *dadd1*^{NP0793} (lower panel) heterozygous flies than in the *dadd1* wild type flies (w^{1118}). In homozygous *dadd1*^{NP1240}/*dadd1*^{NP1240} (upper panel), *dadd1* is even lower that in the heterozygous condition. *rp49* transcript levels remained unchanged in the mutant alleles.

doi:10.1371/journal.pone.0113182.s004 (DOCX)

Figure S5. The dAdd1 proteins co-localize *in vivo* with dAtrx$_L$ and HP1a in some chromatin regions. ChIP assay using total extracts from third instar salivary

glands (SG) prepared from wild-type larvae and S2R+ cells. Graphs represent the percentage of input precipitated using the different antibodies for the same regions. Note that in the rover region only $dAtrx_L$ is enriched. Three independent biological replicates were performed.
doi:10.1371/journal.pone.0113182.s005 (TIF)

Acknowledgments

We would like to thank Dr. Sarah Elgin for kindly providing the BL1 reporter fly stock. Stocks obtained from the Bloomington Drosophila Stock Center (NIH P40OD018537) were used in this study. We also thank Carmen Muñoz and the Laboratorio Nacional de Microscopía Avanzada (LNMA) of IBt, UNAM for technical assistance.

Author Contributions

Conceived and designed the experiments: MZ VVG. Performed the experiments: BLF SMN BHR AC DM VVG. Analyzed the data: ER MZ MV VVG. Contributed reagents/materials/analysis tools: AC ER. Wrote the paper: MZ MV VVG.

References

1. **Gibbons RJ** (2012) α-Thalassemia, Mental Retardation, and Myelodysplastic Syndrome. Cold Spring Harb Perspect Med 2: pii: a011759.
2. **Garrick D, Samara V, McDowell TL, Smith AJ, Dobbie L, et al.** (2004) A conserved truncated isoform of the ATR-X syndrome protein lacking the SWI/SNF-homology domain. Gene 326: 23–34.
3. **Dhayalan A, Tamas R, Bock I, Tattermusch A, Dimitrova E, et al.** (2011) The ATRX-ADD domain binds to H3 tail peptides and reads the combined methylation state of K4 and K9. Hum Mol Genet 20: 2195–2203.
4. **Eustermann S, Yang JC, Law MJ, Amos R, Chapman LM, et al.** (2011) Combinatorial readout of histone H3 modifications specifies localization of ATRX to heterochromatin. Nat Struct Mol Biol 18: 777–782.
5. **Mitson M, Kelley LA, Sternberg MJ, Higgs DR, Gibbons RJ** (2011) Functional significance of mutations in the Snf2 domain of ATRX. Hum Mol Genet 20: 2603–2610.
6. **Emelyanov AD, Konev YA, Vershilova E, Fyodorov DV** (2010) Protein complex of Drosophila ATRX/XNP and HP1a is required for the formation of pericentric beta-heterochromatin in vivo. J Biol Chem 285: 15027–15037.
7. **Gibbons RJ, Wada T, Fisher CA, Malik N, Mitson MJ, et al.** (2008) Mutations in the chromatin-associated protein ATRX. Hum Mutat 29: 796–802.
8. **Goldberg AD, Banaszynski LA, Noh KM, Lewis PW, Elsaesser SJ, et al.** (2010) Distinct factors control histone variant H3.3 localization at specific genomic regions. Cell 140: 678–691.
9. **Law MJ, Lower KM, Voon HP, Hughes JR, Garrick D, et al.** (2010) ATR-X syndrome protein targets tandem repeats and influences allele-specific expression in a size dependent manner. Cell 143: 367–378.
10. **Bassett AR, Cooper SE, Ragab A, Travers AA** (2008) The chromatin remodelling factor dATRX is involved in heterochromatin formation. PLoS ONE 3(5):e2099.

11. **Alekseyenko AA, Gorchakov AA, Zee BM, Fuchs SM, Kharchenko PV, et al.** (2014) Heterochromatin-associated interactions of Drosophila HP1a with dADD1, HIPP1, and repetitive RNAs. Genes Dev 28: 1445–60.

12. **Ren J, Longping W, Gao X, Jin C, Xue Y, et al.** (2009) DOG 1.0: Illustrator of protein domain structures. Cell Res 19: 271–273.

13. **Rambaldi D, Ciccarelli FD** (2009) FancyGene: dynamic visualization of gene structures and protein domain architectures on genomic loci. Bioinformatics 25: 2281–2282.

14. **Larkin MA, Blackshields G, Brown NP, Chenna R, McGettigan PA, et al.** (2007) Clustal W and Clustal X version 2.0. Bioinformatics 23: 2947–2948.

15. **Abascal F, Zardoya R, Posada D** (2005) ProtTest: Selection of best-fit models of protein evolution. Bioinformatics 21: 2104–2105.

16. **Guindon S, Gascuel O** (2003) A simple, fast, and accurate algorithm to estimate large phylogenies by maximum likelihood. Syst Biol 52: 696–704

17. **Le SQ, Gascuel O** (2001) An Improved General Amino Acid Replacement Matrix. Mol Biol Evol 25: 1307–1320.

18. **Letunic I, Bork P** (2011) Interactive Tree Of Life v2: online annotation and display of phylogenetic trees made easy. Nucleic Acids Res 39: (Web Server issue): W475–8.

19. **De Castro E, Sigrist CJA, Gattiker A, Bulliard V, Langendijk-Genevaux PS, et al.** (2006) ScanProsite: detection of PROSITE signature matches and ProRule-associated functional and structural residues in proteins. Nucleic Acids Res 34 (Web server issue):W362–W365.

20. **Arnold K, Bordoli L, Kopp J, Schwede T** (2006) The SWISS-MODEL workspace: a web-based environment for protein structure homology modelling. Bioinformatics 22: 195–201.

21. **Biasini M, Bienert S, Waterhouse A, Arnold K, Studer G, et al.** (2014) SWISS-MODEL: modelling protein tertiary and quaternary structure using evolutionary information. Nucleic Acids Res 42:(Web server issue): W252–8.

22. **Iwase S, Xiang B, Ghosh S, Ren T, Lewis PW, et al.** (2011) ATRX ADD domain links an atypical histone methylation recognition mechanism to human mental-retardation syndrome. Nat Struct Mol Biol 18: 769–76.

23. **Eissenberg JC, Morris G, Reuter G, Hartnett T** (1992) The heterochromatin associated protein HP1 is an essential protein in Drosophila with dosage dependent effects on position effect variegation. Genetics 131: 345–352.

24. **Lu BY, Bishop CP, Eissenberg JC** (1996) Developmental timing and tissue specificity of heterochromatin-mediated silencing. EMBO J 15: 1323–1332

25. **Valadez-Graham V, Yoshioka Y, Velázquez O, Kawamori A, Vázquez M, et al.** (2012). XNP/dATRX interacts with DREF in the chromatin to regulate gene expression. Nucleic Acids Res 40: 1460–74.

26. **Herrera-Cruz M, Cruz G, Valadez-Graham V, Fregoso-Lomas M, Villicaña C, et al.** (2012) Physical and functional interactions between Drosophila homologue of Swc6/p18 Hamlet subunit of the SWR1/SRCAP chromatin-remodeling complex with the DNA repair/transcription factor TFIIH. J Biol Chem 287: 33567–33580.

27. **Kamakaka RT, Kadonaga JT** (1994) The soluble nuclear fraction, a highly efficient transcription extract from Drosophila embryos. Methods Cell Biol 44: 225–235.

28. **Leclerc V, Tassan JP, O'Farrell PH, Nigg EA, Leopold P** (1996) Drosophila Cdk8, a kinase partner of cyclin C that interacts with large subunit of RNA polymerase II. Mol Biol Cell 7: 505–513.

29. **Palomera-Sanchez Z, Bucio-Mendez A, Valadez-Graham V, Reynaud E, Zurita M** (2010) Drosophila p53 is required to increase the levels of the dKDM4B demethylase after UV induced DNA damage to demethylate histone H3-lysine 9. J Biol Chem 285: 31370–31379.

30. **Antão JM, Mason JM, Déjardin J, Kingston RE** (2012) Protein landscape at *Drosophila melanogaster* telomere-associated sequence repeats. Mol Cell Biol 32: 2170–82.

31. **Jimenez G, Ish-Horowicz D** (1997) A chimeric enhancer-of-split transcriptional activator drives neural development and achaete-scute expression. Mol Cell Biol 17: 4355–4362.

32. **Gu T, Elgin SC** (2013) Maternal depletion of Piwi, a component of the RNAi system, impacts heterochromatin formation in Drosophila. PLoS Genet 9: e1003780.

33. **Li Y, Li H** (2012) Many keys to push: diversifying the 'readership' of plant homeodomain fingers. Acta Biochim Biophys Sin (Shanghai) 44: 28–39.

34. **Wang W, Yu H, Long M** (2004) Duplication-degeneration as a mechanism of gene fission and the origin of new genes in Drosophila species. Nat Genet 36: 523–527.

35. **Chauhan C, Zraly CB, Parilla M, Diaz MO, and Dingwall AK** (2012) Histone recognition and nuclear receptor co-activator functions of Drosophila cara mitad, a homolog of the N-terminal portion of mammalian MLL2 and MLL3. Development 139: 1997–2008.

36. **Bhaskar V, Courey AJ** (2002) The MADF-BESS domain factor Dip3 potentiates synergistic activation by Dorsal and Twist. Gene 299: 173–84.

37. **St. Pierre SE, Ponting L, Stefancsik R, McQuilton P, FlyBase Consortium** (2014) FlyBase 102 - advanced approaches to interrogating FlyBase. Nucleic Acids Res 42(D1): D780–D788.

38. **Frydrychova RC, Mason JM, Archer TK** (2008) HP1 is distributed within distinct chromatin domains at Drosophila telomeres. Genetics 180: 121–31.

39. **Park DJ, Pask AJ, Huynh K, Renfree MB, Harley VR, et al.** (2004) Comparative analysis of ATRX, a chromatin remodeling protein. Gene 339: 39–48.

40. **Drané P, Ouararhni K, Depaux A, Shuaib M, Hamiche A** (2010) The death-associated protein DAXX is a novel histone chaperone involved in the replication-independent deposition of H3.3. Genes Dev 24: 1253–65.

41. **Lewis PW, Elsaesser SJ, Noh KM, Stadler SC, and Allis CD** (2010) Daxx is an H3.3-specific histone chaperone and cooperates with ATRX in replication-independent chromatin assembly at telomeres. Proc Natl Acad Sci USA 107: 14075–14080.

42. **Clynes D, Higgs DR, Gibbons RJ** (2013) The chromatin remodeller ATRX: a repeat offender in human disease. Trends Biochem Sci 38: 461–6.

43. **England BP, Admon A, Tjian R** (1992) Cloning of Drosophila transcription factor Adf-1 reveals homology to Myb oncoproteins. Proc Natl Acad Sci USA 89: 683–687.

44. **Casola C, Lawing AM, Betrán E, Feschotte C** (2007) PIF-like transposons are common in Drosophila and have been repeatedly domesticated to generate new host genes. Mol Biol Evol 24: 1872–1888.

45. **Maheshwari S, Wang J, Barbash DA** (2008) Recurrent positive selection of the Drosophila hybrid incompatibility gene Hmr. Mol Biol Evol 25: 2421–2430.

46. **Jung SH, Evans CJ, Uemura C, Banerjee U** (2005) The Drosophila lymph gland as a developmental model of hematopoiesis. Development 132: 2521–2533.

47. **Minakhina S, Steward R** (2006) Melanotic mutants in Drosophila: pathways and phenotypes. Genetics 174: 253–263.

48. **Minakhina S, Tan W, Steward R** (2011) JAK/STAT and the GATA factor Pannier control hemocyte maturation and differentiation in Drosophila. Dev Biol 352: 308–16.

Meyer-Nava et al. BMC Molecular and Cell Biology (2020) 21:17
https://doi.org/10.1186/s12860-020-00257-2

BMC Molecular and Cell Biology

RESEARCH ARTICLE Open Access

Molecular effects of dADD1 misexpression in chromatin organization and transcription

Silvia Meyer-Nava, Amada Torres, Mario Zurita and Viviana Valadez-Graham*

Abstract

Background: dADD1 and dXNP proteins are the orthologs in *Drosophila melanogaster* of the ADD and SNF2 domains, respectively, of the ATRX vertebrate's chromatin remodeler, they suppress position effect variegation phenotypes and participate in heterochromatin maintenance.

Results: We performed a search in human cancer databases and found that ATRX protein levels were elevated in more than 4.4% of the samples analyzed. Using the *Drosophila* model, we addressed the effects of over and under-expression of dADD1 proteins in polytene cells. Elevated levels of dADD1 in fly tissues caused different phenotypes, such as chromocenter disruption and loss of banding pattern at the chromosome arms. Analyses of the heterochromatin maintenance protein HP1a, the dXNP ATPase and the histone post-translational modification H3K9me3 revealed changes in their chromatin localization accompanied by mild transcriptional defects of genes embedded in heterochromatic regions. Furthermore, the expression of heterochromatin embedded genes in null *dadd1* organisms is lower than in the wild-type conditions.

Conclusion: These data indicate that dADD1 overexpression induces chromatin changes, probably affecting the stoichiometry of HP1a containing complexes that lead to transcriptional and architectural changes. Our results place dADD1 proteins as important players in the maintenance of chromatin architecture and heterochromatic gene expression.

Keywords: Heterochromatin, dADD1, ATRX, dXNP

Background

The major factors involved in chromatin dynamics are ATP-dependent chromatin remodeling complexes, which contain an ATPase catalytic subunit, which provides the energy necessary for their function. One of these ATPases is ATRX, first described as a putative member of the helicase superfamily due to its homology with RAD54 that has been implicated in nucleotide excision repair and transcription [1, 2]. Mutations in the human gene are the main cause of a syndrome that includes alpha thalassemia, profound developmental delay, mental retardation, genital abnormalities, and facial dimorphism, among other manifestations [2]. The *ATRX* gene is highly conserved through eukaryotic evolution; for example, mouse and human proteins have 87% homology [3], whereas invertebrates like *Drosophila melanogaster* have 66% [4].

The human mutations usually generate a change in protein functionality and mostly fall into the helicase-ATPase domain in the carboxy terminus, or the ADD motif (named after the three proteins that carry it, **A**TRX-**D**NMT3-**D**NMT3L), composed of a PHD and a GATA-like zinc fingers, which recognize the H3K9me3 and the unmethylated H3K4 combination of histone marks [5]. This domain directs the protein mainly to pericentric heterochromatin [6]. Although there has also been described that the ATRX PxVxL motif can target ATRX through HP1a, and mutations in this motif [7] reduce the localization of ATRX in the heterochromatin [6].

* Correspondence: vvaladez@ibt.unam.mx
Instituto de Biotecnología. Universidad Nacional Autónoma de México, Campus Morelos, Av. Universidad 2001, C.P, 62210 Cuernavaca, Morelos, Mexico

Mutations that affect the function of ATRX have recently been proposed as markers of poor survival in soft tissue sarcomas [8]. It has been highlighted that inactivating mutations in the ATRX/DAXX/H.3.3 complex in cells displaying alternative lengthening of telomeres (ALT) phenotype, including pancreatic neuroendocrine tumors [9], glioblastoma multiform, oligodendrogliomas, medulloblastomas [10] and neuroblastomas [11], support the potential role of ATRX as a tumor suppressor. Endogenous expression of ATRX suppressed the ALT pathway on bone osteosarcoma epithelial human cells [12]. Also, in a murine model of ATRX overexpression, several phenotypes were observed, such as neural tube defects, growth retardation, high mortality, and problems in locomotion and behavior in organisms that survived postnatally [13].

In *Drosophila*, the two main domains of the human ATRX protein are encoded by two different genes *dxnp* and *dadd1*. dXNP proteins conserve a helicase/ATPase domain but lack the ADD domain. The *dadd1* gene encodes three ADD harboring isoforms generated by alternative splicing. Our group and others have shown a physical interaction of these proteins with HP1a and also their localization to heterochromatic regions [14, 15]. We found that in somatic cells, mutations in *dadd1* affect chromosome stability, induce telomeric defects in the fly such as telomeric fusions, and loss of retrotransposon silencing. Lack of dADD1 caused delocalization of HP1a protein from the telomeres, with slight disturbances at other chromosomal sites [16].

Genomic instability is an indication of cancer, and it is supposed to promote tumorigenesis in pre-cancerous lesions, as well as karyotypic diversity during cancer progression. Some of the hypothesis identifies two potential pathways, the loss of tumor suppressor gene functions and/or activation of oncogenes [17].

There have been studies linking different levels of expression of ATRX as drivers of specific phenotypes that give rise to disease and cancer [13, 18, 19]. In the present study, we searched human somatic cancer databases and found that the *ATRX* gene is overexpressed in a wide variety of human cancers. Using a *Drosophila* model of ATRX, we modified the expression levels of dADD1 proteins and evaluated the effects of this overexpression in polytene cells. When dADD1 proteins have higher than wild-type levels, the polytene chromosomes lose compaction and banding pattern. HP1a protein delocalizes and acquires a different distribution within the cell nucleus. To address the roles of the dADD1a and b protein isoforms, we modified the levels of the proteins independently, and overexpression of either isoform leads to changes in the chromatin localization of HP1a, dXNP and also H3K9me3 with differences in the expression of heterochromatin and some euchromatin embedded genes.

We conclude that overexpression of dADD1 proteins titrates the levels of heterochromatin formation proteins leading to chromatin architecture loss, chromosomal instability, and organism death. Our results are discussed in the context of the cellular effects of dADD1 proteins, which are essential for global chromosome stability.

Results

ATRX expression levels in human cancers

Mutations that affect the function of ATRX have been associated with several types of cancers, including glioblastoma and pancreatic cancer [20, 21] and ATRX aberrant expression has been recently proposed as a marker of poor survival in soft tissue sarcomas [8]. On the contrary, higher levels of ATRX protein have not described in human cancers. We decided to analyze the levels of ATRX transcripts in a variety of human somatic cancers using the COSMIC (Catalogue Of Somatic Mutations In Cancer) and THPA (The Human Protein Atlas), database in detail [22, 23]. This search found that ATRX is expressed in all types of cells reviewed on THPA database with high TPM (Transcripts Per Million) values, principally in tissues like parathyroid and thyroid glands, cerebral cortex and endometrium, the thresholds used to categorize over- and under-expression from normal levels is explained in the database. The protein is also present in almost all types of human tissues [23]. According to the Genomic Data Commons (GDC) database, which is a general database, ATRX is one of the most frequently mutated genes associated with cancer, alterations in its expression are present in 7.79% of the reported cases (795/10,202 cases). Variations in gene copy number are only reported in a low number of cases with 1.76% (184/10473 cases) for gain and 1.59% for loss (167/10,473) on GDC and 0.12% (7/5686 samples) for gain and 0.81% (46/5686 samples) for loss on COSMIC, which is a manually curated database.

Advanced filtered query on COSMIC reported 174 (overexpressing) and 39 (underexpressing) cases that had modified levels of ATRX, corresponding to 4.45 and 0.99% of the total of cases registered ($n = 3910$), respectively. Cases with no previous history of treatment to rule out possible secondary effects from any treatment were selected, which gave us a total of 144 overexpressing and 33 under-expressing cases. Additional File 1a shows the distribution of ATRX overexpression in different types of tumors like lung (19%) and breast (26%) tumors are the most abundant type of cancers with alterations in the expression; we did not find any records of central nervous system tumors represented in this group. The mean overexpression revealed a fold change ranking between 3 to 5.5 in comparison to the control tissue (data not shown). Additional File 1b shows the types of tumors associated with a lesser amount of ATRX expression, like lung (38%),

upper aerodigestive tract (18%) and Central Nervous System (CNS) with 5%. Under-expression is not correlated to changes in the gene copy number, indicating that, as the overexpression cases, these changes could result from other molecular events such as gene repression or perhaps mutations in regulatory and coding sequences. Examples of Breast and Lung tissues from the THPA database are shown in the Additional File 1; ATRX immunohistochemistry was performed with the same antibody (Santa Cruz) in healthy breast tissue (Additional File 1c) where we can see nuclear localization in the gland cells. Additional Fig. 1d shows a breast cancer sample with low levels of ATRX and in Additional File 1e and 1f high levels, we can see high levels of ATRX protein in breast cancer samples. Lung tissue immunostaining with the same antibody is shown in g and h; these samples show low ATRX levels. Additional Fig. 1i and j are lung carcinoma examples in which ATRX is overexpressed with strong staining and nuclear localization. These data associate ATRX overexpression to several types of somatic tumors, therefore more in-depth cellular analyses of the molecular effects of ATRX overexpression are essential to study its role as one of the factors that may lead to the appearance or maintenance of a transformed tumor phenotype.

Misexpression of dADD1 disrupts chromatin structure

Human ATRX has two important domains that cooperate to exert its functions, the ADD domain, which recognizes the H3K9me3 and H3K4 unmethylated histone mark, which directs this protein to heterochromatic regions, and the SNF2 domain which is necessary for the correct H3.3 exchange by DAXX [24]. In insects, these two domains are separated and encoded by different genes, *dadd1* encodes orthologues to the amino ADD domain of ATRX and *dxnp* encodes proteins orthologues to the SNF2 domain [15].

The *dadd1* gene encodes three alternative spliced isoforms (see Fig. 1e), in a previous publication we showed that dADD1a tethers HP1a to the telomeres, and in a *Drosophila* line that lacks the *dadd1* gene, a set of telomeric retrotransposons (called the HTT array) which participate in telomeric maintenance and are normally silenced in somatic cells, are expressed. This led to longer telomeres and chromosomal aberrations [16]. The fact that we found that ATRX is overexpressed in a wide variety of human cancers prompted us to study in the *Drosophila* model what would be the molecular effects of overexpressing dADD1 proteins since this domain directs the protein to heterochromatin [25]. We used the UAS-GAL4 system to modify the levels of dADD1 protein isoforms. First, we directed the expression of all dADD1 protein isoforms using a ubiquitous driver (Actin or Tubulin), making genetic crosses between the flies that carried the Actin or Tubulin drivers as described in the Methods Section with the *UAS-dADD1* lines which resulted in organism lethality (Table 1). Since we had determined in our previous publication that the dAdd1a and dAdd1b protein isoforms have different activities, we overexpressed them individually to evaluate their contribution to organism lethality. We achieved similar results when we over-expressed either dADD1a or dADD1b protein isoforms (for a brief description of these lines please refer to the Methods section) [16] (Table 1), and in all the cases the organisms died at early stages of development (data not shown).

Because the ubiquitous over-expression of all or two of dADD1 isoforms led to organism lethality, we decided to drive the expression of dADD1 directly to the salivary glands using the *Sgs3-GAL4* driver (as described in the Methods section) and evaluate chromosome architecture in polytene squashes. In wild-type salivary glands, the chromosome shows the characteristic pattern of bands and interbands in the chromosome, we can also see the chromocenter (dashed box in 1a and 1a'), the telomeres (continuous line boxes in 1a and 1a") and the overall chromosome integrity (Fig. 1a). Overexpression of dADD1 results in a general loss of the chromatin structure (Fig. 1b), the chromocenter becomes fragile (compare dashed boxes of Fig. 1a'and b'), there is a loss of the banding pattern in some regions at the chromosome arms, at the telomeres (arrows and continued line boxes in Fig. 1b and an amplified image in 1b") and dissociated chromosome copies.

To confirm the overexpression of *dADD1* mRNAs, we analyzed the transcript levels in salivary glands obtained from the *UAS-dADD1;Sgs3-Gal4* genotype and compared them to the wild-type salivary glands using the primers described in [15] which are specific for every isoform, *Rp49* primers were used as control. We found that all of the isoforms mRNA levels were two to three-fold higher than the wild-type, compare lanes 1 and 3 in Fig. 1c, which is similar to the fold change observed in the tumors from the COSMIC database (data no shown). Additionally, we used the previously described pan-dADD1 antibody to perform a western blot from total protein extract of salivary glands [15] and found that dADD1 levels were overexpressed at least three-fold in comparison to the wild-type protein levels (compare lanes 1 and 3 in Fig. 1d).

We evaluated changes in DNA and histones content in both wild-type and overexpressed conditions to rule out differences in endoreduplication cycles and chromatin content and we did not observe any significative changes between the wild-type and dADD1 overexpression conditions (See Additional file 2a and b).

The observed phenotype of an overall loss of banding patterns and chromosome compaction when we overexpress dADD1 was somewhat unexpected since, as mentioned

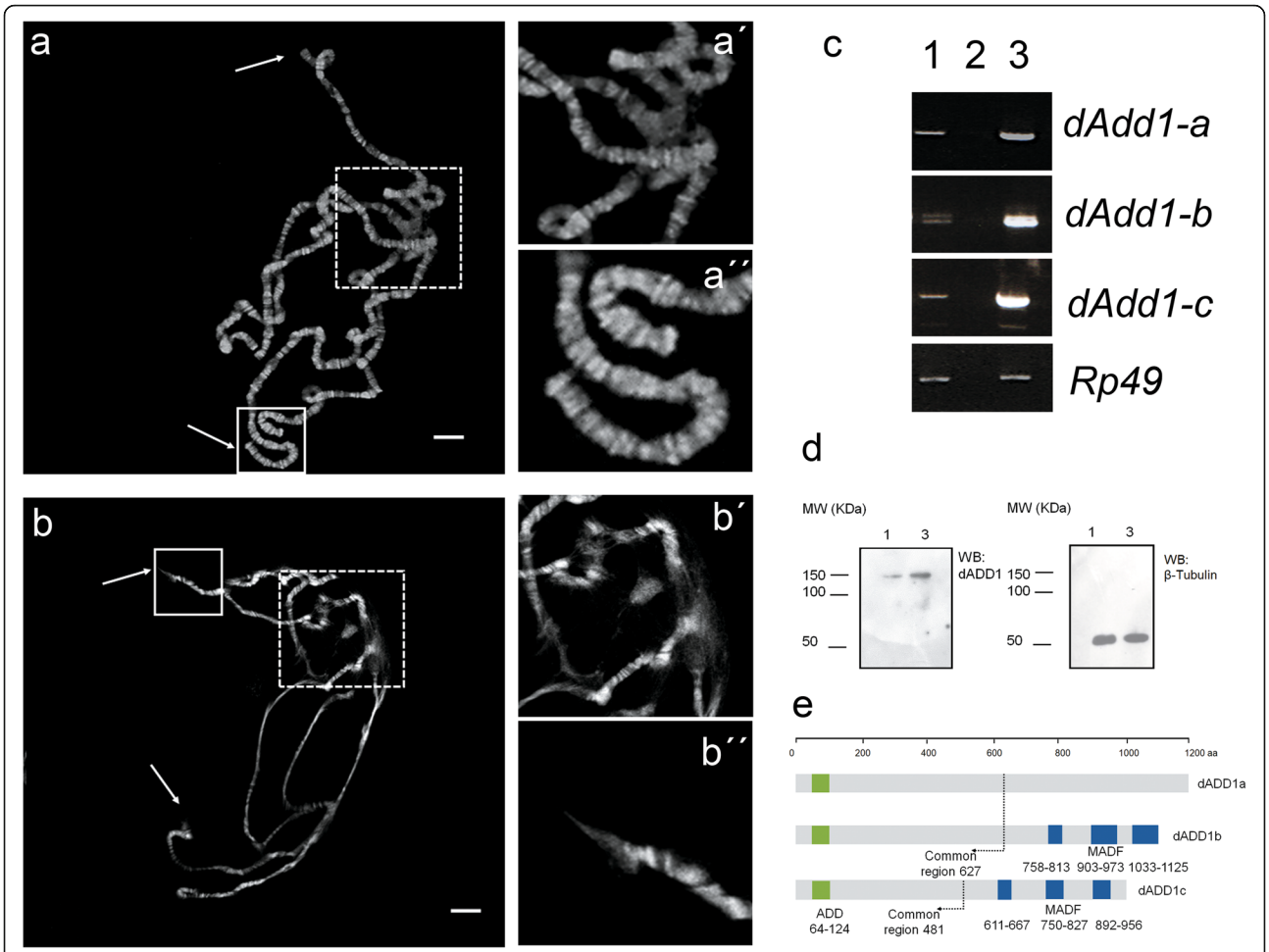

Fig. 1 Modification of dADD1 expression levels results in chromosomal disorganization. **a** Polytene chromosome squash from a wild-type organism. DNA was stained with DAPI (shown in gray), arrows point to telomeric regions, the chromocenter is shown within the dashed box a') magnification of the chromocenter, a") magnification of the telomeres. **b** Polytene chromosome squash from salivary glands in which overexpression of dADD1 isoform was performed using the UAS-GAL4 system, as in "a" arrows point to telomeric regions and the chromocenter is in the dashed box, b') magnification of the chromocenter, b") magnification of a telomeric region. Scale bar 20 μm. **c** Semi-quantitative analysis of the transcript levels of dADD1 isoforms in salivary glands. Lanes in the gel correspond to 1) wild-type, 2) H_2O, 3) *UAS-dadd1; Sgs3-GAL4* genotypes. *Rp49* transcript was used as a control. Note that all transcripts isoforms are overexpressed (compare lanes 1 to 3). **d** Western blot from total protein extracts from salivary glands where pan-dADD1 and anti-β tubulin antibodies were used. Lanes correspond to 1) wild-type and 3) *UAS-dadd1; Sgs3-GAL4,* molecular weight markers are shown on the left side of the panels. On the right side of the panels, the antibodies used for each membrane are specified. **e** Schematic representation of the dADD1 protein isoforms. The ADD domain shared by all isoforms is shown in green; a dashed line delimits the common region. MADF domains of the dADD1b and c isoforms are shown in blue. dADD1a is 1199 aa long (130 kDa), dADD1b is 1125 aa (127 kDa) and dADD1c is 979 aa (112 kDa)

Table 1 Effect of dADD1 overexpression in organism viability

Genotype	Viability [a] (%)
+/+;Tub-GAL4/+	352/372 (94)
+/ UAS-dADD1;+/+	361/361 (100)
+/+; UAS-dADD1a/+	558/558 (100)
+/+; UAS-dADD1b/+	273/273(100)
+/UAS-dADD1;Tub-GAL4/+	0/361 (0)
+/+;Tub-GAL4/UAS-dADD1a	0/558 (0)
+/+;Tub-GAL4/UAS-dADD1b	0/273 (0)

[a]The number of flies gotten over the number of adult flies expected to agree with the healthiest class in each cross

above, we recently reported that dADD1 participates in the silencing and compaction of the telomeric retrotransposons and prevent telomeric fusions. Therefore, we expected that the overexpression could lead to an opposite localized effect (that is more compaction) in some areas of the chromosomes, but this was not the case. In our previous report, we performed rescue experiments in a null *dadd1* background and found that HP1a was restored to the telomeric region when the rescue was performed with dADD1a isoform. However, we also observed that upon dADD1a overexpression, HP1a was lost from the chromocenter in a dADD1a dose-dependent manner [16].

To get further insights into the mechanisms involved in the emergence of these phenotypes, we performed HP1a immunolocalizations in wild-type and dADD1 overexpressing chromosomes. We performed all the immunolocalization experiments to get the overexpressing and wild-type chromosomes at the same time to avoid differences that could be introduced by the immunohistochemistry assay. To evaluate if there was a correlation between the loss of banding pattern and HP1a localization we quantified the number of chromosomes which presented a loss of banding pattern and divided the chromosomes into three groups according to the severity of banding pattern loss: organized (well-defined bands, chromocenter with HP1a signal), moderately affected (still with HP1a signal in the chromocenter but with irregularities in the banding pattern), and severely altered (very little or no signal of HP1a in the chromocenter, many defects in the pattern of banding and thickness of the chromosome arm), examples of each phenotype and classifications are shown in Fig. 2a. The wild-type chromosomes conserved the banding pattern and also the HP1a

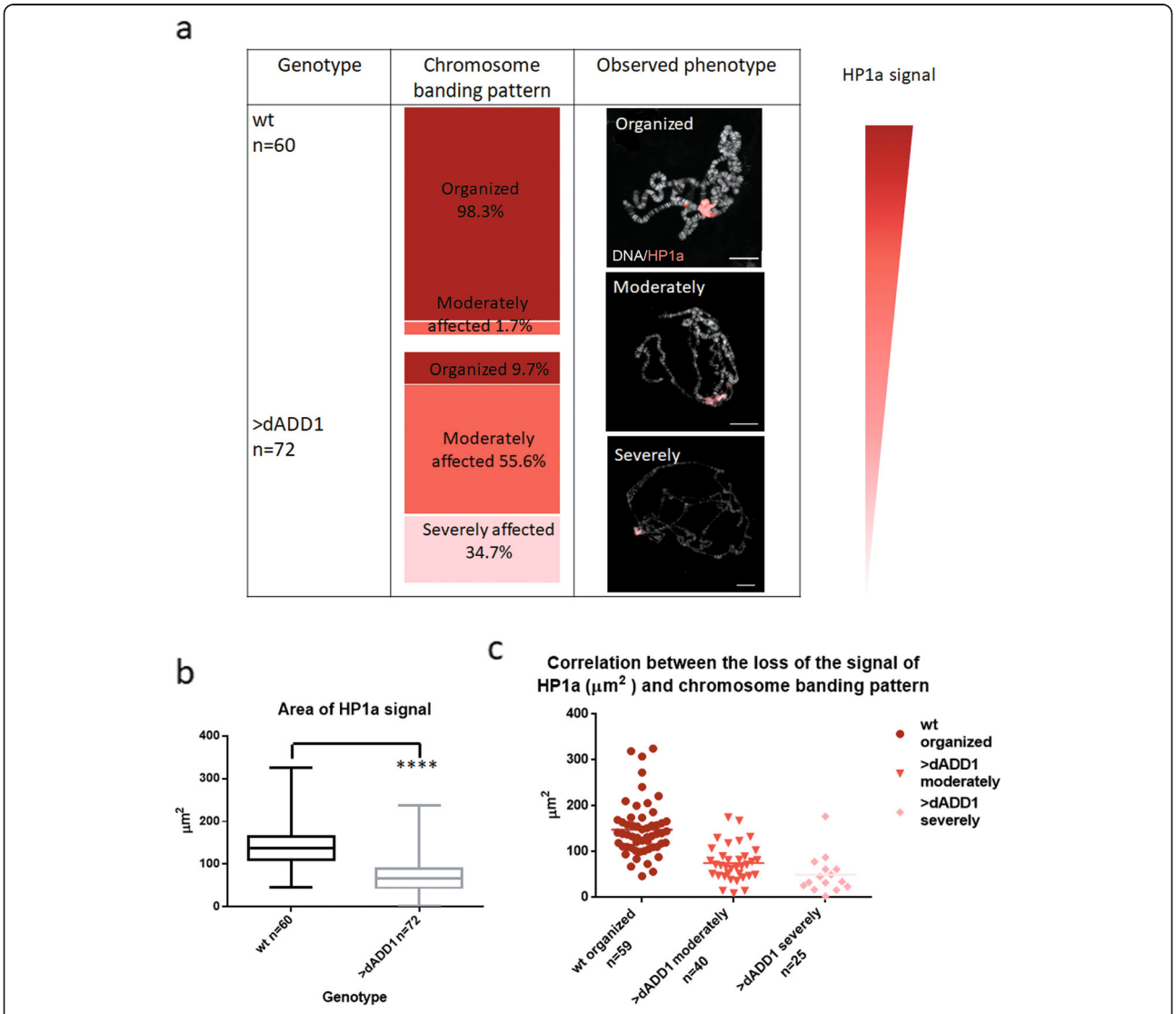

Fig. 2 dADD1 overexpression induces HP1a delocalization, which correlates with loss of chromosome banding pattern at the chromocenter. **a** Classification of the severity of the phenotypes and the amount of HP1a signal observed in the polytene chromosomes. The first column indicates the genotypes analyzed; the second column shows the classification of the chromosomes according to their banding pattern in organized, moderately and severely affected (see text for a detailed explanation on the classification). Different shades of red indicate the intensity of HP1a signal. The third column shows an example of each of these polytene squashes where DNA is evidenced by DAPI staining (shown in gray), HP1a (red) scale bar 20 µm. **b** Area of HP1a signal quantified with ImageJ. The number of chromosomes analyzed for each condition is shown with "n," an Unpaired t-test was performed to determine significance, the Area of HP1a signal is diminished in dADD1 overexpressing chromosomes (>dAdd1 vs. wt). **c** Correlation between HP1a and loss of chromosome banding pattern. Ordinary one-way ANOVA was performed to determine the significance, $p < 0.0001$****

pericentromeric signal, and only 1.7% of the chromosomes had the chromosome banding pattern moderately affected upon the squashing technique; also, the vast majority (98.3%) had a strong HP1a signal. In dADD1 overexpressing chromosomes (>dADD1), only 9.7% of the chromosomes analyzed appeared to maintain an organized chromatin structure, but the majority (90.3%) did not (Fig. 2a). We quantified the area of HP1a signal at the chromocenter (see methods section) and was reduced in dADD1 overexpressing chromosomes (Fig. 2b). To evaluate if the chromosome banding pattern was affected due to HP1 loss, we measured the results obtained from each genotype and HP1a signal intensity, and we observed that indeed, chromosomes have banding pattern loss had less HP1a bound to the chromocenter (Fig. 2c). These experiments indicate that over-expression of dADD1 in a wild-type background results in loss of heterochromatin and compaction mediated at least in part by HP1a loss.

HP1a is delocalized in dADD1 overexpressing cells

In the previous experiments, dADD1 overexpression results in HP1a loss from the chromocenter (Fig. 2). We performed HP1a immunofluorescences in the salivary glands to evaluate whether the loss of HP1a from the chromatin was a result of a change in its sub-nuclear localization.

We directed the expression of dADD1a and dADD1b or all isoforms using the *Sgs3-GAL4* driver to salivary glands and performed HP1a immunofluorescences (see additional File 2c for specific mRNA expression of each isoform evaluated by RT-PCR). In wild-type salivary glands, HP1a appears as a single focalized spot that marks the chromocenter [26]. Figure 3a, first row, and magnified images. Almost 92% of the nuclei counted presented this phenotype; the rest (7%) showed two foci (Fig. 3b and c). Overexpression of dADD1 results in the loss of the HP1a focalized signal, 17% of the observed nuclei presented a wild-type focal distribution, whereas 70% showed a wide distribution in which the HP1a signal appears to be distributed in the nucleoplasm with not bright enriched foci, see also the magnified images of the nuclei (Fig. 3a, second-row genotype > *dADD1*, Fig. 3b second column) and 13% presented the two foci phenotype.

According to these results, we can envision that the HP1a protein present in the nucleoplasm is most likely

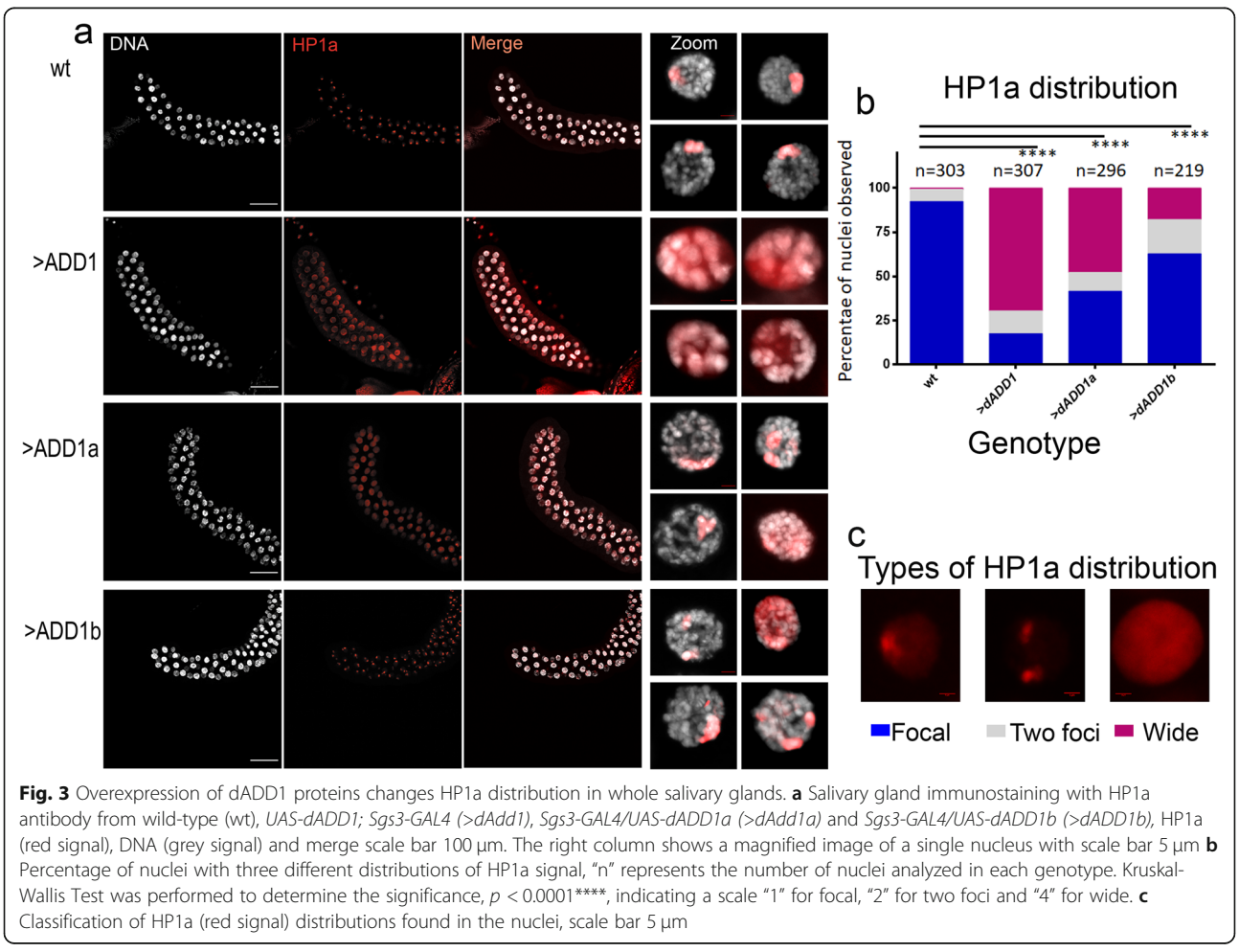

Fig. 3 Overexpression of dADD1 proteins changes HP1a distribution in whole salivary glands. **a** Salivary gland immunostaining with HP1a antibody from wild-type (wt), *UAS-dADD1; Sgs3-GAL4 (>dAdd1)*, *Sgs3-GAL4/UAS-dADD1a (>dAdd1a)* and *Sgs3-GAL4/UAS-dADD1b (>dADD1b)*, HP1a (red signal), DNA (grey signal) and merge scale bar 100 μm. The right column shows a magnified image of a single nucleus with scale bar 5 μm **b** Percentage of nuclei with three different distributions of HP1a signal, "n" represents the number of nuclei analyzed in each genotype. Kruskal-Wallis Test was performed to determine the significance, $p < 0.0001$****, indicating a scale "1" for focal, "2" for two foci and "4" for wide. **c** Classification of HP1a (red signal) distributions found in the nuclei, scale bar 5 μm

lost during the squashing technique; this can account for the lack of HP1a protein in the polytene squashes. On the other hand, the expression of either isoform results in a mixture of the possible phenotypes shown in Fig. 3a, third and fourth row, and magnified images.

In dADD1a overexpression, 48% of the chromosomes presented a wide HP1a distribution (Fig. 3b third column marked >dADD1a). In contrast, dADD1b overexpressing cells exhibited close to 18% wide distribution and had the highest percentage of two foci distribution (19%), but the majority had a wild-type (focal) HP1a distribution (63%) (Fig. 3a, fourth row, and Fig. 3b, 4th column). Overexpression of all dADD1 isoforms had the most profound effect in disrupting the HP1a focal signal, with almost 70% of the observed chromosomes presenting a wide HP1a distribution. Looking at the percentages, the combined dADD1a and dADD1b overexpression is responsible for nearly all of the 70% of HP1a wide distribution (48% plus 18% = 66%) (Fig. 3b), however dADD1a has the most marked effect on HP1a distribution, this could be a result of the reported interaction between these two proteins [14, 27].

We also quantified the area of the nuclei to see if it changed upon dADD1 overexpression, but we could not find any significative differences when we compared it to the control nuclei (Additional file 2d), next we measured the intensity of the DAPI, and we did not observe any differences. These data suggest that dADD1 overexpression does not affect the size of the nuclei nor the amount of DNA in polytene cells (See Additional file 2 d and e).

As mentioned before, dADD1 protein isoforms conserve a common region, which includes the ADD domain, the difference between them is the presence in the carboxy-terminal end of additional MADF domains in the dADD1b protein isoform which are not present in the dADD1a isoform (Fig. 1e). Therefore, the common region may have an essential role in disrupting HP1a foci. The ADD domain recognizes and binds to H3K9me3 in combination with H3K4 without any modification; thus, it was possible that dADD1 overexpression could "compete" with HP1a for binding to the H3K9me3.

H3K9me3 chromatin signal is lost upon dADD1 overexpression

We anticipated at least two possible scenarios. In the first one, dADD1 proteins could "deplete/remove" HP1a from the chromocenter of salivary glands directly via protein-protein interactions. The second one could involve a competition between HP1a and dADD1 for the H3K9me3 binding site [16].

It has been widely demonstrated that H3K9me3 post-translational modification is needed to maintain pericentric heterochromatin and that this histone mark is enriched at the chromocenter of polytene chromosomes [28]. Any perturbation of this histone mark leads to HP1a loss from the chromocenter [29, 30]. Therefore, we decided to evaluate if this mark was conserved in dADD1 overexpressing cells.

We performed double immunostaining of H3K9me3 and HP1a in polytene chromosomes from wild-type or overexpressing dADD1 cells. Representative confocal images are shown in Fig. 4. In wild-type chromosomes, the H3K9me3 (green) and HP1a (red) signals are enriched at the chromocenter as previously described [28], all of the wild-type chromosomes analyzed presented both signals (100%) (Fig. 4a, first column, and Additional file 3a first row). To explain the differences between the wild-type and the overexpressing chromosomes, we quantified the area of HP1a signal on the chromosomes and the intensity of HP1a and H3K9me3 (as described in the methods section). The area of the signal helped us determined the "spreading" of the HP1a domain, and the intensity is a direct measure of the chromatin-bound HP1a or H3K9me3 histone mark. When dADD1 is overexpressed, there was less HP1a signal, and also H3K9me3 was affected (see Additional file 3a third row). When either dADD1a or b protein isoforms are overexpressed, the chromatin banding pattern is still maintained, but there is less HP1a signal (Fig. 4a middle and right column and Fig. 4b), the HP1a quantified area is slightly less affected by the dADD1b overexpression. However, this effect could be because the majority of the chromosomes had a "split" HP1a signal (a representative chromosome is shown in Fig. 4a, right column, and Fig. 4b "area" plot) as if the chromocenter is more fragile and prone to "break" upon the squashing treatment. The signal intensity of both H3K9me3 and HP1a is diminished in the overexpression of both isoforms (Fig. 4b, intensity plots).

Overexpression of dADD1a or dADD1b also affects their own chromosome localization. In dADD1a overexpression, the signal at the chromocenter is lost, and the banding pattern looks more defined than the wild-type, whereas, in the case of dADD1b overexpression, the dADD1 pattern looks punctuated instead of bands but also the signal at the chromocenter is reduced (Additional file 3b).

These results indicate that dADD1 overexpression is not competing with HP1a to bind to its chromatin recognition site, but it could somewhat affect the chromocenter by titrating HP1a or HP1a containing complexes.

dADD1 misexpression affects the expression of some heterochromatic genes

Some genes embedded in heterochromatin need this surrounding context for their correct expression and also require the presence of HP1a [31]. Since HP1a delocalized from many regions upon dADD1 overexpression, we decided to analyze if the expression of these genes was also affected.

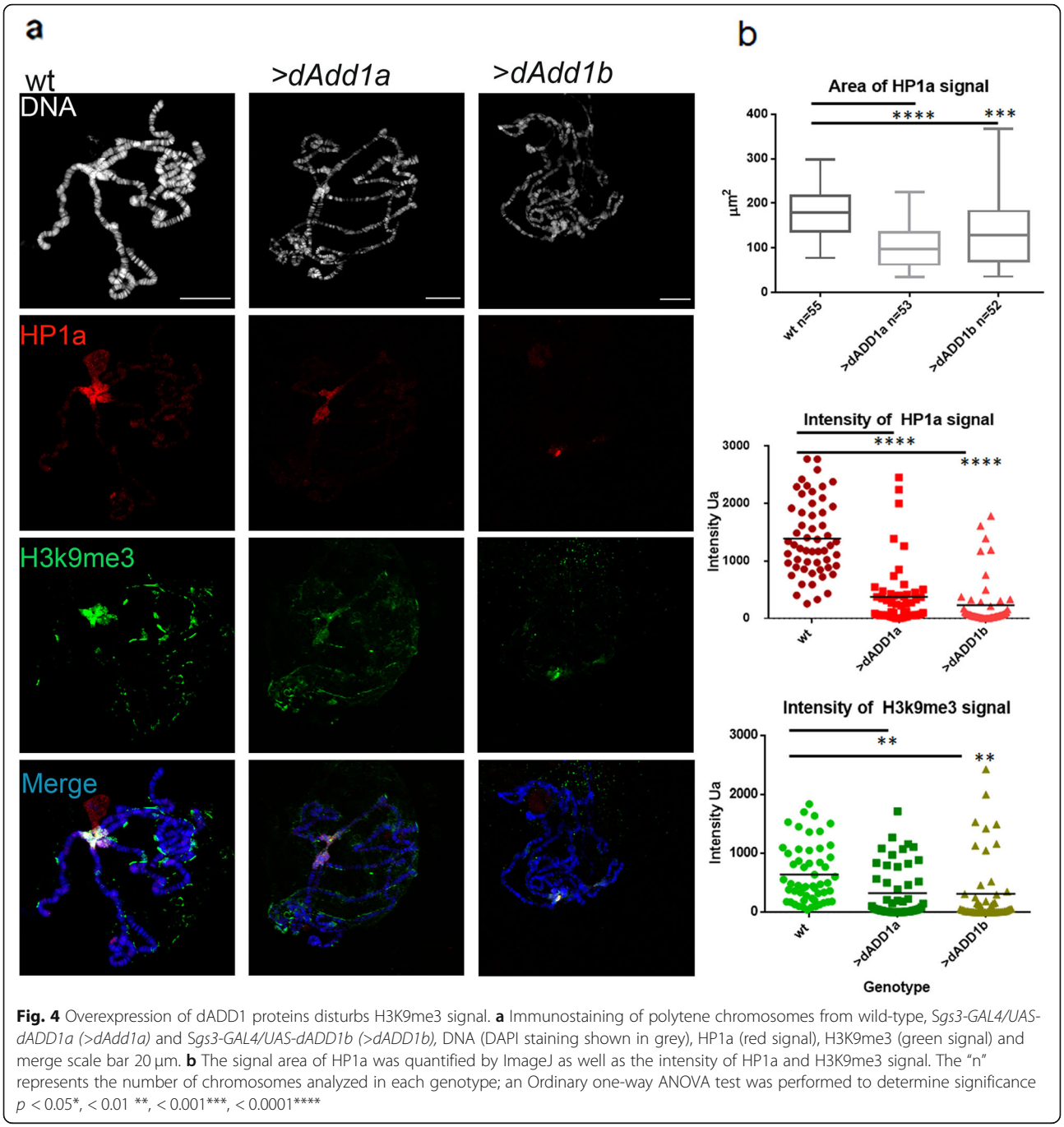

Fig. 4 Overexpression of dADD1 proteins disturbs H3K9me3 signal. **a** Immunostaining of polytene chromosomes from wild-type, *Sgs3-GAL4/UAS-dADD1a (>dAdd1a)* and *Sgs3-GAL4/UAS-dADD1b (>dADD1b),* DNA (DAPI staining shown in grey), HP1a (red signal), H3K9me3 (green signal) and merge scale bar 20 μm. **b** The signal area of HP1a was quantified by ImageJ as well as the intensity of HP1a and H3K9me3 signal. The "n" represents the number of chromosomes analyzed in each genotype; an Ordinary one-way ANOVA test was performed to determine significance $p < 0.05$*, < 0.01 **, < 0.001***, < 0.0001****

We used as a selection guide DamIP chromatin profiling technique in Kc cells [32]. We have certainty of well-known genes located in pericentromeric regions that need HP1a for their proper expression in salivary glands such as *cinnamon (cin)*, *CG7742* [33], *light* (*lt)* [34], and *concertina (cta)* [35] these loci are in different chromosomes and heterochromatic regions [32, 35]. Of others, we decided to evaluate them because they are silenced in salivary glands, such as *kraken (Kra)* and *P-element somatic inhibitor (Psi)* [36]. We also evaluated euchromatic genes as control regions which are not controlled by either HP1a or Su(var)3–9. Using quantitative RT-PCR (qRT-PCR), we analyzed the transcript levels of all these genes in wild-type, dADD1a or b overexpressing salivary glands and also in the null *dadd1* organisms because in our first dADD1 report, we demonstrated the co-localization of HP1a and dADD1 proteins in polytene chromosomes, particularly at the chromocenter, but also at some bands throughout the polytene arms and chromosome four [15].

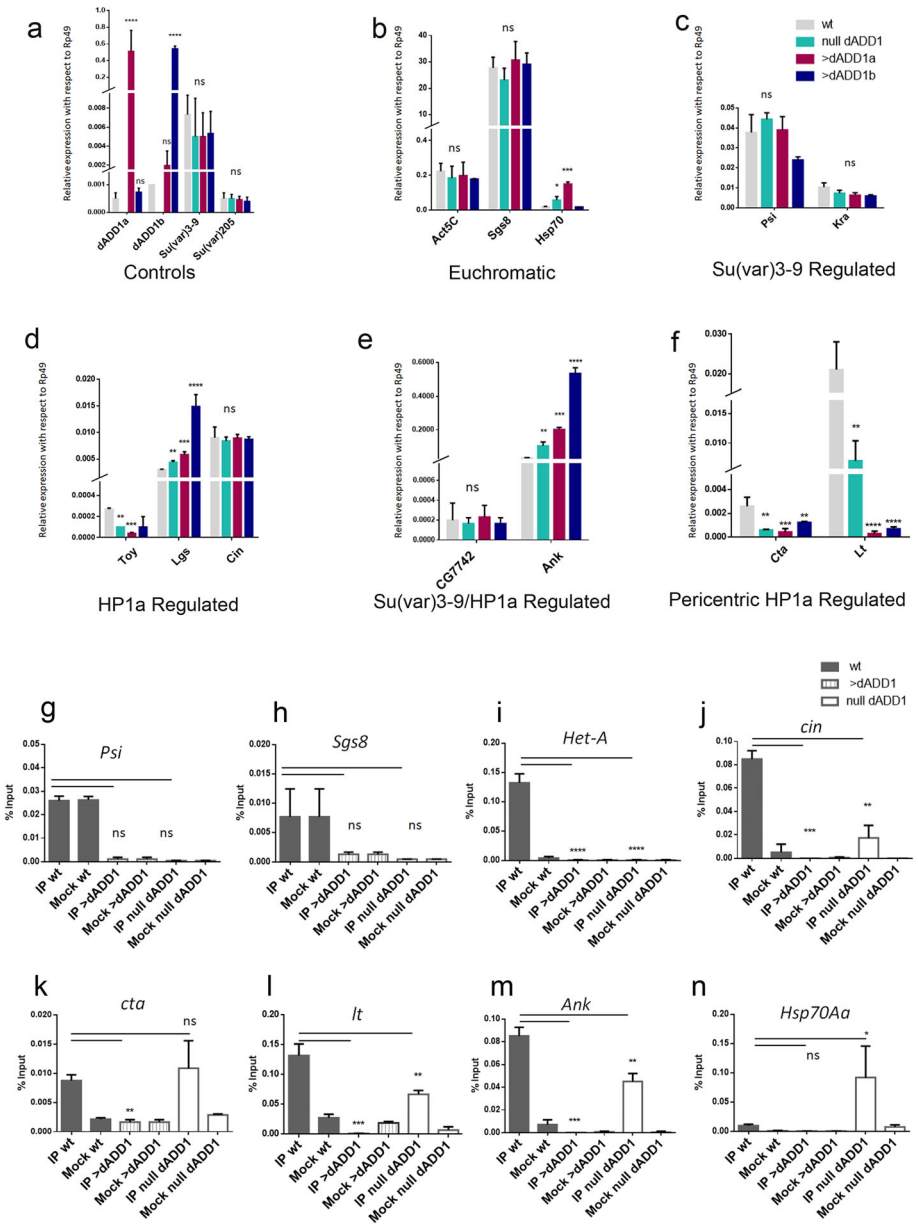

Fig. 5 dADD1 overexpression results in transcriptional silencing of some genes and loss of HP1a. qRT-PCR analyses, wild-type (gray bars), null dADD1 (aqua bars), *Sgs3-GAL4/UAS-dADD1a* (red bars) and *Sgs3-GAL4/UAS-dADD1b* (dark blue bars). Three independent biological replicates were performed. Data are shown as expression relative to *Rp49* transcript. Ordinary one-way ANOVA was executed to determine significance with *P*-values ($p < 0.05$*, < 0.01 **, < 0.001***, < 0.0001****, ns, no significance). **a** controls, **b** euchromatin genes, **c** genes regulated by Su(var)3–9, **d** genes regulated by HP1a, **e** genes regulated by Su(var)3–9 and HP1a, **f** pericentric genes. HP1a protein enrichment at different analyzed promoters. Chromatin immunoprecipitation experiments were performed using the C1A9 antibody (anti-HP1a) and mouse IgG as Mock. *Psi*, *Sgs8* and *Hsp70* are euchromatic regions without HP1a (**g** and **h** and **n**); note there is no enrichment versus the mock in the wild-type condition. Promoters of the Het-A retrotransposon (**i**) and *Cin* (**j**) were evaluated as telomeric and sub-telomeric regions in which HP1a is localized. Cta (**k**) and Lt (**l**) are pericentromeric, and HP1a also regulates them. *Ank* is regulated by Su (var)3–9 and HP1a (**m**). Error bars represent standard deviation. *P*-values ($p < 0.05$*, < 0.01 **, < 0.001***, < 0.0001****, ns, no significance)

We analyzed public data in which they used a Bio-tap tagged dADD1a for ChIP-seq experiments in S2 cells and evaluated the presence of dADD1a in the same genes of Fig. 5. Although S2 cells are embryonic, the position of the genes in the chromosome does not change, and neither does constitutive heterochromatin; therefore, we believe the ChIP-seq data helped us to get further information on dADD1a position in other heterochromatic gene domains. We found that dADD1a is not present in euchromatic genes such as *Sgs8* and

Actin, neither in *Su (var)205* and *Su (var)3–9* nor in genes controlled by Su(var)3–9 such as *Psi* and *kraken* see Additional file 5.

When we looked at genes controlled exclusively by HP1a [37], we only found dADD1a at *toy* and *lgs*, which are located at chromosome four, which is mainly heterochromatic, whereas in *cin* there is not dADD1a (Additional file 5).

In HP1a/Su (var)3–9 controlled genes, dADD1 is localized in *Ank* but not in CG7742. There is also the presence of dADD1 in the pericentromeric genes, *lt* and *cta* (Additional file 5). dADD1a is located at the promoter, but also through the gene bodies of the analyzed genes.

For the qRT-PCR, we used *Rp49* transcript for data normalization since the transcript levels remained very similar in the wild-type and the *dadd1* null or *dadd1* overexpressing salivary glands (data not shown). All the transcripts were analyzed in four genetic backgrounds, wild-type (gray bars), null *dadd1* (aqua bars), *dadd1a* overexpression (red bars) and *dadd1b* overexpression (dark blue bars) (see Fig. 5). First, we analyzed the transcript levels of *dADD1a or b* (Fig. 5a top panel labeled as "controls"). When we overexpress each isoform, higher levels of *dADD1a* or *dADD1b* transcripts were obtained when compared to the wt as expected (Fig. 5a). Next, we analyzed if heterochromatin maintenance genes such as *Su (var)3–9* or *Su (var)205* (the gene that encodes HP1a) transcript levels were affected, but the transcripts remained at similar levels (Fig. 5a), suggesting that the previously observed effects on loss of HP1a and H3K9me3 (Figs. 3 and 4) are not due to loss of transcription of these genes.

Neither euchromatic genes such as *Act5C* and *Sgs8*, nor Su(var)3–9-regulated genes were affected (Fig. 5b, c). The only affected genes were HP1a-regulated genes such as *Toy* and *Lgs* (Fig. 5d); Su(var)3–9/HP1a regulated genes such as *Ank* and pericentric genes such as *Cta* and *light* (Fig. 5f). The majority of these genes were down-regulated in the null *dadd1* organisms or in the overexpression of either *dadd1a* or *b* isoforms. It is worth mentioning that all of these genes also are bound by dADD1 in S2 cells. The only two genes that showed an over-expression either in the null *dadd1* or *dadd1* overexpression genetic backgrounds were *Lgs* and *Ank*, which were overexpressed in all genetic backgrounds when compared to the wild-type. Another gene that resulted de-regulated was *hsp70*; in both the null *dadd1* organisms and *dadd1a* overexpression the transcript was more abundant.

The scheme in Additional file 4 shows the location of the analyzed genes. Particularly, *Lgs* and *Ank* are located within chromosome 4, which is highly heterochromatic but are not pericentric or telomeric. Therefore lack of dADD1 proteins or their overexpression, results in different outcomes depending on the analyzed gene and their chromosomal localization. Down-regulation of heterochromatin embedded genes could be explained by the loss of HP1a in the chromatin, which is known to be required for the correct transcription of some of these genes [37, 38]. To address if there were changes in HP1a binding to these genes, we performed chromatin immunoprecipitation followed by quantitative PCR (ChIP-qPCR). First, we analyzed two genes which are not regulated by HP1a, *Psi* and *Sgs8* do not show any HP1a enrichment versus the mock condition (IgG antibody, see Methods Section and Figs. 5 g and h), next we analyzed a region which we know is target of HP1a, the *Het-A* promoter, as we can see in Fig. 5i, there is an enrichment of HP1a at this region in wild-type individuals. In *dadd1* null organisms, HP1a is no longer present at this site, coinciding with our previous publication; importantly, overexpression of dADD1 proteins also leads to loss of HP1a at this telomeric region. The same effect can be seen in the *light*, *Ank* and *cin* regions, in the case of *light* and *Ank*, we can see that the loss of HP1a leads to opposite effects in gene transcription, *light* is down-regulated and *Ank* is up-regulated, this indicates that there is a differential role for HP1a at these heterochromatic sites, surprisingly, although *cin* loses HP1a in both the null *dadd1* and *dadd1* overexpression, the transcript is not affected (Fig. 5d and j). *cta*, which is also a pericentromeric gene and was down-regulated in all the conditions analyzed, conserves HP1a in the null *dadd1* organisms (Fig. 5k). Another unexpected result came when we analyzed *Hsp70Aa* expression; in null *dadd1* organisms and dADD1a overexpression conditions, this gene is up-regulated, and in a wild-type background, HP1a is not present at this gene, however, in salivary glands from organisms that lack *dadd1*, HP1a becomes enriched at this promoter.

These results demonstrate that dADD1 proteins are important to achieve correct levels of expression of some genes embedded in sub-telomeric or pericentromeric heterochromatin, genes located in chromosome four, which is mainly heterochromatic, but also, at some euchromatic loci.

Overall, our data indicate that misexpression of dADD1 (either over or under expression) has an important impact on chromatin structure and in the localization of HP1a proteins, which leads to differences in heterochromatic and euchromatic gene expression.

dXNP localization is altered upon dADD1 misexpression

The differences observed in gene expression are not only due to HP1a loss, so dADD1 proteins may cooperate with other protein complexes or proteins to control gene expression.

Previous work from our lab identified dXNP as a dADD1 interactor [15]. We decided to analyze if overexpression of dXNP phenocopied the loss of heterochromatin observed upon dADD1 overexpression. We performed genetic crosses between *Sgs3-Gal4* and *UAS-dXNP* lines to direct the expression only to salivary glands. First, we looked at HP1a distribution in complete salivary glands. We found that HP1a focal distribution is maintained, however, when we compare dXNP overexpression to wild-type salivary glands, the chromatin seems more compacted, and the HP1a signal although present, is diminished, see Fig. 6a. We measured the nuclei area and found that it is diminished upon dXNP overexpression (Fig. 6b). Then, we looked at polytene chromosome spreads and analyzed HP1a and dXNP distribution. In wt chromosomes, these proteins co-localized and we also saw telomeric localization of dXNP, as expected, Fig. 6d first row and magnified images. Upon dXNP overexpression, the number of bands increased, as well as the signal at certain heterochromatic regions such as the telomeres (Fig. 6d second row), however, in null *dadd1* organisms or dADD1

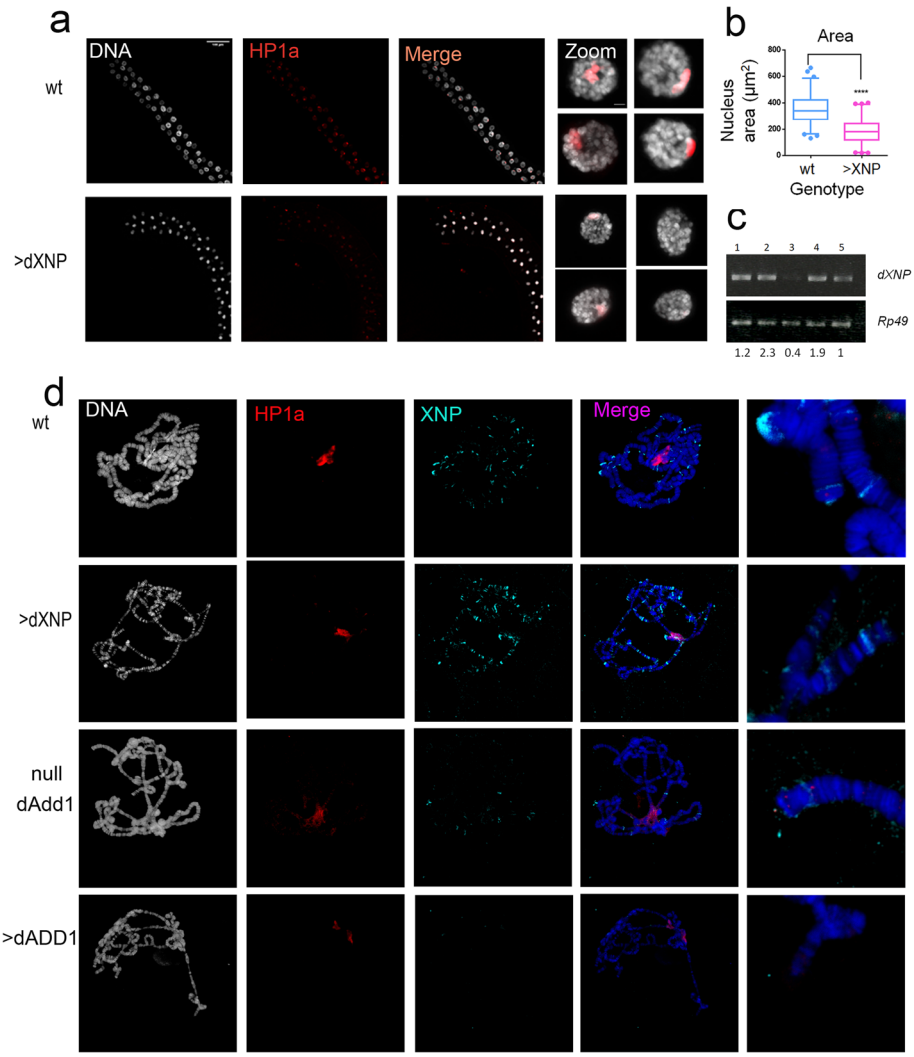

Fig. 6 dADD1 overexpression causes changes in dXNP binding. **a** Salivary gland immunostaining with HP1a antibody from wild-type (wt) and dXNP overexpression *(>dXNP) Sgs3-GAL4/UAS-dXNP*. HP1a (red signal), DNA (grey signal) and merge (scale bar 100 µm). In the right column a magnification of a single nucleus is shown (scale bar 5 µm). **b** Nucleus area quantification showing a reduction in *(>XNP),* wt $n = 341$ and XNP $n = 344$. **c** RT-PCR analysis of the transcript levels of dXNP in salivary glands. Lanes in the gel correspond to 1) wild-type (wt) 2) *Sgs3-Gal4/UAS-XNP (>XNP)*, 3) xnp^2/xnp^3 (a heteroallelic condition in which *dxnp* transcripts are diminished), 4) $dadd1^2/\ dadd1^2$ (null *dadd1*) and 5) *UAS-dadd1; Sgs3-GAL4*(>dADD1), genotypes. *Rp49* transcript was used as a control; the numbers below are the bands quantification with respect to *Rp49* signal intensity. **d** Immunostaining of polytene chromosomes from wild-type (wt), *Sgs3-GAL4/UAS-XNP* (>XNP), $dadd1^2/\ dadd1^2$ (null dAdd1) and *UAS-dADD1; Sgs3-GAL4* (>dADD1), DNA (DAPI staining shown in grey), HP1a (red signal), dXNP (cyan signal) and merge. The right column presents a magnification of the telomeric regions

overexpression, the dXNP signal diminishes, and only a few numbers of bands conserve dXNP protein signal, see Fig. 6d last two rows. Then we analyzed the *dXNP* transcript levels and are normally expressed (compare lines 1 versus 4 and 5 in Fig. 6c). Therefore, lack or overexpression of dADD1 does not affect transcription of this gene, only its chromatin location.

These results demonstrate that upon dADD1 loss, dXNP loses its wild-type chromatin localization as fewer dXNP bands are detected in these chromosomes, which could lead to loss of chromatin compaction. Interestingly, upon dXNP overexpression, there seems to be general chromatin compaction that coincides with the presence of more dXNP bands at polytene chromosomes. These results support the role of dADD1 as essential proteins to maintain a correct chromatin organization, protein localization, and gene expression.

Discussion

Maintenance of a correct chromatin structure is central for cell viability. During the transformation process in cancerous cells, many genes become deregulated, changing several protein levels and allowing the cell to escape normal controls of cell cycle and gene regulation. Currently, many association studies address the role of loss of function mutations of many transcriptional factors and chromatin remodelers in cancer cells, and many databases have been able to concentrate these data to understand this important disease.

ATRX loss of function mutations has been associated with several different cancer cells, from glioblastoma to pancreatic cancer [21]. The number of these mutations has grown in the past few years, and many of them affect the domains important for the wild-type function of the protein [39]. Although the majority of the studies have focused on the loss of function mutations, many reports show overexpression of ATRX in different types of cancer. During the transformation process of the cells, many genes become deregulated and overexpressed, and there is a need for a simplified model to address the roles of the overexpression of these genes.

In this work, we report that somatic cancer cases that have ATRX overexpression are more represented in the databases examined than the under-expression conditions. This data was unexpected since most studies in the functions of ATRX in development come from the loss of function mutants. However, there have also been a few studies in which this protein has been overexpressed, leading to the appearance of similar phenotypes observed in loss of function mutants [13].

Our investigations on the function of dADD1 have led us to develop tools that help us address several questions on the purpose of these proteins. Additionally, the domains are separated in *Drosophila,* and we can study the independent roles of the ADD and the SNF2 domains of the ATRX orthologue.

In this work, we analyzed the effects of the misexpression of one of the central ATRX domains, the ADD domain. This domain shares more than 52% homology with the ADD domain of the human ATRX and also recognizes the combination of K9me3 and unmethylated K4 of histone H3 [14]. The *dadd1* gene encodes three different protein isoforms which conserve the ADD domain; our group has demonstrated that dADD1 proteins are involved in the maintenance of chromosome stability and heterochromatin by tethering HP1a to the telomeres. Additionally, the isoforms participate in the silencing of the telomeric retrotransposons, which in somatic cells are repressed and also direct HP1a binding to the telomeres [16]. Deregulation of this silencing and the lack of HP1a at the telomeres leads to the appearance of chromosomal aberrations and genome instability.

Overexpression of dADD1 proteins resulted in chromatin structure loss, and it caused a general decompaction and the dissociation of chromatin fibers around the chromocenter (Figs. 1 and 2). These phenotypes were stronger when overexpression of all dADD1 isoforms was performed. In wild-type salivary glands, the transcript levels of *dADD1* are low compared to other analyzed transcripts (see Fig. 5). These results indicate that the levels of dADD1 in polytene cells need to be maintained on the lower side to achieve a correct chromatin structure. Recently, Mitzi Kuroda's group identified dADD1 as a strong HP1a interactor and also other factors such as the methyltransferases Eggless/dSETDB1 and Su (var)3–9. These methyltransferases participate in the formation and maintenance of pericentric heterochromatin [39, 40]. Loss of either of these methyltransferases or a shift in their levels affects pericentric heterochromatin H3K9 methylation and HP1a localization [39, 40]. Given that dADD1 interacts with these histone methyltransferases, one possibility is that overexpression of dADD1 proteins breaks the stoichiometry of complexes containing these proteins, affecting the methyltransferases activity, leading to loss of the methylation mark, and HP1a (see Figs. 2 and 4). It is also fundamental to consider that the maintenance and propagation of H3K9me3 also require HP1a since it recruits Su (var)3–9; therefore, disruption of HP1a from the chromocenter might lead to the observed changes in H3K9me3.

Reduction in H3K9me3 signal and HP1a from the chromocenter partially explains the loss of global chromatin structure observed in the polytene chromosomes. Our group has demonstrated that dADD1 also interacts

physically with the ATPase dXNP; this protein does not have a DNA or chromatin binding domain. Consequently, it relies on the interaction with other proteins to reach its targets on the chromatin [41]. dXNP is important for the maintenance of beta heterochromatin and has been shown to interact also with HP1a [42, 43]. dADD1 levels can change HP1a localization, and also affect dXNP binding to chromatin leading to a deregulation of the ATPase activity and loss of chromatin structure, see Fig. 6 [43].

Also, overexpression of either isoform (Additional file 3b) affected dADD1 chromatin binding; therefore, the model of a complex between HP1a, dADD1, dXNP, and a methyltransferase which maintain not only telomeric but pericentric heterochromatin is further supported by our data.

Observations have been made in which overexpressing dXNP in the developing eye and wing causes apoptosis through the JNK pathway [4, 44]. In other studies, overactivation of JAK phosphorylates STAT and STAT92E phosphorylation results in chromatin disruption and loss of HP1a stability [45]. Otherwise, reducing levels of phosphorylated STAT92E or its loss also causes instability in heterochromatin [46]. Both JNK and JAK-STAT are two of the signals that play a primary role during cell fate [47]. This data could be noteworthy for our work because the over-expression of dADD1 proteins could lead to apoptosis via JNK, and it is well-known that STAT abnormal activation by phosphorylation is related to human cancers [48]. Further studies will be needed to clarify this point.

In the literature, there are reports of mutants that phenocopy the chromocenter loss of organization that we observed when we overexpress dADD1. Mutants affecting H3.3 levels or a mutant that substitutes the lysine 9 for an arginine lead to a disorganization of the chromocenter [48, 49].

Vertebrate ATRX is capable of interacting with the histone chaperone DAXX and exchange the H3.3 variant at different heterochromatic regions such as the telomeres and pericentric heterochromatin [25] also, the H3.3 that is deposited helps to maintain the levels H3K9me3 necessary for proper heterochromatin maintenance [25, 50]. In *Drosophila,* the DAXX like protein has been shown to cooperate with ASF1 for the deposition of H3.3 and also with dXNP at certain heterochromatic regions [51]. Thus, it is possible that also dADD1 proteins may be cooperating with this complex to maintain heterochromatin, however to date, there are no studies on histone variant H3.3 in a null *dadd1* background or overexpression condition, but it would be a critical and interest aspect for future research to thoroughly understand the cooperative roles of these proteins.

Heterochromatic foci are needed to maintain a correct chromatin conformation. Proteins that can disrupt these foci may have significant roles as drivers of disease [52, 53]. In our results, we can see that both tested dADD1 isoforms disrupt HP1a foci to different extents; however, the effect is more pronounced when we overexpress the "a" isoform, which has been directly co-precipitated with HP1a. The "b" isoform has additional MADF domains which could in part contribute to other of the observed phenotypes, it is known that in other proteins, the MADF domains recognize repetitive rich sequences which are also present in heterochromatic regions; still, more experiments are required to elucidate the MADF domains function.

It has been demonstrated that human HP1alpha drives phase separation in heterochromatin [54] a feature that is conserved in the *Drosophila* orthologue [54, 55]. Our results place dADD1 proteins as regulators of this HP1a property, probably maintaining a correct local concentration of HP1a oligomers at certain regions such as the telomeres and pericentric heterochromatin. Over and underexpression of dADD1 can disturb the concentration of HP1a and affect phase transition, which could lead to chromatin instability and alterations in gene expression [54, 55].

Our data demonstrate that dADD1 misexpression in the salivary glands affects HP1a, Su (var)3–9, dXNP and dADD1 localization, a set of genes show an important transcriptional effect, whereas other genes remain unaffected. Pericentric genes transcription was similarly affected upon dADD1 overexpression as in the null *dadd1* organisms (Fig. 5) and HP1a binding was also affected in both genetic backgrounds (see Fig. 5k and l) therefore at these pericentromeric genes dADD1 cooperates with HP1a to maintain a correct expression. Transcription from euchromatic genes such as *Sgs8* and *Act5c* was not affected; however the *Hsp70Aa* gene was upregulated in the null and dADD1a overexpression conditions and this effect seems to be independent on the presence of HP1a, this places dADD1 proteins as regulators of this chaperone which has also been observed to be overexpressed in different types of cancers [56]. Another interesting feature of this particular gene is that it has a "poised" Pol II, so it is possible that dADD1 misexpression could also be involved in controlling this "poised" state. It would be important to address if this or other heat-shock proteins which maintain correct homeostasis are also de-regulated in the human cancers in which ATRX is overexpressed.

In *Drosophila* salivary gland cells, gene transcription remains highly regulated despite the loss of HP1a foci and a concomitant loss of chromatin architecture. Chromatin from salivary glands is polytenized; thus, the transcriptional defects may be somehow "buffered" by other gene copies. This buffering effect may not be conserved in other cells and tissues as overexpression of dADD1

using a ubiquitous driver results in organism lethality (Table 1).

Contrary to what we observed with dADD1 overexpression, dXNP overexpression leads to chromatin compaction, evidenced by an increase of dXNP bands in polytene chromosomes, even at the telomeric regions and a decrease in the nucleus area (Fig. 6a and b). Also, it was highly difficult to obtain full spread chromosomes due to the high compaction (Fig. 6c). The dXNP protein lacks a DNA or chromatin binding domain, our group and others have shown that dXNP is able to interact with transcription factors such as DREF or chromatin-binding proteins such as HP1a. dXNP may reach chromatin via DREF or other factors and through the SNF2 domain promotes heterochromatinization, so an excess of dXNP could also affect gene expression or, as has been demonstrated, lead to cell death [45].

In the fly, this is the first study that presents the effect mediated by overexpression of the orthologues of the ADD and SNF2 domain of ATRX. Further investigation will be necessary and exciting to address the impact of dADD1 overexpression in a context in which we could suppress lethality, to evaluate if the cells acquire characteristics or phenotypes associated with cancer features. Also, we believe that further studies to understand why ATRX is overexpressed in the tumor cells is necessary. At present we know that this overexpression is not highly correlated to gene copy number loss or duplication which leads us to think that perhaps de-regulation of proteins that act in the control region of ATRX could be responsible for its overexpression, therefore, it would be interesting to understand the contribution of these factors to the transformed phenotype [57].

Conclusions

The results presented here provide new evidence that dADD1 overexpression disrupts chromatin structure, affecting the localization of chromatin binding proteins such as HP1a, dXNP and H3K9me3 inducing chromosomal instability and organism death. Also, our group recently described dADD1 as a negative regulator of the expression of telomeric retrotransposons; however, in this study, we demonstrate dADD1 proteins are also required for correct heterochromatic and euchromatic gene transcription. Further genetic and biochemical characterization of dADD1 isoforms is necessary to understand their roles in the maintenance of chromatin stability and heterochromatic gene regulation.

Methods

Search on public data bases

Clinical relevance of mutation on ATRX was revised on the NCBI Genomic DATA Commons (GDC, https://portal.gdc.cancer.gov/) [58]. GDC is a general collecting portal that includes all cancer genomics studies data that the users are updating. Transcriptome expression pattern of ATRX on normal and cancer human samples were explored on the Human Protein Atlas (THPA, https://www.proteinatlas.org/, [58, 59] specialized proteome database and the manually curated Catalogue of Somatic Mutation in Cancer (COSMIC, https://cancer.sanger.ac.uk/cosmic, [41] last accessed at 18 February of 2019. Advanced search on COSMIC was filtered using the criteria of "Gene Expression (mRNA)" "over/under-expressed." We downloaded each case, verified the full report and corroborated common samples between the Human Protein Atlas (THPA) and COSMIC databases. We selected the cases that do no report previous history of treatment (to avoid differences in expression due to chemical or irradiation treatments) and that had full available expression data.

Fly stocks and genetic crosses

The wild-type flies used in this study were w^{1118}. Fly stocks were maintained at 25 °C with standard food. All stocks were outcrossed with w^{1118}; *Sp/CyO; TM6B, Tb*^{1}*/MKRS* flies. *UAS-dADD1* (ID 200280 Kyoto stock center) were crossed to GAL4 drivers *Tub-GAL4* (ID 5138), *Act5C-GAL4* (ID 4414), *Sgs3-GAL4* (ID 6870). *His2Av-RFP* (ID BL23651), *UAS-XNP* (ID BL 26645), Xnp^{2} (ID BL 26643) and Xnp^{3} (ID BL 26644) were obtained from the Bloomington Drosophila Stock Center NIH P40OD018537. At least 100 flies were examined for each genotype. The generation of transgenic lines over-expressing of each isoform is explained in [16] Briefly, to generate the transgenic lines to conditionally direct the expression of dADD1 isoforms, the cDNA encoding either the A or B isoforms, was cloned into the pUAST vector carrying four UAS sequences [59]. Plasmid DNAs were sent to the Bestgene Company to obtain the transgenic *UAS-dADD1a* or *UAS-dADD1b* lines. Lines harboring insertions into the third chromosome were saved and balanced. The *dadd1*^{2} null allele was generously provided by Dr. Mitzi Kuroda and has been described in [14].

Immunostaining of polytene chromosomes, salivary glands, and signal quantifications.

Immunostaining of polytene chromosomes was performed as described in [41] with a modification in the spreading procedure with Lacto-acetic acid solution [60]. All controls and tested genotypes were processed at the same time to avoid variations in the immunohistochemistry procedures. Anti-HP1a (C1A9 from DSHB) antibody was used at 1:1000, anti-pandADD1 [15] and Anti-Histone H3K9me3 were used 1:50 (Abcam 8898) and anti-dXNP was used 1:10. Salivary gland immunohistochemistry was performed as described in [61]. Secondary antibodies Alexa fluor 488 or 568 (Invitrogen) were used at 1:300 and 1:100. Images were taken on a confocal laser scanning

microscope (Olympus FV1000) with a 60x and 20x objective at the Laboratorio Nacional de Microscopia Avanzada (LNMA, UNAM). Images were processed using ImageJ. For polytene chromosomes, the intensity of the signal of HP1a or H3K9me3 was measured with ImageJ only by selecting the chromocenter and taking into account only the red or green signal in combination with the DNA signal (in blue) to eliminate the possible background.

Western blot

Third instar wandering larvae were rinsed in ice-cold PBS 1X; 10 pairs of salivary glands were dissected from each analyzed genotype. Samples were boiled in Laemmli buffer, and proteins were separated in an 8% acrylamide/bis-acrylamide denaturing gels. Detection of the proteins was then carried out as previously described [15]. Anti-β-Tubulin (E7 from DSHB) antibody was used at 1:3000, and anti-pandADD1 was used as described before [15].

Real-time RT-PCR assay

RNA was obtained using the Trizol reagent (Invitrogen) from 10 third instar larvae salivary glands. 1 mg of total RNA was converted to cDNA using reverse transcriptase enzyme and oligo-dT (Invitrogen). *Rp49* was used as a control for these experiments. The primers used for *dAdd1, a, b* and *Rp49* transcripts were the same as [15]. Other primer sequences are as follows (5′-3′):

Name	Forward	Reverse
Su (var)3–9	GTGCGCTTCAAGAACGAACT	GCGGCCTTTTGGCAATTACT
Su (var)205	GGGCAAGAAAATCG ACAACCC	GGCCATTATTGTCGGAGGCA
Act5C	GGTTGCAGCTTTAGTGGTCG	GGCACAGTATGGGAGACA CC
Sgs8	TGCTCGTTGTCGCCGTC	GCCGCTCAAGACCCTCCATA
Psi	TCCAGGGAAAGAACGACGAA	CGCTCCAGATTGCTGGTTGA
Kraken	CGGAACTTTCGCCAGAGACAA	CTATCCGGCGAATCAGGCAT
Toy	CGTTGCGGAACGAACATCAT	CATCGTTGCAATCGGTTGTG
Lgs	GTACCACAACAGCAAACCCC	TGGGCTTGGTCGCCTACTTT
Cin	ACACGGTACAAAAGACCGCC	TCCACTTGCACTACGCAATCT
CG7742	ATGGCCAAGTGGAACGAACT	AATCCTCTGGCACTGAACCG
Ank	TTTCGTTCTTACGTGCTGCTC	TGTGCAAAGGGGTGAATCCT
Cta	ACGCGGCTTTGAGGAGTAC	GACTAGCTACCACAATATCC
Lt	TTTGAGGAGGCAATGGAACTT	CAGCCAGGCCGTCA TAAAGA

Real-time PCR was performed as in [16]. Reactions were set up in duplicates, and the LightCycler Fast Start DNA Master SYBR Green 1 was used (Roche). Real-time quantitative PCR was performed by using a LightCycler 1.5 Instrument by Roche. PCR conditions were 95 °C for 10 min, followed by 40 cycles at 95 °C for 10s, alignment temperature for 10s, and 72 °C for 18 s. The alignment temperature was 65–60 °C. The threshold cycle (Ct) was used for assessing relative levels of respect to the housekeeping gene *Rp49*. The relative levels on mutant genotypes were compared to the corresponding levels on the wild-type strain to obtain the fold difference using the formula 2-ΔΔCT = [(CT gene of interest − CT internal control) sample A − (CT gene of interest − CT internal control) sample B] previously reported for relative transcript quantification [62]. Quantification of transcript abundance was measured with technical duplicates and three independent biological replicates were analyzed.

Chromatin immunoprecipitation, qPCR, and data analyses

Chromatin immunoprecipitation from salivary glands was performed as [16] using Het-A primers. Data were expressed as % Input = 100*log2(dCt normalized ChIP), where dCt normalized ChIP = Ct sample – [Ct input*Input dilution factor)]. Two independent biological experiments were performed each with three technical replicates.

Statistical analysis

All the graphs and statistical analyses were performed with GraphPad Prism 6. Data assuming normality and homogeneity of variance were analyzed with one-way ANOVA. Non-parametric data were evaluated with one-way ANOVA on ranks. Statistical significance was set at ($p < 0.05$*, < 0.01 **, < 0.001***, < 0.0001****). For data on the amount of DNA and Area of HP1a signal between two populations, an Unpaired t-test was performed. Kruskal-Wallis test was used to analyze data from HP1a distribution in salivary glands.

Data analysis

Previously reported ChIP-seq data for S2 cells were obtained from Gene Expression Omnibus (GEO) database. GSM1363103, GSM1363104, GSM136105 and GSM136106 raw data from dADD1 (CG8290) [14]. Sequences were mapped to the dm6 reference genome using bowtie2 v 2.3.4.1 [63]. PCR duplicates were removed with samtools v1.7–2 [64]. Peak calling was conducted utilizing MACS v2.1.1.1 [65], requiring peaks to have a P-value of 1e-10. All genomics intersections were conducted with bedtools v.2.26 [66], peaks were called with the input control and visualized with the IGV genome browser [67].

Supplementary information

Supplementary information accompanies this paper at https://doi.org/10.1186/s12860-020-00257-2.

Additional file 1. Distribution of cases by cancer type expressed as a percentage with a) ATRX overexpression and b) ATRX underexpression.

Databases last accessed on February 18, 2019. C) Healthy breast sample tissue (Patient id: 3544) from a 45 years old female patient showing ATRX immunohistochemistry, d) Breast duct carcinoma sample (Patient id: 1874) from an 80-year-old patient. e) Breast duct carcinoma sample (Patient id: 4193) from a 43-year-old patient with a high signal of ATRX. f) Lobular carcinoma sample (Patient id: 4789) from a 49-year-old patient with a high signal of ATRX. g) Healthy Lung sample tissue (Patient id: 1678) from a 57-years-old female patient showing ATRX immunohistochemistry, h) Adenocarcinoma from female 51 years old (Patient id: 2041) showing low signal of ATRX, i) Squamous cell carcinoma from Male, 64 years old (Patient id:4090), j) Squamous cell carcinoma from Male, 72 years old (Patient id:4896) with high signal of ATRX. The immunohistochemistry was performed with the same antibody sc-15,408 from Santa Cruz Biotechnology. Image credit: Human Protein Atlas.

Additional file 2 The amount of DNA and chromatin does not change during dADD1 overexpression. a) DNA quantification in salivary glands over-expressing all the isoforms. An unpaired t-test was performed to determine significance. No significant differences were found. b) H2Av-RFP visualization of salivary glands with an H2Av-RFP transgenic line (red signal) the amount of chromatin between wild-type and over-expression of dADD1 does not change H2Av-RFP signal intensity. c) Transcript analyzes by RT-PCR lane 1) *Sgs3-GAL4*, lane 2) UAS-*dADD1a,* lane 3) UAS-*dADD1b,* lane 4) *Sgs3*-GAL4/UAS-*dADD1a* and lane 5) *Sgs3*-GAL4/UAS-*dADD1b. rp49* transcript was used as a control. Parameters of area (d) and intensity (e) of wild-type and overexpression conditions were quantified. Ordinary one-way ANOVA was performed to determine significance. No significant differences were found. For each genotype we counted the number of nuclei wt $n = 303$, *UAS-dADD1; Sgs3-GAL4* $n = 307$, *Sgs3*-GAL4/UAS-*dADD1a*, $n = 296$, *Sgs3*-GAL4/UAS-*dADD1b* $n = 219$. The quantification was made with ImageJ.

Additional file 3 Overexpression of all dADD1 isoforms disturbs H3K9me3 and dADD1 signal. a) Immunostaining of polytene chromosomes from wild-type, and over-expressing dADD1 a and b proteins., DNA (grey signal), HP1a (red signal), H3K9me3 (green) and Merge scale bar 20 μm. b) Immunostaining of polytene chromosomes from wild-type and over-expressing dADD1 proteins. Genotype: *Sgs3*-GAL4/UAS-*dADD1a* and *Sgs3*-GAL4/UAS-*dADD1b,* DNA (grey signal), pan-dAdd1 (green), HP1a (red signal) and Merge scale bar 20 μm.

Additional file 4 Schematic representation of *Drosophila* polytene chromosomes and the location of the transcripts analyzed in Fig. 5. The numbers below each chromosome correspond to cytological map locations. Genes targeted by HP1a are shown in red, genes targeted by Su (var)3–9 are shown in green and in yellow, the genes that are regulated by both proteins. Euchromatic genes are represented with blue lines. A black circle represents the chromocenter.

Additional file 5 Localization of dADD1a protein in the analyzed genes. dADD1a (pink peaks) is located principally at the promoter, and through the gene bodies in all the pericentric genes (*cta and lt*). Also, at *Ank* controlled by HP1a/Su (var)3–9. dADD1a is not present in euchromatic genes such as *Sgs8*, *Actin* and *Hsp70Aa* neither in *Su (var)205* and *Su (var)3–9* nor in genes controlled by Su (var)3–9 such as *Psi* and *kraken* or HPla exclusively controlled genes as *toy* or *lgs*.

Additional file 6 Raw data.

Abbreviations

ADD: A zinc finger domain named after three proteins: ATRX, DNMT3 and DNMT3L; ASF1: Anti-Silencing function 1 protein; ATRX: Alpha-thalassemia and Mental Retardation X-related; dADD1: Drosophila ADD containing domain protein 1; dXNP: Drosophila X-linked Nuclear Protein; H3K4: Lysine 4 of Histone H3; H3K9me3: Trimethylation of lysine 9 of histone H3; HP1a: Heterochromatin Protein 1 variant a; JAK: Janus Kinase; JNK: c-Jun N terminal Kinase; Pol II: RNA Polymerase II; RAD54: DNA repair and recombination protein 54; STAT92E: Signal Transducer and Activator Transcription and 92E band

Acknowledgments

We thank Carlos Castelán Angel for support in bioinformatic analysis. Carmen Muñoz for media preparation. Arturo Pimentel, Andrés Saralegui and Dr. Chris Wood from the LMNA for advice on the use of the microscopes.

Authors' contributions

VV-G performed leading research, VV-G conceived and designed the experiments, SM-N conceived, designed and conducted experiments, AT performed data mining and bio-informatic analyses, VV-G, SM-N, AT and MZ analyzed data, VV-G and MZ obtained funding, VV-G wrote the manuscript with input from all the authors. All authors read and approved the manuscript.

Funding

This study was supported by Consejo Nacional de Ciencia y Tecnología (177393 and A1-S-8239 to VV-G; 219673 and 250588 to MZ) and Programa de Apoyo a Proyectos de Investigación e Innovación Tecnológica (204915 and 200118 to VV-G). SM-N received a scholarship from the Consejo Nacional de Ciencia y Tecnología (354993).

Availability of data and materials

All data generated during this study is included in this published article. The data sets analyzed during the current study are available at the public databases mentioned in the Methods section of this article.
Raw figures have been added as an Additional file 6.

Ethics approval and consent to participate

This article does not contain any studies with humans or animals performed by any of the authors.

Consent for publication

Not applicable.

Competing interests

The authors declare that they have no competing interests.

Received: 31 May 2019 Accepted: 4 March 2020
Published online: 23 March 2020

References

1. Stayton C, et al. Cloning and characterization of a new human Xq13 gene, encoding a putative helicase. Hum Mol Genet. 1994;3:1957–202197d0a00c-cd1e-70b9-d02b-07dfd7fb2b35.
2. Gibbons RJ, Picketts DJ, Villard L, Higgs DR. Mutations in a putative global transcriptional regulator cause X-linked mental retardation with α-thalassemia (ATR-X syndrome). Cell. 1995;80(6):837–45.
3. Picketts DJ, Tastan AO, Higgs DR, Gibbons RJ. Comparison of the human and murine ATRX gene identifies highly conserved, functionally important domains. Mamm Genome. 1998;9(5):400–3.
4. Lee NG, Hong YK, Yu SY, Han SY, Geum D, Cho KS. dXNP, a Drosophila homolog of XNP/ATRX, induces apoptosis via Jun-N-terminal kinase activation. FEBS Lett. 2007;581(14):2625–32.
5. Argentaro A, et al. Structural consequences of disease-causing mutations in the ATRX-DNMT3-DNMT3L (ADD) domain of the chromatin-associated protein ATRX. Proc Natl Acad Sci. 2007;104(29):11939–44.
6. Eustermann S, et al. Combinatorial readout of histone H3 modifications specifies localization of ATRX to heterochromatin. Nat Struct Mol Biol. 2011;18(7):777–82.
7. McDowell TL, et al. Localization of a putative transcriptional regulator (ATRX) at pericentromeric heterochromatin and the short arms of acrocentric chromosomes. Proc Natl Acad Sci. 1999;96(24):13983–8.
8. Lu H-C, et al. Aberrant ATRX protein expression is associated with poor overall survival in NF1-MPNST. Oncotarget. 2018;9(33):23018–28.
9. Jiao Y, et al. DAXX/ATRX, MEN1, and mTOR Pathway Genes Are Frequently Altered in Pancreatic Neuroendocrine Tumors. *Science*. 2011;331(6021):1199 LP–1203.
10. Heaphy CM, et al. Altered telomeres in tumors with ATRX and DAXX mutations. Science. 2011;333(6041):425.
11. Molenaar JJ, et al. Sequencing of neuroblastoma identifies chromothripsis and defects in neuritogenesis genes. Nature. 2012;483:589.
12. Clynes D, et al. Suppression of the alternative lengthening of telomere pathway by the chromatin remodelling factor ATRX. Nat Commun. 2015;6:7538.
13. Berubé NG, Jagla M, Smeenk C, De Repentigny Y, Kothary R, Picketts DJ. Neurodevelopmental defects resulting from ATRX overexpression in transgenic mice. Hum Mol Genet. 2002;11(3):253–61.
14. Alekseyenko AA, Gorchakov AA, Zee BM, Fuchs SM, Kharchenko PV, Kuroda MI. Heterochromatin-associated interactions of Drosophila HP1a with dADD1, HIPP1, and repetitive RNAs. Genes Dev. 2014;28(13):1445–60.

15. López-Falcón B, et al. Characterization of the Drosophila group ortholog to the amino-terminus of the alpha-thalassemia and mental retardation X-linked (ATRX) vertebrate protein. PLoS One. 2014;9(12):1–25.
16. Chavez J, et al. dAdd1 and dXNP prevent genome instability by maintaining HP1a localization at Drosophila telomeres. Chromosoma. 2017;126(6):697–712.
17. Lee EYHP, Muller WJ. Gout Breast Cancer: Oncogenes and tumor suppressor genes. Cold Spring Harb Perspect Biol. 2010;2(10):a003236.
18. Danussi C, et al. Atrx inactivation drives disease-defining phenotypes in glioma cells of origin through global epigenomic remodeling. Nat Commun. 2018;9(1):1–15.
19. Hampton TA, et al. SEREX analysis for tumor antigen identification in a mouse model of adenocarcinoma. Cancer Gene Ther. 2000;7(3):446–55.
20. Mukherjee J, et al. Mutant IDH1 cooperates with ATRX loss to drive the alternative lengthening of telomere phenotype in glioma. Cancer Res. 2018;78(11):2966–77.
21. Singhi AD, et al. Alternative lengthening of telomeres and loss of DAXX/ATRX expression predicts metastatic disease and poor survival in patients with pancreatic neuroendocrine tumors. Clin Cancer Res. 2017;23(2):600–9.
22. Campbell PJ, Forbes Simon A, Beare D, Boutselakis H, Bamford S, Bindal N, Tate J, Cole CG, Ward S, Dawson E, Ponting L, Stefancsik R, Harsha B, Kok CY, Jia M, Jubb H, Sondka Z, Thompso S. COSMIC: somatic cancer genetics at high-resolution. Nucleic Acids Res. 2016;45(D1):D777–83.
23. Uhlén M, et al. Tissue-based map of the human proteome. *Science*. 2015; 347(6220):1260419.
24. Lewis PW, Elsaesser SJ, Noh K-M, Stadler SC, Allis CD. Daxx is an H3.3-specific histone chaperone and cooperates with ATRX in replication-independent chromatin assembly at telomeres. Proc Natl Acad Sci. 2010; 107(32):14075–80.
25. Voon HPJ, et al. ATRX plays a key role in maintaining silencing at interstitial heterochromatic loci and imprinted genes. Cell Rep. 2015;11(3):405–18.
26. Eissenberg JC, Elgin SC. The {HP1} protein family: getting a grip on chromation. Curr Opin Genet Dev. 2000;10:204.
27. Swenson JM, Colmenares SU, Strom AR, Costes SV, Karpen GH. The composition and organization of Drosophila heterochromatin are heterogeneous and dynamic. *Elife*. 2016;5:1–37.
28. Schotta G, et al. Central role of Drosophila SU (VAR)3-9 in histone H3-K9 methylation and heterochromatic gene silencing. EMBO J. 2002;21(5):1121–31.
29. Rudolph T, et al. Heterochromatin Formation in Drosophila Is Initiated through Active Removal of H3K4, vol. 2; 2007. p. 103–15.
30. Wood JG, et al. Chromatin remodeling in the aging genome of Drosophila. Aging Cell. 2010;9(6):971–8.
31. Cryderman DE, Vitalini MW, Wallrath LL. Heterochromatin protein 1a is required for an open chromatin structure. Transcription. 2011;2(2):95–9.
32. Greil F, et al. Distinct HP1 and Su (var)3-9 complexes bind to sets of developmentally coexpressed genes depending on chromosomal location. Genes Dev. 2003;17(22):2825–38.
33. Fanti L, Berloco M, Piacentini L, Pimpinelli S. Chromosomal distribution of heterochromatin protein 1 (HP1) in Drosophila: a cytological map of euchromatic HP1 binding sites. Genetica. 2003;117(2–3):135–47.
34. Lu BY, Emtage PC, Duyf BJ, Hilliker AJ, Eissenberg JC. Heterochromatin protein 1 is required for the normal expression of two heterochromatin genes in Drosophila. Genetics. 2000;155(2):699–708.
35. Penke TJR, McKay DJ, Strahl BD, Gregory Matera A, Duronio RJ. Direct interrogation of the role of H3K9 in metazoan heterochromatin function. Genes Dev. 2016;30(16):1866–80.
36. Hallson G, et al. The Drosophila cohesin subunit Rad21 is a trithorax group (trxG) protein. Proc Natl Acad Sci. 2008;105(34):12405–10.
37. Eissenberg JC, James TC, Foster-Hartnett DM, Hartnett T, Ngan V, Elgin SC. Mutation in a heterochromatin-specific chromosomal protein is associated with suppression of position-effect variegation in Drosophila melanogaster. Proc Natl Acad Sci U S A. 1990;87(24):9923–7.
38. Eissenberg JC, Elgin SCR. HP1a: a structural chromosomal protein regulating transcription. Trends Genet. 2014;30(3):103–10.
39. Schwartzentruber J, et al. Driver mutations in histone H3.3 and chromatin remodelling genes in paediatric glioblastoma. Nature. 2012; 482(7384):226–31.
40. Brower-Toland B, Riddle NC, Jiang H, Huisinga KL, Elgin SCR. Multiple SET methyltransferases are required to maintain normal heterochromatin domains in the genome of Drosophila melanogaster. Genetics. 2009;181(4): 1303–19.
41. Valadez-Graham V, et al. XNP/dATRX interacts with DREF in the chromatin to regulate gene expression. Nucleic Acids Res. 2012;40(4):1460–74.
42. Bassett AR, Cooper SE, Ragab A, Travers AA. The Chromatin Remodelling Factor dATRX Is Involved in Heterochromatin Formation, vol. 3; 2008. p. 5.
43. Emelyanov AV, Konev AY, Vershilova E, Fyodorov DV. Protein complex of Drosophila ATRX/XNP and HP1a is required for the formation of pericentric beta-heterochromatin in vivo. J Biol Chem. 2010;285(20):15027–37.
44. Hong YK, et al. dXNP/DATRX increases apoptosis via the JNK and dFOXO pathway in Drosophila neurons. Biochem Biophys Res Commun. 2009; 384(2):160–6.
45. Xu N, Emelyanov AV, Fyodorov DV, Skoultchi AI. Drosophila linker histone H1 coordinates STAT-dependent organization of heterochromatin and suppresses tumorigenesis caused by hyperactive JAK-STAT signaling; 2014. p. 1–13.
46. Shi S, et al. Drosophila STAT is required for directly maintaining HP1 localization and heterochromatin stability. Nat Cell Biol. 2008;10(4):489–96.
47. Ahmed-de-Prado S, Diaz-Garcia S, Baonza A. JNK and JAK/STAT signalling are required for inducing loss of cell fate specification during imaginal wing discs regeneration in Drosophila melanogaster. Dev Biol. 2018;441(1):31–41.
48. Pencik J, et al. JAK-STAT signaling in cancer: from cytokines to non-coding genome. Cytokine. 2016;87:26–36.
49. Penke TJR, McKay DJ, Strahl BD, Gregory Matera A, Duronio RJ. Functional redundancy of variant and canonical histone H3 lysine 9 modification in drosophila. Genetics. 2018;208(1):229–44.
50. Udugama M, et al. Histone variant H3.3 provides the heterochromatic H3 lysine 9 tri-methylation mark at telomeres. Nucleic Acids Res. 2015;43(21): 10227–37.
51. A. H. Fromental-Ramain C., Philippe Ramain. The Drosophila DAXX-like protein (DLP) cooperates with ASF1 for H3.3 deposition and heterochromatin formation. Mol Cell Biol. 2017;37(12):1–18.
52. Zhang R, et al. Formation of macroH2A-containing senescence-associated heterochromatin foci and senescence driven by ASF1a and HIRA. Dev Cell. 2005;8(1):19–30.
53. Zhu Q, et al. BRCA1 tumour suppression occurs via heterochromatin-mediated silencing. Nature. 2011;477(7363):179–84.
54. Larson AG, et al. Liquid droplet formation by HP1α suggests a role for phase separation in heterochromatin. Nature. 2017;547(7662):236–40.
55. Strom AR, Emelyanov AV, Mir M, Fyodorov DV, Darzacq X, Karpen GH. Phase separation drives heterochromatin domain formation. Nature. 2017; 547(7662):241–5.
56. Elmallah MIY, Cordonnier M, Vautrot V. Membrane-anchored heat-shock protein 70 (Hsp70) in cancer. Cancer Lett. 2020;469:134–41.
57. Tang P, Frankenberg S, Argentaro A, Graves JM, Familari M. Comparative analysis of the ATRX promoter and 5′ regulatory region reveals conserved regulatory elements which are linked to roles in neurodevelopment, alpha-globin regulation and testicular function. BMC Res. Notes. 2011;4(1):200.
58. Grossman RL, et al. Toward a shared vision for Cancer genomic data. N Engl J Med. 2016;375(12):1109–12.
59. Brand AH, Perrimon N. Targeted gene expression as a means of altering cell fates and generating dominant phenotypes. Development. 1993;118(2):401–15.
60. Johansen KM, et al. Polytene chromosome squash methods for studying transcription and epigenetic chromatin modification in Drosophila using antibodies. Methods. 2009;48(4):387–97.
61. Reynaud E, Lomeli H, Vazquez M, Zurita M. The Drosophila melanogaster homologue of the Xeroderma Pigmentosum D gene product is located in Euchromatic regions and has a dynamic response to UV light-induced lesions in Polytene chromosomes. Mol Biol Cell. 1999;10(4):1191–203.
62. Schmittgen TD, Livak KJ. Analyzing real-time PCR data by the comparative CT method. Nat Protoc. 2008;3(6):1101–8.
63. Langmead B, Salzberg SL. Fast gapped-read alignment with bowtie 2. Nat Methods. 2012;9(4):357–9.
64. Li H, et al. The sequence alignment/map format and SAMtools. Bioinformatics. 2009;25(16):2078–9.
65. Zhang Y, et al. Model-based analysis of ChIP-Seq (MACS). Genome Biol. 2008;9(9):R137.
66. Quinlan AR, Hall IM. BEDTools: a flexible suite of utilities for comparing genomic features. Bioinformatics. 2010;26(6):841–2.
67. Robinson JT, et al. Integrative genomics viewer. Nat Biotechnol. 2011;29(1): 24–6.

Publisher's Note

Funding sources: None.

Disclosure: Dr Anne Marano is a principal investigator for a study for Viela Bio, a phase I trial of VIB7734 in patients with systemic lupus erythematosus, cutaneous lupus erythematosus, Sjögren syndrome, systemic sclerosis, polymyositis, and dermatomyositis. MS Petty and Dr Cardones have no conflicts of interest to declare.

IRB approval status: Reviewed and approved by the Duke University IRB (approval 00084622).

Reprints not available from the authors.

Correspondence to: Anne L. Marano, MD, 234 Crooked Creek Parkway, Ste 300, Durham, NC 27713

E-mail: Anne.marano@duke.edu

REFERENCES

1. Hejazi EZ, Werth VP. Cutaneous lupus erythematosus: an update on pathogenesis, diagnosis and treatment. *Am J Clin Dermatol*. 2016;17:135-146.
2. Guicciardi F, Atzori L, Marzano AV, et al. Are there distinct clinical and pathological features distinguishing idiopathic from drug-induced subacute cutaneous lupus erythematosus? A European retrospective multicenter study. *J Am Acad Dermatol*. 2019;81:403-411.
3. Laurinaviciene R, Sandholdt LH, Bygum A. Drug-induced cutaneous lupus erythematosus: 88 new cases. *Eur J Dermatol*. 2017;27:28-33.
4. Marzano AV, Lazzari R, Polloni I, Crosti C, Fabbri P, Cugno M. Drug-induced subacute cutaneous lupus erythematosus: evidence for differences from its idiopathic counterpart. *Br J Dermatol*. 2011;165:335-341.
5. Drenkard C, Parker S, Aspey LD, et al. Racial disparities in the incidence of primary chronic cutaneous lupus erythematosus in the southeastern US: the Georgia Lupus Registry. *Arthritis Care Res (Hoboken)*. 2019;71:95-103.

https://doi.org/10.1016/j.jaad.2020.03.002

A cross-sectional report on melasma among Hispanic patients: Evaluating the role of oral tranexamic acid versus oral tranexamic acid plus hydroquinone

To the Editor: Oral tranexamic acid (TA) has been described as a game changer as a solo agent in the treatment for refractory moderate to severe melasma.[1] Its therapeutic mechanism has been postulated to address the vascular component in melasma. However, optimal dose, duration, and studies on depigmenting creams are limited.[2] A retrospective treatment outcome analysis, at a single center over a 1-year period (June 2018 to June 2019), of patients with melasma receiving oral TA 650 mg daily ± hydroquinone (HQ) 4% cream was performed. This report describes the main clinical characteristics and impact on patients' quality of life (QOL). The primary outcome was the modified Melasma Area and Severity Index (mMASI) score, and impact on QOL was assessed using the Spanish Melasma on Quality of Life questionnaire (Sp-MELASQOL). Patients were evaluated to exclude the risk of thrombosis. The mMASI was calculated by 2 dermatologists blinded to treatment groups. Pearson correlation, paired *t* test, and unpaired *t*-test with Welch's correction were used. A *P* value of less than .05 was considered statistically significant.

Fifty-three patients' charts with sufficient documentation on progress and the degree of improvement at weeks 8 and 20 were included. The main background clinical characteristics are summarized in Table I. Twenty-seven patients (50.94%) received oral TA 650 mg daily (mean baseline mMASI score, 8.25), and 26 (49.05%) received oral TA 650 mg daily plus HQ 4% cream (mean baseline mMASI score, 8.20). At week 20 of treatment, there was a 46% reduction in mMASI score in the TA group versus 61% in the TA plus HQ 4% cream group; this difference was significant ($P = .048$). Mild adverse effects to TA were reported in 7 patients. Notably, there was a 49% reduction in the Sp-MELASQOL score in the combined group compared with 29% with oral TA alone. The overall clinical response rate observed aligns with that reported in previous studies. Zhu et al,[3] in a randomized study, reported no significant differences in the MASI and melanin index among 500; 750; 1,000; or 1,500 mg oral TA. Del Rosario et al,[2] in a randomized study of 39 patients taking 250 mg TA twice daily, reported a 49% reduction in mMASI score compared with 18% in the control placebo group. To our knowledge, this is the first treatment outcome analysis among Hispanic patients. Our data indicated that combined therapy appears superior to oral TA alone. Padhi and Pradhan reported a more significant improvement in MASI score with oral TA 250 mg twice daily in conjunction with a triple combination depigmented cream compared with the triple combination alone,[4] and Karn et al,[5] in a prospective randomized controlled trial, found a significantly higher clinical improvement with oral TA 250 mg twice daily combined with topical HQ versus topical HQ alone. Our data support the use of oral TA plus HQ 4% as a combined therapy for moderate to severe melasma with better clinical and QOL results.

Ileana E. Arreola Jauregui, MD,[a] Gabriel Huerta Rivera, MD,[a] Manuel Soria Orozco, MD,[b] Silvia

Table I. Background clinical parameters and treatment outcomes (N = 53)

Characteristics	Value
Sex, n (%)	
Male	2 (3.77)
Female	51 (96.22)
Skin phototype	
II	2 (3.77)
III	22 (41.50)
IV	24 (45.28)
V	5 (9.43)
Age at onset, y	
Mean ± SD	33.5 ± 8.2
Minimum, maximum	17, 50
Years of melasma before starting oral TA	
Mean ± SD	11.03 ± 8.4
Minimum, maximum	1, 36
Clinical parameters	
Main affection, n (%)	
Centrofacial	28 (52.83)
Malar	19 (35.84)
Mandibular	6 (11.32)
Melasma Severity Score, n (%)	
Mild (mMASI of 2.7-4.9)	5 (9.43)
Moderate (mMASI of 5-7.2)	20 (37.73)
Severe (mMASI of 7.3 or more)	28 (52.83)

Treatment outcomes	mMASI	Sp-MELASQOL
Group: 650 mg TA daily		
Baseline	8.25	36.88
Week 8	6.51	—
Week 20	4.4	26.2
Group: 650 mg TA + HQ 4% daily		
Baseline	8.20	32.80
Week 8	5.57	—
Week 20	3.12	16.69
Adverse effects to TA (n = 7), n		
Breast pain	4	
Abdominal pain/inflammation	1	
Arthralgias	1	
Hypo-oligomenorrhea	1	

HQ, Hydroquinone; *mMASI*, Modified Melasma Area and Severity Index; *Sp-MELASQOL*, Spanish-language Melasma Quality of life; *TA*, tranexamic acid.

Meyer-Nava, MSc,[c] Juan E. Paniagua Santos, MD,[a] Juan B. López Zaldo, MD,[a] Ilse Meyer-Nava, MD,[a] Clara Madrid Carrillo, MD,[a] Iara E. Zaldo Rolón, MD,[a] Aline E. Baeza Echeverría, MD,[a] and Minerva Vázquez Huerta, MD[a]

From the Derma Center Aesthetic Clinic Laser, Guadalajara, Mexico[a]; Department of Dermatology, Civil Hospital of Guadalajara, Mexico[b]; and Biotechnology Institute National Autonomous University of Mexico, Morelos Campus, Cuernavaca.[c]

Funding sources: None.

Conflicts of interest: None disclosed.

IRB approval status: Not applicable.

Reprints not available from the authors.

Correspondence to: Manuel Soria Orozco, MD, Department of Dermatology, Civil Hospital of Guadalajara, Av Hospital 278, Sector Hidalgo, CP 44280, Guadalajara, Jalisco Mexico

E-mail: manuelspitz@hotmail.com

REFERENCES

1. Lee HC, Thng TG, Goh CL. Oral tranexamic acid (TA) in the treatment of melasma: a retrospective analysis. *J Am Acad Dermatol*. 2016;75(2):385-392.
2. Del Rosario E, Florez-Pollack S, Zapata L Jr, et al. Randomized, placebo-controlled, double-blind study of oral tranexamic acid in the treatment of moderate-to-severe melasma. *J Am Acad Dermatol*. 2018;78(2):363-369.
3. Zhu CY, Li Y, Sun QN, et al. Analysis of the effect of different doses of oral tranexamic acid on melasma: a multicentre prospective study. *Eur J Dermatol*. 2019;29(1):55-58.
4. Padhi T, Pradhan S. Oral tranexamic acid with fluocinolone-based triple combination cream versus fluocinolone-based triple combination cream alone in melasma: an open labeled randomized comparative trial. *Indian J Dermatol*. 2015;60(5):520.
5. Karn D, Kc S, Amatya A, et al. Oral tranexamic acid for the treatment of melasma. *Kathmandu Univ Med J (KUMJ)*. 2012;10(40):40-43.

https://doi.org/10.1016/j.jaad.2020.02.072

Characterizing index keratinocytic carcinomas in commercially insured adults younger than age 50 years in the United States

To the Editor: More than 3 million people are affected by keratinocyte carcinomas (KCs) in the United States, an often-cited estimate from Medicare claims and population survey data for patients 65 years old and older.[1] However, less is known about KCs in younger populations. In this retrospective cohort study, we used health administrative claims data to characterize index KC in commercially insured adults aged 18 to 50 years.

We interrogated the IBM MarketScan Commercial Database, a claims database containing 20 to 40 million US employees (2011-2017), using a previously validated algorithm[2] pairing International Classification of Diseases diagnosis codes with Current Procedural Terminology procedural codes to identify index KC. Enrollees (aged 18-50 inclusive) with 12-months continuous enrollment prior to their index service date were captured. Enrollees with any prior malignancy history of the lip or skin;

cells

MDPI

Review

Insights into HP1a-Chromatin Interactions

Silvia Meyer-Nava, Victor E. Nieto-Caballero, Mario Zurita and Viviana Valadez-Graham *

Instituto de Biotecnología, Departamento de Genética del Desarrollo y Fisiología Molecular, Universidad Nacional Autónoma de México, Cuernavaca Morelos 62210, Mexico; smeyer@ibt.unam.mx (S.M.-N.); vnieto@lcg.unam.mx (V.E.N.-C.); marioz@ibt.unam.mx (M.Z.)

* Correspondence: vvaladez@ibt.unam.mx; Tel.: +527773291631

Received: 26 June 2020; Accepted: 21 July 2020; Published: 9 August 2020

Abstract: Understanding the packaging of DNA into chromatin has become a crucial aspect in the study of gene regulatory mechanisms. Heterochromatin establishment and maintenance dynamics have emerged as some of the main features involved in genome stability, cellular development, and diseases. The most extensively studied heterochromatin protein is HP1a. This protein has two main domains, namely the chromoshadow and the chromodomain, separated by a hinge region. Over the years, several works have taken on the task of identifying HP1a partners using different strategies. In this review, we focus on describing these interactions and the possible complexes and subcomplexes associated with this critical protein. Characterization of these complexes will help us to clearly understand the implications of the interactions of HP1a in heterochromatin maintenance, heterochromatin dynamics, and heterochromatin's direct relationship to gene regulation and chromatin organization.

Keywords: heterochromatin; HP1a; genome stability

1. Introduction

Chromatin is a complex of DNA and associated proteins in which the genetic material is packed in the interior of the nucleus of eukaryotic cells [1]. To organize this highly compact structure, two categories of proteins are needed: histones [2] and accessory proteins, such as chromatin regulators and histone-modifying proteins. Both kinds of proteins participate in maintaining the structure of chromatin and regulating gene expression [3]. The primary unit of chromatin is the nucleosome [4], which is formed by an octamer of histones, with two copies of histones H2A, H2B, H3, and H4 (also called the canonical or core histones) [4]. The histone H1 has been referred to as a "linker" because a single copy is positioned on the DNA between each nucleosome [5]. Deciphering the procedures that control chromatin packaging has become a significant issue in understanding developmental programs and disease states.

There are two primary types of chromatin in the nucleus: heterochromatin and euchromatin [6]. Heterochromatin is abundant in compacted, highly condensed, silenced, and repetitious sequences found near centromeric and telomeric locations. By contrast, euchromatin includes the majority of transcriptionally active genes [7]. Through staining different types of cells, Emil Heitz conceived the term "heterochromatin" more than 90 years ago, observing retention of this more compact structure throughout the cell cycle [8]. These core heterochromatic structures have become an essential area of study because of their role in gene silencing [9].

In all eukaryotes, constitutive heterochromatin is established early in development. During the 1960s, satellite sequences were identified, sequenced, and mapped to pericentromeric and telomeric regions of metaphase chromosomes located at the nuclear periphery of interphase cells [10]. With the development of automatic sequencing over the decades that followed, studies on vertebrates have

determined that the genome is rich in repetitive sequences that, for example, account for more than 50% of the human genome. There are many types of these repetitive elements: some are composed of retrotransposon sequences, others of long and short interspersed elements known as LINEs, SINEs, Alu sequences, in addition to minor and major satellite sequences. These sequences need to be silenced to avoid chromosome instability, and several mechanisms cooperate toward maintaining this silencing. These mechanisms include DNA methylation, histone post-transcriptional modifications, histone deacetylation, binding of chromatin proteins, and non-coding RNA and RNA interference pathways [11–13]. Embryonic stem cells have, in general, less heterochromatin than differentiated cells. This characteristic confers plasticity. As differentiation advances, cells gain heterochromatin. Disruption of any of these heterochromatin maintenance mechanisms leads to chromosome instability and can sometimes lead to diseases such as cancer.

The mechanisms of heterochromatin formation and maintenance have been highly conserved throughout the evolution of eukaryotic cells, and understanding these mechanisms using less complex animal models has helped us to advance understanding in this important field.

Based on cytological criteria, one-third of the *Drosophila melanogaster* genome, including the telomeres, pericentric regions, and chromosome 4, is considered as the heterochromatin [14]. As development and differentiation progress, regions regarded as heterochromatin become more abundant as differentiated cells undergo heterochromatinization to promote gene repression and prevent inappropriate gene expression. One mechanism for achieving this is for cells to anchor chromatin to the nuclear lamina resulting in gene inactivation [15]; alternatively, the heterochromatin/euchromatin borders may be defined [16], for example, by changing the profile of chromatin as differentiation progresses, i.e., as stem cells differentiate into the mature cell type [17].

The primary mechanism used to maintain differential expression patterns is the silencing of genes, which involves packaging them in structures inaccessible to DNA-binding proteins [18]. The silencing of a specific gene or chromosomal region requires covalent modification by enzymes or complexes harboring subunits that recognize these modifications and facilitate their physical association with histones [19] and their extension throughout the chromatin fiber, creating a compacted structure (heterochromatin) which is generally believed to be inaccessible to transcription-promoting factors [20]. Heterochromatinization then becomes one of the primary mechanisms used to silence chromosomal regions.

In 1930, experiments using X-ray treatment of flies have shown that genes that were translocated from euchromatic regions to the vicinity of pericentric heterochromatin, acquired a motley pattern of expression [21]. This effect, which is caused by the repressive properties of heterochromatin, was called position effect variegation (PEV) and has been exploited from the 1980s onward for the systematic examination of factors that regulate heterochromatin formation. One of the proteins identified through this screening is heterochromatin protein 1 (HP1). It is a highly conserved protein [22] that was initially discovered in *Drosophila* by the group of Grigliatti in a study in which the authors found more than 50 loci that acted as suppressors of PEV. The authors identified that the protein encoded by the *Su(var)2-5* locus works as a dosage-dependent modifier of PEV [23]. Since then, various studies have shown that this protein is essential for the establishment and maintenance of heterochromatin.

HP1 proteins are conserved in a variety of organisms, including fission yeast (as Swi6 and Chp2) [24,25] and also vertebrates such as amphibians (e.g., frog (xHP1α and xHP1γ)) [26], birds (e.g., chicken (HP1α, HP1β, and HP1γ)) [27], and mammals (such as mice (HP1α, HP1β, and HP1γ)) [28]. Various functions have been described for each member of the family throughout the life cycle of a cell: heterochromatin formation and maintenance, gene silencing, telomere capping, DNA repair, and control of gene expression [14]. Mutations that affect HP1 protein activities have a significant impact on organism development. For example, in *Drosophila*, null mutants for HP1a are lethal at the embryonic stage [29]. Although the HP1 isoforms are very similar structurally, they have different functions, and null mutants for HP1a cannot be rescued by HP1b or HP1c. Thus, HP1 proteins have been revealed to interact with a wide variety of proteins, forming different complexes [30–32].

In this review, we present a general overview of HP1 proteins, their conserved domains, and their interactions with other proteins. We focus mainly on HP1a to provide a layered view of its interactions as well as their possible impacts on functions and heterochromatin maintenance.

2. Functions of Conserved HP1a Domains

HP1a has two highly conserved domains, the N-terminal chromodomain (CHD) that is located in numerous chromosomal proteins [18] and a C-terminal chromoshadow domain (CSD), which are separated by a hinge region of variable length (Hin). The CHD is found in many chromosomal proteins whose primary function is in the maintenance of chromatin structure and gene regulation [33]. The specificity of the CHD for certain modified histone residues is one of the features that direct the binding of these proteins to specific regions in the chromatin [34,35]. HP1 proteins specifically bind to dimethylated and trimethylated H3K9 (H3K9me2 and H3K9me3) through their CHD. This binding of this histone mark to CHD occurs via the region Gln5 to Ser10. These amino acids form a β-sheet that aligns, antiparallel, with two β-sheets that are formed by the regions Glu23 to Val26 and Asn60 and Asp62 in the chromodomain, thus creating a structure of three β-sheets in the form of a sandwich [36] (Figure 1). The HP1a CHD also interacts with the tail of the linker histone H1.4 that is methylated at lysine 26, resulting in greater compaction of chromatin [37]. HP1 has been considered as a sign of repression because it is mainly found in silenced chromatin. Any null mutations in *Su(var)2-5* (HP1a coding gene) and the replacement of H3K9 with arginine (H3K9R) to block HP1a binding are lethal to the organism [38–40]. In *Drosophila* HP1a, a single amino acid substitution within the CHD (V26M) is present in the $Su(var)2\text{-}5^{02}$ allele; for this allele, heterozygous flies show the suppression of gene silencing by heterochromatin [38]. Furthermore, a significant reduction of HP1a occupancy near the centromeres and a decrease in survival until the third larval stage have been shown in flies that have a null allele of *Su(var)2-5* and are trans-heterozygous for $Su(var)2\text{-}5^{02}$ [41]. In agreement with these results, the crucial role of V26 in forming the hydrophobic pocket of CHD that binds to H3K9me has been demonstrated through crystallographic studies [36]. Thus, the CHD is essential for the whole protein to target this heterochromatin mark, and a simple amino acid substitution can be lethal to the organism.

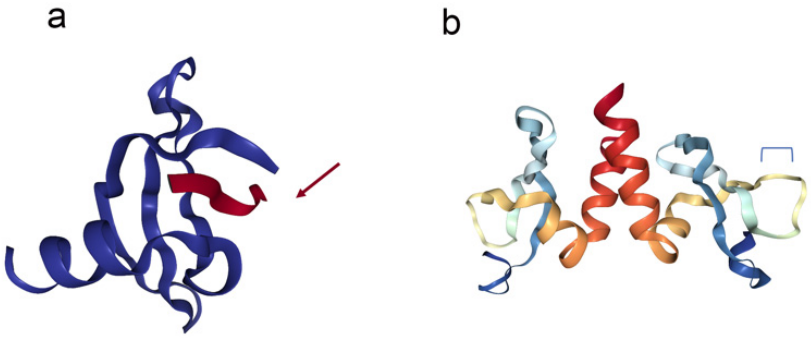

Figure 1. The crystal structure of the CHD (left) and CSD (right) of HP1a. (**a**) The left image is a representation of the chromodomain (blue ribbons) of HP1 complexed with histone H3K9me3 from *Drosophila* (red ribbon mark with red arrow). The CHD (69 aa in length), is made up of three β-sheet antiparallel chains flanked by an α-helix on the C-terminal. The histone tail (16 aa) inserts as a β-strand, completing the β-sandwich architecture of the CHD. (**b**) On the right side is the CSD with the C-terminal region (rainbow ribbons) of HP1a from *Drosophila*. The CSD (87 aa) is a dimeric domain and consists of three antiparallel β-sheet chains flanked by two α-helices. The blue bracket represents the interaction site of the PxVxL peptide. Images were created with the PDB (Protein Data Bank) ID 1KNE [36], 3P7J [42], and NGL Viewer [43].

The second domain shares identity with the amino acid sequence of the CHD and was thus named the chromoshadow domain (CSD) [44]. A function critical for the formation of heterochromatin is

preserved within this domain [45], which facilitates the dimerization of HP1 proteins and also directs interactions with other proteins that carry the conserved pentapeptide motif, PxVxL (x = any amino acid) (Table 1) [46,47]. The structure of the CSD is roughly similar to that of the CHD (three β-sheets packed against two α-helices) [48]. For example, a single amino acid replacement inside the CSD (I161E) prevents the dimerization of mouse HP1β [33]. The absence of dimerization also triggers the loss of contact with nuclear factors carrying PxVxL motifs as well as non-PxVxL partners [49,50]. By contrast, a single amino acid replacement elsewhere in the CSD (W170A) of mouse HP1β does not preclude dimerization but disturbs interactions with PxVxL partner proteins [33]. Consequently, the binding to PxVxL proteins and the conditions for HP1 dimerization can be eliminated independently.

Table 1. Proteins or factors in mammals and *Drosophila* that were revealed as directly bound with the known domains of HP1a/HP1α.

Protein or Cellular Component	Organism	Methodology	References
		CHD	
Methylated H3K9	*Drosophila*	IF, FAITC, NMR	[51]
H2Av	*Drosophila*	IF, tagIP, rPD,	[52]
RpII215	*Drosophila*	IP, WB, rPD	[7,53]
Nuclear envelope	Mouse	IF, BA	[54]
H3	Mouse	IP, FW, rPD	[31,55]
H1	Mouse	rPD, FW	[55]
Methylated H3K9	Mouse	rPD	[56]
Methylated H3K9	Human	rPD, SPRA	[57]
CTIP2	Human	rPD, IP	[58,59]
Methylated H1.4K26	Human	BD, IP, rPD, IF	[31,37]
DNMT1	Human	rPD	[60]
		CSD	
Hip/HP4	*Drosophila*	Y2H, tagIP, rPD, IF, tag-WB	[61,62]
AF10/Alh	*Drosophila*	transPD	[42,63]
Su(var)3-7	*Drosophila*	Y2H, IP, IF, WB	[64,65]
PIWI	*Drosophila*	Y2H, IP, IF, NMR, Y2H	[42,66,67]
Kdm4A	*Drosophila*	transIP, tag-WB, MW, WB, fingerprinting, MS	[68–70]
Ssrp	*Drosophila*	transPD, WB, IP, tandem affinity technology, tagIP, tag-WB	[53,71]
Su(var)3-9	*Drosophila*	transPD, At, ATC, WB, Y2H, IP, tag-WB, tagIP, fingerprinting, IF, MS	[53,68,70,72,73]
Su(var)2-HP2	*Drosophila*	IP, At, Y2H, NMR, FAITC, PP, tagIP, fingerprinting, co-sedimentation, molecular weight, molecular sieving, MS	[42,68,70,74,75]
XNP/dATRX	*Drosophila*	transIP, transPD, MS, IF, WB	[68,76–78]
HP6	*Drosophila*	IP, WB, transPD, tag-WB	[79]
egg	*Drosophila*	transIP, fingerprinting, rPD	[53,68]
G9a	*Drosophila*	IP, WB, rPD	[53]
ova	*Drosophila*	IP, Y2H	[80]
HP1-BP84	Mouse	Y2H	[81]
TIF1α	Mouse	Y2H, rPD	[50,81,82]
CAF-1 p150	Mouse	Y2H, rPD, IF, GFC, NMR	[33,83]
mSNF2β	Mouse	Y2H	[50]
KAP1/TIFβ	Mouse	IP, rPD, IF, SPRA, GFC	[50,55,83]
H4	Mouse	In vitro cross-linking	[31]
MeCP2	Mouse	tagIP	[84]
KAP1/TIFβ	Human	Y2H, IP, rPD, IF, GFC	[83,85]
SP100	Human	Y2H, rPD, transPD, IF	[86]
Polycomb	Human	IP, rPD, IF	[33]
ATRX	Human	Y2H, IF, rPD	[85,87]
CAF-1 p150	Human	rPD	[50]
Ku70	Human	Y2H, IP, rPD	[88]
$TAF_{II}130$	Human	Y2H, exPD, transPD	[89]
Ki-67	Human	Y2H, exPD, IF, ChIP	[90]
BRG1	Human	IP, rPD, TransPD, IF	[91]
SUV39H1	Human	rPD, Y2H	[49]
NIPBL/hScc2	Human	rPD	[85,92]
HP1-BP74	Human	rPD	[85]
LBR (Lamin B receptor)	Human	rPD, Y2H, IP	[85,93]

Table 1. *Cont.*

Protein or Cellular Component	Organism	Methodology	References	
CSD				
Sgo1	Human	Y2H, MS. IP	[92,94]	
POGZ	Human	Y2H, MS	[92]	
BARD1	Human	tragIP, transPD	[95]	
KDM2A	Human	IP, transPD, IF	[96]	
LRIF1	Human	IP, transPD	[97]	
Haspin	Human	tragIP, rPD	[98]	
MacroH2A1.2	Human	IP, transPD	[99]	
Hinge				
HP-BP74 H1-like	Mouse	Y2H, FW, rPD	[55,81]	
MITR, HDAC4/5	Mouse	IP, rPD	[100]	
Combination of Domains				
ORC1-6	*Drosophila*	tagIP	CHD, CSD	[30]
Mcm10	*Drosophila*	proximity ligation assay, IF, IP, WB, transPD, tag-WB, Y2H	CHD, CSD	[101,102]
SuUR	*Drosophila*	Y2H, rPD, transPD, WB, IP, MS, tagIP, fingerprinting	Hin + CSD	[68,93]
Caf1-180	*Drosophila*	transPD, tag-WB, WB, transIP, fingerprinting, IP	Hin + CSD	[68,103]
Cav/HOAP	*Drosophila*	tagIP, IF, IP, exPD	Hin + CSD	[79,104–107]
Parp-2	Mouse	rPD	Hin + CSD	[108]
TIf1β	Mouse	rPD	Hin + CSD	[108]
ARFL5	Human	Y2H, rPD	CHD + CSD	[109]
INCENP	Human	Y2H, tranPD	Hin + CSD	[94,110]

Methodology: BA, binding assays; ChIP, chromatin immunoprecipitation; IP, co-immunoprecipitation using extract; exPD, pull-down assay using extracts; FAITC, fluorescence anisotropy, isothermal titration calorimetry; FW, far-western analysis; IF, immunofluorescence co-localization; rPD, pull-down assay using recombinant proteins; tragIP, immunoprecipitation with in-vitro translated protein; transPD, pull-down assay using in-vitro translated protein; SPRA, surface plasmon resonance analysis; Y2H, yeast two-hybrid assay; WB, western blot; NMR, nuclear magnetic resonance; PP, predetermined participant; tag-WB, western blot assay performed when specific antibodies for the protein of interest are not available; At, autoradiography; fingerprinting, peptide mass fingerprinting; MS, identification by mass spectrometry; BiFC, bimolecular fluorescence complementation.

At first, the hinge region was thought of as being only a linker region [111] because it is the region corresponding to the greatest amino acid variability within HP1 proteins. Moreover, other studies have suggested that its structure is flexible and disorganized [56,57,112,113]. However, the hinge region has been found to contribute to facilitating specific interactions [26,42,47,114,115] and is also highly receptive to subsequent post-translation modifications, especially phosphorylation [112,116,117]. Furthermore, changes within this region were shown to alter the location, interactions, and function of HP1 proteins, thus making it a critical control region in the regulation of HP1 proteins [117–119].

Both the CHD and the CSD have been the focus of extensive structural analyses [33,36,48], which have determined that each domain forms a hydrophobic pocket. Recently, using cryogenic electron microscopy, Machida et al. reported the three-dimensional structure of a complex containing dinucleosomes with H3K9me3 modification and human HP1 isoforms. In these structures, two H3K9me3 nucleosomes are joined by a symmetric HP1 dimer (for example, an α with an α). The linker DNA between the nucleosomes does not interact directly with HP1, thereby allowing the nucleosome to be remodeled by ATP-utilizing chromatin assembly factor (ACF) [120]. This is an important observation because it changes the view of heterochromatin from being stable and rigid regions to regions that can also be highly malleable and where diverse cellular mechanisms, such as DNA repair or transcription, can take place.

Just as the CHD is preserved within the protein, the proteins of the HP1 family have been conserved throughout evolution. Most eukaryotes have three primary genes encoding variants of HP1 proteins with different functions. Humans have three principal isoforms of HP1 (referred to as HP1α, HP1β, and HP1γ) [121]. *Drosophila* also expresses three primary isoforms of HP1, encoded by different genes (HP1a, HP1b, and HP1c), which are ubiquitously expressed in adult fly [122] (Figure 2a). Flies also

have two germline-specific isoforms, HP1d (Rhino) and HP1e. Rhino is expressed in the ovaries and involved in transposon silencing in the germline via piRNA clusters [123]. HP1e is expressed in the testes and is essential for paternal chromosome segregation through embryonic mitosis [122].

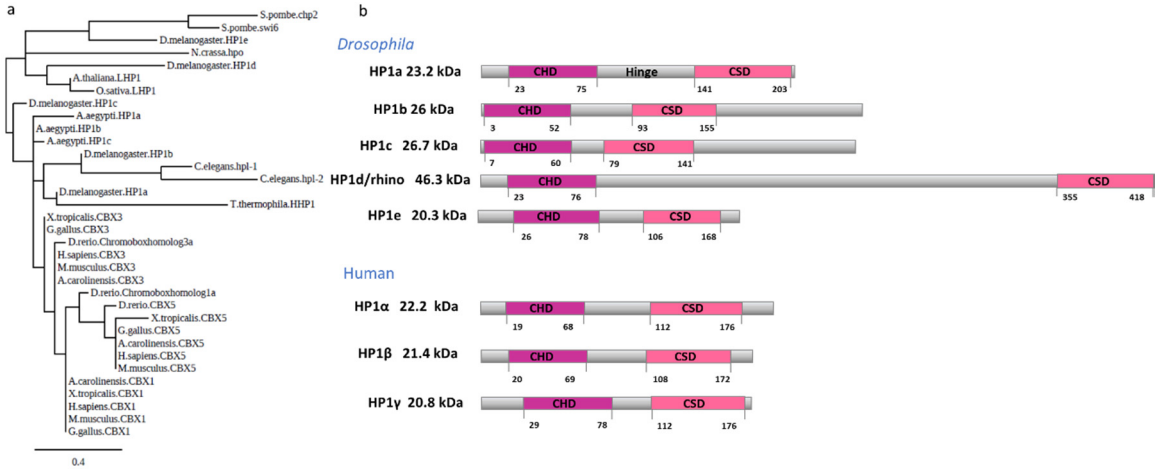

Figure 2. HP1 is preserved during evolution. (**a**) Maximum likelihood phylogenetic analysis of the HP1 protein information of the containing proteins as computed by PhyML. The amino acid sequences were analyzed from the following organisms: *Tetrahymena thermophila*, *Schizosaccharomyces pombe*, *Neurospora crassa*, *Arabidopsis thaliana*, *Oryza sativa*, *Caenorhabditis elegans*, *Aedes aegypti*, *Drosophila melanogaster*, *Xenopus tropicalis*, *Anolis carolinensis*, *Danio rerio*, *Gallus gallus*, *Mus musculus*, and *Homo sapiens*. (**b**) Diagram of HP1 proteins in *Drosophila* and humans. The chromodomain is shown in magenta, and the chromoshadow is in rose. The molecular weight is indicated to the left, with the amino acid localization of the domains displayed below each protein.

Regarding their functions, the paralogs of this family show considerable differences in location. The *Drosophila* HP1a and mammalian HP1α are predominantly localized to heterochromatin [47,55,62,124]. HP1b (both *Drosophila* and mammalian) is present in heterochromatin and euchromatin, whereas HP1c localizes to euchromatin and yields gene-specific contributions to transcriptional regulation [125]. Given these differences in location, it seems that these paralogs can form different complexes or interact at various places in chromatin.

Although HP1 proteins share high similarity with respect to both their amino acid sequences and their comprising domains, they present differences in the disposition of these domains [44], with many such differences observed between *Drosophila* paralogs [126]. For example, the HP1a CHD is located between amino acids 20 and 80, whereas in HP1b and c, the CHD domain is located almost at the beginning of the protein. The hinge region is shorter in HP1b and c compared to HP1a and is the least conserved region among all *Drosophila* homologs [127]. The hinge region connecting the two main domains seems to enable the CHD and CSD to move independently of each other in the native protein [33].

Further, in vitro studies have shown that phosphorylation of the most N-terminal portion of HP1α inhibits DNA binding but promotes phase separation by creating subcompartments where the same protein can be located in chromatin with distinct grades of compaction [128]. This N-terminal part is almost entirely absent in β and γ (see Figure 2b). Lastly, in the C-terminal part after the CSD domain, HP1a has three amino acids. By comparison, HP1b and HP1c each have a C-terminal extension region (CTE) with a length of 85 and 96 amino acids, respectively. Analysis of these CTE sequences did not reveal any similarities either between them or with any reported domains, and further studies of their contribution to the function of these proteins will be of great importance [53].

Although the CHDs of all three HP1 proteins are involved in the recognition and binding of H3K9me2/3, they do not bind with the same affinity. In competition experiments to test the binding affinity to the trimethylation mark, HP1c always presented the lowest affinity; later, it was

confirmed that this mark is not recognized by HP1c in vivo [53]. The overexpression of HP1b causes pericentromeric heterochromatin decompaction accompanied by a reduction in binding of HP1a to H3K9me2, suggesting that the presence of HP1b prevents the function of HP1a in heterochromatin [129]. Moreover, when the N-terminal and hinge regions of HP1α are exchanged into HP1β, chimeric protein droplets are formed [128]. This competition leads to differences in the paralog location, and a gradient is observed in which HP1a or α is found in heterochromatic regions characterized by potent DNA compaction and phase separation activities. This is followed by HP1b or β in areas where there is a change from heterochromatin to euchromatin, whereby the enrichment of HP1b or β works as a bridge, allowing for the recruitment of gene activators which contribute to maintaining open chromatin states. Finally, HP1c or γ are found in euchromatin areas with entirely different partners [71,125,130]. This process requires different interactors, and the different variables may contribute to dissolving the phases [128]. In the following sections, we focus our attention on the described interactions with HP1a to better understand how these interactions regulate heterochromatic domains.

3. HP1a Conserved Domains Direct Specific Protein Interactions

In addition to histone recognition, interactions with non-histone chromosomal proteins might serve as an additional mechanism for association between HP1a and chromatin. In Table 1, we detail the direct HP1 interactors revealed in humans, mice, and flies using different methods, such as yeast two-hybrid and pull-down assays. In some cases, the interactions have been confirmed through other indirect methods, such as IP, WB, and IF. In 2014, Alekseyenko et al. performed BioTAP-labeling of the HP1a protein and described new HP1a-binding proteins in addition to RNAs [68]. To characterize the organization and regulation of heterochromatin, Swenson et al. isolated some previously known HP1a interactors as well as others that were completely new. The authors also showed the distribution and dynamic localization patterns during the cell cycle of some interaction partners [70]. In Table 2, we list the HP1a interactors in *Drosophila melanogaster*—not necessarily direct interactors—for which the exact domain(s) of interaction within HP1a have not been characterized.

Table 2. HP1a interactors in *Drosophila* for which the interaction domains within HP1a have not been identified.

Protein or Cellular Component	Methodology	Reference
Arp6	IF	[131,132]
E(bx)	WB	[133]
Nap1	WB	[133]
Su(var) 3-3	IP, WB, transIP, fingerprinting	[68,134]
POF	IF	[135,136]
Ndc80	transIP, fingerprinting	[137]
HP5	MS, IP, WB,	[68,70,138]
Pep	IP, WB	[7]
moi	transPD, tag-WB	[107]
ACF	transPD	[130]
Dp1	IP, WB,	[7]
vig	IP, WB	[139]
vig2	IP, WB, rPD	[139]
Hmt4-20	IF	[62]
dre4	tandem affinity purification, multidimensional protein identification technology, WB	[71]
ver	transPD, tag-WB	[140]
HP1c	transPD, WB	[53,71]
Atg8a	PA	[138]
CG11474	PA	[138]
Atf-2	IP, WB	[141]
qin	transIP, WB, IP, tag-WB	[142]

Table 2. *Cont.*

Protein or Cellular Component	Methodology	Reference
mu2	transIP, WB, Y2H, IP, tag-WB, transPD	[143]
CG15356	FAITC, PP	[42]
jnj	transIP, WB	[144]
SMC5	transIP, WB	[144]
Hrb87F	transIP, WB	[7,145]
Hrb98DE	transIP, WB	[145]
bon	IP, WB	[73]
fru	IP, WB	[73]
eyg	IP, WB, transIP	[146]
Hers	cosedimentation, WB, IP	[73]
woc	FAITC, PP	[75]
H1	rPD, WB, tagIP	[147,148]
Su(var)2-10	IP, At, Y2H, NMR, FAITC, PP, transIP, fingerprinting, cosedimentation, molecular weight, molecular sieving	[42,68,74,75]
Lhr	Y2H, transIP, WB, IP, fingerprinting, tag-WB	[68,149–151]
Hmr	IP, WB, tag-WB, transIP, fingerprinting	[68,149,150]
STAT92E	IP, rPD, IF, transPD, tag-WB	[152,153]
MED26	IP, WB, ATC	[154]
MED17	IP, WB	[154]
Incenp	transIP, fingerprinting	[68]
borr	transIP, fingerprinting	[68]
HIPP1	transIP, WB, fingerprinting	[68]
CAP	transIP, fingerprinting	[68]
SMC1	transIP, fingerprinting	[68]
Yeti	transPD, tag-WB	[155]
Mau2	transIP, fingerprinting	[68]
Nipped-B	transIP, fingerprinting	[68]
vtd	transIP, fingerprinting	[68]
Odj	transIP, fingerprinting, Y2H, MS	[68,70,156,157]
vers	transIP, fingerprinting	[68]
HP1b	transIP, fingerprinting, rPD	[53,62,68]
dADD1	transIP, tag-WB, fingerprinting, WB, MS	[68,70,78]
tea	transIP, fingerprinting	[68]
sle	transIP, fingerprinting	[68]
CG43736	transIP, fingerprinting	[68]
E(var)3-9	transIP, fingerprinting	[68]
CG1815	transIP, fingerprinting	[68]
NSD	transIP, fingerprinting	[68]
CG7692	transIP, fingerprinting, MS	[68,70]
CG1737	transIP, fingerprinting	[68]
CG30403	transIP, fingerprinting	[68]
Jra	IP, WB, transIP, MS	[158]
Rrp6	coimmunoprecipitation, tag-WB, transIP, WB	[159]
Pc	IP, WB	[160]
Su(z)12	IP, WB	[160]
E(z)	IP, WB	[160]
HipHop	transPD, WB, IP, chromatography technology, molecular sieving, MW	[105,106]
CG8108	transIP, fingerprinting, MS	[68,70]
Sse	transIP, tag-WB, transPD, WB	[161]
Hsc70-3	MS	[70]
βTub56D	MS	[70]
Chd64	MS	[70]
Hsp83	MS	[70]
Act5C	MS	[70]
rictor	transIP, fingerprinting	[162]

Table 2. *Cont.*

Protein or Cellular Component	Methodology	Reference
Tsr	MS	[70]
dmt	Y2H, transIP, MS	[163]
DNApol-ε255	proximity ligation assay, fluorescence microscopy	[101]
Gnf1	IP, WB, proximity ligation assay, fluorescence microscopy	[101]
Ubx	IF, BiFC	[164]
abd-A	IF, BiFC	[164]
sov	transIP, fingerprinting	[68,165]
H3	exPD, FAITC, FW, NMR, PP	[45,51,53,71,125]
bbx	Y2H	[157]
tj	Y2H	[157]

Methodology: IP, co-immunoprecipitation using extract; exPD, pull-down assay using extracts; FAITC, fluorescence anisotropy isothermal titration calorimetry; FW, far-Western analysis; IF, immunofluorescence co-localization; rPD, pull-down assay using recombinant proteins; transPD, pull-down assay using in-vitro translated protein; Y2H, yeast two-hybrid assay; WB, western blot; PA, predictive algorithms; NMR, nuclear magnetic resonance; PP, predetermined participant; GI, genetic interference; tag-WB, western blot assay performed when specific antibodies for the protein of interest are not available; At, autoradiography; fingerprinting, peptide mass fingerprinting; MS, identification by mass spectrometry; BiFC, bimolecular fluorescence complementation.

To identify putative direct HP1a interactors among those presented in Table 2, we searched for the PxVxL motif, a pentapeptide known to bind between the CSD dimer interface formed through the C termini of HP1 [33,47,166–168]. The following proteins contain this motif (Figure 3): Dp1, CG15356, Eyg, Woc, Su (var) 2–10, STAT92E, MED26, Vtd, dADD1, CG43736, DNApol-ε255, Gnf1, and Sov.

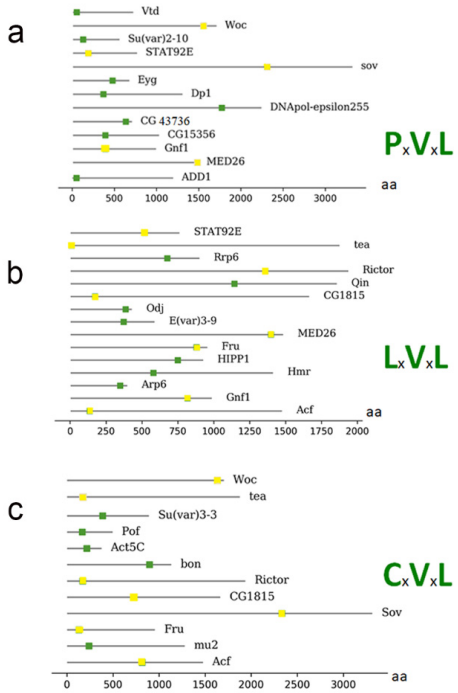

Figure 3. Representation of proteins that have a possible motif for interaction with HP1a from Table 2. (**a**) The proteins connected to the motif PxVxL and the location of the motif within the amino acid sequence. (**b**) Illustration of the proteins with the LxVxL motif and the location of the motif within the amino acid sequence. (**c**) Illustration of the proteins with the CxVxL motif and the location of the motif within the amino acid sequence. The bottom bar indicates the position of the amino acids within the proteins. Proteins that present more than one motif are repeated, and the motif is represented as a yellow box.

Other motifs can also bind to the HP1 CSD domain. These are known as degenerate motifs, which retain similar characteristics to the classical PxVxL pentamer; some of them have conserved V and L residues, such as LxVxL and CxVxL [96,168,169]. The following proteins were found to contain the LxVxL motif: Arp6, ACF, Qin, Fru, Su (var) 2–10, Hmr, STAT92E, MED26, HIPP1, Odj, Tea, CG43736, E (var) 3-9, CG1815, Rrp6, Rictor, and Gnf1.

We also searched for and found the degenerate motif CxVxL [76] in the following proteins: Su(var) 3-3, POF, ACF, mu2, Bon, Fru, Woc, Tea, CG1815, Rictor, and Sov.

Furthermore, some proteins harbor more than one motif (represented as a yellow box; Figure 3), including WOC (without children), which encodes a transcription factor with zinc fingers and an AT-hook domain for sequence-specific DNA binding. WOC is involved in telomere capping and transcriptional regulation, and was also found to be co-immunoprecipitated and show immunofluorescent co-localization with HP1b and c [75,125]. Additionally, the signal transducer and activator of the transcription protein at 92E (Stat92E), which encodes a transcription factor that shuttles between the cytosol and nucleus and functions in the JAK/STAT pathway [153], presented one PxVxL motif and one LxVxL motif. These motifs can accommodate several interaction options—for example, an interaction with both HP1a and HP1b or c, or even an interaction with other proteins.

Gene ontology analysis revealed that all proteins from Figure 3 are chromatin proteins and that no other processes were enriched (data not shown). Moreover, 69% of proteins (9 of 13) from Table 1, with known direct binding to CSD, were found to have the PxVxL or similar motifs. However, only 35% of proteins (30 of 86) presented in Table 2 were found to have the PxVxL or similar motifs. This analysis indicates that many proteins from Table 2 could interact with HP1a indirectly (i.e., by association with other direct interactors or via RNAs [68,113]. Another possibility is that proteins from Table 2 lacking PxVxL or similar motifs may interact with HP1a directly, but via unknown motifs. In addition, some proteins appear to have more than one possible motif for binding, which may give more weight to the theory that they can bind in different complexes—i.e., if one site is occupied, the other can be used, depending on the partners with which they are associated, thus representing another level of regulation.

Although many of the proteins described here harbor the HP1a-binding domain (Figure 3), this domain is not necessarily the only feature required to establish an interaction with HP1a; binding with other residues may be required to form a stable interaction. Therefore, it will be important to analyze the +1 and −1 positions of the PxVxL motif, where V is position 0. These amino acids could also intervene in different ways to facilitate protein binding. Furthermore, it will be essential to identify whether different degenerate motifs have different affinities, i.e., CxVxL or LxVxL, since we found several proteins that contain more than one domain for binding with HP1a.

4. HP1a Interaction with Insulator and Architectural Proteins

Insulators were first defined as regulatory elements that maintain the correct separation of different gene domains, thereby preventing enhancer–promoter communication and/or blocking the expansion of heterochromatin silencing. They also mediate intra- and interchromosomal interactions, which are involved in the large-scale organization of the genome [170,171].

Since the 1980s, it has been known that there are DNA sequences that delimit and isolate a region of chromatin in the *Drosophila* heat shock locus [172,173]. Since then, many of these sequences and the factors that bind to them have been characterized [174,175]. CTCF (CCCTC binding factor) was initially identified as a repressor capable of binding to promoters in chicken and mammalian MYC genes [176]. CTCF was later shown to have an insulator function because it indirectly regulates gene expression by preventing binding between promoters and enhancers or nearby silencers, thus avoiding the inappropriate activation or silencing of certain genes [177]. Recent advances in Hi-C technique have shown that CTCF can mediate the interactions between the boundaries of topologically associating domains (TADs) resulting in the formation of chromatin loops [178]. It should be noted that not all TADs are flanked by CTCF [179].

Although it is not known exactly how CTCF assists in loop formation, a "loop extrusion" model has been proposed. This model suggests that cohesin, which is composed of SMC proteins (structural maintenance of chromosomes) and Rad21 (which is an ortholog of *Drosophila* verthandi (*vtd*)) are directed to the chromatin with the help of the NIPBL protein. Together they "pull" the DNA strand until the cohesin ring is blocked with CTCF [180]. It is currently unclear whether the same mechanism operates in *Drosophila*. However, ChIP-seq experiments have identified several architectural proteins (APs) which are co-localized with CTCF at several sites in the genome.

APs are characterized by promoting contacts between regulatory elements through the formation of loops; thus, they have a role in determining the organization and architecture of chromatin [181,182]. Furthermore, it has been shown that APs can contribute to the establishment of TADs [183]. Some of them include suppressor of hairy-wing (Su(Hw)) [184], dCTCF, the *D. melanogaster* ortholog of mammalian CCCTC-binding factor [185], Boundary Element Associated Factors (BEAF-32A and B) [183], GAGA Associated Factor (GAF) [186], and Zeste-white 5 (Zw5) [187]. Others that have recently been identified include Elba (made up of 3 proteins), Elba1, Elba2, and Elba3 [188], Pita, the zinc-finger protein interacting with CP190 (ZIPIC) [181], Clamp [189], and Ibf-1 and 2 [190].

Typically, the proteins bound to the insulator sequences are necessary but not sufficient for the activity of insulators. Several cofactors are also required to establish physical contacts and anchor them to nuclear structures. In *Drosophila*, proteins such as the modifier of mdg4 (Mod (mdg4)) [191,192] and centrosomal protein of 190kDa (CP190) [193]; cohesins (like Rad21/Vtd); and condensins (like Cap-H2) are present in different combinations in all types of insulators and fulfill these functions [194].

A protein which interacts with HP1a and has a possible role in insulator function is HIPP1 (HP1 and insulator partner protein 1) [68]. Our bioinformatic analysis has shown that HIPP1 could directly associate with HP1a via a PxVxL-related motif (Figure 3b). This protein has a crotonase-fold domain, which makes it a homolog of the human protein chromodomain Y-like (CDYL). In vertebrates, this protein is involved in negatively regulating crotonylation, a modification associated with active promoters [195–197]. The function of this protein during development is not essential [198]. Its location is mainly pericentric, but it also binds to several euchromatin regions and interacts with AP proteins such as Su(Hw), Mod(mdg4), and CP190 [199]. HIPP1 functions stabilize the interactions between CP190 and the Su(Hw)-dependent complex [200]. In this article, we include HIPP1 as a possible architectural protein in Table 3, although this function has not yet been fully demonstrated. We found that the degenerate motif of binding with HP1a (Figure 3b) is located at the most terminal part of the protein. The degenerate motif begins at amino acid 752, and the crotonase domain extends from amino acid 675 to 778. This suggests that HIPP1 interactions with HP1a could affect (negatively or positively) its crotonase activity to some extent. Moreover, the crotonase domain seems to have a role in the interaction of HIPP1 with Su (Hw). Presently, there are no data on whether crotonase activity could be affected by interactions with these proteins. This is an important question to address experimentally in the future.

Since HIPP1 contains possible motifs for direct interactions with HP1a, we examined whether such motifs are also present in other APs. The results are summarized in Table 3. The cohesin complex is an important factor in maintaining the structure of chromosomes. In mammals, the cohesin complex co-localizes with CTCF throughout the genome. In many of these sites, CTCF performs its function of enhancer-blocking [201,202]. In *Drosophila,* there is no co-localization observed between CTCF and the cohesin complex [203], but cohesins do co-localize with other APs, such as CP190 [193]. Through a ChIP-chip analysis, it was determined that Nipped-B and cohesins are located preferably in active sites and are absent from the silenced sites [204].

The Rad21 homolog in *Drosophila* is known as Vtd which is a cohesin subunit involved in the ring formation of the cohesion complex. According to our analysis, Vtd has a PxVxL motif responsible for a possible direct binding with HP1a (Figure 3a). HP1a also interacts with the Nip-b protein, which topologically loads the cohesin ring complex onto the chromosomes. The existence of the

Drosophila ortholog of NIPBL was also confirmed using mass spectrometry, but we could not find a motif in this protein that may be involved in direct binding to HP1a (Table 3).

Table 3. Architectural proteins of *Drosophila* and motifs for possible interaction with HP1a protein.

Protein	PxVxL	CxVxL	LxVxL
CTCF			
Su(Hw)			
BEAF-32			
pita			
ZIPIC			
Ibf1			
Ibf2			
Mod(mdg4)			
CP190			
Cap-H2			X
Elba1			
Elba2			
Elba3	X		
Shep			
Zw5		X	
Clamp			
GAF	X		
Nip-b			
Vtd	X		
SA			X
Smc1			
Smc2			X
Smc3			
HIPP1			X

The Cap-H2 protein has an LxVxL binding motif beginning at 159 aa (N-terminal); also, in Stromalin (SA), this domain is present in the middle of the protein, and the same domain was found in Smc2 in the C-terminal. In Elba3, the canonical binding site, PxVxL, is found at 156 aa and for GAF, this canonical motif is present in the N-terminal. Finally, Zw5 has a putative binding domain, CxVxL, at 449 aa, the most C-terminal part of the protein (Table 3). This opens the door to possible interactions of HP1a with architectural complexes which, in the future, would be interesting to address experimentally.

To better understand whether HP1a is co-localized with APs, we analyzed previously published modENCODE chromatin immunoprecipitation (ChIP-seq) data in *Drosophila* for the region spanning *Abd-A* and *Abd-B* loci (Figure 4). This region has very complicated regulation, and the insulator function is essential for the correct expression of genes within this region [205–207] such that the active or silenced state of one domain does not extend to an adjacent one. ChIP assays detected the presence of APs such as CP190 or CTCF, not only at the border elements but also at the promoters of genes such as *Abd-b* [203,208,209]. The interactions between protein insulators, on the one hand, manage to form loops that leave out entire domains. On the other hand, elements in the domain are brought in close contact with the gene promoter, thereby mediating correct gene expression [210–212].

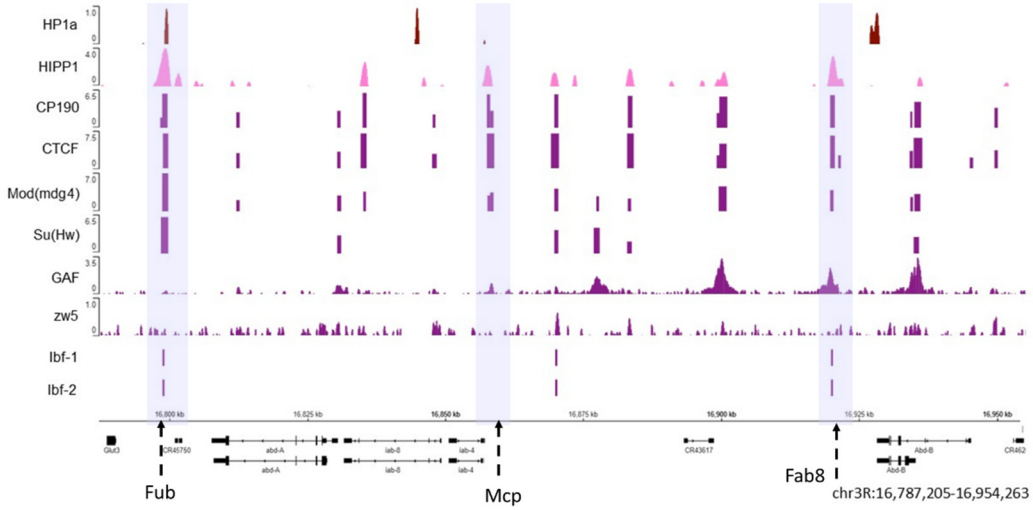

Figure 4. The HP1a and HIPP1 proteins co-localize at homeotic genes along with the AP. The HP1a and HIPP1 proteins co-localize at the Fub insulator (the first violet box) in the *Abd-a* gene along with CP190, Su (Hw), CTCF, and Mod (mdg4), and Ibf 1 and 2. From the previously published ChIP data on S2 cells, we find HP1a (dark red), HIPP1 (pink), and some architecture proteins (purple). The adjacent insulators Mcp and Fab8 do not co-localize with HP1a (center and right violet boxes). The regions with insulators are marked with dotted arrows inside a violet shadow. At the bottom are the *Abd-a* and *Abd-b* genes and their locations; the reference in kilobases.

As shown in Figure 4, both HP1a (dark red) and HIPP1 (pink) are present at the Fub insulator where APs, such as CP190, Su (Hw), CTCF, and Mod (mdg4) are also observed (the violet box where the Fub insulator region is present). Other known insulators are Mcp and Fab8 (highlighted in the middle and right violet boxes) [213], where APs can be observed but do not co-localize with HP1a. Moreover, not all architectural proteins are present in all the insulator loci at the same time. The *Abd-b* gene is silenced in S2 cells, and HP1a appears enriched at the *Abd-b* promoter and is flanked by APs.

For the architectural proteins with available ChIP-seq data, we analyzed the percentage of peaks that co-localized with HP1a peaks genome-wide and estimated the significance of co-localization using the permutation test at a confidence of 95% (Figure S1). The co-localization between peaks of HP1a and HIPP1reaches 42% (p-value 0.0181), followed by Su (Hw) (28%, p-value 0.0001), CP190 (26%, p-value 0.0001), Mod (mdg4) (24%, p-value 0.0001), GAF (16%, p-value 0.0001). Although 20% of HP1a peaks co-localize with CTCF peaks, this co-localization was not statistically significant (p-value 0.4221), the same case was observed for Zw5 (13%, p-value 0.0001, z-score-3.876).

The HP1a CSD domain potentially mediates all the interactions with proteins that were evaluated. This indicates that binding possibly occurs with homodimers or heterodimers of HP1a at specific regions of chromatin. The regions where we assessed the presence of architectural proteins were not constitutive heterochromatin; rather, they represent islands of facultative heterochromatin in the euchromatin. Thus, a disruption of heterochromatin may take place, where HP1a dimers cannot be formed. Subsequently, the binding of HP1a with HMTases could be impaired, which would prevent the spreading of heterochromatinization. Chromatin insulators are essential components of genome architecture across eukaryotes [214,215]. It seems plausible that HIPP1, Vtd, Nip-b, and HP1a cooperate to maintain the insulating complexes and define edges of loops, thereby facilitating the correct separation of heterochromatin and euchromatin.

5. HP1a Interaction Partners in Silenced Chromatin

Constitutive heterochromatin represents a substantial fraction of eukaryotic genomes; it plays an important role in the maintenance of genome stability and silencing of repetitive elements. Nonetheless, further studies are needed to fully understand its formation and maintenance throughout development

and cell differentiation. Thorough localization studies of HP1a in *Drosophila* and mammals have shown that HP1a proteins associate with regions of constitutive heterochromatin around the centromeres and at the telomeres which are rich in repetitive DNA sequences. For example, in polytene chromosomes of *Drosophila*, mainly the chromocenter (i.e., regions of pericentric chromatin) and the telomeres are stained with HP1 antibodies [22].

Constitutive heterochromatin is established early in development. In *Drosophila,* it starts during MBT (in cycle 13) [216,217]. The proposed model involves a complex that contains a methyltransferase (Eggless/SetDB1) of histone H3 lysine 9 and HP1a. The histone mark H3K9me (di or tri methylated) acts as a binding site for HP1a, which binds through its CHD to these chromatin marks, possibly with the involvement of other stabilizing interactions [51,56,57]. It is known that HP1a crosslinks nucleosomes which form condensed heterochromatic structures. For example, in yeast, HP1a also strengthens the association of the HMTase SUV39H1 to chromatin [49]. SUV39H1 methylates nearby unmethylated H3 tails at lysine 9 via its SET domain, creating new H3K9me-binding sites for HP1a. Thus, this three-component system could explain the spreading and maintenance of heterochromatic gene silencing [218,219]. The structures may then be further stabilized through interactions with additional heterochromatic factors. This interaction is preserved in both mammals and *Drosophila* (see Table 1) [49,72,73].

Several groups have carried out chromosomal rearrangement experiments where a euchromatic gene was translocated to a heterochromatic environment and, as a result of being present in this environment, became silenced with the help of several factors, mainly HP1a [38,220,221]. Subsequently, experiments were carried out to direct HP1a to euchromatin regions, such as region 31 of the *Drosophila* 2L arm. Three of the four studied genes within this region were silenced by HP1a and the methyltransferase Su(var)3-9 [222]. These studies demonstrated HP1a to be an essential protein that promotes heterochromatin formation and gene silencing.

Different methyltransferases can work in conjunction with HP1a. For example, in null HP1 mutants, localization of Su(var)3-9 is no longer limited to the chromocenter but spreads across the chromosomes [72]. Studies using mutants suggest that there is a sequential order in which interactions are established [223]. Another member of this complex is the zinc-finger protein Su (var) 3-7, which appears to function as an effector downstream of Su (var) 3-9 and HP1a. This protein has heterochromatic localization, very similar to that of HP1a on polytene chromosomes in pericentric regions and on chromosome 4 [64]. In addition to decreasing the dose of this protein, it reduces PEV [224]. Increasing the quantity of the product of Su (var) 3-7 prompts heterochromatin extension and epigenetic gene silencing [225]. The formation of heterochromatin is a critical developmental process. Su (var) 3-3, whose homolog in mammals is LSD1, removes H3K4me1/2 marks in early embryonic development. This led to the establishment of a balance between demethylase and methyltransferase Su (var) 3-9, contributing to the maintenance of heterochromatic domains [134].

The heterochromatin–euchromatin borders have previously been described cytologically [226,227] and, later, with ChIP-array analysis of genome distribution of H3K9me2 mark, and were named the "epigenomic borders" [16]. Interestingly, the epigenomic borders varied in different cell lines or tissues studied which lead authors to propose that additional mechanisms besides sequence-specific binding can establish these borders [16]. To identify the borders of pericentric heterochromatin domains more precisely, we analyzed publicly available ChIP-seq profiles in S2 cells for HP1a, along with Su (var) 3-9, Su (var) 3-7, and H3K9me3 (Figure 5, see also Material and Methods). We examined a section near the chromocenter (the black circle at the top of thde schematic representation). A clear enrichment of HP1a along with the other examined proteins and histone marks is seen in the pericentromeric region highlighted with a red rectangle. Further from the centromere (7.3 Mb), this enrichment sharply declines thus indicating the border between heterochromatin and euchromatin. APs such as CTCF and CP190 are clearly enriched just after the border in the euchromatin which is consistent with the function of these proteins to keep chromatin domains isolated from each other [170,181,208,209,228,229] and of CP190 to mark active promoters in *Drosophila* [193]. Therefore, APs may play a role in defining

this border. Thus, HP1a can cooperate with other factors at these epigenomic borders to maintain a correct chromatin structure. Interestingly, H3K9 acetylation is still present within the beginning of constitutive heterochromatin, co-localizing with CP190 and some CTCF peaks. These bivalent signatures may facilitate pericentromeric gene transcription, as was observed for some genes [230]. Throughout the chromosome, other HP1a sites co-localize with H3K9ac (blue shaded box, Figure 5). The HP1a enrichment sets the epigenomic border for 2R chromosome arm at 7.3 Mb position, while the epigenomic border described in [16] was set at 7.4 Mb (highlighted red square in Figure 5).

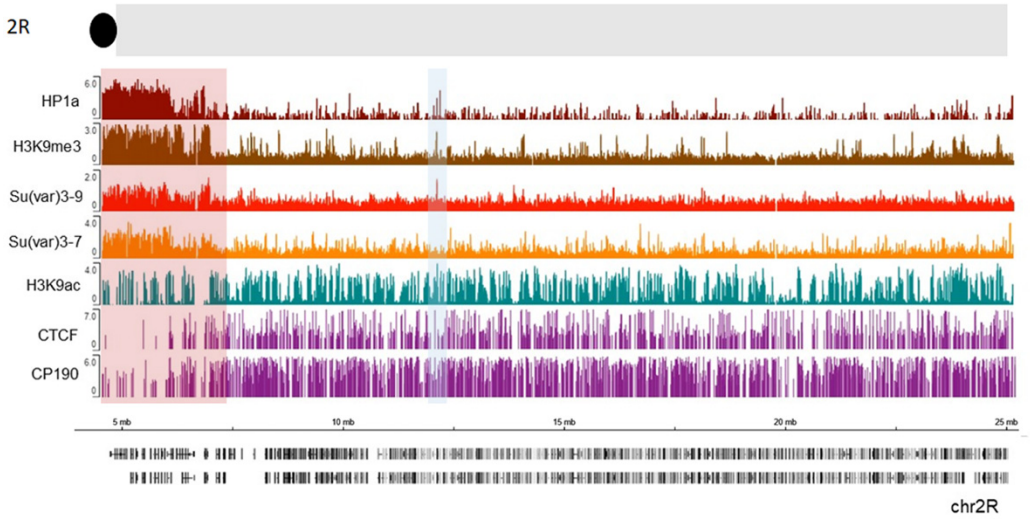

Figure 5. HP1a, together with other proteins, delimits epigenomic borders. Previously published ChIP data on S2 cells were used, where we see HP1a (dark red), Su(var) 3-9 (light red), Su(var) 3-7 (orange), H3k9me3 mark (brown), H3k9ac (green), CTCF, and CP190 (purple). The regions with a pericentric border are marked with a red rectangle according to Riddle et al. The co-localization of HP1a with H3K9ac mark is shaded in blue.

Another interactor of HP1a is dADD1 [68]. dADD1 is an ortholog of the N-terminal domain of mammalian ATRX protein [78] and has a motif for interaction with HP1a in the most N-terminal portion (54 aa) (Figure 3a). This is also found within a region conserved between the three isoforms encoded by this gene. We observed that the dADD1-a isoform is the only isoform that immunoprecipitated together with HP1a [78]. Although the other isoforms have the ability to associate and therefore be immunoprecipitated, this was not observed for any of the conditions we have evaluated so far. Rescue experiments in a null *dadd1* background demonstrated that HP1a was restored to the telomeric region when the rescue was performed with dADD1a [231] but not with dADD1b. However, we also observed that upon dADD1a overexpression, HP1a was lost from the chromocenter in a dADD1a dose-dependent manner. When dADD1 proteins have higher than wild-type levels, the polytene chromosomes become decompacted and lose their banding pattern. The HP1a protein and H3K9me3 mark delocalize and acquire a different distribution within the cell nucleus [232].

These results show that dADD1 proteins are regulators of HP1a, likely maintaining the correct local concentration of HP1a oligomers at certain regions, such as the telomeres and pericentric heterochromatin. The over- and underexpression of dADD1 can disturb the concentration of HP1a and likely affect phase transition, which could lead to chromatin instability and alterations in gene expression [232].

Moreover, it has been demonstrated that human HP1α promotes phase separation of heterochromatin from euchromatin [128], which is also exhibited by the *Drosophila* ortholog [128,233]. The HP1 proteins possibly involved in orchestrating these separations and play an important role in defining their possible environments and interactions. For example, HP1a could be enriched at heterochromatin regions together with a methyltransferase (as with dADD1), forming gel-type droplets

with a specific environment. Interestingly, dADD1a possesses intrinsically disordered regions in the C-terminal region (650–696, 716–763, 791–1069, 1112–1132, and 1154–1199 aa) that can contribute to phase separation [234].

The contribution of HP1a to the maintenance of telomeric heterochromatin works via two main functions: as part of the CAP along with proteins such as HOAP (cav) [106,107] and the repression of telomeric retrotransposons in cooperation with piRNAs [235]. Notably, HP1a localization at this heterochromatic site does not depend on its chromodomain but rather on its interaction with dADD1a in somatic cells [231]. The interaction of HP1a and dADD1 at the telomeric region seems to be conserved because ATRX also co-localizes with HP1α at the telomeres in human cells. HP1a's functions at telomeres seem to depend on the interactions of different proteins and even RNAs. In mammalian embryonic stem cells, ATRX (Alpha-Thalassemia with mental Retardation X-related) [236] has been shown to complex with TRIM28 and SETDB1 recruited by H3K9me3 in retrotransposon regions [237,238]. We have described the interaction of the helicase part of ATRX (XNP) together with the ADD domain (dADD1) in *Drosophila* in conjunction with HP1a. Furthermore, Kuroda's laboratory was able to immunoprecipitate EGG/dSETDB1 and the Bonus protein (Trim28 homolog) together with dADD1 [68]. These proteins could form a complex and perform a similar function to their mammalian counterparts at retrotransposon regions in *Drosophila*.

6. HP1a Interaction Partners in Euchromatin

It is well known that HP1a does not only localize to regions of constitutive heterochromatin. A fraction of HP1a is also present within euchromatic regions of the chromosomes. For example, in polytene chromosomes of *Drosophila*, HP1a is found at about 200 sites within the chromosome arms [14,127]. Moreover, using DamID technique numerous HP1a binding regions within euchromatic parts of *Drosophila* chromosome arms from various non-polytene tissues were revealed [15,17,239,240]. This points to the repressive action of HP1 within euchromatin, an interpretation supported by studies demonstrating the recruitment of HP1a by different transcriptional repressors [81,82] and the reported upregulation of some HP1-bound genes in euchromatin upon mutation of HP1a in *Drosophila* [222].

Numerous experimental data demonstrate that HP1 by itself can induce heterochromatic structures and may, in fact, directly stimulate gene silencing within euchromatin. When HP1 binds to the euchromatin regions of *Drosophila* chromosomes through an ectopic binding domain, this process is almost always sufficient to enable the establishment of heterochromatin and silence neighboring reporter genes [241]. Furthermore, redirecting HP1α or HP1a through a GAL/lacR system to euchromatic regions in mammalian or *Drosophila* cells causes local condensation of higher-order chromatin structure and gene repression [3]. These experiments suggest that HP1 could indeed play a role in gene repression within euchromatic regions of chromosomes. The participation of HP1 in the regulation of euchromatic regions is even more complex and goes beyond its well-established role in gene silencing.

Unexpectedly, at some euchromatic loci, HP1 association clearly corresponds to the elevated gene expression. For example, HP1a is recruited to some of the ecdysone-induced or heat shock-induced puffs of *Drosophila* polytene chromosomes, generated due to strong decondensation of chromatin linked to gene activation [242], implying the modulating role of HP1a in their expression. The association of HP1 with such sites seems to be RNA-dependent since HP1 association with Hsp70 heat shock locus is only observed in the presence of RNA [242]. We also observed dADD1 enrichment at the Hsp70 locus under native conditions [232] (Figure 6). When heat shock is induced, this area becomes free of nucleosomes, the poised RNA pol II begins to elongate which results in rapid activation of transcription [243]. Another group also analyzed the presence of Xnp (the helicase part that completes the mammalian ortholog ATRX) at this locus along with Hira and the H3.3 histone variant. The authors proposed that Xnp could recognize nucleosome-free sites and work to avoid transcriptional problems or defects in subsequent DNA repair [244]. Many questions remain to be answered regarding the role of these proteins at this locus. For example, whether they strengthen the ability of HP1a to maintain a silenced state or if their presence is necessary to promote rapid transcription upon cell insult.

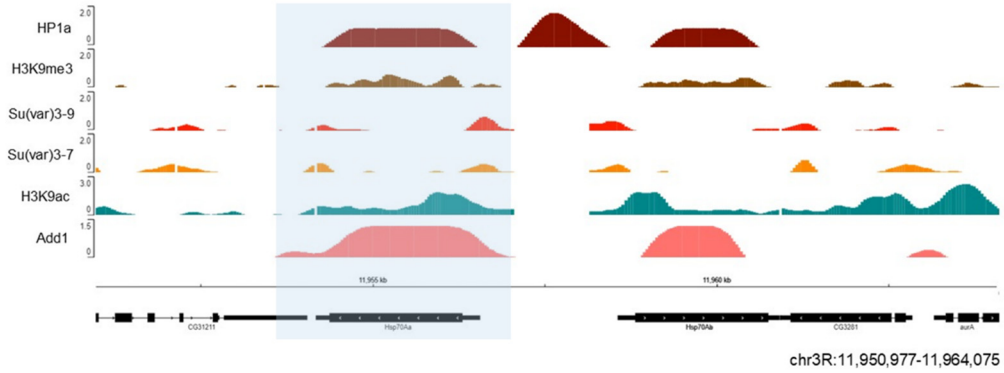

Figure 6. HP1a and dADD1 proteins co-localize at the Hsp70 locus. Previously published ChIP-seq data on S2 cells were used, where we see HP1a (dark red), dADD1 (salmon) HP1a, Su (var) 3-9 (light red), Su (var) 3-7 (orange), H3k9me3 mark (brown), and H3k9ac (green). At the bottom are the gene Hsp70 Aa (blue box) and its location, with the reference in kilobases.

Furthermore, some genes located within pericentric heterochromatin require a heterochromatic environment for their normal expression. The mutations of HP1a reduce the expression of *light* and *rolled* genes, the first to be described [245]. These genes are essential for the organism and reside naturally in heterochromatin blocks on chromosome 2. Later studies observed that a complex of HP1a and Su(var)3-9 generates very compact chromatin in these blocks [246].

High-resolution mapping of the HP1a-binding sites in *Drosophila* shows that HP1 is excluded from the promoter and is restricted to the transcribed regions of actively expressed genes [135,239]. Furthermore, HP1a depletion causes downregulation of a subset of active genes [247]. The interaction of HP1 with RNA may mediate the association of HP1 at euchromatic regions within the genome. HP1a interactions with RNA, most likely in collaboration with other interactions, recruit HP1a to these sites, where it plays a role in the promotion of gene expression [7]. This is supported by studies indicating that the section of HP1a responsible for RNA binding is the hinge [26].

It has been observed that HP1b and HP1c isoforms are more localized in the euchromatic chromosome arms than HP1a [47,222,248,249]. Lee et al. have shown that all HP1 isoforms interact with the phosphorylated at serine 2 or 5 RNA pol II, but do so with different affinities [53]. Various localization patterns of HP1 isoforms on chromosomes may be mediated by different complexes in which these isoforms are involved (Figure 7).

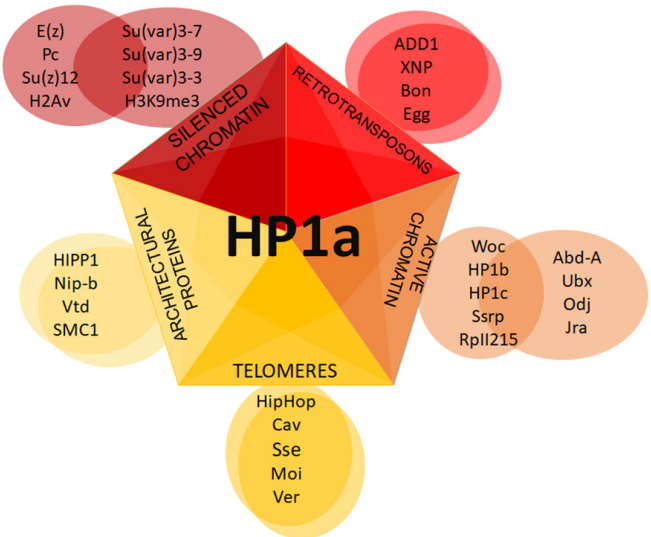

Figure 7. Putative HP1a complexes at different chromatin regions. Schematic representation of distinct complexes formed with HP1a.

7. Future Directions

Although there have been detailed genetic and biochemical studies of HP1's roles in heterochromatin establishment and maintenance, its position at euchromatic regions and in association with RNA has not been thoroughly characterized. Valuable studies have shed light on the multiple proteins that interact with HP1a. In this extended review, we addressed whether the proteins found in association with HP1a could bear putative motifs that allow direct interaction with HP1 proteins. The identification of HP1a interactors at different chromatin regions is essential to understand the different roles of these protein complexes. We found that among the reported interactors, only a handful conserve motifs for CSD domain interactions (Figure 3). Experimental studies to test if these motifs function in vivo in binding to CSD would be of great importance and could extend our understanding of the biological significance of the interactions.

We also raise the possibility of HP1 interactions with architectural proteins. Indeed, we found that several architectural proteins harbor conserved putative HP1-interacting motifs (Table 3). Further experimentation will be required to understand the role of HP1a in conjunction with architectural proteins and their possible cooperation in the organization of chromatin structure [71].

Very recently, it has been shown that pericentric heterochromatin also establishes well-defined territories through contact with different proteins via the H3K9me2 mark. Most importantly, the maintenance of these territories and the established pericentromeric contacts also influence active genome regions. The protein complexes associated with these domains could also have an essential role in the formation of higher-order chromatin structures [250].

8. Materials and Methods

Protein domain structure illustration

The search for possible motifs for interaction with HP1a in protein sequences and the representation of the location of the domain were executed using Python 2.7. The obtained data are presented in Figure 3 and Table 3.

Alignments and phylogenetic inference analyses

Multiple protein sequence alignments were performed using MUSCLE [251]. Maximum likelihood phylogenetic analysis was computed by PhyML [252] using a Dayhoff matrix as a substitution model with 100 bootstraps. The tree was edited using FigTree with the protein domain architecture information of chromodomain and chromoshadow of the containing proteins as predicted by ScanProsite [253]. The data are presented in Figure 2.

ChIP-seq analyses and data visualization

All datasets used in this study were retrieved as processed data from the GEO Omnibus database (http://www.ncbi.nlm.nih.gov/geo/) and shown in Supplementary Material Table S1 [254,255]. ChIP-seq data were visualized using the Integrative Genome Browser [256]. Values from all ChIP-seq datasets represent log2 enrichment values, except in the case of Pol II and H3K27ac, where the values are the combined counts of fragment centers for all replicates.

The percentage of co-localizing peaks between HP1a and the architectural proteins was obtained with the R Bioconductor package. To select the epigenomic borders, the global height of HP1a ChIP-seq peaks summit was measured along the genome. The median height was obtained, this provided a value of 0.9 arbitrary units (a.u.). Chromosome 2R peaks were analyzed every 0.5 Mb from the centromere to the telomere. The median of HP1a peaks near the chromocenter has a value of 3.12 a.u., and it extends to approximately 7 Mb, where it changes to 1.4 a.u. and then decays to 0.5 a.u. When the value decayed below the global median, the edge was marked. Importantly, Su (var) 3-9 and H3K9me3 peaks presented a similar behavior. Genomic coordinates were converted from dm3 to dm6 using FlyBase [257]. The epigenomic boundary set with HP1a was at 7.3Mb whereas in Riddle et al. [16] it was at 7.4 Mb in chromosome 2R. All the coordinates are from the reference genome dm6. Data obtained with these tools are presented in Figures 4–6 and S1.

Supplementary Materials: The following are available online at http://www.mdpi.com/2073-4409/9/8/1866/s1, Table S1: Publicly available ChIP-seq data for S2 cells; Figure S1: Permutation test for overlap between HP1a and architectural proteins.

Author Contributions: S.M.-N. and V.V.-G. wrote the manuscript, S.M.-N. and V.E.N.-C. performed data mining and bioinformatic analyses, S.M.-N., V.V.-G. and M.Z. performed revisions and editing. All authors read and approved the manuscript.

Funding: This work was supported by the Consejo Nacional de Ciencia y Tecnología (A1-S-8239 to V.V.-G.) and Programa de Apoyo a Proyectos de Investigación e Innovación Tecnológica (204915 and 200118 to V.V.-G.); S.M.-N. received a scholarship from the Consejo Nacional de Ciencia y Tecnología (354993).

Acknowledgments: We would like to thank Lola Flores for helpful comments and Alfonso León Del Río for critical reading of the manuscript and helpful suggestions.

Conflicts of Interest: The authors declare no conflict of interest.

References

1. Felsenfeld, G.; Groudine, M. Controlling the double helix. *Nature* **2003**, *42*, 448–453. [CrossRef] [PubMed]
2. Luger, K.; Dechassa, M.L.; Tremethick, D.J. New insights into nucleosome and chromatin structure: An ordered state or a disordered affair? *Nat. Rev. Mol. Cell Biol.* **2012**, *13*, 436–447. [CrossRef]
3. Brueckner, L.; van Arensbergen, J.; Akhtar, W.; Pagie, L.; van Steensel, B. High-throughput assessment of context-dependent effects of chromatin proteins. *Epigenetics Chromatin.* **2016**, *9*, 1–17. [CrossRef] [PubMed]
4. Luger, K.; Mader, A.W.; Richmond, R.K.; Sargent, D.F.; Richmond, T.J. Crystal structure of the nucleosome resolution core particle at 2.8 A. *Nature* **1997**, *389*, 251–260. [CrossRef] [PubMed]
5. Bayona-Feliu, A.; Casas-Lamesa, A.; Reina, O.; Bernués, J.; Azorín, F. Linker histone H1 prevents R-loop accumulation and genome instability in heterochromatin. *Nat. Commun.* **2017**, *8*, 1. [CrossRef] [PubMed]
6. Richards, E.J.; Elgin, S.C.R. Epigenetic codes for heterochromatin formation and silencing: Rounding up the usual suspects. *Cell* **2002**, *108*, 489–500. [CrossRef]
7. Piacentini, L.; Fanti, L.; Negri, R.; Del Vescovo, V.; Fatica, A.; Altieri, F.; Pimpinelli, S. Heterochromatin Protein 1 (HP1a) positively regulates euchromatic gene expression through RNA transcript association and interaction with hnRNPs in Drosophila. *PLoS Genet.* **2009**, *5*, e1000670. [CrossRef]
8. Passarge, E. Emil Heitz and the concept of heterochromatin: Longitudinal chromosome differentiation was recognized fifty years ago. *Am. J. Hum. Genet.* **1979**, *31*, 106–115.
9. Dillon, N. Heterochromatin structure and function. *Biol. Cell* **2004**, *96*, 631–637. [CrossRef] [PubMed]
10. Britten, R.J.; Kohne, D.E. Repeated sequences in DNA. *Science* **1968**, *161*, 529–540. [CrossRef] [PubMed]
11. Fodor, B.D.; Shukeir, N.; Reuter, G.; Jenuwein, T. Mammalian *Su* (*var*) genes in chromatin control. *Annu. Rev. Cell Dev. Biol.* **2010**, *26*, 471–501. [CrossRef] [PubMed]
12. Guthmann, M.; Burton, A.; Torres-Padilla, M. Expression and phase separation potential of heterochromatin proteins during early mouse development. *EMBO Rep.* **2019**, *20*, 1–11. [CrossRef] [PubMed]
13. Nishibuchi, G.; Déjardin, J. The molecular basis of the organization of repetitive DNA-containing constitutive heterochromatin in mammals. *Chromosom. Res.* **2017**, *25*, 77–87. [CrossRef] [PubMed]
14. Fanti, L.; Pimpinelli, S. HP1: A functionally multifaceted protein. *Curr. Opin. Genet. Dev.* **2008**, *18*, 169–174. [CrossRef] [PubMed]
15. Pindyurin, A.V.; Ilyin, A.A.; Ivankin, A.V.; Tselebrovsky, M.V.; Nenasheva, V.V.; Mikhaleva, E.A.; Pagie, L.; van Steensel, B.; Shevelyov, Y.Y. The large fraction of heterochromatin in Drosophila neurons is bound by both B-type lamin and HP1a. *Epigenetics Chromatin.* **2018**, *11*, 1–17. [CrossRef] [PubMed]
16. Riddle, N.C.; Minoda, A.; Kharchenko, P.V.; Alekseyenko, A.A.; Schwartz, Y.B.; Tolstorukov, M.Y.; Gorchakov, A.A.; Jaffe, J.D.; Kennedy, C.; Linder-Basso, D.; et al. Plasticity in patterns of histone modifications and chromosomal proteins in *Drosophila* heterochromatin. *Genome Res.* **2011**, *21*, 147–163. [CrossRef]
17. Marshall, O.J.; Brand, A.H. Chromatin state changes during neural development revealed by in vivo cell-type specific profiling. *Nat. Commun.* **2017**, *8*, 1–9. [CrossRef]
18. Grewal, S. Heterochromatin and epigenetic control of gene expression. *Science* **2003**, *301*, 798–802. [CrossRef]
19. Wang, X.; Moazed, D. DNA sequence-dependent epigenetic inheritance of gene silencing and histone H3K9 methylation. *Science* **2017**, *91*, 88–91. [CrossRef]

20. Riddle, N.C.; Jung, Y.L.; Gu, T.; Alekseyenko, A.A.; Asker, D.; Gui, H.; Kharchenko, P.V.; Minoda, A.; Plachetka, A.; Schwartz, Y.B.; et al. Enrichment of HP1a on drosophila chromosome 4 genes creates an alternate chromatin structure critical for regulation in this heterochromatic domain. *PLoS Genet.* **2012**, *8*, e1002954. [CrossRef]
21. Muller, H.J.; Altenburg, E. The frequency of translocations produced by X-rays in Drosophila. *Genetics* **1930**, *15*, 283-311. [PubMed]
22. James, T.C.; Elgin, S.C. Identification of a nonhistone chromosomal protein associated with heterochromatin in Drosophila melanogaster and its gene. *Mol. Cell. Biol.* **1986**, *6*, 3862–3872. [CrossRef] [PubMed]
23. Sinclair, D.A.R.; Mottus, R.C.; Grigliatti, T.A. Genes which suppress position-effect variegation in Drosophila melanogaster are clustered. *MGG Mol. Gen. Genet.* **1983**, *191*, 326–333. [CrossRef]
24. Lorentz, A.; Ostermann, K.; Fleck, O.; Schmidt, H. Switching gene swi6, involved in repression of silent mating-type loci in fission yeast, encodes a homologue of chromatin-associated proteins from Drosophila and mammals. *Gene* **1994**, *143*, 139–143. [CrossRef]
25. Thon, G.; Verhein-hansen, J. Four chromo-domain proteins of schizosaccharomyces pombe differentially repress transcription at various chromosomal locations. *Genetics* **2000**, *155*, 551–568. [PubMed]
26. Meehan, R.R.; Kao, C.F.; Pennings, S. HP1 binding to native chromatin in vitro is determined by the hinge region and not by the chromodomain. *EMBO J.* **2003**, *22*, 3164–3174. [CrossRef] [PubMed]
27. Istomina, N.E.; Shushanov, S.S.; Springhetti, E.M.; Karpov, V.L.; Krasheninnikov, I.A.; Stevens, K.; Zaret, K.S.; Singh, P.B.; Grigoryev, S.A. Insulation of the chicken beta-globin chromosomal domain from a chromatin-condensing protein, MENT. *Mol. Cell. Biol.* **2003**, *23*, 6455–6468. [CrossRef]
28. Wreggett, K.A.; Hill, F.; James, P.S.; Hutchings, A.; Butcher, G.W.; Singh, P.B. A mammalian homologue of Drosophila heterochromatin protein 1 (HP1) is a component of constitutive heterochromatin. *Cytogenet. Cell Genet.* **1994**, *66*, 99–103. [CrossRef]
29. Cowell, I.G.; Aucott, R.; Mahadevaiah, S.K.; Burgoyne, P.S.; Huskisson, N.; Bongiorni, S.; Prantera, G.; Fanti, L.; Pimpinelli, S.; Wu, R.; et al. Heterochromatin, HP1 and methylation at lysine 9 of histone H3 in animals. *Chromosoma* **2002**, *111*, 22–36. [CrossRef]
30. Pak, D.T.; Pflumm, M.; Chesnokov, I.; Huang, D.W.; Kellum, R.; Marr, J.; Romanowski, P.; Botchan, M.R. Association of the origin recognition complex with heterochromatin and HP1 in higher eukaryotes. *Cell* **1997**, *91*, 311–323. [CrossRef]
31. Polioudaki, H.; Kourmouli, N.; Drosou, V.; Bakou, A.; Theodoropoulos, P.A.; Singh, P.B.; Giannakouros, T.; Georgatos, S.D. Histones H3/H4 form a tight complex with the inner nuclear membrane protein LBR and heterochromatin protein 1. *EMBO Rep.* **2001**, *2*, 920–925. [CrossRef] [PubMed]
32. Raffa, G.D.; Ciapponi, L.; Cenci, G.; Gatti, M. Terminin: A protein complex that mediates epigenetic maintenance of Drosophila telomeres. *Nucleus* **2011**, *2*, 383-391. [CrossRef] [PubMed]
33. Brasher, S.V.; Smith, B.O.; Fogh, R.H.; Nietlispach, D.; Thiru, A.; Nielsen, P.R.; Broadhurst, R.W.; Ball, L.J.; Murzina, N.V.; Laue, E.D. The structure of mouse HP1 suggests a unique mode of single peptide recognition by the shadow chromo domain dimer. *EMBO J.* **2000**, *19*, 1587–1597. [CrossRef] [PubMed]
34. Hendzel, M.J.; Wei, Y.; Mancini, M.A.; Van Hooser, A.; Ranalli, T.; Brinkley, B.R.; Bazett-Jones, D.P.; Allis, C.D. Mitosis-specific phosphorylation of histone H3 initiates primarily within pericentromeric heterochromatin during G2 and spreads in an ordered fashion coincident with mitotic chromosome condensation. *Chromosoma* **1997**, *106*, 348–360. [CrossRef] [PubMed]
35. Hirota, T.; Lipp, J.J.; Toh, B.H.; Peters, J.M. Histone H3 serine 10 phosphorylation by Aurora B causes HP1 dissociation from heterochromatin. *Nature* **2005**, *438*, 1176–1180. [CrossRef] [PubMed]
36. Jacobs, S.A.; Khorasanizadeh, S. Structure of HP1 chromodomain bound to a lysine 9-methylated histone H3 tail. *Science* **2002**, *295*, 2080–2083. [CrossRef]
37. Daujat, S.; Zeissler, U.; Waldmann, T.; Happel, N.; Schneider, R. HP1 binds specifically to Lys26-methylated histone H1.4, whereas simultaneous Ser27 phosphorylation blocks HP1 binding. *J. Biol. Chem.* **2005**, *280*, 38090–38095. [CrossRef]
38. Eissenberg, J.C.; James, T.C.; Foster-Hartnett, D.M.; Hartnett, T.; Ngan, V.; Elgin, S.C. Mutation in a heterochromatin-specific chromosomal protein is associated with suppression of position-effect variegation in Drosophila melanogaster. *Proc. Natl. Acad. Sci. USA* **1990**, *87*, 9923-9927. [CrossRef]
39. Penke, T.J.R.; McKay, D.J.; Strahl, B.D.; Matera, A.G.; Duronio, R.J. Direct interrogation of the role of H3K9 in metazoan heterochromatin function. *Genes Dev.* **2016**, *30*, 1866–1880. [CrossRef]

40. Penke, T.; McKay, D.J.; Strahl, B.D.; Matera, A.G.; Duronio, R.J. Functional redundancy of variant and canonical histone H3 lysine 9 modification in drosophila. *Genetics* **2018**, *208*, 229–244. [CrossRef]
41. Fanti, L.; Giovinazzo, G.; Berloco, M.; Pimpinelli, S. The heterochromatin protein 1 prevents telomere fusions in Drosophila. *Mol. Cell* **1998**, *2*, 527–538. [CrossRef]
42. Mendez, D.L.; Kim, D.; Chruszcz, M.; Stephens, G.E.; Minor, W.; Khorasanizadeh, S.; Elgin, S.C. The HP1a disordered C terminus and chromo shadow domain cooperate to select target peptide partners. *ChemBioChem* **2011**, *12*, 1084–1096. [CrossRef] [PubMed]
43. Rose, A.S.; Bradley, A.R.; Valasatava, Y.; Duarte, J.M.; Prlic, A.; Rose, P.W. NGL viewer: Web-based molecular graphics for large complexes. *Bioinformatics* **2018**, *34*, 3755–3758. [CrossRef] [PubMed]
44. Kwon, S.H.; Workman, J.L. HP1c casts light on dark matter. *Cell Cycle* **2011**, *10*, 625–630. [CrossRef] [PubMed]
45. Azzaz, A.M.; Vitalini, M.W.; Thomas, A.S.; Price, J.P.; Blacketer, M.J.; Cryderman, D.E.; Zirbel, L.N.; Woodcock, C.L.; Elcock, A.H.; Wallrath, L.L.; et al. Human heterochromatin protein 1α promotes nucleosome associations that drive chromatin condensation. *J. Biol. Chem.* **2014**, *289*, 6850–6861. [CrossRef] [PubMed]
46. Nielsen, S.J.; Schneider, R.; Bauer, U.M.; Bannister, A.J.; Morrison, A.; O'Carroll, D.; Firestein, R.; Cleary, M.; Jenuwein, T.; Herrera, R.E.; et al. Rb targets histone H3 methylation and HP1 to promoters. *Nature* **2001**, *412*, 561–565. [CrossRef]
47. Smothers, J.F.; Henikoff, S. The hinge and chromo shadow domain impart distinct targeting of HP1-like proteins. *Mol. Cell. Biol.* **2001**, *21*, 2555–2569. [CrossRef]
48. Cowieson, N.P.; Partridge, J.F.; Allshire, R.C.; McLaughlin, P.J. Dimerisation of a chromo shadow domain and distinctions from the chromodomain as revealed by structural analysis. *Curr. Biol.* **2000**, *10*, 517–525. [CrossRef]
49. Yamamoto, K.; Sonoda, M. Self-interaction of heterochromatin protein 1 is required for direct binding to histone methyltransferase, SUV39H1. *Biochem. Biophys. Res. Commun.* **2003**, *301*, 287–292. [CrossRef]
50. Lechner, M.S.; Begg, G.E.; Speicher, D.W.; Rauscher, F.J. Molecular determinants for targeting heterochromatin protein 1-mediated gene silencing: Direct chromoshadow domain-KAP-1 corepressor interaction is essential. *Mol. Cell. Biol.* **2000**, *20*, 6449–6465. [CrossRef]
51. Jacobs, S.A.; Taverna, S.D.; Zhang, Y.; Briggs, S.D.; Li, J.; Eissenberg, J.C.; Allis, C.D.; Khorasanizadeh, S. Specificity of the HP1 chromo domain for the methylated N-terminus of histone H3. *EMBO J.* **2001**, *20*, 5232–5241. [CrossRef] [PubMed]
52. Verni, F.; Cenci, G. The drosophila histone variant H2A.V works in concert with HP1 to promote kinetochore-driven microtubule formation. *Cell Cycle* **2015**, *14*, 577–588. [CrossRef] [PubMed]
53. Lee, D.H.; Ryu, H.W.; Kim, G.W.; Kwon, S.H. Comparison of three heterochromatin protein 1 homologs in Drosophila. *J. Cell Sci.* **2019**, *132*, jcs222729. [CrossRef] [PubMed]
54. Kourmouli, N.; Theodoropoulos, P.A.; Dialynas, G.; Bakou, A.; Politou, A.S.; Cowell, I.G.; Singh, P.B.; Georgatos, S.D. Dynamic associations of heterochromatin protein 1 with the nuclear envelope. *EMBO J.* **2000**, *19*, 6558–6568. [CrossRef] [PubMed]
55. Nielsen, A.L.; Oulad-Abdelghani, M.; Ortiz, J.A.; Remboutsika, E.; Chambon, P.; Losson, R. Heterochromatin formation in mammalian cells: Interaction between histones and HP1 Proteins. *Mol. Cell* **2001**, *7*, 729–739. [CrossRef]
56. Lachner, M.; O'Carroll, D.; Rea, S.; Mechtler, K.; Jenuwein, T. Methylation of histone H3 lysine 9 creates a binding site for HP1 proteins. *Nature* **2001**, *410*, 116–120. [CrossRef] [PubMed]
57. Bannister, A.J.; Zegerman, P.; Partridge, J.F.; Miska, E.A.; Thomas, J.O.; Allshire, R.C.; Kouzarides, T. Selective recognition of methylated lysine 9 on histone H3 by the HP1 chromo domain. *Nature* **2001**, *410*, 120–124. [CrossRef]
58. Rohr, O.; Lecestre, D.; Chasserot-Golaz, S.; Marban, C.; Avram, D.; Aunis, D.; Leid, M.; Schaeffer, E. Recruitment of tat to heterochromatin protein HP1 via interaction with CTIP2 inhibits human immunodeficiency virus type 1 replication in microglial cells. *J. Virol.* **2003**, *77*, 5415–5427. [CrossRef]
59. Marban, C.; Redel, L.; Suzanne, S.; Van Lint, C.; Lecestre, D.; Chasserot-Golaz, S.; Leid, M.; Aunis, D.; Schaeffer, E.; Rohr, O. COUP-TF interacting protein 2 represses the initial phase of HIV-1 gene transcription in human microglial cells. *Nucleic Acids Res.* **2005**, *33*, 2318–2331. [CrossRef]
60. Smallwood, A.; Estève, P.O.; Pradhan, S.; Carey, M. Functional cooperation between HP1 and DNMT1 mediates gene silencing. *Genes Dev.* **2007**, *21*, 1169–1178. [CrossRef]

61. Schwendemann, A.; Matkovic, T.; Linke, C.; Klebes, A.; Hofmann, A.; Korge, G. Hip, an HP1-interacting protein, is a haplo- and triplo-suppressor of position effect variegation. *Proc. Natl. Acad. Sci. USA* **2008**, *105*, 204–209. [CrossRef]
62. Hines, K.A.; Cryderman, D.E.; Flannery, K.M.; Yang, H.; Vitalini, M.W.; Hazelrigg, T.; Mizzen, C.A.; Wallrath, L.L. Domains of heterochromatin protein 1 required for drosophila melanogaster heterochromatin spreading. *Genetics* **2009**, *182*, 967–977. [CrossRef] [PubMed]
63. Linder, B.; Gerlach, N.; Jäckle, H. The Drosophila homolog of the human AF10 is an HP1-interacting suppressor of position effect variegation. *EMBO Rep.* **2001**, *2*, 211–216. [CrossRef] [PubMed]
64. Cléard, F.; Delattre, M.; Spierer, P. SU(VAR)3-7, a Drosophila heterochromatin-associated protein and companion of HP1 in the genomic silencing of position-effect variegation. *EMBO J.* **1997**, *16*, 5280–5288. [CrossRef] [PubMed]
65. Delattre, M.; Spierer, A.; Tonka, C.H.; Spierer, P. The genomic silencing of position-effect variegation in Drosophila melanogaster: Interaction between the heterochromatin-associated proteins Su(var)3-7 and HP1. *J. Cell Sci.* **2000**, *113*, 4253–4261. [PubMed]
66. Yin, H.; Lin, H. An epigenetic activation role of Piwi and a Piwi-associated piRNA in Drosophila melanogaster. *Nature* **2007**, *450*, 304–308. [CrossRef]
67. Brower-Toland, B.; Findley, S.D.; Jiang, L.; Liu, L.; Yin, H.; Dus, M.; Zhou, P.; Elgin, S.C.; Lin, H. Drosophila PIWI associates with chromatin and interacts directly with HP1a. *Genes Dev.* **2007**, *21*, 2300–2311. [CrossRef] [PubMed]
68. Alekseyenko, A.A.; Gorchakov, A.A.; Zee, B.M.; Fuchs, S.M.; Kharchenko, P.V.; Kuroda, M.I. Heterochromatin-associated interactions of Drosophila HP1a with dADD1, HIPP1, and repetitive RNAs. *Genes Dev.* **2014**, *28*, 1445–1460. [CrossRef]
69. Lin, C.H.; Li, B.; Swanson, S.; Zhang, Y.; Florens, L.; Washburn, M.P.; Abmayr, S.M.; Workman, J.L. Heterochromatin Protein 1a stimulates histone H3 Lysine 36 demethylation by the drosophila KDM4A demethylase. *Mol. Cell* **2008**, *32*, 696–706. [CrossRef] [PubMed]
70. Swenson, J.M.; Colmenares, S.U.; Strom, A.R.; Costes, S.V.; Karpen, G.H. The composition and organization of Drosophila heterochromatin are heterogeneous and dynamic. *eLife* **2016**, *5*, 1–37. [CrossRef] [PubMed]
71. Kwon, S.H.; Florens, L.; Swanson, S.K.; Washburn, M.P.; Abmayr, S.M.; Workman, J.L. Heterochromatin protein 1 (HP1) connects the FACT histone chaperone complex to the phosphorylated CTD of RNA polymerase II. *Genes Dev.* **2010**, *24*, 2133–2145. [CrossRef] [PubMed]
72. Schotta, G.; Ebert, A.; Krauss, V.; Fischer, A.; Hoffmann, J.; Rea, S.; Jenuwein, T.; Dorn, R.; Reuter, G. Central role of Drosophila SU(VAR)3-9 in histone H3-K9 methylation and heterochromatic gene silencing. *EMBO J.* **2002**, *21*, 1121–1131. [CrossRef] [PubMed]
73. Ito, H.; Sato, K.; Koganezawa, M.; Ote, M.; Matsumoto, K.; Hama, C.; Yamamoto, D. Fruitless recruits two antagonistic chromatin factors to establish single-neuron sexual dimorphism. *Cell* **2012**, *149*, 1327–1338. [CrossRef] [PubMed]
74. Shaffer, C.D.; Stephens, G.E.; Thompson, B.A.; Funches, L.; Bernat, J.A.; Craig, C.A.; Elgin, S.C. Heterochromatin protein 2 (HP2), a partner of HP1 in Drosophila heterochromatin. *Proc. Natl. Acad. Sci. USA* **2002**, *99*, 14332–14337. [CrossRef] [PubMed]
75. Mendez, D.L.; Mandt, R.E.; Elgin, S.C. Heterochromatin protein 1a (HP1a) partner specificity is determined by critical amino acids in the chromo shadow domain and C-terminal extension. *J. Biol. Chem.* **2013**, *288*, 22315–22323. [CrossRef] [PubMed]
76. Bassett, A.R.; Cooper, S.E.; Ragab, A.; Travers, A.A. The chromatin remodelling factor dATRX is involved in heterochromatin formation. *PLoS ONE* **2008**, *3*, 5. [CrossRef]
77. Emelyanov, A.V.; Konev, A.Y.; Vershilova, E.; Fyodorov, D.V. Protein complex of Drosophila ATRX/XNP and HP1a is required for the formation of pericentric beta-heterochromatin in vivo. *J. Biol. Chem.* **2010**, *285*, 15027–15037. [CrossRef]
78. López-Falcón, B.; Meyer-Nava, S.; Hernández-Rodríguez, B.; Campos, A.; Montero, D.; Rudiño, E.; Vázquez, M.; Zurita, M.; Valadez-Graham, V. Characterization of the Drosophila group ortholog to the amino-terminus of the alpha-thalassemia and mental retardation X-linked (ATRX) vertebrate protein. *PLoS ONE* **2014**, *9*, e113182. [CrossRef]

79. Joppich, C.; Scholz, S.; Korge, G.; Schwendemann, A. Umbrea, a chromo shadow domain protein in Drosophila melanogaster heterochromatin, interacts with Hip, HP1 and HOAP. *Chromosom. Res.* **2009**, *17*, 19–36. [CrossRef]
80. Yang, F.; Quan, Z.; Huang, H.; He, M.; Liu, X.; Cai, T.; Xi, R. Ovaries absent links dLsd1 to HP1a for local H3K4 demethylation required for heterochromatic gene silencing. *eLife* **2019**, *8*, 1–21. [CrossRef]
81. Le Douarin, B.; Nielsen, A.L.; Garnier, J.M.; Ichinose, H.; Jeanmougin, F.; Losson, R.; Chambon, P. A possible involvement of TIF1 alpha and TIF1 beta in the epigenetic control of transcription by nuclear receptors. *EMBO J.* **1996**, *15*, 6701–6715. [CrossRef] [PubMed]
82. Nielsen, A.L.; Ortiz, J.A.; You, J.; Oulad-Abdelghani, M.; Khechumian, R.; Gansmuller, A.; Chambon, P.; Losson, R. Interaction with members of the heterochromatin protein 1 (HP1) family and histone deacetylation are differentially involved in transcriptional silencing by members of the TIF1 family. *EMBO J.* **1999**, *18*, 6385–6395. [CrossRef] [PubMed]
83. Murzina, N.; Verreault, A.; Laue, E.; Stillman, B. Heterochromatin dynamics in mouse cells: Interaction between chromatin assembly factor 1 and HP1 proteins. *Mol. Cell* **1999**, *4*, 529–540. [CrossRef]
84. Agarwal, N.; Hardt, T.; Brero, A.; Nowak, D.; Rothbauer, U.; Becker, A.; Leonhardt, H.; Cardoso, M.C. MeCP2 interacts with HP1 and modulates its heterochromatin association during myogenic differentiation. *Nucleic Acids Res.* **2007**, *35*, 5402–5408. [CrossRef]
85. Lechner, M.S.; Schultz, D.C.; Negorev, D.; Maul, G.G.; Rauscher, F.J. The mammalian heterochromatin protein 1 binds diverse nuclear proteins through a common motif that targets the chromoshadow domain. *Biochem. Biophys. Res. Commun.* **2005**, *331*, 929–937. [CrossRef]
86. Seeler, J.S.; Marchio, A.; Sitterlin, D.; Transy, C.; Dejean, A. Interaction of SP100 with HP1 proteins: A link between the promyelocytic leukemia-associated nuclear bodies and the chromatin compartment. *Proc. Natl. Acad. Sci. USA* **1998**, *95*, 7316–7321. [CrossRef]
87. McDowell, T.L.; Gibbons, R.J.; Sutherland, H.; O'Rourke, D.M.; Bickmore, W.A.; Pombo, A.; Turley, H.; Gatter, K.; Picketts, D.J.; Buckle, V.; et al. Localization of a putative transcriptional regulator (ATRX) at pericentromeric heterochromatin and the short arms of acrocentric chromosomes. *Proc. Natl. Acad. Sci. USA* **1999**, *96*, 13983–13988. [CrossRef]
88. Song, K.; Jung, Y.; Jung, D.; Lee, I. Human Ku70 Interacts with Heterochromatin Protein 1a. *J. Biol. Chem.* **2001**, *276*, 8321–8327. [CrossRef]
89. Vassallo, M.F.; Tanese, N. Isoform-specific interaction of HP1 with human TAFII130. *Proc. Natl. Acad. Sci. USA* **2002**, *99*, 5919–5924. [CrossRef]
90. Scholzen, T.; Endl, E.; Wohlenberg, C.; van der Sar, S.; Cowell, I.G.; Gerdes, J.; Singh, P.B. The Ki-67 protein interacts with members of the heterochromatin protein 1 (HP1) family: A potential role in the regulation of higher-order chromatin structure. *J. Pathol.* **2002**, *196*, 135–144. [CrossRef]
91. Nielsen, P.R.; Nietlispach, D.; Mott, H.R.; Callaghan, J.; Bannister, A.; Kouzarides, T.; Murzin, A.G.; Murzina, N.V.; Laue, E.D. Structure of the HP1 chromodomain bound to histone H3 methylated at lysine 9. *Nature* **2002**, *416*, 103–107. [CrossRef] [PubMed]
92. Nozawa, R.S.; Nagao, K.; Masuda, H.T.; Iwasaki, O.; Hirota, T.; Nozaki, N.; Kimura, H.; Obuse, C. Human POGZ modulates dissociation of HP1α from mitotic chromosome arms through Aurora, B. activation. *Nat. Cell Biol.* **2010**, *12*, 719–727. [CrossRef] [PubMed]
93. Ye, Q.; Worman, H.J. Interaction between an integral protein of the nuclear envelope inner membrane and human. *J. Biol. Chem.* **1996**, *271*, 14653–14656. [CrossRef] [PubMed]
94. Kang, J.; Chaudhary, J.; Dong, H.; Kim, S.; Brautigam, C.A.; Yu, H. Mitotic centromeric targeting of HP1 and its binding to Sgo1 are dispensable for sister-chromatid cohesion in human cells. *Mol. Biol. Cell* **2011**, *22*, 1181–1190. [CrossRef] [PubMed]
95. Wu, W.; Nishikawa, H.; Fukuda, T.; Vittal, V.; Asano, M.; Miyoshi, Y.; Klevit, R.E.; Ohta, T. Interaction of BARD1 and HP1 is required for BRCA1 retention at sites of DNA damage. *Cancer Res.* **2015**, *75*, 1311–1321. [CrossRef] [PubMed]
96. Borgel, J.; Tyl, M.; Schiller, K.; Pusztai, Z.; Dooley, C.M.; Deng, W.; Wooding, C.; White, R.J.; Warnecke, T.; Leonhardt, H.; et al. KDM2A integrates DNA and histone modification signals through a CXXC/PHD module and direct interaction with HP1. *Nucleic Acids Res.* **2017**, *45*, 1114–1129. [CrossRef]

97. Akram, S.; Yang, F.; Li, J.; Adams, G.; Liu, Y.; Zhuang, X.; Chu, L.; Liu, X.; Emmett, N.; Thompson, W.; et al. LRIF1 interacts with HP1α to coordinate accurate chromosome segregation during mitosis. *J. Mol. Cell Biol.* **2018**, *10*, 527–538. [CrossRef]
98. Yi, Q.; Chen, Q.; Liang, C.; Yan, H.; Zhang, Z.; Xiang, X.; Zhang, M.; Qi, F.; Zhou, L.; Wang, F. HP1 links centromeric heterochromatin to centromere cohesion in mammals. *EMBO Rep.* **2018**, *19*, e45484. [CrossRef] [PubMed]
99. Kim, J.M.; Shin, Y.; Lee, S.; Kim, M.Y.; Punj, V.; Shin, H.I.; Kim, K.; Koh, J.M.; Jeong, D.; An, W. MacroH2A1.2 inhibits prostate cancer-induced osteoclastogenesis through cooperation with HP1α and H1.2. *Oncogene* **2018**, *37*, 5749–5765. [CrossRef]
100. Zhang, C.L.; McKinsey, T.A.; Olson, E.N. Association of class II histone deacetylases with heterochromatin protein 1: Potential role for histone methylation in control of muscle differentiation. *Mol. Cell. Biol.* **2002**, *22*, 7302–7312. [CrossRef]
101. Vo, N.; Suong, D.N.A.; Yoshino, N.; Yoshida, H.; Cotterill, S.; Yamaguchi, M. Novel roles of HP1a and Mcm10 in DNA replication, genome maintenance and photoreceptor cell differentiation. *Nucleic Acids Res.* **2017**, *45*, 1233–1254. [CrossRef] [PubMed]
102. Apger, J.; Reubens, M.; Henderson, L.; Gouge, C.A.; Ilic, N.; Zhou, H.H.; Christensen, T.W. Multiple functions for drosophila Mcm10 suggested through analysis of two mcm10 mutant alleles. *Genetics* **2010**, *185*, 1151–1165. [CrossRef] [PubMed]
103. Roelens, B.; Clémot, M.; Leroux-Coyau, M.; Klapholz, B.; Dostatni, N. Maintenance of heterochromatin by the large subunit of the CAF-1 replication-coupled histone chaperone requires its interaction with HP1a through a conserved motif. *Genetics* **2017**, *205*, 125–137. [CrossRef] [PubMed]
104. Cenci, G.; Ciapponi, L.; Marzullo, M.; Raffa, G.D.; Morciano, P.; Raimondo, D.; Burla, R.; Saggio, I.; Gatti, M. The Analysis of Pendolino (peo) mutants reveals differences in the fusigenic potential among drosophila telomeres. *PLoS Genet.* **2015**, *11*, e1005260. [CrossRef] [PubMed]
105. Vedelek, B.; Blastyák, A.; Boros, I.M. Cross-species interaction between rapidly evolving telomere-specific drosophila proteins. *PLoS ONE* **2015**, *10*, e142771. [CrossRef] [PubMed]
106. Gao, G.; Walser, J.C.; Beaucher, M.L.; Morciano, P.; Wesolowska, N.; Chen, J.; Rong, Y.S. HipHop interacts with HOAP and HP1 to protect Drosophila telomeres in a sequence-independent manner. *EMBO J.* **2010**, *29*, 819–829. [CrossRef] [PubMed]
107. Raffa, G.D.; Siriaco, G.; Cugusi, S.; Ciapponi, L.; Cenci, G.; Wojcik, E.; Gatti, M. The Drosophila modigliani (moi) gene encodes a HOAP-interacting protein required for telomere protection. *Proc. Natl. Acad. Sci. USA* **2009**, *106*, 7–12. [CrossRef]
108. Quénet, D.; Gasser, V.; Fouillen, L.; Cammas, F.; Sanglier-Cianferani, S.; Losson, R.; Dantzer, F. The histone subcode: Poly(ADP-ribose) polymerase-1 (Parp-1) and Parp-2 control cell differentiation by regulating the transcriptional intermediary factor TIF1 and the heterochromatin protein HP1. *FASEB J.* **2008**, *22*, 3853-3865. [CrossRef]
109. Lin, C.; Li, C.; Huang, P.; Lee, F.S. A developmentally regulated ARF-like 5 protein (ARL5), localized to nuclei and nucleoli, interacts with heterochromatin protein 1. *J. Cell Sci.* **2002**, *115*, 4433–4445. [CrossRef]
110. Ainsztein, A.M.; Kandels-Lewis, S.E.; Mackay, A.M.; Earnshaw, W.C. INCENP centromere and spindle targeting: Identification of essential conserved motifs and involvement of heterochromatin protein HP1. *J. Cell Biol.* **1998**, *143*, 1763–1774. [CrossRef]
111. Ye, Q.; Callebaut, I.; Pezhman, A.; Courvalin, J.-C.; Worman, H.J. Domain-specific interactions of human HP1-type chromosomain proteins and inner nuclear membrane protein LBR. *J. Biol. Chem.* **1997**, *271*, 14983–14989. [CrossRef] [PubMed]
112. Lomberk, G.; Wallrath, L.L.; Urrutia, R. The heterochromatin protein 1 family. *Genome Biol.* **2006**, *7*, 1–8. [CrossRef] [PubMed]
113. Keller, C.; Adaixo, R.; Stunnenberg, R.; Woolcock, K.J.; Hiller, S.; Bühler, M. HP1 Swi6 mediates the recognition and destruction of heterochromatic RNA transcripts. *Mol. Cell* **2012**, *47*, 215–227. [CrossRef] [PubMed]
114. Wang, G.; Ma, A.; Chow, C.M.; Horsley, D.; Brown, N.R.; Cowell, I.G.; Singh, P.B. Conservation of heterochromatin protein 1 function. *Mol. Cell. Biol.* **2000**, *20*, 6970–6983. [CrossRef] [PubMed]
115. Shareef, M.M.; King, C.; Damaj, M.; Badagu, R.; Huang, D.W.; Kellum, R. Drosophila Heterochromatin Protein 1 (HP1)/Origin Recognition Complex (ORC) Protein is associated with HP1 and ORC and functions in heterochromatin- induced silencing. *Mol. Biol. Cell* **2001**, *12*, 1671–1685. [CrossRef] [PubMed]

116. Badugu, R.K.; Yoo, Y.; Singh, P.B.; Kellum, R. Mutations in the heterochromatin protein 1 (HP1) hinge domain affect HP1 protein interactions and chromosomal distribution. *Chromosoma* **2005**, *113*, 370–384. [CrossRef]
117. Zhao, T.; Heyduk, T.; Eissenberg, J.C. Phosphorylation site mutations in heterochromatin Protein 1 (HP1) reduce or eliminate silencing activity. *J. Biol. Chem.* **2001**, *276*, 9512–9518. [CrossRef]
118. Gaudin, V.; Libault, M.; Pouteau, S.; Juul, T.; Zhao, G.; Lefebvre, D.; Grandjean, O. Mutations in LIKE HETEROCHROMATIN PROTEIN 1 affect flowering time and plant architecture in Arabidopsis. *Development* **2001**, *128*, 4847–4858.
119. Bawa-Khalfe, T.; Lu, L.S.; Zuo, Y.; Huang, C.; Dere, R.; Lin, F.M.; Yeh, E.T. Differential expression of SUMO-specific protease 7 variants regulates epithelial-mesenchymal transition. *Proc. Natl. Acad. Sci. USA* **2012**, *109*, 17466–17471. [CrossRef]
120. Machida, S.; Takizawa, Y.; Ishimaru, M.; Sugita, Y.; Sekine, S.; Nakayama, J.I.; Wolf, M.; Kurumizaka, H. Structural basis of heterochromatin formation by human HP1. *Mol. Cell* **2018**, *69*, 385–397. [CrossRef] [PubMed]
121. Saunders, W.S.; Chue, C.; Goebl, M.; Craig, C.; Clark, R.F.; Powers, J.A.; Eissenberg, J.C.; Elgin, S.C.; Rothfield, N.F.; Earnshaw, W.C. Molecular cloning of a human homologue of Drosophila heterochromatin protein HP1 using anti-centromere autoantibodies with anti-chromo specificity. *J. Cell Sci.* **1993**, *104*, 573–582. [PubMed]
122. Vermaak, D.; Henikoff, S.; Malik, H.S. Positive selection drives the evolution of rhino, a member of the heterochromatin protein 1 family in drosophila. *PLoS Genet.* **2005**, *1*, e10009. [CrossRef] [PubMed]
123. Klattenhoff, C.; Xi, H.; Li, C.; Lee, S.; Xu, J.; Khurana, J.S.; Zhang, F.; Schultz, N.; Koppetsch, B.S.; Nowosielska, A.; et al. The Drosophila HP1 homolog rhino is required for transposon silencing and piRNA production by dual-strand clusters. *Cell* **2009**, *138*, 1137–1149. [CrossRef] [PubMed]
124. Fanti, L.; Berloco, M.; Piacentini, L.; Pimpinelli, S. Chromosomal distribution of heterochromatin protein 1 (HP1) in drosophila: A cytological map of euchromatic HP1 binding sites. *Genetica* **2003**, *117*, 135–147. [CrossRef]
125. Font-Burgada, J.; Rossell, D.; Auer, H.; Azorín, F. Drosophila HP1c isoform interacts with the zinc-finger proteins WOC and Relative-of-WOC to regulate gene expression. *Genes Dev.* **2008**, *22*, 3007–3023. [CrossRef] [PubMed]
126. Vermaak, D.; Malik, H.S. Multiple roles for heterochromatin protein 1 genes in drosophila. *Annu. Rev. Genet.* **2009**, *43*, 467–492. [CrossRef]
127. Li, Y.; Kirschmann, D.A.; Wallrath, L.L. Does heterochromatin protein 1 always follow code? *Proc. Natl. Acad. Sci. USA* **2002**, *99*, 16462–16469. [CrossRef]
128. Larson, A.G.; Elnatan, D.; Keenen, M.M.; Trnka, M.J.; Johnston, J.B.; Burlingame, A.L.; Agard, D.A.; Redding, S.; Narlikar, G.J. Liquid droplet formation by HP1α suggests a role for phase separation in heterochromatin. *Nature* **2017**, *547*, 236–240. [CrossRef]
129. Zhang, D.; Wang, D.; Sun, F. Drosophila melanogaster heterochromatin protein HP1b plays important roles in transcriptional activation and development. *Chromosoma* **2011**, *120*, 97–108. [CrossRef]
130. Abel, J.; Eskeland, R.; Raffa, G.D.; Kremmer, E. Imhof. Drosophila HP1c is regulated by an auto-regulatory feedback loop through its binding partner Woc. *PLoS ONE* **2009**, *4*, e5089. [CrossRef]
131. Frankel, S.; Sigel, E.A.; Craig, C.; Elgin, S.C.R.; Mooseker, M.S.; Tsakonas, S.A. An actin-related protein in Drosophila colocalizes with heterochromatin protein 1 in pericentric heterochromatin. *J. Cell Sci.* **1997**, *110*, 1999–2012. [PubMed]
132. Kato, M.; Sasaki, M.; Mizuno, S.; Harata, M. Novel actin-related proteins in vertebrates: Similarities of structure and expression pattern to Arp6 localized on Drosophila heterochromatin. *Gene* **2001**, *268*, 133–140. [CrossRef]
133. Stephens, G.E.; Xiao, H.; Lankenau, D.H.; Wu, C.; Elgin, S.C.R. Heterochromatin protein 2 interacts with Nap-1 and NURF: A link between heterochromatin-induced gene silencing and the chromatin remodeling machinery in Drosophila. *Biochemistry* **2006**, *45*, 14990–14999. [CrossRef] [PubMed]
134. Rudolph, T.; Yonezawa, M.; Lein, S.; Heidrich, K.; Kubicek, S.; Schäfer, C.; Phalke, S.; Walther, M.; Schmidt, A.; Jenuwein, T.; et al. Heterochromatin formation in drosophila is initiated through active removal of H3K4. *Mol. Cell.* **2007**, *2*, 103–115. [CrossRef] [PubMed]
135. Johansson, A.M.; Stenberg, P.; Pettersson, F.; Larsson, J. POF and HP1 bind expressed exons, suggesting a balancing mechanism for gene regulation. *PLoS Genet.* **2007**, *3*, e30209. [CrossRef] [PubMed]

136. Tzeng, T.-Y.; Lee, C.-H.; Chan, L.-W.; Shen, C.-K.J. Epigenetic regulation of the Drosophila chromosome 4 by the histone H3K9 methyltransferase dSETDB1. *Proc. Natl. Acad. Sci. USA* **2007**, *104*, 12691–12696. [CrossRef]
137. Przewloka, M.R.; Zhang, W.; Costa, P.; Archambault, V.; D'Avino, P.P.; Lilley, K.S.; Laue, E.D.; McAinsh, A.D.; Glover, D.M. Molecular analysis of core kinetochore composition and assembly in drosophila melanogaster. *PLoS ONE* **2007**, *2*, e478. [CrossRef]
138. Guruharsha, K.G.; Rual, J.F.; Zhai, B.; Mintseris, J.; Vaidya, P.; Vaidya, N.; Beekman, C.; Wong, C.; Rhee, D.Y.; Cenaj, O.; et al. A protein complex network of drosophila melanogaster. *Cell* **2011**, *147*, 690–703. [CrossRef]
139. Gracheva, E.; Dus, M.; Elgin, S.C.R. Drosophila RISC component VIG and its homolog Vig2 impact heterochromatin formation. *PLoS ONE* **2009**, *4*, e6182. [CrossRef]
140. Raffa, G.D.; Raimondo, D.; Sorino, C.; Cugusi, S.; Cenci, G.; Cacchione, S.; Gatti, M.; Ciapponi, L. Verrocchio, a Drosophila OB fold-containing protein, is a component of the terminin telomere-capping complex. *Genes Dev.* **2010**, *24*, 1596–1601. [CrossRef]
141. Seong, K.; Li, D.; Shimizu, H.; Nakamura, R.; Ishii, S. Inheritance of stress-induced, ATF-2-dependent epigenetic change. *Cell* **2011**, *145*, 1049–1061. [CrossRef] [PubMed]
142. Anand, A.; Kai, T. The tudor domain protein Kumo is required to assemble the nuage and to generate germline piRNAs in Drosophila. *EMBO J.* **2011**, *31*, 870–882. [CrossRef] [PubMed]
143. Dronamraju, R.; Mason, J.M. MU2 and HP1a regulate the recognition of double strand breaks in Drosophila melanogaster. *PLoS ONE* **2011**, *6*, e25439. [CrossRef] [PubMed]
144. Chiolo, I.; Minoda, A.; Colmenares, S.U.; Polyzos, A.; Costes, S.V.; Karpen, G.H. Double-strand breaks in heterochromatin move outside of a dynamic HP1a domain to complete recombinational repair. *Cell* **2011**, *144*, 732–744. [CrossRef] [PubMed]
145. Tan, H.; Qurashi, A.; Poidevin, M.; Nelson, D.L.; Li, H.; Jin, P. Retrotransposon activation contributes to fragile X premutation rCGG-mediated neurodegeneration. *Hum. Mol. Genet.* **2012**, *21*, 57–65. [CrossRef] [PubMed]
146. Salvany, L.; Requena, D.; Azpiazu, N. Functional association between eyegone and HP1a mediates wingless transcriptional repression during development. *Mol. Cell. Biol.* **2012**, *32*, 2407–2415. [CrossRef] [PubMed]
147. Kavi, H.; Emelyanov, A.V.; Fyodorov, D.V.; Skoultchi, A.I. Independent biological and biochemical functions for individual structural domains of drosophila linker histone H1. *J. Biol. Chem.* **2016**, *291*, 15143–15155. [CrossRef]
148. Lu, X.; Wontakal, S.N.; Kavi, H.; Kim, B.J.; Guzzardo, P.M.; Emelyanov, A.V.; Xu, N.; Hannon, G.J.; Zavadil, J.; Fyodorov, D.V.; et al. Drosophila H1 regulates the genetic activity od heterochromatin by recruitment of su(var)3-9. *Science* **2013**, *340*, 78–81. [CrossRef]
149. Thomae, A.W.; Schade, G.O.; Padeken, J.; Borath, M.; Vetter, I.; Kremmer, E.; Heun, P.; Imhof, A. Article A pair of centromeric proteins mediates reproductive isolation in drosophila species. *Dev. Cell* **2013**, *27*, 412–424. [CrossRef]
150. Satyaki, P.R.; Cuykendall, T.N.; Wei, K.H.; Brideau, N.J.; Kwak, H.; Aruna, S.; Ferree, P.M.; Ji, S.; Barbash, D.A. The Hmr and Lhr hybrid incompatibility genes suppress a broad range of heterochromatic repeats. *PLoS Genet.* **2014**, *10*, e1004240. [CrossRef]
151. Brideau, N.J.; Barbash, D.A. Functional conservation of the Drosophila hybrid incompatibility gene Lhr. *BMC E Biol.* **2011**, *11*. [CrossRef] [PubMed]
152. Xu, N.; Emelyanov, A.V.; Fyodorov, D.V.; Skoultchi, A.I. Drosophila linker histone H1 coordinates STAT-dependent organization of heterochromatin and suppresses tumorigenesis caused by hyperactive JAK-STAT signaling. *Epigenetics Chromatin.* **2014**, *7*. [CrossRef] [PubMed]
153. Shi, S.; Larson, K.; Guo, D.; Lim, S.J.; Dutta, P.; Yan, S.J.; Li, W.X. Drosophila STAT is required for directly maintaining HP1 localization and heterochromatin stability. *Nat. Cell Biol.* **2008**, *10*, 489–496. [CrossRef] [PubMed]
154. Marr, S.K.; Lis, J.T.; Treisman, J.E.; Ii, T.M. Viability and is found at both active genes and pericentric heterochromatin in drosophila melanogaster. *Mol. Cell. Biol.* **2014**, *34*, 2710–2720. [CrossRef] [PubMed]
155. Messina, G.; Damia, E.; Fanti, L.; Atterrato, M.T.; Celauro, E.; Mariotti, F.R.; Accardo, M.C.; Walther, M.; Vernì, F.; Picchioni, D.; et al. Yeti, an essential Drosophila melanogaster gene, encodes a protein required for chromatin organization. *J. Cell Sci.* **2014**, *127*, 2577–2588. [CrossRef] [PubMed]

156. van Bemmel, J.G.; Filion, G.J.; Rosado, A.; Talhout, W.; de Haas, M.; van Welsem, T.; van Leeuwen, F.; van Steensel, B. Resource a network model of the molecular organization of chromatin in drosophila. *Mol. Cell* **2013**, *49*, 759–771. [CrossRef]
157. Shokri, L.; Inukai, S.; Hafner, A.; Weinand, K.; Hens, K.; Vedenko, A.; Gisselbrecht, S.S.; Dainese, R.; Bischof, J.; Furger, E.; et al. A comprehensive drosophila melanogaster transcription factor interactome. *Cell Rep.* **2019**, *27*, 955–970.e7. [CrossRef]
158. Liu, Y.; Zhang, D. HP1a/KDM4A is involved in the autoregulatory loop of the oncogene gene c-Jun. *Epigenetics* **2015**, *10*, 453–459. [CrossRef]
159. Eberle, A.B.; Jordán-Pla, A.; Gañez-Zapater, A.; Hessle, V.; Silberberg, G.; von Euler, A.; Silverstein, R.A.; Visa, N. An interaction between RRP6 and SU(VAR)3-9 Targets RRP6 to heterochromatin and contributes to heterochromatin maintenance in drosophila melanogaster. *PLoS Genet.* **2015**, *11*, e1005523. [CrossRef]
160. Cabrera, J.R.; Olcese, U.; Horabin, J.I. A balancing act: Heterochromatin protein 1a and the polycomb group coordinate their levels to silence chromatin in Drosophila. *Epigenetics Chromatin.* **2015**, *8*, 1–21. [CrossRef]
161. Cipressa, F.; Morciano, P.; Bosso, G.; Mannini, L.; Galati, A.; Raffa, G.D.; Cacchione, S.; Musio, A.; Cenci, G. A role for Separase in telomere protection. *Nat. Commun.* **2016**, *7*, 1–9. [CrossRef]
162. Vinayagam, A.; Kulkarni, M.M.; Sopko, R.; Sun, X.; Hu, Y.; Nand, A.; Villalta, C.; Moghimi, A.; Yang, X.; Mohr, S.E.; et al. An integrative analysis of the InR/PI3K/Akt network identifies the dynamic response to insulin signaling. *Cell Rep.* **2016**, *16*, 3062–3074. [CrossRef] [PubMed]
163. Yamada, T.; Tahara, E.; Kanke, M.; Kuwata, K.; Nishiyama, T. Drosophila dalmatian combines sororin and shugoshin roles in establishment and protection of cohesion. *EMBO J.* **2017**, *36*, 1513–1527. [CrossRef] [PubMed]
164. Bischof, J.; Duffraisse, M.; Furger, E.; Ajuria, L.; Giraud, G.; Vanderperre, S.; Paul, R.; Björklund, M.; Ahr, D.; Ahmed, A.W.; et al. Generation of a versatile BiFC ORFeome library for analyzing protein—Protein interactions in live Drosophila. *eLife* **2018**, *7*. [CrossRef] [PubMed]
165. Jankovics, F.; Bence, M.; Sinka, R.; Faragó, A.; Bodai, L.; Pettkó-Szandtner, A.; Ibrahim, K.; Takács, Z.; Szarka-Kovács, A.B.; Erdélyi, M. Drosophila small ovary gene is required for transposon silencing and heterochromatin organization, and ensures germline stem cell maintenance and differentiation. *Development* **2018**, *145*, 23. [CrossRef]
166. Thiru, A.; Nietlispach, D.; Mott, H.R.; Okuwaki, M.; Lyon, D.; Nielsen, P.R.; Hirshberg, M.; Verreault, A.; Murzina, N.V.; Laue, E.D. Structural basis of HP1/PXVXL motif peptide interactions and HP1 localisation to heterochromatin. *EMBO J.* **2004**, *23*, 489–499. [CrossRef]
167. Lomberk, G.; Bensi, D.; Fernandez-Zapico, M.E.; Urrutia, R. Evidence for the existence of an HP1-mediated subcode within the histone code. *Nat. Cell Biol.* **2006**, *8*, 407–415. [CrossRef]
168. Stephens, G.E.; Slawson, E.E.; Craig, C.A.; Elgin, S.C. Interaction of Heterochromatin Protein 2 with HP1 Defines a Novel HP1-Binding. *Biochemistry* **2005**, *44*, 13394–13403. [CrossRef]
169. Eustermann, S.; Yang, J.C.; Law, M.J.; Amos, R.; Chapman, L.M.; Jelinska, C.; Garrick, D.; Clynes, D.; Gibbons, R.J.; Rhodes, D.; et al. Combinatorial readout of histone H3 modifications specifies localization of ATRX to heterochromatin. *Nat. Struct. Mol. Biol.* **2011**, *18*, 777–782. [CrossRef]
170. van Bortle, K.; Corces, V.G. Nuclear organization and genome function. *Annu. Rev. Cell Dev. Biol.* **2012**, *28*, 163–187. [CrossRef]
171. Beishline, K.; Vladimirova, O.; Tutton, S.; Wang, Z.; Deng, Z.; Lieberman, P.M. CTCF driven TERRA transcription facilitates completion of telomere DNA replication. *Nat. Commun.* **2017**, *8*, 1–10. [CrossRef] [PubMed]
172. Lis, J.T.; Simon, J.A.; Sutton, C.A. New heat shock puffs and β-galactosidase activity resulting from transformation of Drosophila with an hsp70-lacZ hybrid gene. *Cell* **1983**, *35*, 403–410. [CrossRef]
173. Kellum, R.; Schedl, P. A position-effect assay for boundaries of higher order chromosomal domains. *Cell* **1991**, *64*, 941–950. [CrossRef]
174. Udvardy, A.; Maine, E.; Schedl, P. The 87A7 chromomere. Identification of novel chromatin structures flanking the heat shock locus that may define the boundaries of higher order domains. *J. Mol. Biol.* **1985**, *185*, 341–358. [CrossRef]
175. Li, Q.; Starnatoyannopoulos, G. Hypersensitive site 5 of the human B Locus control region functions as a chromatin insulator. *Blood* **1994**, *84*, 1399–1401. [CrossRef]

176. Filippova, G.N.; Fagerlie, S.; Klenova, E.M.; Myers, C.; Dehner, Y.; Goodwin, G.; Neiman, P.E.; Collins, S.J.; Lobanenkov, V.V. An exceptionally conserved transcriptional repressor, CTCF, employs different combinations of zinc fingers to bind diverged promoter sequences of avian and mammalian c-myc oncogenes. *Mol. Cell. Biol.* **1996**, *16*, 2802–2813. [CrossRef]
177. Felsenfeld, G.; Bell, A.C. Methylation of a CTCF-dependent boundary controls imprinted expressionof the *Igf2* gene. *Nature* **2000**, *405*, 482–485.
178. Rao, S.S.; Huntley, M.H.; Durand, N.C.; Stamenova, E.K.; Bochkov, I.D.; Robinson, J.T.; Sanborn, A.L.; Machol, I.; Omer, A.D.; Lander, E.S.; et al. A 3D map of the human genome at kilobase resolution reveals principles of chromatin looping. *Cell* **2014**, *159*, 1665–1680. [CrossRef]
179. Dixon, J.R.; Selvaraj, S.; Yue, F.; Kim, A.; Li, Y.; Shen, Y.; Hu, M.; Liu, J.S.; Ren, B. Topological domains in mammalian genomes identified by analysis of chromatin interactions. *Nature* **2012**, *485*, 376–380. [CrossRef]
180. Brackley, C.A.; Johnson, J.; Michieletto, D.; Morozov, A.; Nicodemi, M.; Cook, P.; Marenduzzo, D. Nonequilibrium chromosome looping via molecular slip links. *Phys. Rev. Lett.* **2017**, *119*, 1–5. [CrossRef]
181. Maksimenko, O.; Bartkuhn, M.; Stakhov, V.; Herold, M.; Zolotarev, N.; Jox, T.; Buxa, M.K.; Kirsch, R.; Bonchuk, A.; Fedotova, A.; et al. Two new insulator proteins, Pita and ZIPIC, target CP190 to chromatin. *Genome Res.* **2015**, *25*, 89–99. [CrossRef] [PubMed]
182. Van Bortle, K.; Nichols, M.H.; Li, L.; Ong, C.T.; Takenaka, N.; Qin, Z.S.; Corces, V.G. Insulator function and topological domain border strength scale with architectural protein occupancy. *Genome Biol.* **2014**, *15*, R82. [CrossRef] [PubMed]
183. Yang, J.; Ramos, E.; Corces, V.G. The BEAF-32 insulator coordinates genome organization and function during the evolution of Drosophila species. *Genome Res.* **2012**, *22*, 2199–2207. [CrossRef] [PubMed]
184. Roseman, R.R.; Pirrotta, V.; Geyer, P.K. The su(Hw) protein insulates expression of the drosophila melanogaster white gene from chromosomal position-effects. *EMBO J.* **1993**, *12*, 435–442. [CrossRef] [PubMed]
185. MacDonald, W.A.; Menon, D.; Bartlett, N.J.; Sperry, G.E.; Rasheva, V.; Meller, V.; Lloyd, V.K. The drosophila homolog of the mammalian imprint regulator, CTCF, maintains the maternal genomic imprint in drosophila melanogaster. *BMC Biol.* **2010**, *8*, 105. [CrossRef] [PubMed]
186. Ohtsuki, S.; Levine, M. GAGA mediates the enhancer blocking activity of the eve promoter in the drosophila embryo. *Genes Dev.* **1998**, *12*, 3325–3330. [CrossRef]
187. Gaszner, M.; Vazquez, J.; Schedl, P. The Zw5 protein, a component of the scs chromatin domain boundary, is able to block enhancer-promoter interaction. *Genes Dev.* **1999**, *13*, 2098–2107. [CrossRef]
188. Aoki, T.; Sarkeshik, A.; Yates, J.; Schedl, P. Elba, a novel developmentally regulated chromatin boundary factor is a hetero-tripartite DNA binding complex. *eLife* **2012**, *1*, 1–24. [CrossRef]
189. Bag, I.; Dale, R.K.; Palmer, C.; Lei, E.P. The zinc-finger protein CLAMP promotes gypsy chromatin insulator function in Drosophila. *J. Cell Sci.* **2019**, *132*, 6. [CrossRef]
190. Cuartero, S.; Fresán, U.; Reina, O.; Planet, E.; Espinàs, M.L. Ibf1 and Ibf2 are novel CP190-interacting proteins required for insulator function. *EMBO J.* **2014**, *33*, 637–647. [CrossRef]
191. Gerasimova, T.I.; Gdula, D.A.; Gerasimov, D.V.; Simonova, O.; Corces, V.G. A drosophila protein that imparts directionality on a chromatin insulator is an enhancer of position-effect variegation. *Cell* **1995**, *82*, 587–597. [CrossRef]
192. Savitsky, M.; Kim, M.; Kravchuk, O.; Schwartz, Y.B. Distinct roles of chromatin insulator proteins in control of the Drosophila bithorax complex. *Genetics* **2016**, *202*, 601–617. [CrossRef] [PubMed]
193. Bartkuhn, M.; Straub, T.; Herold, M.; Herrmann, M.; Rathke, C.; Saumweber, H.; Gilfillan, G.D.; Becker, P.B.; Renkawitz, R. Active promoters and insulators are marked by the centrosomal protein 190. *EMBO J.* **2009**, *28*, 877–888. [CrossRef] [PubMed]
194. Pherson, M.; Misulovin, Z.; Gause, M.; Dorsett, D. Cohesin occupancy and composition at enhancers and promoters are linked to DNA replication origin proximity in Drosophila. *Genome Res.* **2019**, *29*, 602–612. [CrossRef] [PubMed]
195. Lahn, B.T.; Tang, Z.L.; Zhou, J.; Barndt, R.J.; Parvinen, M.; Allis, C.D.; Page, D.C. Previously uncharacterized histone acetyltransferases implicated in mammalian spermatogenesis. *Proc. Natl. Acad. Sci. USA* **2002**, *99*, 8707–8712. [CrossRef] [PubMed]
196. Caron, C.; Pivot-Pajot, C.; van Grunsven, L.A.; Col, E.; Lestrat, C.; Rousseaux, S.; Khochbin, S. Cdyl: A new transcriptional co-repressor. *EMBO Rep.* **2003**, *4*, 877–882. [CrossRef]

197. Liu, S.; Yu, H.; Liu, Y.; Liu, X.; Zhang, Y.; Bu, C.; Yuan, S.; Chen, Z.; Xie, G.; Li, W.; et al. Chromodomain protein CDYL acts as a Crotonyl-CoA hydratase to regulate histone crotonylation and spermatogenesis. *Mol. Cell* **2017**, *67*, 853–866. [CrossRef]
198. Glenn, S.E.; Geyer, P.K. Investigation of the developmental requirements of drosophila HP1 and insulator protein partner, HIPP1. *G3 Genes Genomes Genet.* **2019**, *9*, 345–357. [CrossRef]
199. Stow, E.C.; An, R.; Schoborg, T.A.; Davenport, N.M.; Simmons, J.R. A drosophila insulator interacting protein suppresses enhancer-blocking function and modulates replication timing. *bioRxiv* **2019**. [CrossRef]
200. Melnikova, L.; Molodina, V.; Erokhin, M.; Georgiev, P.; Golovnin, A. HIPP1 stabilizes the interaction between CP190 and Su(Hw) in the drosophila insulator complex. *Sci. Rep.* **2019**, *9*, 1–13. [CrossRef]
201. Parelho, V.; Hadjur, S.; Spivakov, M.; Leleu, M.; Sauer, S.; Gregson, H.C.; Jarmuz, A.; Canzonetta, C.; Webster, Z.; Nesterova, T.; et al. Cohesins functionally associate with CTCF on mammalian chromosome arms. *Cell* **2008**, *132*, 422–433. [CrossRef] [PubMed]
202. Rubio, E.D.; Reiss, D.J.; Welcsh, P.L.; Disteche, C.M.; Filippova, G.N.; Baliga, N.S.; Aebersold, R.; Ranish, J.A.; Krumm, A. CTCF physically links cohesin to chromatin. *Proc. Natl. Acad. Sci. USA.* **2008**, *105*, 8309–8314. [CrossRef] [PubMed]
203. Holohan, E.E.; Kwong, C.; Adryan, B.; Bartkuhn, M.; Herold, M.; Renkawitz, R.; Russell, S.; White, R. CTCF genomic binding sites in Drosophila and the organisation of the bithorax complex. *PLoS Genet.* **2007**, *3*, e30112. [CrossRef]
204. Misulovin, Z.; Schwartz, Y.B.; Li, X.Y.; Kahn, T.G.; Gause, M.; MacArthur, S.; Fay, J.C.; Eisen, M.B.; Pirrotta, V.; Biggin, M.D.; et al. Association of cohesin and Nipped-B with transcriptionally active regions of the drosophila melanogaster genome. *Chromosoma* **2008**, *117*, 89–102. [CrossRef] [PubMed]
205. Karch, F.; Galloni, M.; Sipos, L.; Gausz, J.; Gyurkovics, H.; Sched, P. Mcp and Fab-7: Molecular analysis of putative boundaries of cis-regulatory domains in the bithorax complex of drosophila melanogaster. *Nucleic Acids Res.* **1994**, *22*, 3138–3146. [CrossRef]
206. Cavalli, G.; Paro, R. The Drosophila Fab-7 chromosomal element conveys epigenetic inheritance during mitosis and meiosis. *Cell* **1998**, *93*, 505–518. [CrossRef]
207. Pérez-Lluch, S.; Cuartero, S.; Azorín, F.; Espinàs, M.L. Characterization of new regulatory elements within the drosophila bithorax complex. *Nucleic Acids Res.* **2008**, *36*, 6926–6933. [CrossRef]
208. Moon, H.; Filippova, G.; Loukinov, D.; Pugacheva, E.; Chen, Q.; Smith, S.T.; Munhall, A.; Grewe, B.; Bartkuhn, M.; Arnold, R.; et al. CTCF is conserved from Drosophila to humans and confers enhancer blocking of the Fab-8 insulator. *EMBO Rep.* **2005**, *6*, 165–170. [CrossRef]
209. Mohan, M.; Bartkuhn, M.; Herold, M.; Philippen, A.; Heinl, N.; Bardenhagen, I.; Leers, J.; White, A.R.; Renkawitz-Pohl, R.; Saumweber, H.; et al. The drosophila insulator proteins CTCF and CP190 link enhancer blocking to body patterning. *EMBO J.* **2007**, *26*, 4203–4214. [CrossRef]
210. Muller, M.; Hagstrom, K.; Gyurkovics, H.; Pirrotta, V.; Schedl, P. The Mcp element from the Drosophila melanogaster bithorax complex mediates long-distance regulatory interactions. *Genetics* **1999**, *153*, 1333–1356.
211. Sipos, L.; Gyurkovics, H. Long-distance interactions between enhancers and promoters: The case of the Abd-B domain of the Drosophila bithorax complex. *FEBS J.* **2005**, *272*, 3253-3259. [CrossRef] [PubMed]
212. Kyrchanova, O.; Toshchakov, S.; Podstreshnaya, Y.; Parshikov, A.; Georgiev, P. Functional interaction between the Fab-7 and Fab-8 boundaries and the upstream promoter region in the drosophila Abd-B gene. *Mol. Cell. Biol.* **2008**, *28*, 4188–4195. [CrossRef] [PubMed]
213. Postika, N.; Metzler, M.; Affolter, M.; Müller, M.; Schedl, P.; Georgiev, P.; Kyrchanova, O. Boundaries mediate long-distance interactions between enhancers and promoters in the drosophila bithorax complex. *PLoS Genet.* **2018**, *14*, e1007702. [CrossRef] [PubMed]
214. Heger, P.; Marin, B.; Bartkuhn, M.; Schierenberg, E.; Wiehe, T. The chromatin insulator CTCF and the emergence of metazoan diversity. *Proc. Natl. Acad. Sci. USA* **2012**, *109*, 17507–17512. [CrossRef] [PubMed]
215. Heger, P.; George, R.; Wiehe, T. Successive gain of insulator proteins in arthropod evolution. *Evolution* **2013**, *67*, 2945–2956. [CrossRef] [PubMed]
216. Seller, C.A.; Cho, C.-Y.; O'Farrell, P.H. Rapid embryonic cell cycles defer the establishment of heterochromatin by Eggless/SetDB1 in drosophila. *Genes Dev.* **2019**, *33*, 403–417. [CrossRef]
217. Armstrong, R.L.; Duronio, R.J. Phasing in heterochromatin during development. *Genes Dev.* **2019**, *33*, 379–381. [CrossRef]

218. Fuks, F.; Hurd, P.J.; Deplus, R.; Kouzarides, T. The DNA methyltransferases associate with HP1 and the SUV39H1 histone methyltransferase. *Nucleic Acids Res.* **2003**, *31*, 2305–2312. [CrossRef]
219. Muramatsu, D.; Kimura, H.; Kotoshiba, K.; Tachibana, M.; Shinkai, Y. Pericentric H3K9me3 Formation by HP1 Interaction-defective Histone Methyltransferase Suv39h1. *Cell Struct. Funct.* **2016**, *41*, 145–152. [CrossRef]
220. Eissenberg, J.C.; Elgin, S.C. The HP1 protein family: Getting a grip on chromation. *Curr. Opin. Genet. Dev.* **2000**, *10*, 204. [CrossRef]
221. Eissenberg, J.C.; Elgin, S.C.R. HP1a: A structural chromosomal protein regulating transcription. *Trends Genet.* **2014**, *30*, 103–110. [CrossRef] [PubMed]
222. Hwang, K.K.; Eissenberg, J.C.; Worman, H.J. Transcriptional repression of euchromatic genes by Drosophila heterochromatin protein 1 and histone modifiers. *Proc. Natl. Acad. Sci. USA* **2001**, *98*, 11423–11427. [CrossRef] [PubMed]
223. Singh, P.B.; Georgatos, S.D. HP1: Facts, open questions, and speculation. *J. Struct. Biol.* **2002**, *140*, 10–16. [CrossRef]
224. Reuter, G.; Giarre, M.; Farah, J.; Gausz, J.; Spierer, A.; Spierer, P. Dependence of position-effect variegation in Drosophila on dose of a gene encoding an unusual zinc-finger protein. *Nature* **1990**, *6263*, 219–223. [CrossRef] [PubMed]
225. Tschiersch, B.; Hofmann, A.; Krauss, V.; Dorn, R.; Korge, G.; Reuter, G. The protein encoded by the Drosophila position-effect variegation suppressor gene Su(var)3-9 combines domains of antagonistic regulators of homeotic gene complexes. *EMBO J.* **1994**, *13*, 3822–3831. [CrossRef] [PubMed]
226. Hoskins, R.A.; Smith, C.D.; Carlson, J.W.; Carvalho, A.B.; Halpern, A.; Kaminker, J.S.; Kennedy, C.; Mungall, C.; Sullivan, B.A.; Sutton, G.; et al. Heterochromatic sequences in a drosophila whole-genome shotgun assembly. *Genome Biol.* **2002**, *3*, 1–16. [CrossRef]
227. Hoskins, R.A.; Carlson, J.W.; Kennedy, C.; Acevedo, D.; Evans-Holm, M.; Frise, E.; Wan, K.H.; Park, S.; Mendez-Lago, M.; Rossi, F.; et al. Sequence finishing and mapping of drosophila melanogaster heterochromatin. *Science* **2007**, *316*, 1625–1628. [CrossRef]
228. Ciavatta, D.; Rogers, S.; Magnuson, T. Drosophila CTCF Is Required for Fab-8 enhancer blocking activity in S2 Cells. *J. Mol. Biol.* **2007**, *373*, 233–239. [CrossRef] [PubMed]
229. Bonchuk, A.; Maksimenko, O.; Kyrchanova, O.; Ivlieva, T.; Mogila, V.; Deshpande, G.; Wolle, D.; Schedl, P.; Georgiev, P. Functional role of dimerization and CP190 interacting domains of CTCF protein in drosophila melanogaster. *BMC Biol.* **2015**, *13*, 1–23. [CrossRef] [PubMed]
230. Brower-Toland, B.; Riddle, N.C.; Jiang, H.; Huisinga, K.L.; Elgin, S.C.R. Multiple SET methyltransferases are required to maintain normal heterochromatin domains in the genome of drosophila melanogaster. *Genetics* **2009**, *181*, 1303–1319. [CrossRef] [PubMed]
231. Chavez, J.; Murillo-Maldonado, J.M.; Bahena, V.; Cruz, A.K.; Castañeda-Sortibrán, A.; Rodriguez-Arnaiz, R.; Zurita, M.; Valadez-Graham, V. dAdd1 and dXNP prevent genome instability by maintaining HP1a localization at Drosophila telomeres. *Chromosoma* **2017**, *126*, 697–712. [CrossRef] [PubMed]
232. Meyer-Nava, S.; Torres, A.; Zurita, M.; Valadez-Graham, V. Molecular effects of dADD1 misexpression in chromatin organization and transcription. *BMC Mol. Cell Biol.* **2020**, *2*, 1–17. [CrossRef] [PubMed]
233. Strom, A.R.; Emelyanov, A.V.; Mir, M.; Fyodorov, D.V.; Darzacq, X.; Karpen, G.H. Phase separation drives heterochromatin domain formation. *Nature* **2017**, *547*, 241–245. [CrossRef] [PubMed]
234. Ishida, T.; Kinoshita, K. PrDOS: Prediction of disordered protein regions from amino acid sequence. *Nucleic Acids Res.* **2007**, *35*, 460–464. [CrossRef] [PubMed]
235. Frydrychova, R.C.; Biessmann, H.; Mason, J.M. Regulation of telomere length in Drosophila. *Cytogenet. Genome Res.* **2009**, *122*, 356–364. [CrossRef] [PubMed]
236. Gibbons, R.J.; Picketts, D.J.; Villard, L.; Higgs, D.R. Mutations in a putative global transcriptional regulator cause X-linked mental retardation with α-thalassemia (ATR-X syndrome). *Cell* **1995**, *80*, 837–845. [CrossRef]
237. Sadic, D.; Schmidt, K.; Groh, S.; Kondofersky, I.; Ellwart, J.; Fuchs, C.; Theis, F.J.; Schotta, G. Atrx promotes heterochromatin formation at retrotransposons. *EMBO Rep.* **2015**, *16*, 836–850. [CrossRef]
238. Valle-García, D.; Qadeer, Z.A.; McHugh, D.S.; Ghiraldini, F.G.; Chowdhury, A.H.; Hasson, D.; Dyer, M.A.; Recillas-Targa, F.; Bernstein, E. ATRX binds to atypical chromatin domains at the 3′ exons of zinc finger genes to preserve H3K9me3 enrichment. *Epigenetics* **2016**, *11*, 398–414. [CrossRef]

239. de Wit, E.; Greil, F.; van Steensel, B. High-resolution mapping reveals links of HP1 with active and inactive chromatin components. *PLoS Genet.* **2007**, *3*, e30038. [CrossRef]
240. Ilyin, A.A.; Stolyarenko, A.D.; Klenov, M.S.; Shevelyov, Y.Y. Various modes of HP1a interactions with the euchromatic chromosome arms in Drosophila ovarian somatic cells. *Chromosoma* **2020**. [CrossRef]
241. Li, Y.; Danzer, J.R.; Alvarez, P.; Belmont, A.S.; Wallrath, L.L. Effects of tethering HP1 to euchromatic regions of the Drosophila genome. *Development* **2003**, *130*, 1817–1824. [CrossRef] [PubMed]
242. Piacentini, L.; Fanti, L.; Berloco, M.; Perrini, B.; Pimpinelli, S. Heterochromatin protein 1 (HP1) is associated with induced gene expression in Drosophila euchromatin. *J. Cell Biol.* **2003**, *161*, 707–714. [CrossRef] [PubMed]
243. Petesch, S.J.; Lis, J.T. Rapid, transcription-independent loss of nucleosomes over a large chromatin domain at Hsp70 Loci. *Cell* **2008**, *134*, 74–84. [CrossRef] [PubMed]
244. Schneiderman, I.J.; Orsi, G.A.; Hughes, K.T.; Loppin, B.; Ahmad, K. Nucleosome-depleted chromatin gaps recruit assembly factors for the H3.3 histone variant. *Proc. Natl. Acad. Sci. USA* **2012**, *109*, 19721–19726. [CrossRef] [PubMed]
245. Lu, B.Y.; Emtage, P.C.; Duyf, B.J.; Hilliker, A.J.; Eissenberg, J.C. heterochromatin protein 1 is required for the normal expression of two heterochromatin genes in drosophila. *Genetics* **2000**, *155*, 699–708. [PubMed]
246. Danzer, J.R.; Wallrath, L.L. Mechanisms of HP1-mediated gene silencing in Drosophila. *Development* **2004**, *131*, 3571–3580. [CrossRef]
247. de Lucia, F.; Ni, J.Q.; Vaillant, C.; Sun, F.L. HP1 modulates the transcription of cell-cycle regulators in drosophila melanogaster. *Nucleic Acids Res.* **2005**, *33*, 2852–2858. [CrossRef]
248. Minc, E.; Courvalin, J.; Buendia, B. HP1γ associates associates with euchromatin and heterochromatin in mammalian nuclei and chromosomes. *Cytogenet Cell Genet.* **2005**, *284*, 279–284.
249. Vakoc, C.R.; Mandat, S.A.; Olenchock, B.A.; Blobel, G.A. Histone H3 lysine 9 methylation and HP1γ are associated with transcription elongation through mammalian chromatin. *Mol. Cell* **2005**, *19*, 381–391. [CrossRef]
250. Lee, Y.C.G.; Ogiyama, Y.; Martins, N.M.C.; Beliveau, B.J.; Acevedo, D.; Wu, C.-T.; Cavalli, G.; Karpen, G.H. Pericentromeric heterochromatin is hierarchically organized and spatially contacts H3K9me2 islands in euchromatin. *PLoS Genet.* **2020**, *16*, e1008673.
251. Edgar, R.C. MUSCLE: Multiple sequence alignment with high accuracy and high throughput. *Nucleic Acids Res.* **2004**, *32*, 1792–1797. [CrossRef] [PubMed]
252. Guindon, S.; Gascuel, O. A simple, fast, and accurate algorithm to estimate large phylogenies by maximum likelihood. *Syst. Biol.* **2003**, *52*, 696–704. [CrossRef] [PubMed]
253. de Castro, E.; Sigrist, C.J.A.; Gattiker, A.; Bulliard, V.; Langendijk-Genevaux, P.S.; Gasteiger, E.; Bairoch, A.; Hulo, N. ScanProsite: Detection of PROSITE signature matches and ProRule-associated functional and structural residues in proteins. *Nucleic Acids Res.* **2006**, *34*, 362–365. [CrossRef] [PubMed]
254. Contrino, S.; Smith, R.N.; Butano, D.; Carr, A.; Hu, F.; Lyne, R.; Rutherford, K.; Kalderimis, A.; Sullivan, J.; Carbon, S.; et al. modMine: Flexible access to modENCODE data. *Nucleic Acids Res.* **2012**, *40*, D1082–D1088. [CrossRef]
255. Ong, C.T.; van Bortle, K.; Ramos, E.; Corces, V.G. XPoly(ADP-ribosyl)ation regulates insulator function and intrachromosomal interactions in drosophila. *Cell* **2013**, *155*, 148–159. [CrossRef] [PubMed]
256. Thorvaldsdóttir, H.; Robinson, J.T.; Mesirov, J.P. Integrative Genomics Viewer (IGV): High-performance genomics data visualization and exploration. *Brief. Bioinform.* **2012**, *14*, 178–192. [CrossRef]
257. Thurmond, J.; Goodman, J.L.; Strelets, V.B.; Attrill, H.; Gramates, L.S.; Marygold, S.J.; Mathews, B.B.; Millburn, G.; Antonazzo, G.; Trovisco, V.; et al. FlyBase 2.0: The next generation. *Nucleic Acids Res.* **2018**, *47*, D759–D765. [CrossRef]

jove JOURNAL OF VISUALIZED EXPERIMENTS
1 Alewife Center #200
Cambridge, MA 02140
tel. 617.945.9051
www.jove.com

Standard Manuscript Template

TITLE:
Immunofluorescent staining for visualization of heterochromatin associated proteins in Drosophila salivary glands.

AUTHORS AND AFFILIATIONS:
Silvia Meyer-Nava[1], Mario Zurita[1] and Viviana Valadez-Graham*[1]
silvia.meyer@ibt.unam.mx, marioz@ibt.unam.mx, viviana.valadez@mail.ibt.unam.mx
1 Instituto de Biotecnología, Departamento de Genética del Desarrollo y Fisiología Molecular, Universidad Nacional Autónoma de México, Cuernavaca Morelos 62210, México.
*Author to whom correspondence should be addressed.

KEYWORDS:
Drosophila melanogaster
heterochromatin
salivary glands
chromatin
immunostaining
HP1a

SUMMARY:
This protocol aims to visualize heterochromatin aggregates in *Drosophila* polytene cells.

ABSTRACT:
Visualization of heterochromatin aggregates by immunostaining can be challenging. Many mammalian components of chromatin are conserved In *Drosophila melanogaster;* therefore, it is an excellent model to study heterochromatin formation and maintenance. Polytenized cells, such as the ones found in salivary glands of third instar *D. melanogaster* larvae, provide an excellent tool to observe the chromatin amplified nearly a thousand times and have allowed researchers to study changes in the distribution of heterochromatin in the nucleus. Although the observation of heterochromatin components can be carried out directly in polytene chromosome preparations, the localization of some proteins can be altered by the severity of the treatment. Therefore, the direct visualization of heterochromatin in cells complements this type of study. In this protocol, we describe the immunostaining techniques used for this tissue, the use of secondary fluorescent antibodies, and confocal microscopy to observe with greater precision and detail these heterochromatin aggregates.

INTRODUCTION:
Since the early studies of Emil Heitz [1], heterochromatin has been considered an important regulator of cellular processes such as gene expression, meiotic and mitotic separation of chromosomes, and the maintenance of genome stability [2–4].

Heterochromatin is mainly divided into two types, constitutive heterochromatin, which characteristically defines repetitive sequences and transposable elements and is present at

specific chromosome sites such as the telomeres and centromeres. This type of heterochromatin is mainly defined epigenetically by specific histone marks such as the di or tri-methylation of lysine 9 of histone H3 (H3K9me3) and the binding of the Heterochromatin protein 1a (HP1a) [5,6]. On the other hand, facultative heterochromatin localizes through the chromosome's arms and consists mainly of developmentally silenced genes [7,8]. Immunostaining of heterochromatin blocks in metaphase cells, or the observation of heterochromatin aggregates in interphase cells, has led much light in understanding the formation and function of heterochromatic regions [9].

The use of *Drosophila* as a model system has allowed the development of essential tools to study heterochromatin without the use of electron microscopy [10]. Since the description of position effect variegation and the discovery of heterochromatin-associated proteins such as HP1a, and histone post-translational modifications, many groups developed several immunohistochemical techniques that allow visualization of these heterochromatic regions [10,11].

These techniques are based on the use of specific antibodies that recognize heterochromatin-associated proteins or histone marks, for every cell type and antibody, the fixation and permeabilization conditions must be determined empirically. Also, conditions may vary if additional mechanical processes such as squashing techniques are used. In this protocol, we describe the use of *Drosophila* salivary glands to study heterochromatic foci, salivary glands have polytenized cells that contain more than 1000 copies of the genome thus providing an amplified view of most of the chromatin features, with the exception of satellite DNA and some heterochromatic regions which are under replicated, nevertheless, heterochromatin regions are easily visualized in polytene chromosome preparations, but sometimes the squashing techniques may disrupt characteristic chromatin-bound complexes or the chromatin architecture, therefore, immunolocalization of proteins in whole salivary gland tissue can surpass these undesired effects. We have used this protocol to detect several chromatin bound proteins, and we have demonstrated that using this protocol combined with mutant *Drosophila* stocks can be useful to study heterochromatin disruption [12].

PROTOCOL:

1. Third instar larvae culture: To optimize the 3° instar larvae culture, first collect 5-to-10-day old adults and place 50 (25 males and 25 females) in a broad neck bottle of standard media for a 1 Liter of Medium: 100 grams of yeast, 100 grams of unrefined whole cane sugar, 16 grams of Agar, 10 ml of propionic acid and 14 grams of gelatin. Dissolve all ingredients except the yeast in 800 ml of tap water and then dissolve the yeast. Autoclave immediately for 30 minutes. Afterward, let the media cool down to 60 Celsius degrees and add propionic acid, final concentration 0.01%, let the bottle stand until gelatin is formed.

    1.1 Place the bottle with the flies in a controlled temperature incubator at 25 Celsius degrees until the number of eggs laid is 50 (approximately 12 hours for the wild-type strain). After the incubation time is over, remove the adults and transfer them to a new bottle to repeat the procedure. Let the embryos grow at 18° C for 72 hours (if you want to know more about *Drosophila* stock maintenance conditions, see Tennessen & Thymmel) [13].

2. Larvae collection: For larvae collection makes sure choose the wandering larvae which do not have everted spiracles. After the eversion of the spiracles, the larva enters the prepupal stage, while retaining excellent polytene chromosomes suitable for analysis. Only after 12 hours do the cells of the salivary gland begin to prepare for programmed cell death[14,15].

2.1 Take fifteen 3°instar larvae and put them in a watch glass to wash them, then transfer them to an ice-cold saline solution or PBS (PBS 1L 1x: 137 mM NaCl, 2.7 mM KCl, 10mM Na_2HPO_4, 2 mM KH_2PO_4, adjust pH 7.4).

2.2 Dissect 15 to 30 pairs of salivary glands (NOTE: or as many as possible in 30 minutes) in cold PBS with protease inhibitors under the stereoscopic microscope. Transfer the salivary glands to a 1.5ml Eppendorf tube with ice-cold PBS.

2.3 Wash once with 1 ml PBS plus protease inhibitors (NOTE: wait for the tissue to reach the bottom of the tube). After the wash removes the PBS with a 1000ul pipette taking care not to touch the tissue. Alternatively, dissect the salivary glands in 5ml of PBS to eliminate the need for this washing step and proceed to step number 3 by transferring the salivary glands to 0.5ml of the Ruvkun fixing buffer described below.

3. Salivary gland tissue fixation: After removing the PBS from the last step, directly add 0.5 ml of 1X Ruvkun fixing buffer, plus 50% methanol (add 0.5 ml of methanol) plus 2% formaldehyde and incubate for 2 hours at 4 Celsius degrees with mild rotation (Ruvkun 2x solution: 160mM KCl, 40mM NaCl, 20mM EGTA, 30mM PIPES pH 7.4).

4. Salivary gland tissue wash: Carry out one 5-minute rotation wash with Tris/Triton buffer (100 mM tris pH 7.4, 1% Triton X-100 and 1 mM EDTA) adding 1ml. (NOTE: wait for the tissue to reach the bottom of the tube).

5. Permeabilization step: Incubate the salivary glands in 1 ml Tris/Triton X-100 (the same as above). For some proteins it might be necessary to add 1% β-mercaptoethanol. Incubate for 2 hours at 37 ° C with mild shaking (300 rpm).

6. Preservation step (optional): In case you do not proceed immediately to the incubation with the antibody, the tissue can be preserved as follows: Wash with 1 ml BO_3 buffer (0.01 M H_3BO_3 pH 9.2 + 0.01 M NaOH) and then incubate in BO_3 / 10 mM DTT at 37 ° C with mild shaking (300 rpm) for 15 minutes. At the end of the incubation period, perform a wash with 1 ml of BO_3 buffer alone (NOTE: wait for the tissue to reach the bottom of the tube Add 1ml of PBS. You can preserve the tissue in this solution at 4 degrees Celsius for up to 48 hours and then proceed with the next step. This step is particularly helpful when you are working with different mutant strains which may present a delayed life cycle, so you can perform the immunodetection at the same time along with the controls.

7. Tissue blocking step: Incubate the salivary glands in 1 ml of buffer B (PBS + 0.1% BSA + 0.5% Triton X-100 + 1 mM EDTA) for 2 hours at room temperature with rotation.

8. Immunostaining: Remove all buffer B and add buffer A (buffer B with 1% BSA) plus antibody of interest (we use the HP1a C1A9c (concentrated antibody) from Hybridoma Bank up to 1:3000,

when using the C1A9s (supernatant) we have tried from 1:100 to a 1:500 dilution and any dilution between this rank works well) overnight at 4°C with rotation. At this point it is important that the shaking does not raise bubbles which might damage the antibody.

9. Immunostaining washing step: Give 3 x 15-minute washes with buffer B under stirring at room temperature using 1 ml each time. The glands are transferred to buffer B together with the secondary antibody coupled to a fluorophore for 2 hours under rotation at 4°C (secondary antibody Alexa fluor 568 Invitrogen were used 1:3000). At this step, it is important to cover the tube with aluminum paper foil to protect the secondary antibody from the light.

10. Carry out 2 x 15-minute wash at room temperature while rotation with 1ml of Buffer B.

11. Incubate with a DNA marker such as Sytox (take 2µl of stock 5 mM and dissolved in 1 ml of Buffer B) or Hoechst (take 1µl of stock 10 mg/mL and dissolved in 1 ml of Buffer B) for 10 minutes at room temperature with rotation.

12. Carry out one wash with Buffer B and once with PBS, each wash lasting 10 minutes while rotating at room temperature (NOTE: remember to protect it from the light).

13. Finally, mount the salivary glands on a slide, making a pool with a coverslip. Put the salivary glands in the middle of the pool and cover with AF1 citifluor to avoid the formation of bubbles extending the viscous liquid all over the place, then seal all the sides with clear nail polish. Observe under a fluorescence or confocal microscope. If the sample is not going to be observed on the same day, store from light at 4°C.

14. GraphPad Prism 6 was used to generate all graphs and statistical analyses. The data from HP1a distribution in salivary glands was analyzed using the Kruskal-Wallis test. Statistical significance was set at ($p < 0.05$*, < 0.01 **, < 0.001***, < 0.0001****).

REPRESENTATIVE RESULTS:

Representative results of HP1a immunostaining in *Drosophila* salivary glands are shown in Figure 1. A positive result is to observe one focal point (a) (heterochromatic aggregate or condensate). A negative result is no signal or a dispersed signal. Sometimes a double signal can be observed, that is, with a double point (c), but it usually occurs in smaller quantities.

To analyze the data, they can be represented as bar graphs, comparing the distribution of HP1a with different mutant backgrounds. For example, in Figure 2 we can see that 98% of the nuclei present distribution of one point, 2% of two foci in wt. In the mutant, the proportion change, and the presence of two foci increase to 40%.

Figure 3 shows representative H3k9me3 immunostaining results in Drosophila salivary glands. Observing one focal point (b) is a favorable result (heterochromatic aggregate or condensate). A double or triple signal in (c), can be seen on rare occasions, but only in small quantities.

FIGURE AND TABLE LEGENDS:

Figure 1. Representative confocal microscopy image from salivary gland immunostaining with HP1a antibody from wild type (wt). a) DNA (cyan signal), HP1a (magenta signal), and merge scale bar 100 µm. In immunostaining for HP1a, a nucleus with a focal point is marked with a white arrow and a nucleus with two foci with a dotted line box. The right column shows a magnified image of a single nucleus with scale bar 5 µm b) focal distribution, c) two foci distribution. Both nuclei are marked with a white dashed line.

Figure 2. Examples result from counting nuclei distribution with HP1a immunostaining. The first bar represents the counting of the wild-type nuclei (wt), as in Figure 1. The second bar represents a mutant.

Figure 3. Representative confocal microscopy image from salivary gland immunostaining with H3K9me3 antibody from wild type (wt). a) DNA (cyan signal), H3K9me3 (magenta signal) and merge scale bar 100 µm. In immunostaining for H3K9me3.The right column shows a magnified image of a single nucleus with scale bar 5 µm b) a nucleus with a focal distribution, c) three foci distribution. Both nuclei are marked with a white dashed line.

DISCUSSION:

The cellular function of eukaryotic organisms can define the 3D structure within the nucleus, which is supported by interactions between different proteins with chromatin and various molecules including RNA. In the last three years, the biological condensates that have had relevance, including heterochromatin have taken a fundamental role in the determination of the phase separation promoting the distinct nuclear spatial organization of active and repressive chromatin [16–18].

Heterochromatin is essential to preserve cell functions and identity. Previously it was thought that these dense areas were not transcribed, but now that we have more powerful technologies and we can see that it is not only transcribed but also a fundamental process to maintain the scaffold of the nucleus and are sensitive to developmental or pathological processes [12,19]. Besides, certain genes embedded in pericentric heterochromatin need a heterochromatic environment to function properly. HP1a mutations reduce the expression of the light and rolled genes, which were the first to be discovered [19]. These genes are essential for the organism's survival and are found in heterochromatin blocks. As a result, despite its ability to induce silencing, this peculiar genome component has the potential to be very dynamic. [20] In a complex balance between chromatin-bound and diffuse types that can be controlled by various biological contexts, heterochromatin-associated proteins such as HP1a also exist. It was also recently suggested that phase-separation properties are shown by the assembly of heterochromatin condensates [21,22].

There are several papers in which the authors carried out whole-mount immunostaining of *Drosophila* salivary gland nuclei using different and sometimes simpler protocols[23,24]. In this case we adapted a protocol first described in *C. elegans* [25], and subsequently used in *Drosophila* salivary glands by several groups [26–29] and combined it with the use of confocal microscopy and

mutant organisms. This protocol also allows to visualize different types of proteins, including transcription factors such as XPD, XPB and TBP[27], but also heterochromatin bound proteins such as HP1a and histone marks such as H3K9me3, which positions it as a protocol for broad use in this tissue. It also presents the advantage that the tissue can be stored at an intermediate step without affecting polytene chromosome banding.

This protocol is reliable and cost-effective due to the use of a specific antibody to view the HP1a protein. The critical step in this protocol is to avoid losing the glands during washes and waiting for the tissue to bottom out. The advantage of using salivary glands is that you easily get a 3D view of the nucleus and its conformation, in contrast to the polytene chromosome technique which requires a mechanical disruption of the cell and can damage the chromatin. While performing this protocol, you should take special care during the washing steps, if not carefully performed, the tissue will break, and you will not be able to obtain high quality images.

If it is desired to evaluate the importance of the lack of binding of RNA to the regions or proteins that are being observed, it is necessary to add a wash with Buffer C and add 100 µM of RNAse. This wash should be carried out for one hour at 37 °C as previously described. Washing should be done before the step where you add molecules to observe the DNA (between steps 10 and 11).

Confocal microscopy may not seem like a very new methodology to address questions of heterochromatin condensates [25,30], but it has been extremely useful to identify delocalization of the HP1a protein in *Drosophila* nuclei, which suggests severe problems in chromatin structure that can be evaluated with other techniques more thoroughly. Despite its limitation, and combined with high-resolution microscopy it can be used as a first approach to apply novel techniques to clarify the biological activity that modulates heterochromatin condensate assembly, control, and functions[31]. Some of these new methodologies that focus on the molecular and biophysical interactions between heterochromatin, RNA, and heterochromatin-associated proteins are gathered from this set of methods to test heterochromatin condensates.

ACKNOWLEDGMENTS:
We thank Marco Antonio Rosales Vega for taking some of the confocal images, Carmen Muñoz for media preparation and Dr. Arturo Pimentel, M.C. Andrés Saralegui, and Dr. Chris Wood from the LMNA for advice on the use of the microscopes.

DISCLOSURES:
The authors declare that they have no competing interests.

REFERENCES:
1. Berger F. Emil Heitz, a true epigenetics pioneer. *Nature Reviews Molecular Cell Biology*. 2019;20(10):572. doi:10.1038/s41580-019-0170-y
2. Irick H. A new function for heterochromatin. *Chromosoma*. 1994;103(1):1-3. doi:10.1007/BF00364720
3. Kasinathan B, Colmenares S, McConnell H, Young J, Karpen G, Malik H. Innovation of

heterochromatin functions drives rapid evolution of essential ZAD-ZNF genes in Drosophila. *Elife*. Published online 2020:1-31. doi:10.1101/2020.07.08.192740

4. Lifschytz E, Hareven D. Heterochromatin markers: Arrangement of obligatory heterochromatin, histone genes and multisite gene families in the interphase nucleus of D. melanogaster. *Chromosoma*. 1982;86(4):443-455. doi:10.1007/BF00330120
5. Eissenberg JC, Elgin SCR. HP1a: A structural chromosomal protein regulating transcription. *Trends in Genetics* . 2014;30(3):103-110. doi:10.1016/j.tig.2014.01.002
6. Lee YCG, Ogiyama Y, Martins NMC, et al. Pericentromeric heterochromatin is hierarchically organized and spatially contacts H3K9me2 islands in euchromatin. *PLoS Genetics*. 2020;16(3):1-27. doi:10.1371/journal.pgen.1008673
7. Koryakov DE, Walther M, Ebert A, Lein S, Zhimulev IF, Reuter G. The SUUR protein is involved in binding of SU(VAR)3-9 and methylation of H3K9 and H3K27 in chromosomes of Drosophila melanogaster. *Chromosome Research*. 2011;19(2):235-249. doi:10.1007/s10577-011-9193-8
8. Cao R, Wang L, Wang H, et al. Role of Histone H3 Lysine 27 Methylation in Polycomb-Group Silencing. *Science (80-)*. 2002;298(5595):1039 LP - 1043. doi:10.1126/science.1076997
9. Hines KA, Cryderman DE, Flannery KM, et al. Domains of heterochromatin protein 1 required for Drosophila melanogaster heterochromatin spreading. *Genetics*. 2009;182(4):967-977. doi:10.1534/genetics.109.105338
10. Elgin SCR, Reuter G. Position-effect variegation, heterochromatin formation, and gene silencing in Drosophila. *Cold Spring Harbor Perspectives in Biology*. 2013;5(8):1-26. doi:10.1101/cshperspect.a017780
11. Eissenberg JC, Elgin SCR. HP1a: A structural chromosomal protein regulating transcription. *Trends in Genetics*. 2014;30(3):103-110. doi:10.1016/j.tig.2014.01.002
12. Meyer-Nava S, Torres A, Zurita M, Valadez-graham V. Molecular effects of dADD1 misexpression in chromatin organization and transcription. *BMC Molecular and Cell Biology*. 2020;2:1-17. doi:https://doi.org/10.1186/s12860-020-00257-2
13. Tennessen JM, Thummel CS. Coordinating growth and maturation - Insights from drosophila. *Current Biology*. 2011;21(18):R750-R757. doi:10.1016/j.cub.2011.06.033
14. Cai W, Jin Y, Girton J, Johansen J, Johansen KM. Preparation of drosophila polytene chromosome squashes for antibody labeling. *Journal of Visualized Experiments.* 2010;(36):1-4. doi:10.3791/1748
15. Bainbridge SP, Bownes M. Staging the metamorphosis of Drosophila melanogaster. *J Journal of Embryology and Experimental Morphology.* 1981;Vol.66(1967):57-80.
16. Larson AG, Elnatan D, Keenen MM, et al. Liquid droplet formation by HP1α suggests a role for phase separation in heterochromatin. *Nature*. 2017;547(7662):236-240. doi:10.1038/nature22822
17. Larson AG, Narlikar GJ. The Role of Phase Separation in Heterochromatin Formation, Function, and Regulation. *Biochemistry*. 2018;57(17):2540-2548. doi:10.1021/acs.biochem.8b00401
18. Keenen MM, Larson AG, Narlikar GJ. *Visualization and Quantitation of Phase-Separated Droplet Formation by Human HP1α*. *Methods in Enzymology*. 2018. doi:10.1016/bs.mie.2018.09.034
19. Lu BY, Emtage PC, Duyf BJ, Hilliker a J, Eissenberg JC. Heterochromatin protein 1 is required

for the normal expression of two heterochromatin genes in Drosophila. *Genetics*. 2000;155(2):699-708.

20. Marsano RM, Giordano E, Messina G, Dimitri P. A New Portrait of Constitutive Heterochromatin: Lessons from Drosophila melanogaster. *Trends in Genetics*. 2019. doi:10.1016/j.tig.2019.06.002
21. Strom AR, Emelyanov A V., Mir M, Fyodorov D V., Darzacq X, Karpen GH. Phase separation drives heterochromatin domain formation. *Nature*. 2017;547(7662):241-245. doi:10.1038/nature22989
22. Sanulli S, Trnka MJ, Dharmarajan V, et al. HP1 reshapes nucleosome core to promote phase separation of heterochromatin. *Nature*. 2019;575(7782):390-394. doi:10.1038/s41586-019-1669-2
23. Dialynas G, Delabaere L, Chiolo I. Arp2/3 and Unc45 maintain heterochromatin stability in Drosophila polytene chromosomes. *Experimental Biology and Medicine*. 2019. 244(15):1362-1371. doi:10.1177/1535370219862282
24. Kolesnikova TD, Semeshin VF, Andreyeva EN, et al. Induced decondensation of heterochromatin in drosophila melanogaster polytene chromosomes under condition of ectopic expression of the supressor of underreplication gene. *Fly (Austin)*. 2011;5(3):181-190. doi:10.4161/fly.5.3.16729
25. Bettinger JC, Lee K, Rougvie AE. Stage-specific accumulation of the terminal differentiation factor LIN-29 during Caenorhabditis elegans development. *Development*. 1996;122(8):2517-2527.
26. Messina G, Damia E, Fanti L, et al. Yeti, an essential Drosophila melanogaster gene, encodes a protein required for chromatin organization. *Journal of Cell Science*. 2014. 127(11):2577-2588. doi:10.1242/jcs.150243
27. Aguilar-Fuentes J, Fregoso M, Herrera M, et al. p8/TTDA overexpression enhances UV-irradiation resistance and suppresses TFIIH mutations in a Drosophila trichothiodystrophy model. *PLOS Genetics*. 2008;4(11):1-9. doi:10.1371/journal.pgen.1000253
28. Reynaud E, Lomeli H, Vazquez M, Zurita M. The Drosophila melanogaster Homologue of the Xeroderma Pigmentosum D Gene Product Is Located in Euchromatic Regions and Has a Dynamic Response to UV Light-induced Lesions in Polytene Chromosomes. *Molecular Biology of the Cell*.1999;10(4):1191-1203. doi:10.1091/mbc.10.4.1191
29. Farkaš R, Mechler BM. The timing of Drosophila salivary gland apoptosis displays an I(2)gl-dose response. *Cell Death & Differentiation*. 2000;7(1):89-101. doi:10.1038/sj.cdd.4400621
30. Zhang P, Spradling AC. The Drosophila salivary gland chromocenter contains highly polytenized subdomains of mitotic heterochromatin. *Genetics*. 1995;139(2):659-670.
31. Stormo BM, Fox DT. Polyteny: still a giant player in chromosome research. *Chromosome Research* . 2017;25(3-4):201-214. doi:10.1007/s10577-017-9562-z